NASA-CR-197678

KSC-DF-3772

UNIVERSITY OF CENTRAL FLORIDA

COLLEGE OF ENGINEERING
ELECTRICAL AND COMPUTER ENGINEERING

156 p

FINAL REPORT

ANALYSIS OF MAGNETIC FIELD LEVELS AT KSC

PRINCIPAL INVESTIGATOR

Christos G. Christodoulou

August 5, 1994

Sponsored by:

National Aeronautics and Space Administration

KENNEDY SPACE CENTER

NAG - 0126

N95-26808
Unclas
G3/45 0039727
(NASA-CR-197678) ANALYSIS OF MAGNETIC FIELD LEVELS AT KSC Final Report (University of Central Florida) 156 p

SCOPE

The scope of this work is to evaluate the magnetic field levels of distribution systems and other equipment at KSC. Magnetic fields levels in several operational areas and various facilities are investigated. Three dimensional mappings and contour are provided along with the measured data. Furthermore, the portion of magnetic fields generated by the 60 Hz fundamental frequency and the portion generated by harmonics are examined. Finally, possible mitigation techniques for attenuating fields from electric panels are discussed.

Contents

1 INTRODUCTION

In the past, the concern was with the electric fields only emitted from high-voltage transmission lines, since they were the most visible sources. However, recently the emphasis has shifted to the effects of magnetic fields. Since, these fields are current-dependent and not voltage-dependent, they are stronger in the vicinity of high current conductors. This type of conductors are now most common at lower circuit voltages in the residential and commercial distribution areas.

Most of the magnetic fields produced by distribution systems emanate from any imbalanced currents between phase and neutral conductors, or from ground currents returning through the ground and pipes. Minimizing these currents are of paramount importance.

In this study several measurements were taken at various sites at KSC. The measurements were taken both as functions of time and distance from the source. Furthermore, the measurements were done at the fundamental 60 Hz frequency and its harmonics.

Three dimensional plots and contour plots of the magnetic field intensity levels have been obtained for a variety of sites at Kennedy Space Center, including a prototype building and shop with several electrical equipment.

Basically, a large number of sources of magnetic fields were identified and measured. More specifically, these measurements covered :

- Power Lines
- Transformers
- Ground Currents
- Electric panels

- Several industrial equipment
- Several offices (in a prototype building)

Several calculations and measurements were completed and samples of results are included in this report. All measurements and data are provided along with this report on floppy disks and back-up tapes. These results can be used for further parametric studies in the future by other researchers as well.

All measurements were done by using the EMDEX II field meter designed by EPRI.

The sections to follow herein are divided into calculations, results, conlusions, recommendations and future projects as proposed in our unsolicited proposal.

2 CALCULATIONS

2.1 Magnetic Field Calculation

The EMDEX II field meter (designed by EPRI- Appendix I) is used in this study. This programmable meter can measure the orthogonal vector components of the magnetic field through its three internal sensors. In some of the results to follow herein a single combined value is given. This combined value, called the resultant, reflects the strength of the magnetic field. It is defined as:

$$R = \sqrt{B_x^2 + B_y^2 + B_z^2} \tag{1}$$

where:

B_x x vector component of B field

B_y y vector component of B field

B_z z vector component of B field

All values are in milliGauss (mG) units and B is the magnetic field density vector.

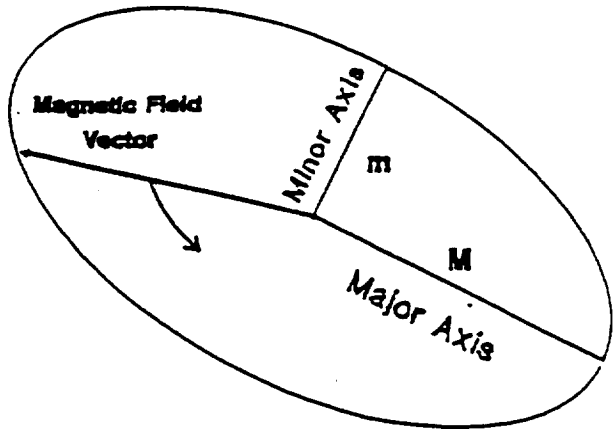

Figure 1: Major and minor axes for elliptical polarized fields

2.2 Magnetic field measurements for different polarizations

Magnetic field vectors change as a function of time. The magnetic field can have any type of polarization. It is important to know what part of the field the measurements represent in each case. The most general polarization is the *elliptical* polarization shown in Figure 1. This type of field is produced by 3-phase distribution and transmission lines [1].

In our measurements the maximum value obtained corresponds to the major axis of the ellipse. The resultant value reflects the values of both axes.

Two special cases of the elliptical polarization exist. The circular(Figure 2) and the linear polarization (Figure 3). In the circular polarization the major and minor axes are equal. In the linear case the minor axes is equal to zero. For the linear polarization the measured resulatnt is equal to the major axis. For the circularly polarized field the resultant is $\sqrt{2}\times$ larger than the magnitude of the major axis.

2.3 Fundamental Frequency Calculations

Measurements are made over two frequency ranges:

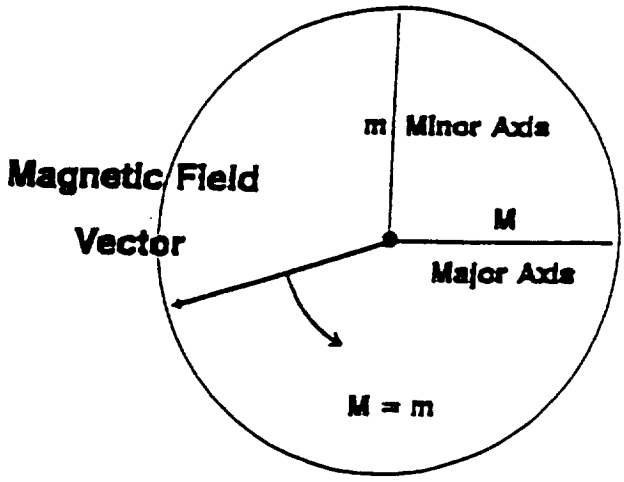

Figure 2: Axes for circular polarization

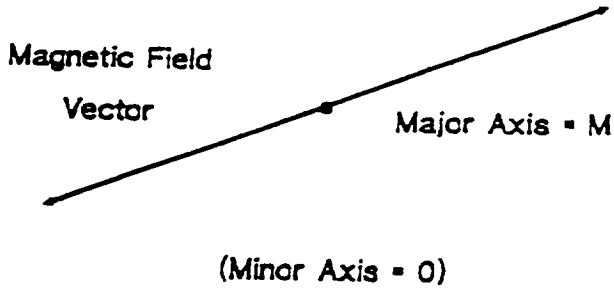

Figure 3: Linear polarization

- the broadband measured from 40 to 800 Hz that also includes the fundamental 60 Hz frequency.

- harmonic measured from 100 to 800 Hz .

The calculated magnitude of the magnetic field at the fundamental frequency is found from the following expression [2] :

$$F_c = \sqrt{B_m^2 - H_m^2} \qquad for \;\; H_m \leq B_m \tag{2}$$

where:

b_m is the rms value of the measured broadband component, and

H_m is the rms value of the measured harmonic component.

If $H_m \geq B_m$ then the fundamental value $F_c = 0$.

Appendix II includes an error analysis for the calculated fundamental value of the magnetic field.

2.4 Power Lines

For power lines, if the the current flowing in the line is known then one can use the Biot-Savart Law to determine the value of the magnetic field given by:

$$H_\phi = \frac{I(z)}{2\pi}\frac{1}{\rho} \tag{3}$$

where z is the axis of the power line and ρ the distance from the line.

For horizontal conductors, such as a three phase horizontal power line the following formula should be used[3-4]:

$$\begin{aligned} \vec{B} \;\; = \;\; & -2\,I_n \left[\frac{(y-d_n)}{r_{cn}^2} - \frac{(y+d_n+\alpha)}{r_{in}^2}\right] \hat{a}_z \\ & + \;\; 2\,I_n \left[\frac{(x-h_n)}{r_{cn}^2} - \frac{(x-h_n)}{r_{in}^2}\right] \hat{a}_y \;\; \text{mG} \;\; \text{in RMS} \end{aligned} \tag{4}$$

where:

$$r_{cn} = \left[(x-h_n)^2 + (y-d_n)^2\right]^{1/2} \quad (5)$$

$$r_{in} = \left[(x-h_n)^2 + (y+d_n+\alpha)^2\right]^{1/2} \quad (6)$$

$$\alpha = \sqrt{(2)}\,\delta\, e^{-j\pi/4} \quad (7)$$

$$\delta = 503\,(\rho_g/f)^{1/2} \quad (8)$$

ρ_g is the earth resistivity, I_n is the conductor current and f the frequency. This formula takes into account the induced eddy currents in a conducting earth.

2.5 Calculation for Magnetic Shielding

Several materials for magnetic shielding exist. The ones we used in our work are the *Co-netic* and Netic materialas provided by the Magnetic Shielding Corporation [2]. These materials are usually used for building shielding enclosures so that any of the magnetically sensitive equipment can be protected from any outside interference. Our problem is the opposite. We want to shield sources of magnetic fields. In general the shield attracts flux lines to itself and diverts the magnetic field away from sensitive components.

The shielding efficiency of a magnetic material is given in terms of its attenuation ratio. This is the ratio of the measured field before shielding to that after shielding. Each layer of material has its own attenuation ratio. If more attenuation is required more layers can be used. This attenuation ratio (in dB) is given by:

$$A = \frac{\mu \cdot t}{D} \quad (9)$$

where

μ is the permeability of the material

t the thickness of the material.

D is the diameter or diagonal of the shield.

For more details on the saturation and other characteristics of these two types of materials see Appendix III .

3 STUDY RESULTS

In this section several examples of measurements are presented and discussed. It should be mentioned that not all measured data appear in this report. All data can be found in the data disks provided with the report. A large number of measurements can also be found in the 50% and 75% reports. The results here are separated into:

- Power Lines
- Transformers
- Ground Currents
- Electric panels
- Several industrial equipment
- Several offices (in a prototype building)

3.1 Power Lines

Figure 4 depicts the path taken for measuring the fields in the vicinity of a power line. Figures 5 and 6 show the intensities as a function of distance and in a three dimensional format, respectively. The EMDEX II sensor used in our measurements is not capable of measuring values over 3,000 mGauss. Since power lines emanate large magnetic field levels, measurements from power lines are limited to a few cases.

Fig. 4

File:POWERLN.MDX

< Data Point • Event □ Begin Path ▪ End Path

Label:Around power line

Units: feet

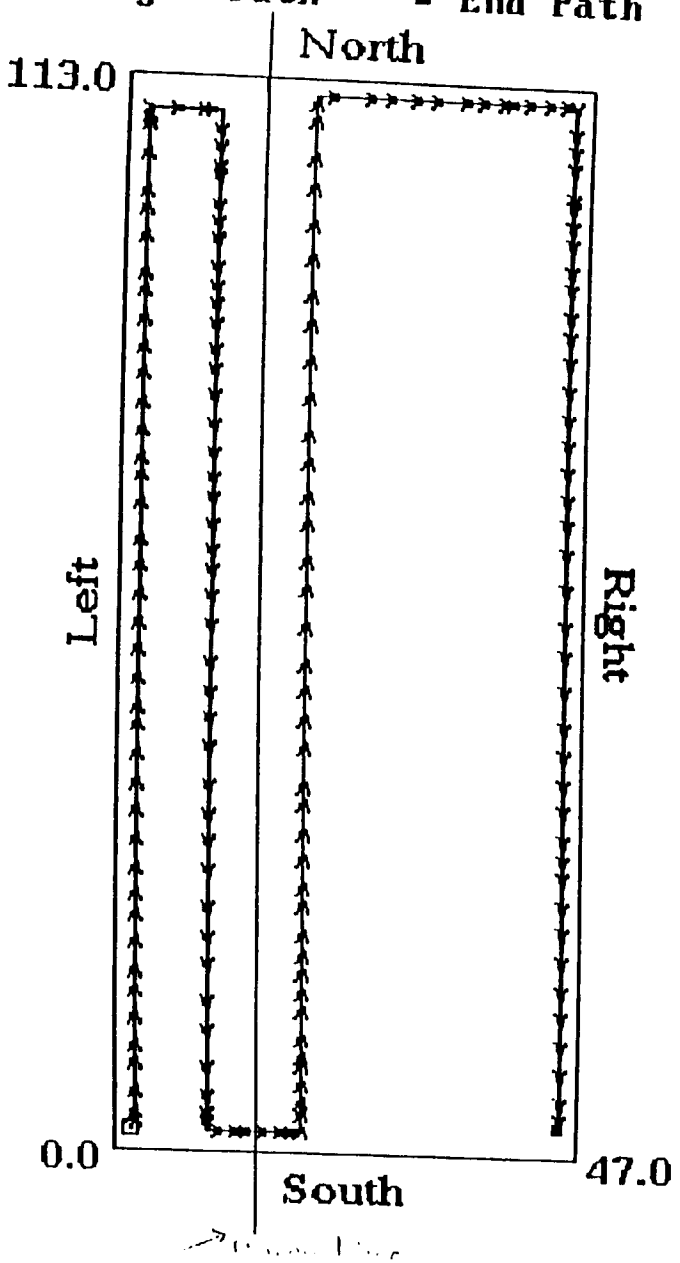

Fig. 5

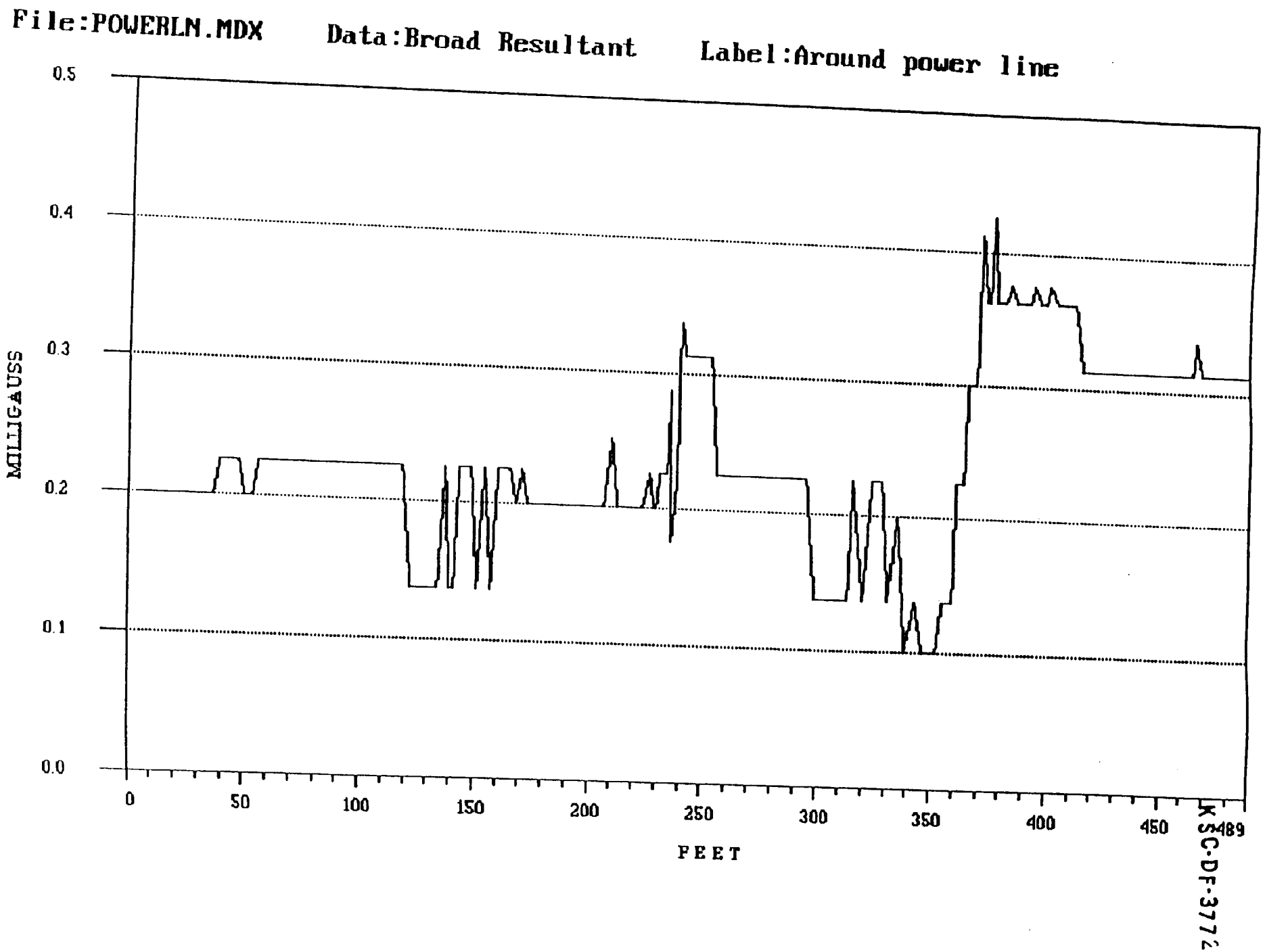
File:POWERLN.MDX
Data:Broad Resultant
Label:Around power line
0.5
0.4
0.3
0.2
0.1
0.0
MILLIGAUSS
0
50
100
150
200
250
300
350
400
450
489
FEET
KSC-DF-3772

Fig. 6

File:POWERLN.MDX Data:Broad Resultant Label:Around power line

Units: feet

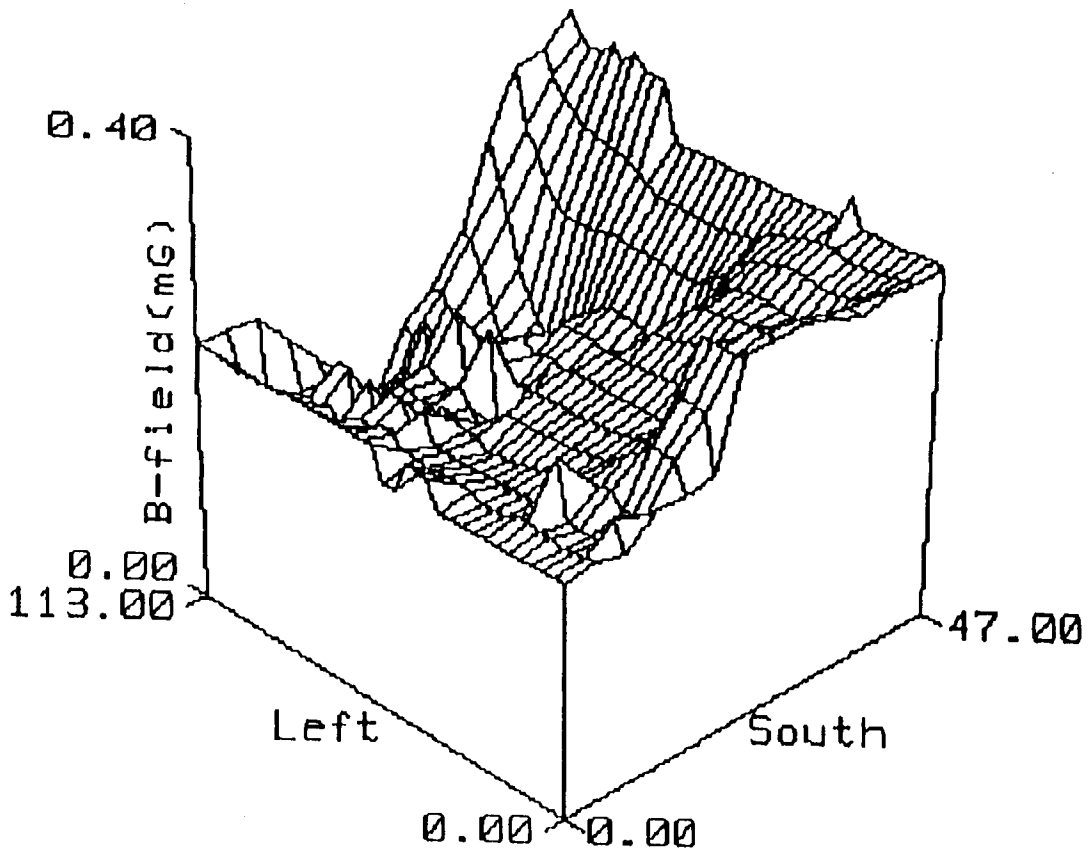

3.2 Transformers

Figures 7 through 12 correspond to measurements from an OCR (Oil Circuit Recloser) and a LBS (Load Break Switch). Two different paths were selected, as shown in Figures 7 and 10. The intensities obtained for these two paths are depicted in Figures 8 and 11. Their 3-dimensional representation is shown in Figures 9 and 12, respectively. These measurements demonstrate the dependence of the magnetic field data on the path taken around the source under study. The path taken in each measurement should always be checked before any results are interpreted. Although several paths could have been chosen, here two paths are enough to demonstrate this point. One path (Figure 8) gives a maximum value of 100 mG whereas the other path (Figure 11) yields a maximum of 30 mG.

In Figure 13, the path taken for measuring the magnetic field intensity in the vicinity of a load break switch is shown. In Figure 14, we can see that the level of magnetic field is slightly over 1 milligauss for the entire path. Figure 15 , depicts the measurements path for a transformer (labeled # 115). Figure 16, shows that the levels from such a transformer are almost 20 times larger than those from a load break switch. These kind of results are important in determining which sources are the main sources that generate high magnetic fields at KSC. Figure 17 depicts a three dimensional plot in the vicinity of the transformer.

File:POWERLN.MDX

< Data Point • Event □ Begin Path ▪ End Path

Label:OCR 6

Units: feet

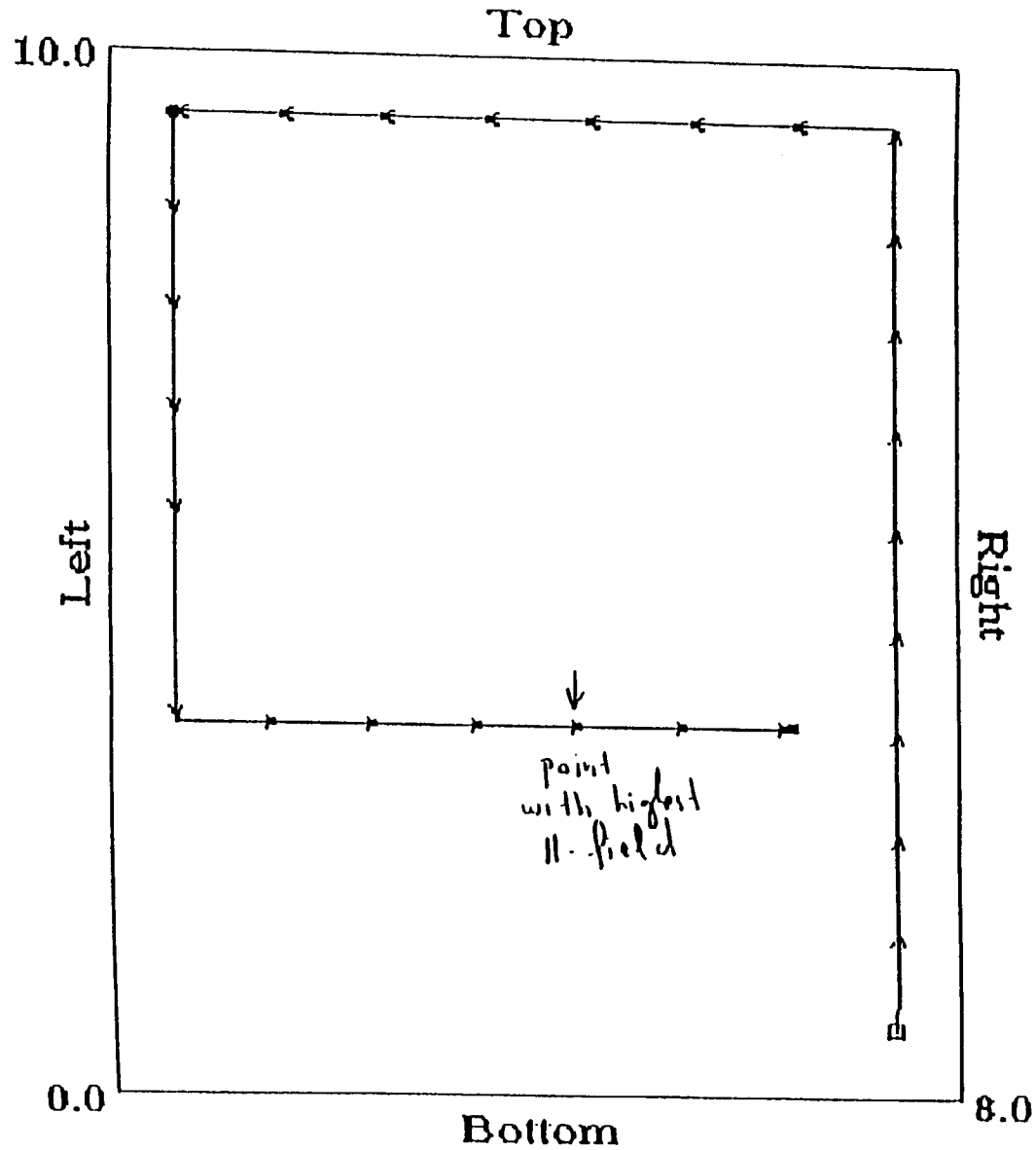

Fig. 8

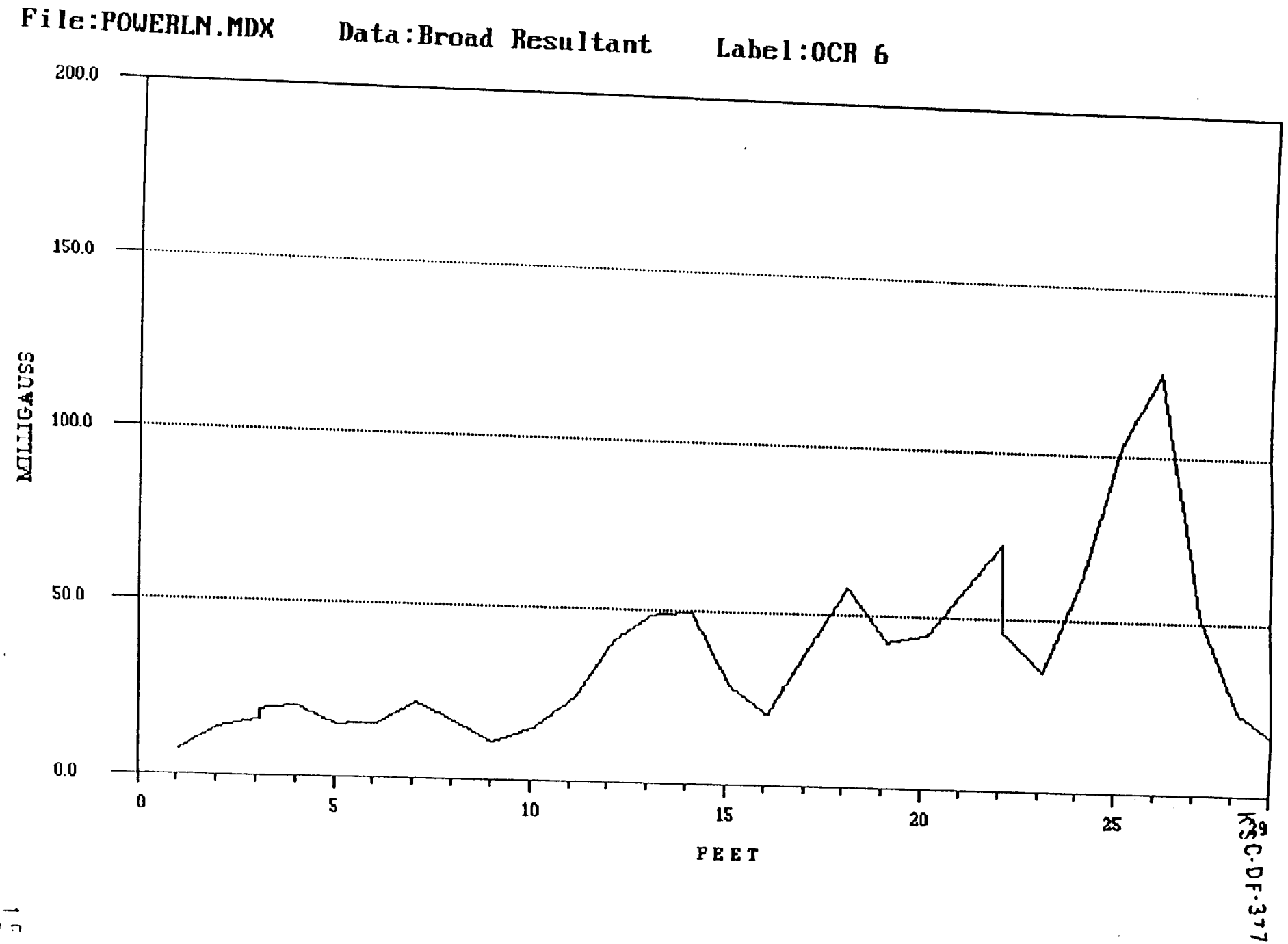
File:POWERLN.MDX
Data:Broad Resultant
Label:OCR 6
200.0
150.0
100.0
50.0
0.0
MILLIGAUSS
0
5
10
15
20
25
FEET
KSC-DF-377

Fig. 9

File:POWERLN.MDX Data:Broad Resultant Label:OCR 6

Units: feet

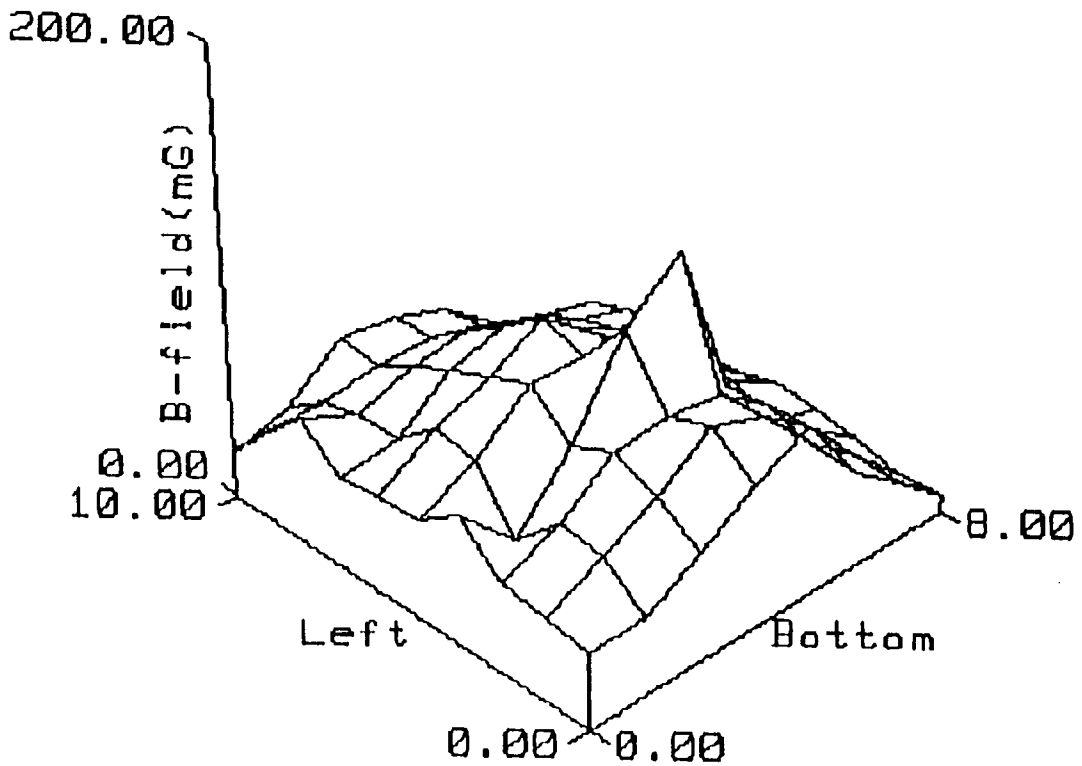

File:OCT_19.MDX

Fig. 10

< Data Point • Event □ Begin Path ▪ End Path

Label:LBS #56 / OCR #6

Units: feet

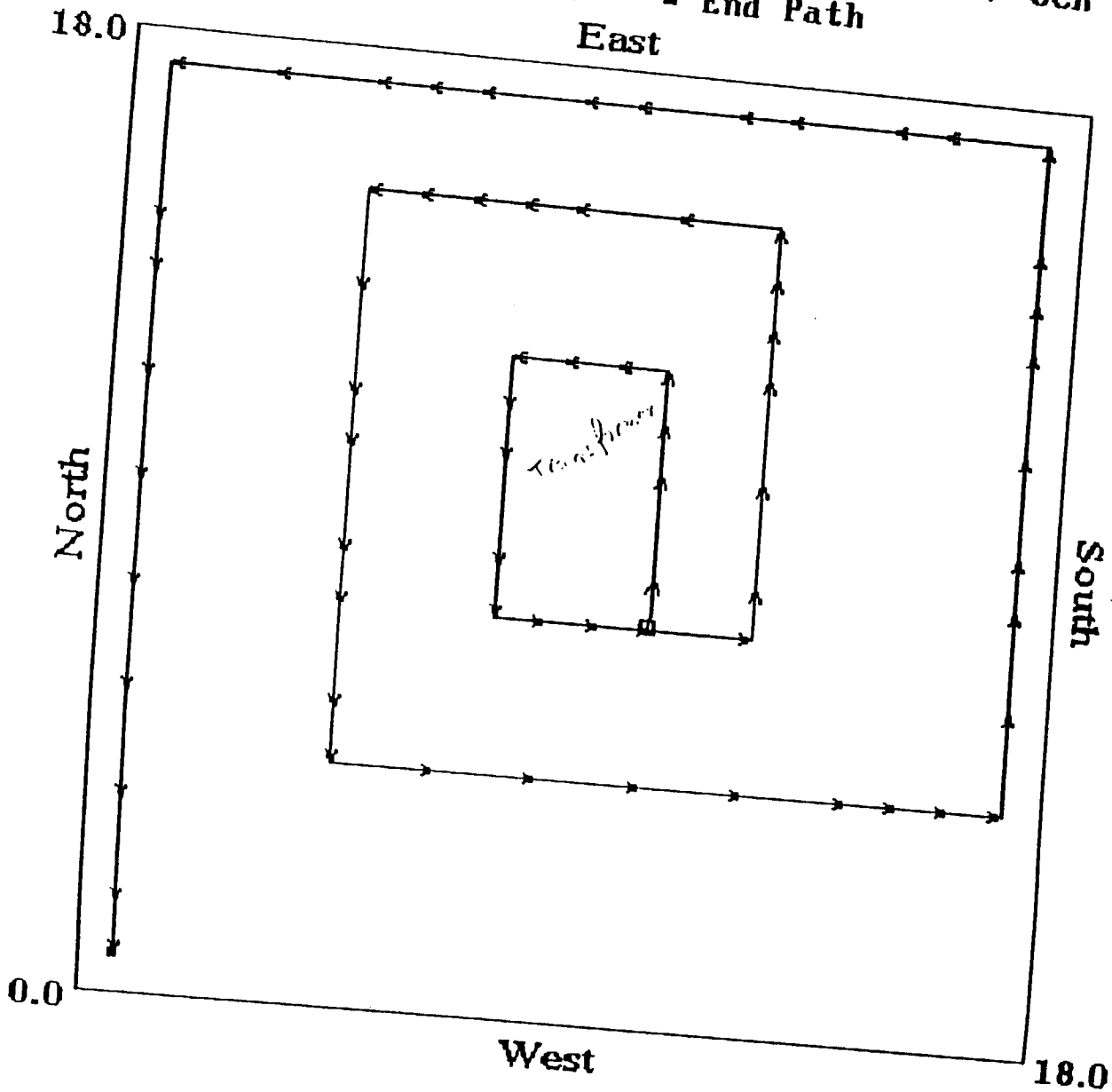

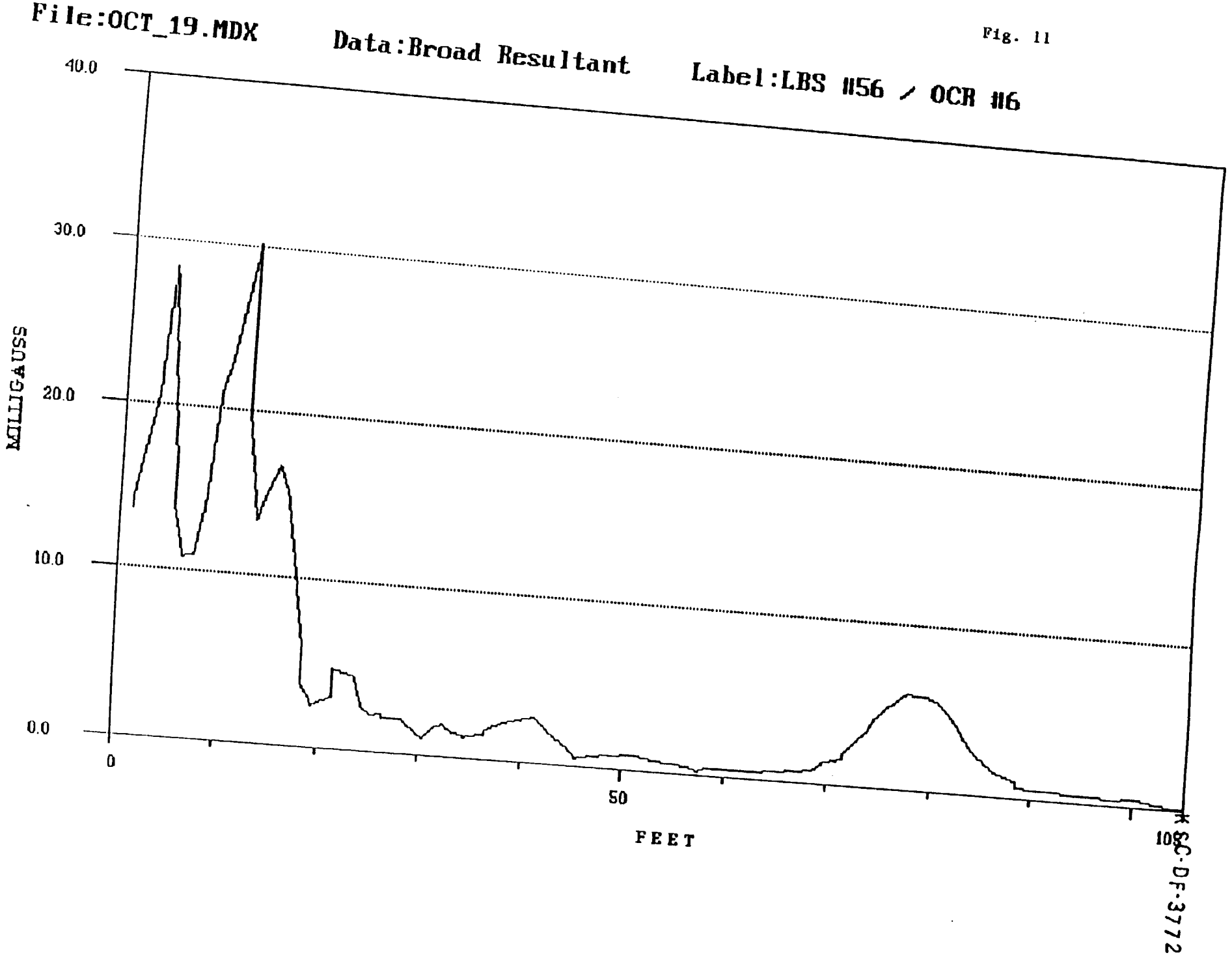

Fig. 11

K&C-DF-3772

Fig. 12

File:OCT_19.MDX Data:Broad Resultant Label:LBS #56 / OCR #6

Units: feet

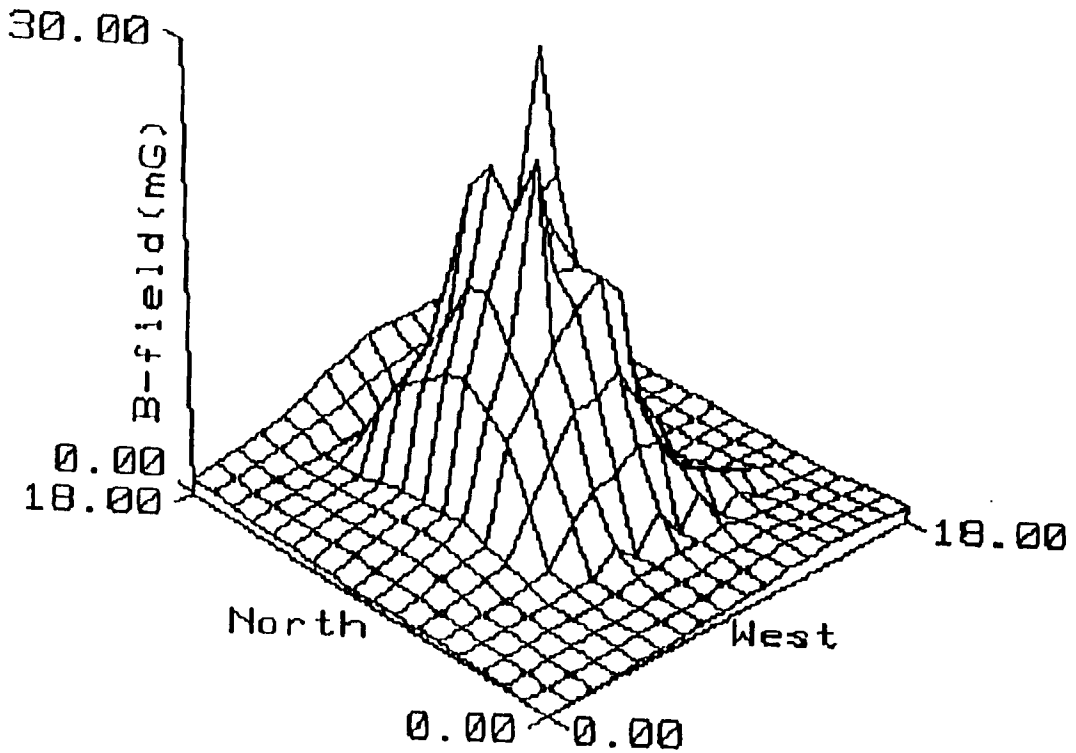

Fig. 13

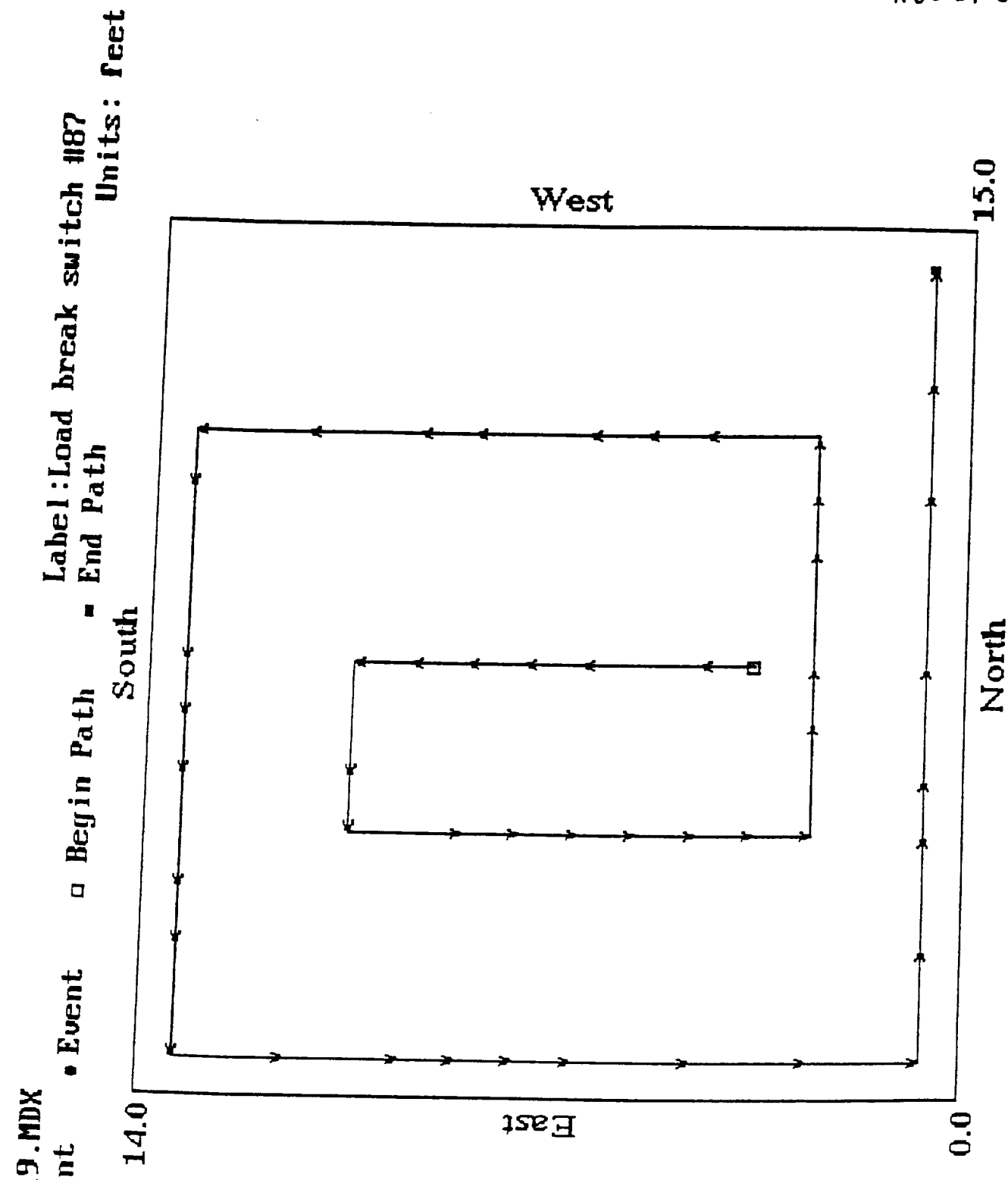
File:OCT_19.MDX
Data Point
Event
Begin Path
End Path
Label:Load break switch #87
Units: feet
West
15.0
South
North
14.0
East
0.0

Fig. 14

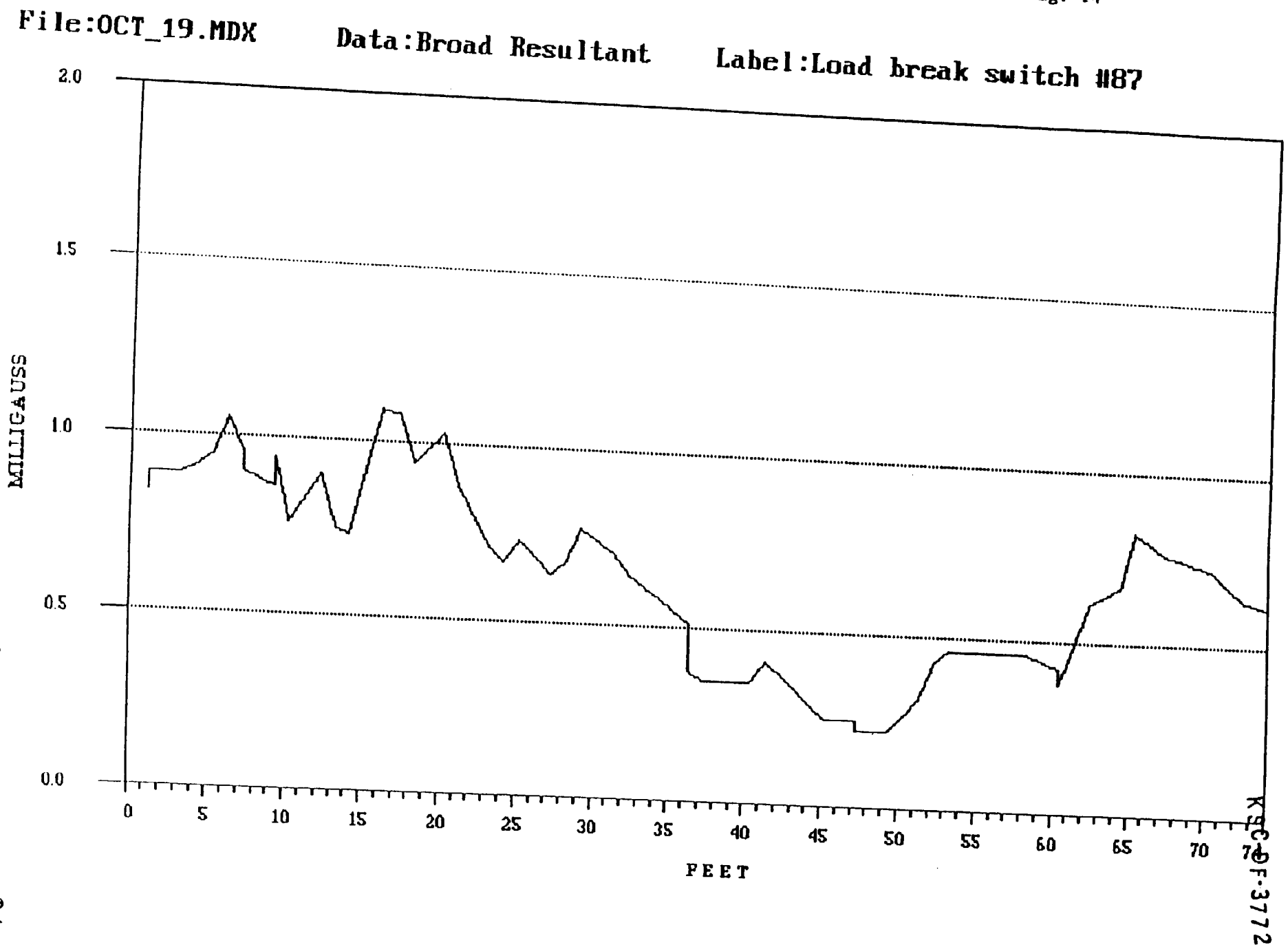
File:OCT_19.MDX
Data:Broad Resultant
Label:Load break switch #87
2.0
1.5
1.0
0.5
0.0
MILLIGAUSS
0
5
10
15
20
25
30
35
40
45
50
55
60
65
70
FEET
KS-36F-3772

Fig. 15

File:OCT_19.MDX

< Data Point • Event ▫ Begin Path ▪ End Path Label:Transformer #115

Units: feet

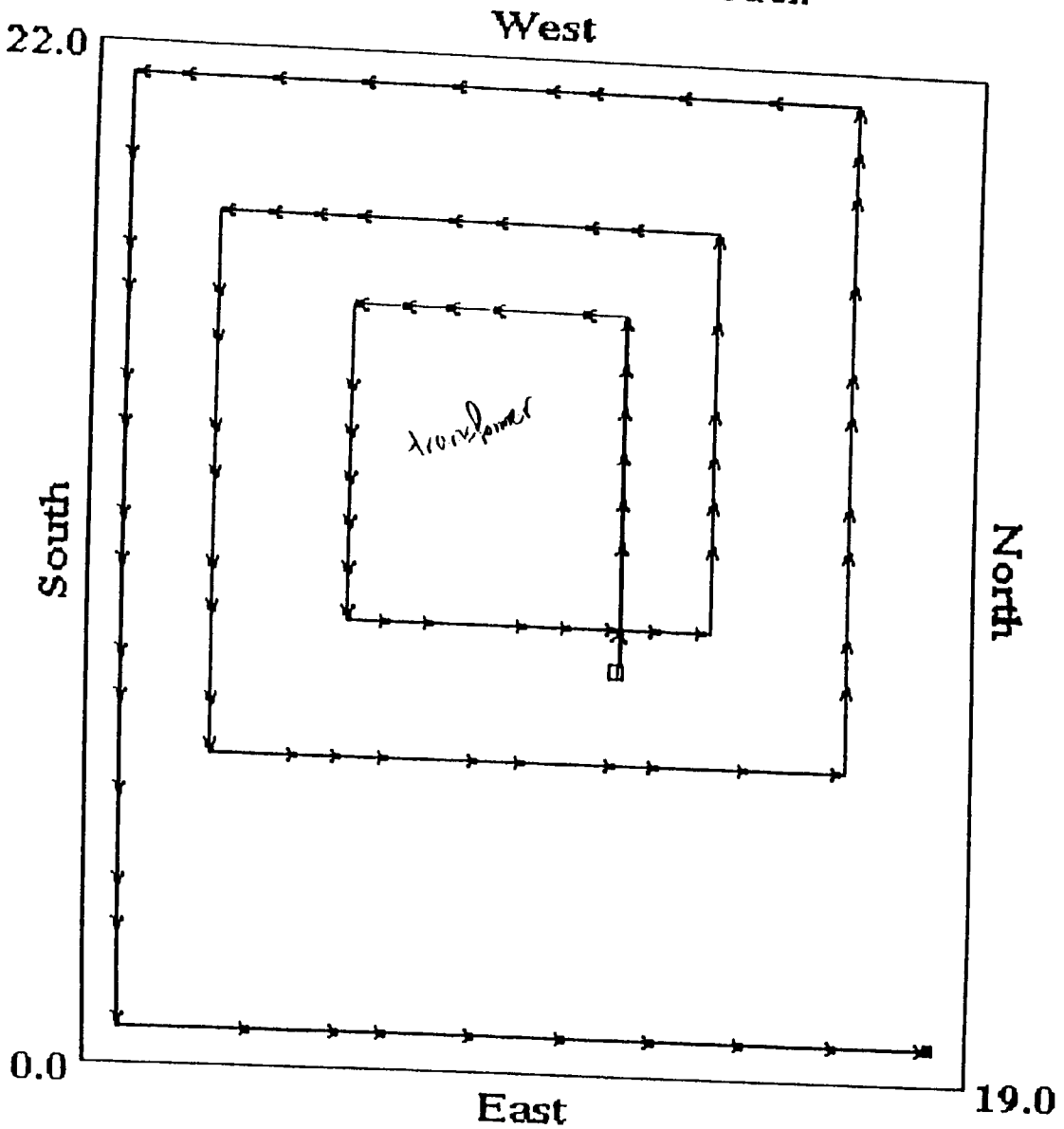

Fig. 16

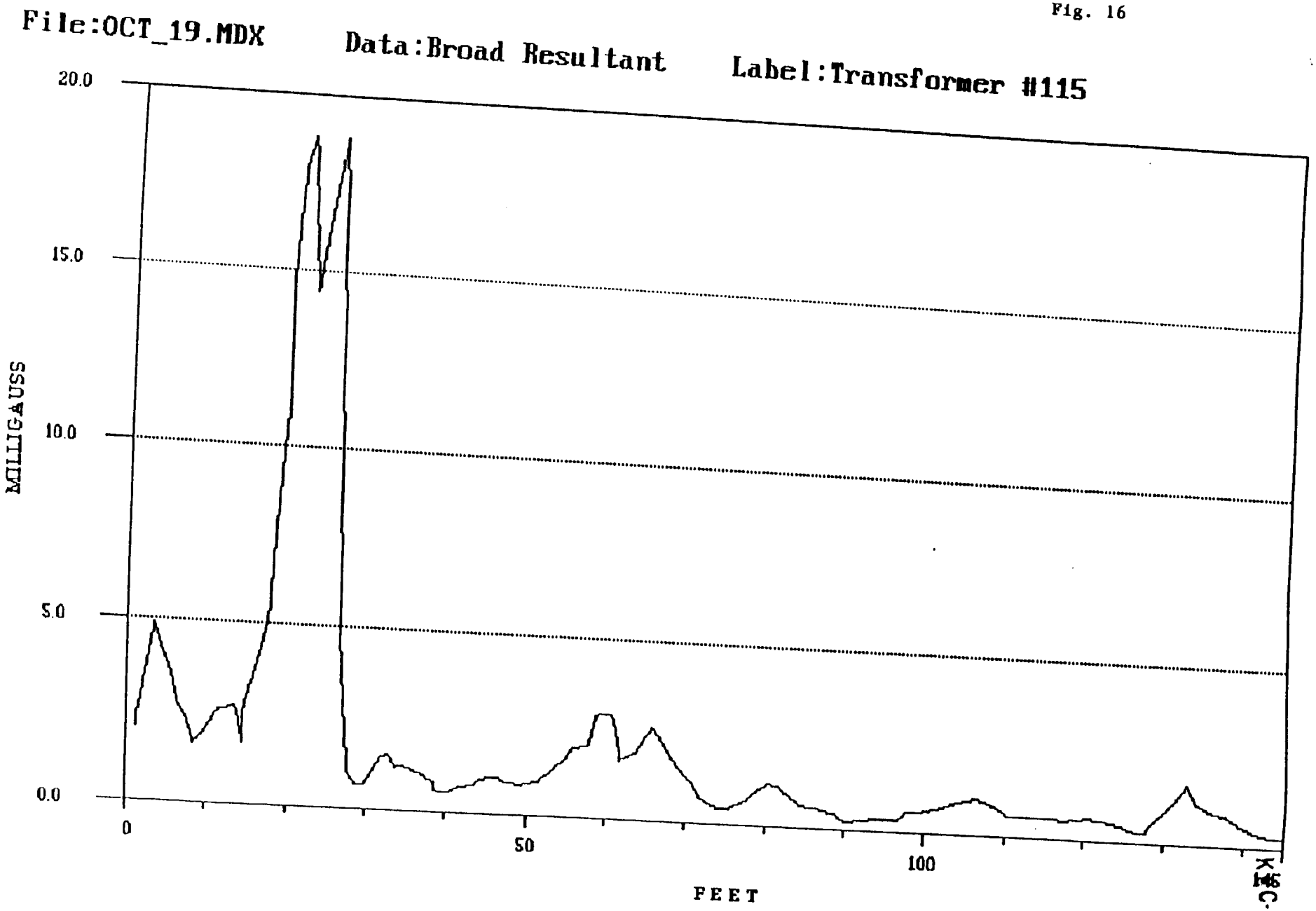

KEC-DF-3772

File:OCT_19.MDX Data:Broad Resultant Label:Transformer #115

Units: feet, mG

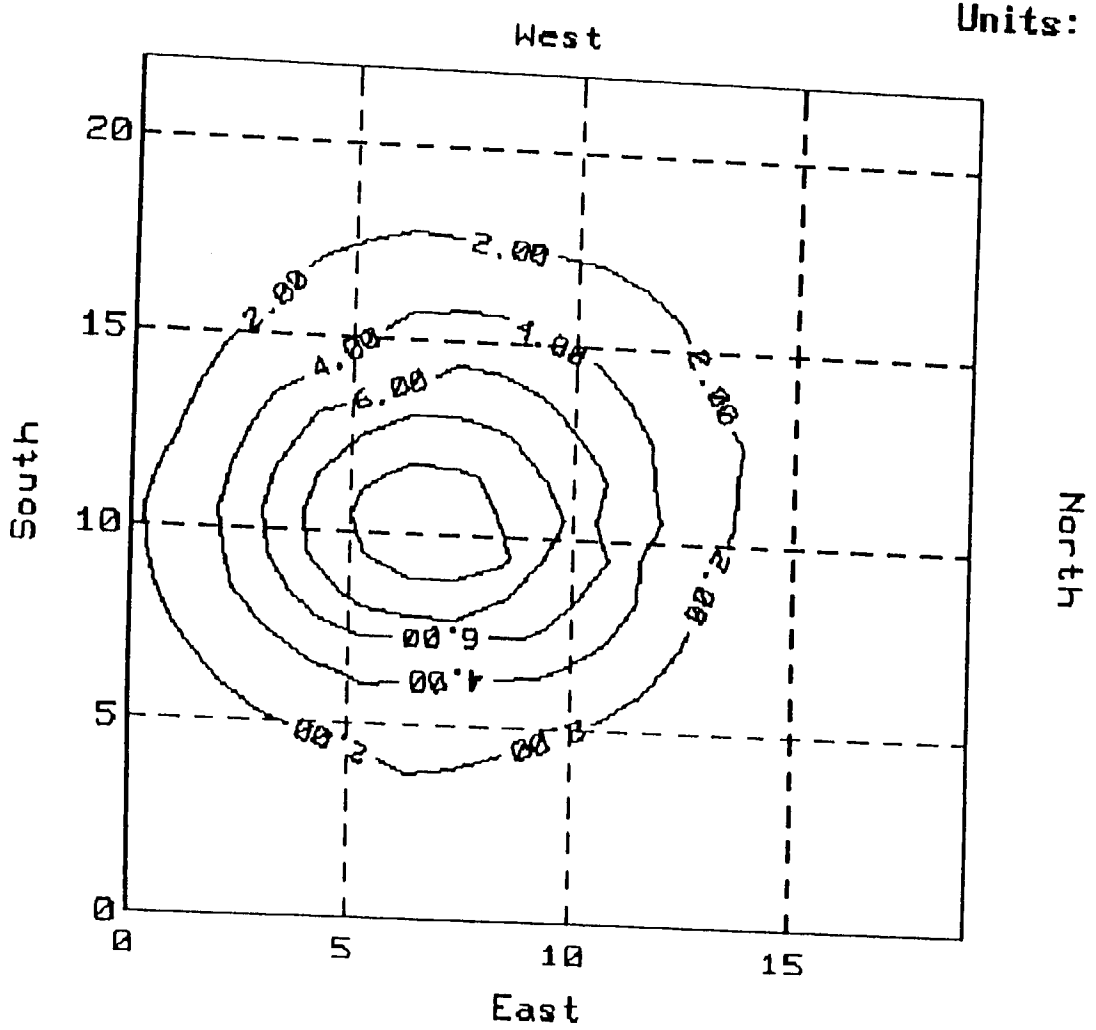

3.3 Measurements versus time

Next, some of measurements taken were versus time instead of distance. These type of measurements are important in determining the frequency, time, and duration of occurence of any high level magnetic field intensities. In Figures 18 through 31 the results from a conference room tested over a period of a week are shown. It can be seen that the magnetic field level does not exceed the 1 mGauss mark any time in this particular room. It was interesting to observe that the highest readings occured, every day, between 8 and 5 o'clock. This should not come as a surprise since these are the hours when most lights and equipment are on. Measurements were done at the fundamental (Figures 22-26) and harmonic (Figure 27-31) frequencies. Most of the contribution to the magnetic field was primarily due to the fundamental frequency.

Fig. 18

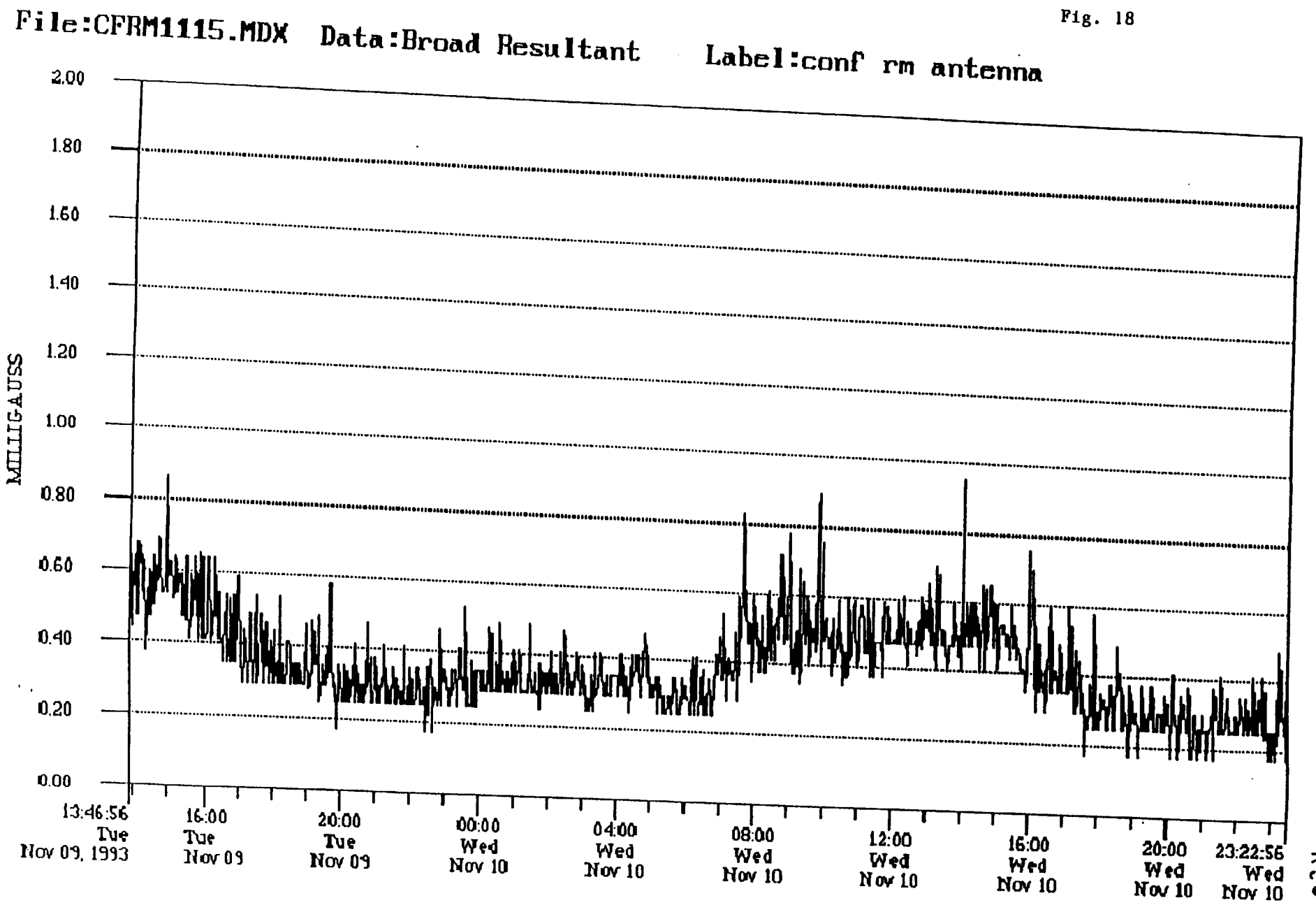
File:CFRM1115.MDX Data:Broad Resultant Label:conf rm antenna
MILLIGAUSS
2.00
1.80
1.60
1.40
1.20
1.00
0.80
0.60
0.40
0.20
0.00
13:46:56 Tue Nov 09, 1993
16:00 Tue Nov 09
20:00 Tue Nov 09
00:00 Wed Nov 10
04:00 Wed Nov 10
08:00 Wed Nov 10
12:00 Wed Nov 10
16:00 Wed Nov 10
20:00 Wed Nov 10
23:22:56 Wed Nov 10

File:CFRM1115.MDX Data:Broad Resultant Label:conf rm antenna

Fig. 19

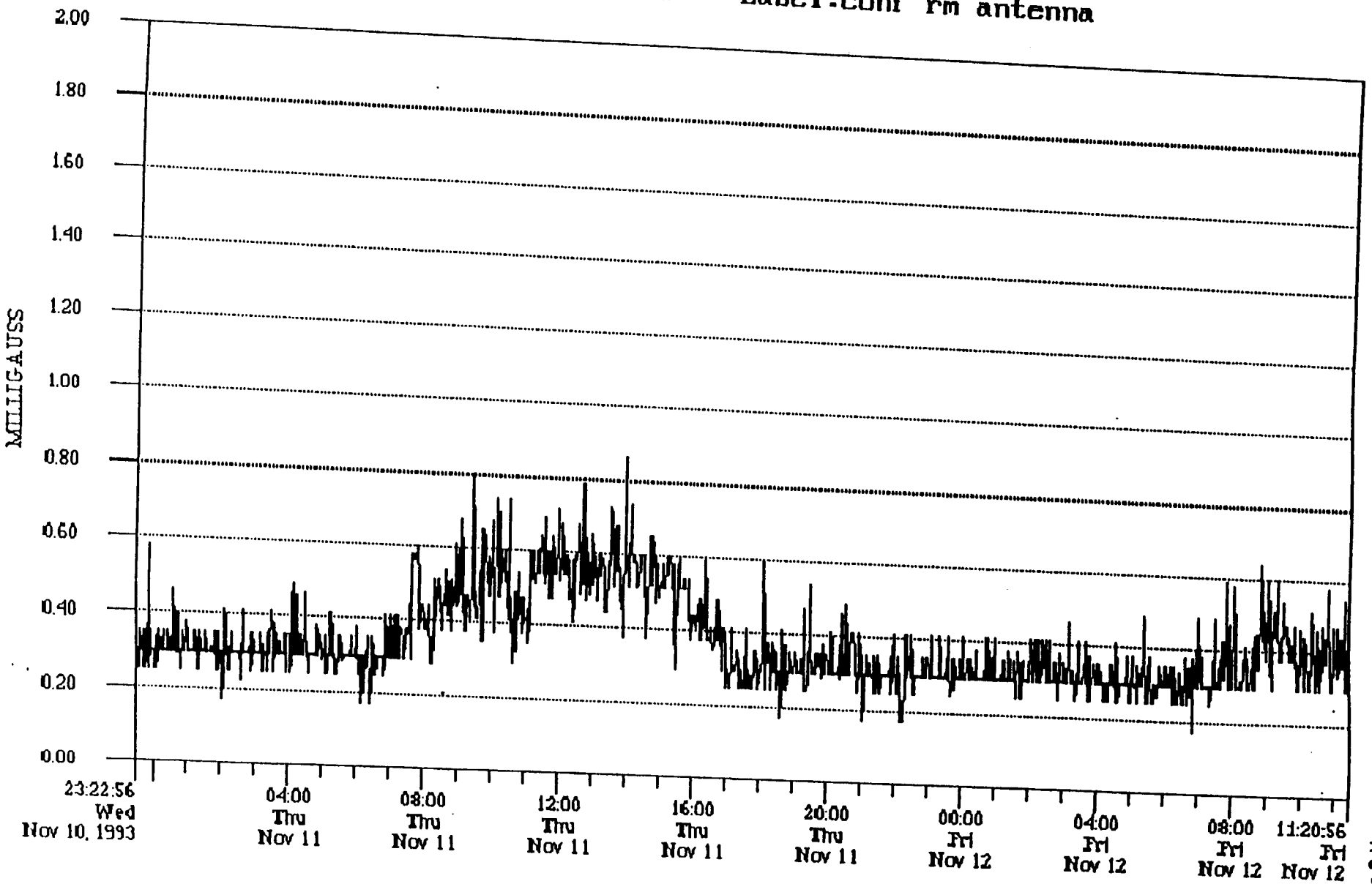

Fig. 20

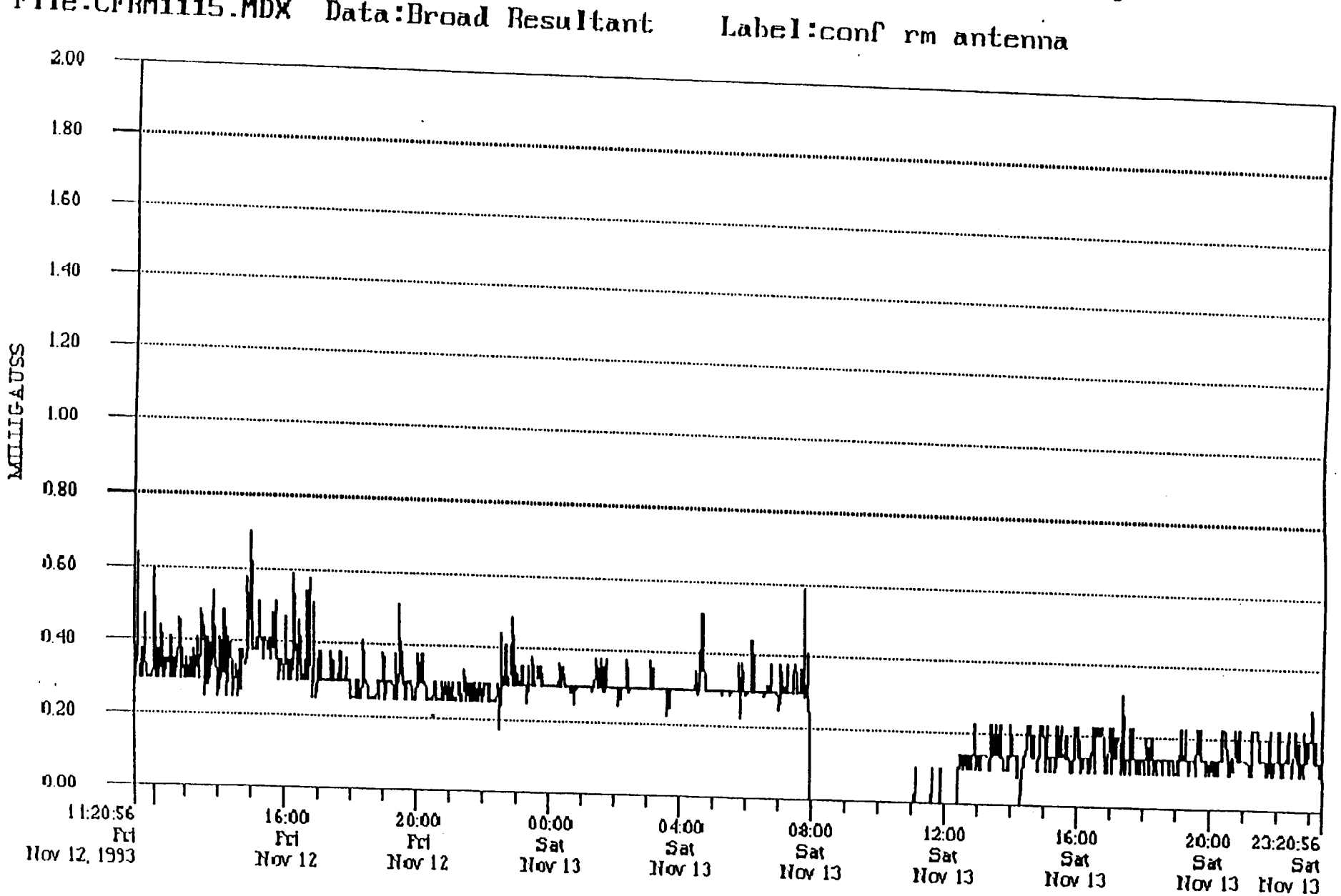
File:CFRM1115.MDX Data:Broad Resultant Label:conf rm antenna
MILLIGAUSS
2.00
1.80
1.60
1.40
1.20
1.00
0.80
0.60
0.40
0.20
0.00
11:20:56 Fri Nov 12, 1993
16:00 Fri Nov 12
20:00 Fri Nov 12
00:00 Sat Nov 13
04:00 Sat Nov 13
08:00 Sat Nov 13
12:00 Sat Nov 13
16:00 Sat Nov 13
20:00 Sat Nov 13
23:20:56 Sat Nov 13

Fig. 21

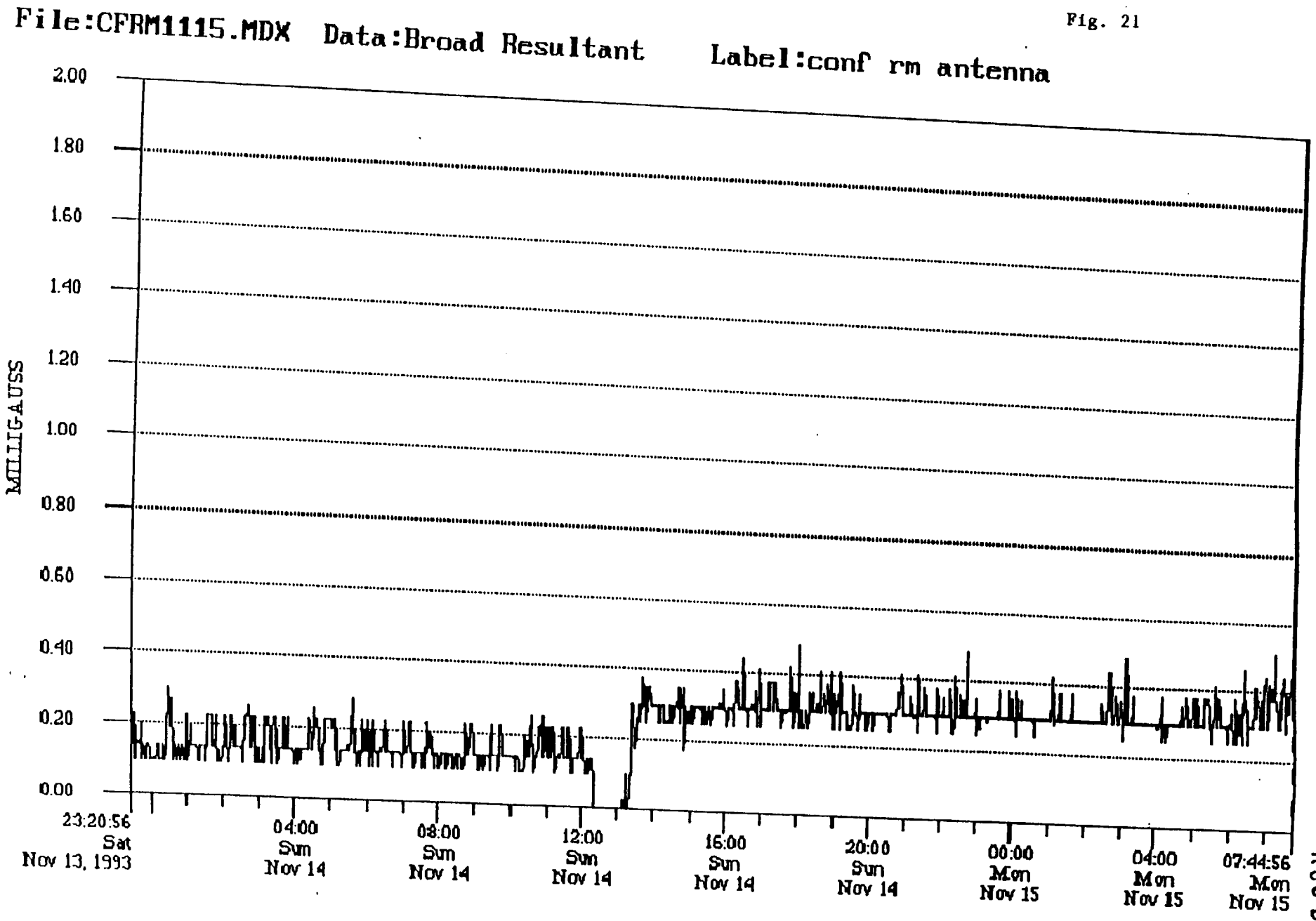

KSC-DF-377

File:CFRM1115.MDX Data:Fund Resultant Label:conf rm antenna

Fig. 22

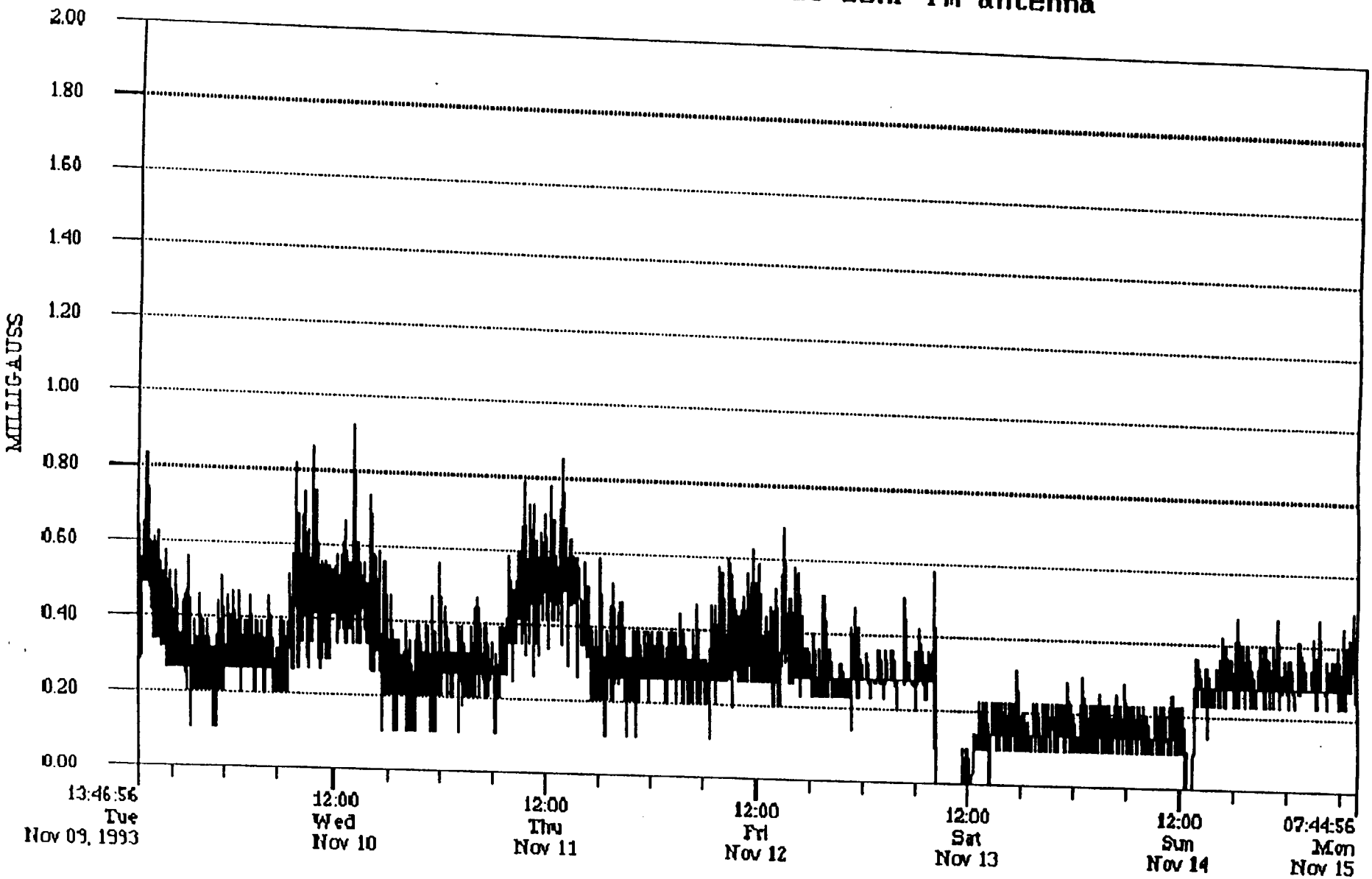

KSC-DF-3772

Fig. 23

File:CFRM1115.MDX Data:Fund Resultant Label:conf rm antenna

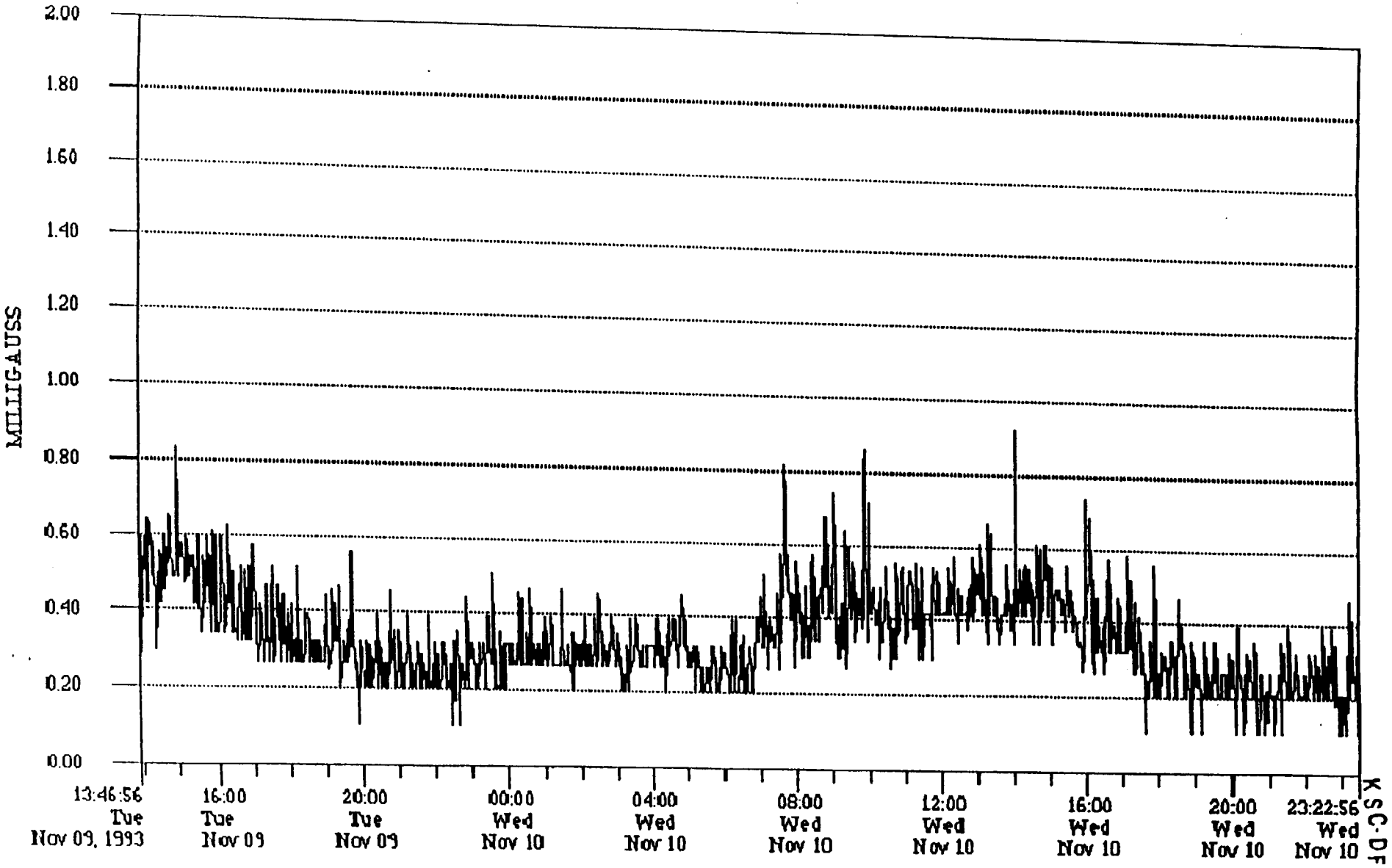

Fig. 24

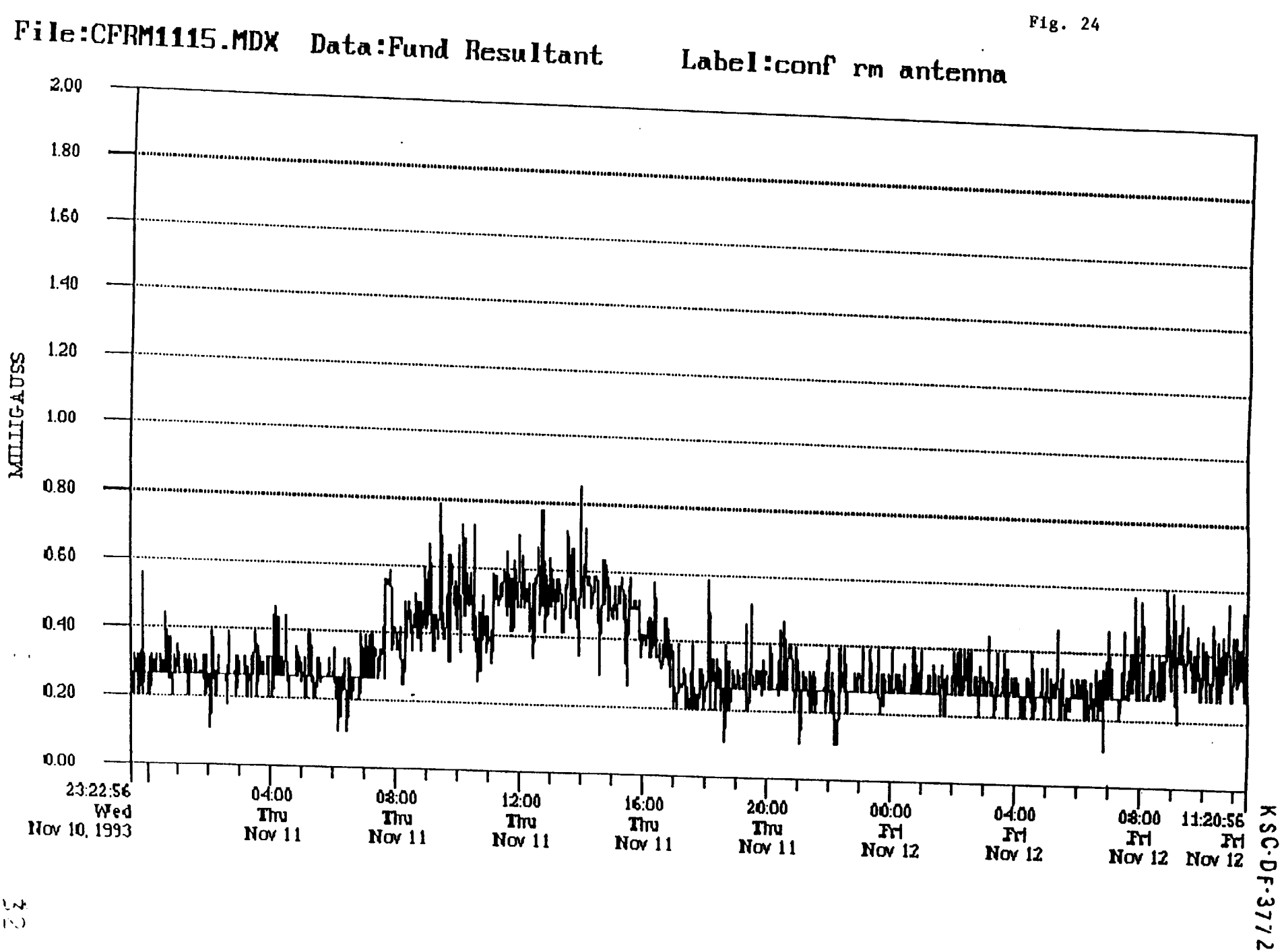

KSC-DF-3772

Fig. 25

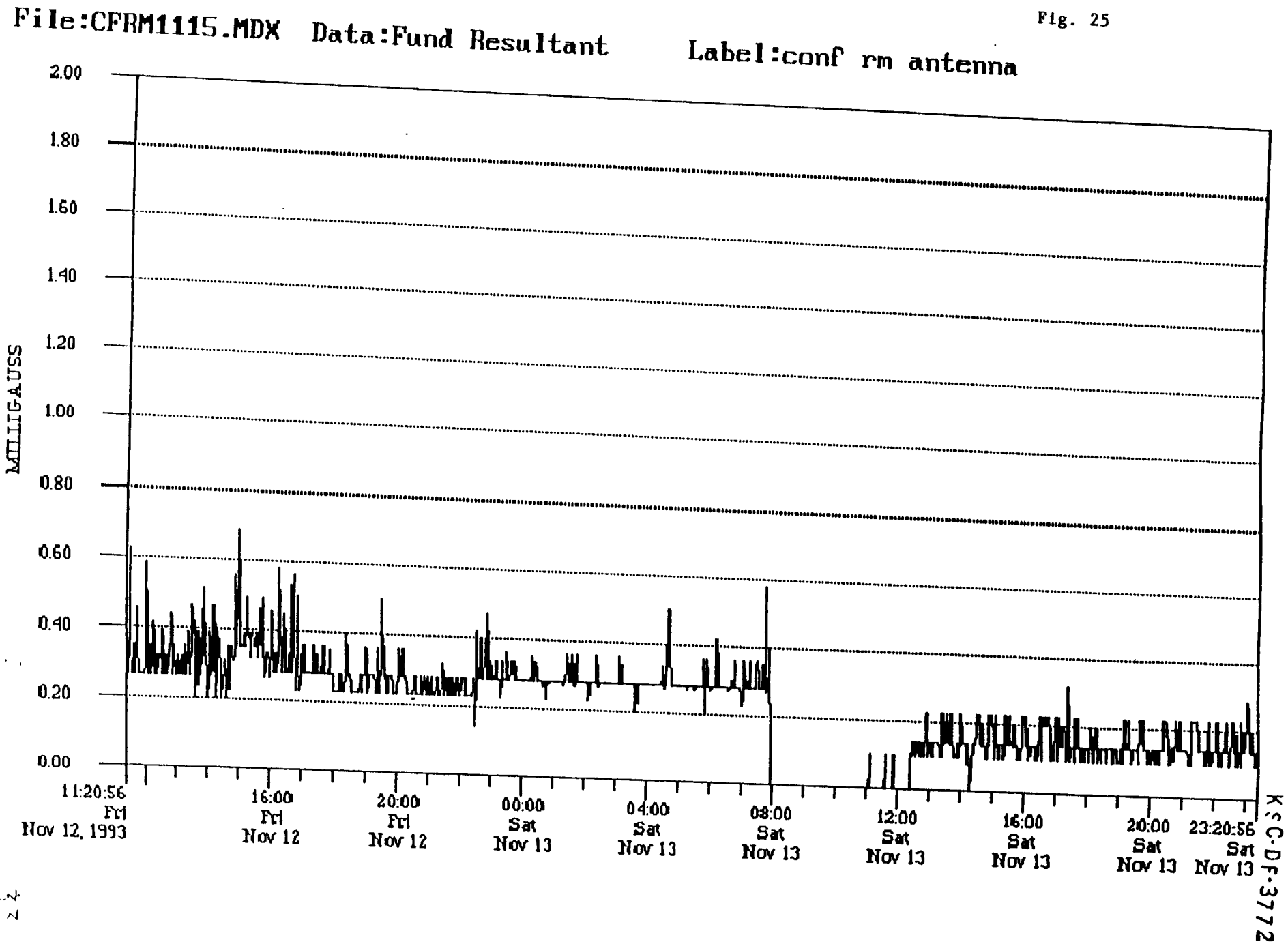
File:CFRM1115.MDX Data:Fund Resultant Label:conf rm antenna
MILLIGAUSS
2.00
1.80
1.60
1.40
1.20
1.00
0.80
0.60
0.40
0.20
0.00
11:20:56 Fri Nov 12, 1993
16:00 Fri Nov 12
20:00 Fri Nov 12
00:00 Sat Nov 13
04:00 Sat Nov 13
08:00 Sat Nov 13
12:00 Sat Nov 13
16:00 Sat Nov 13
20:00 Sat Nov 13
23:20:56 Sat Nov 13
KSC-DF-3772

File:CFRM1115.MDX Data:Fund Resultant Label:conf rm antenna

Fig. 26

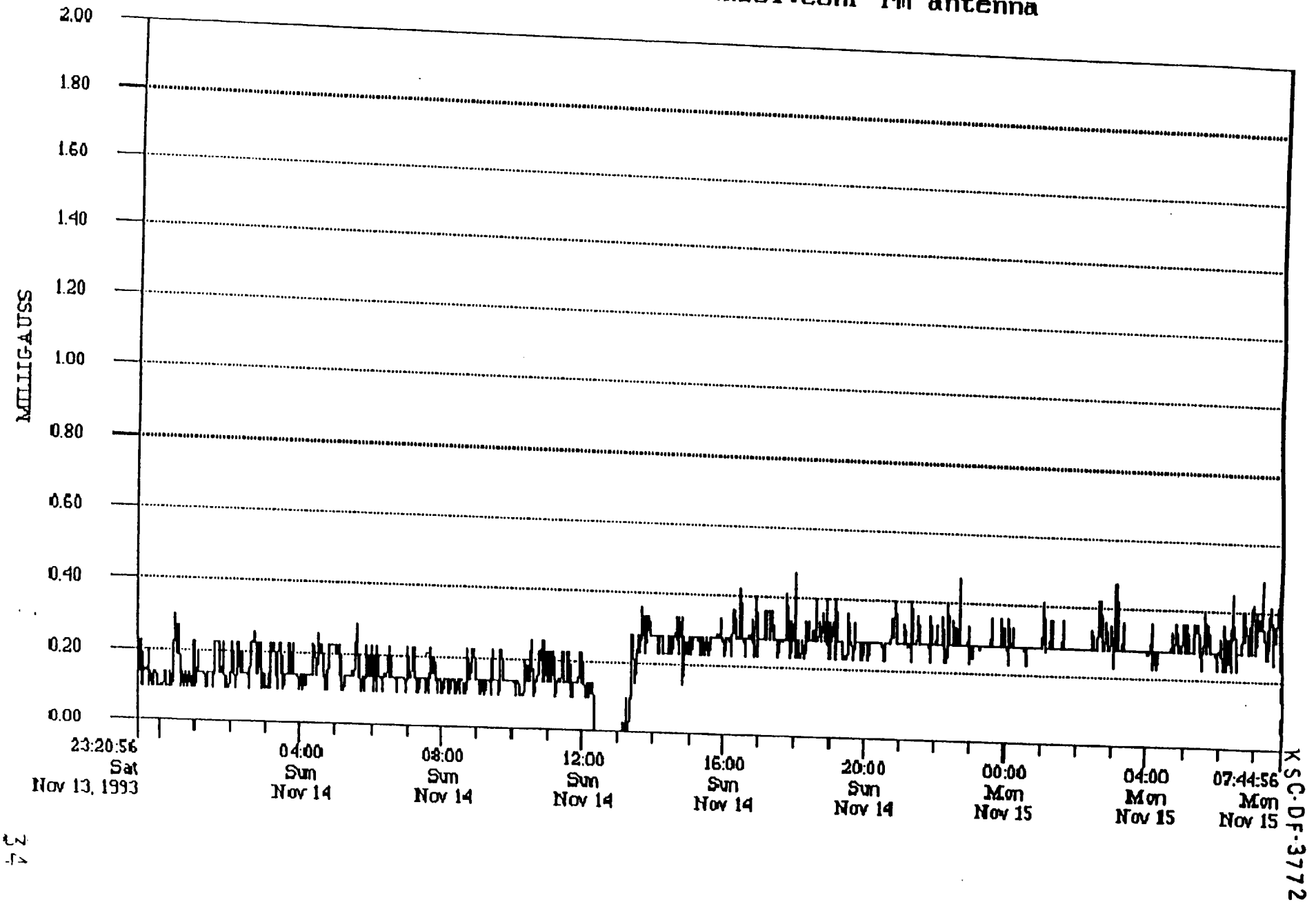

File:CFRM1115.MDX Data:Harm Resultant Label:conf rm antenna

Fig. 27

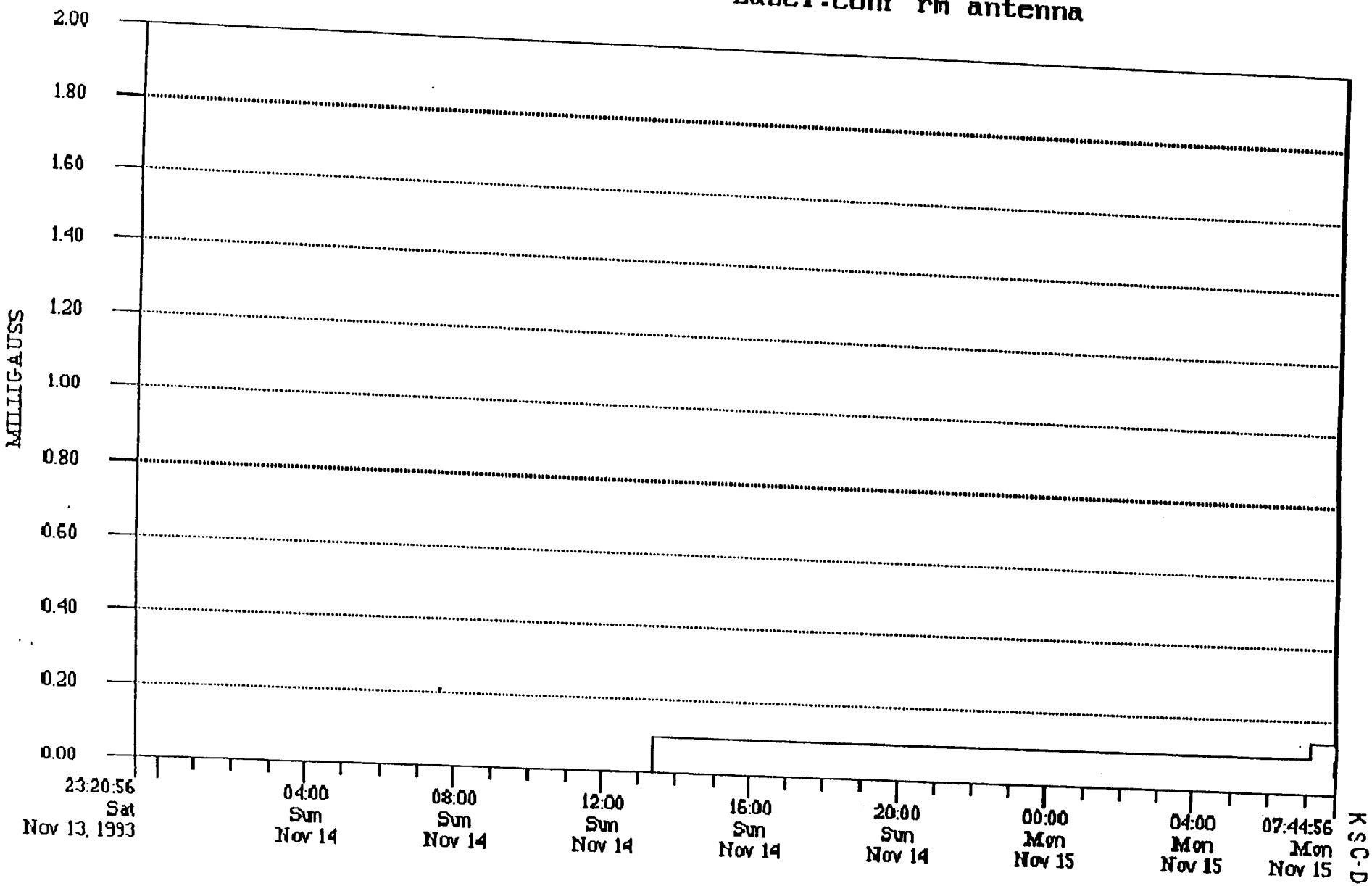

KSC-DF-3772

Fig. 28

File:CFRM1115.MDX Data:Harm Resultant Label:conf rm antenna

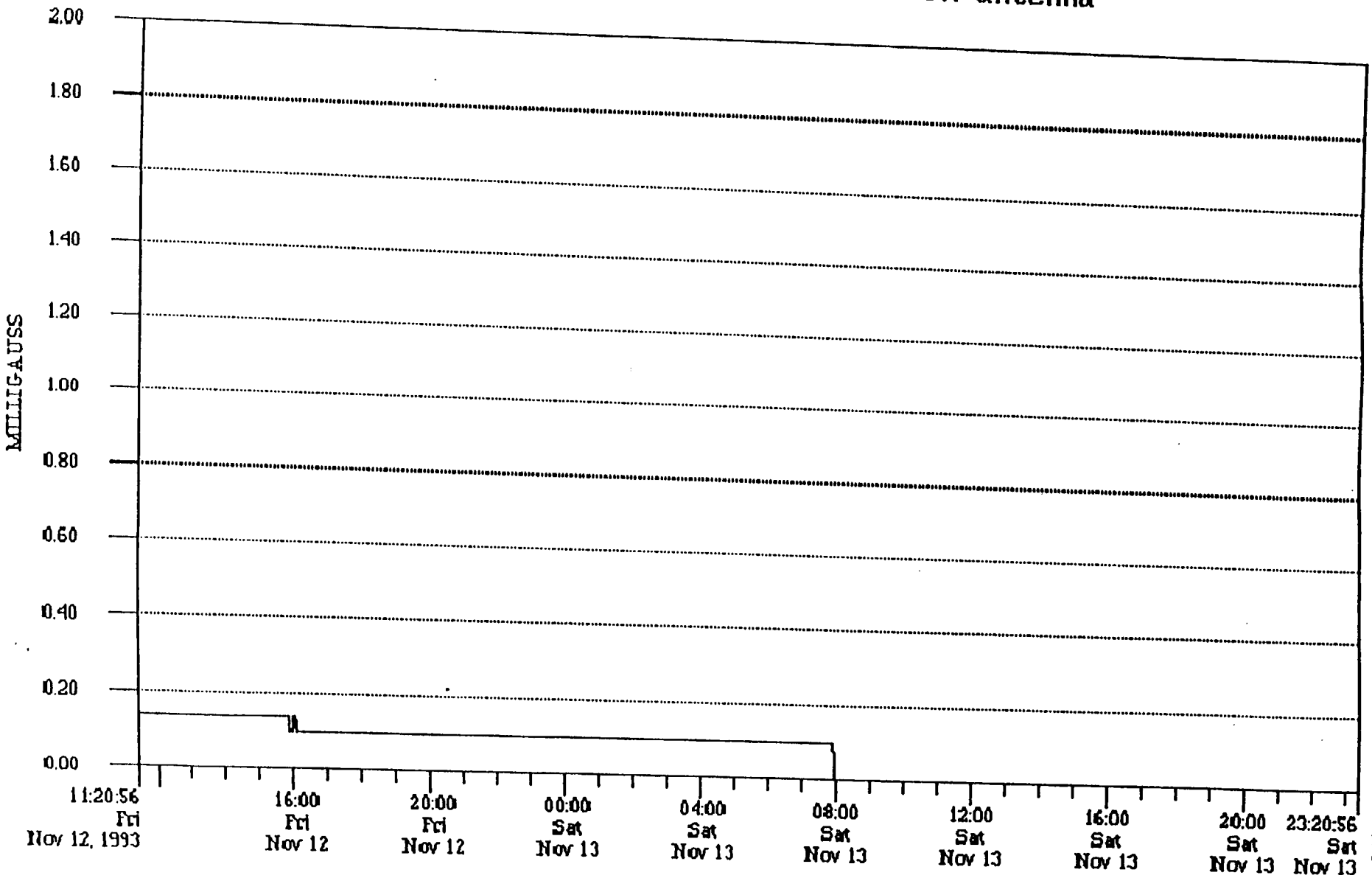

File:CFRM1115.MDX Data:Harm Resultant Label:conf rm antenna

Fig. 29

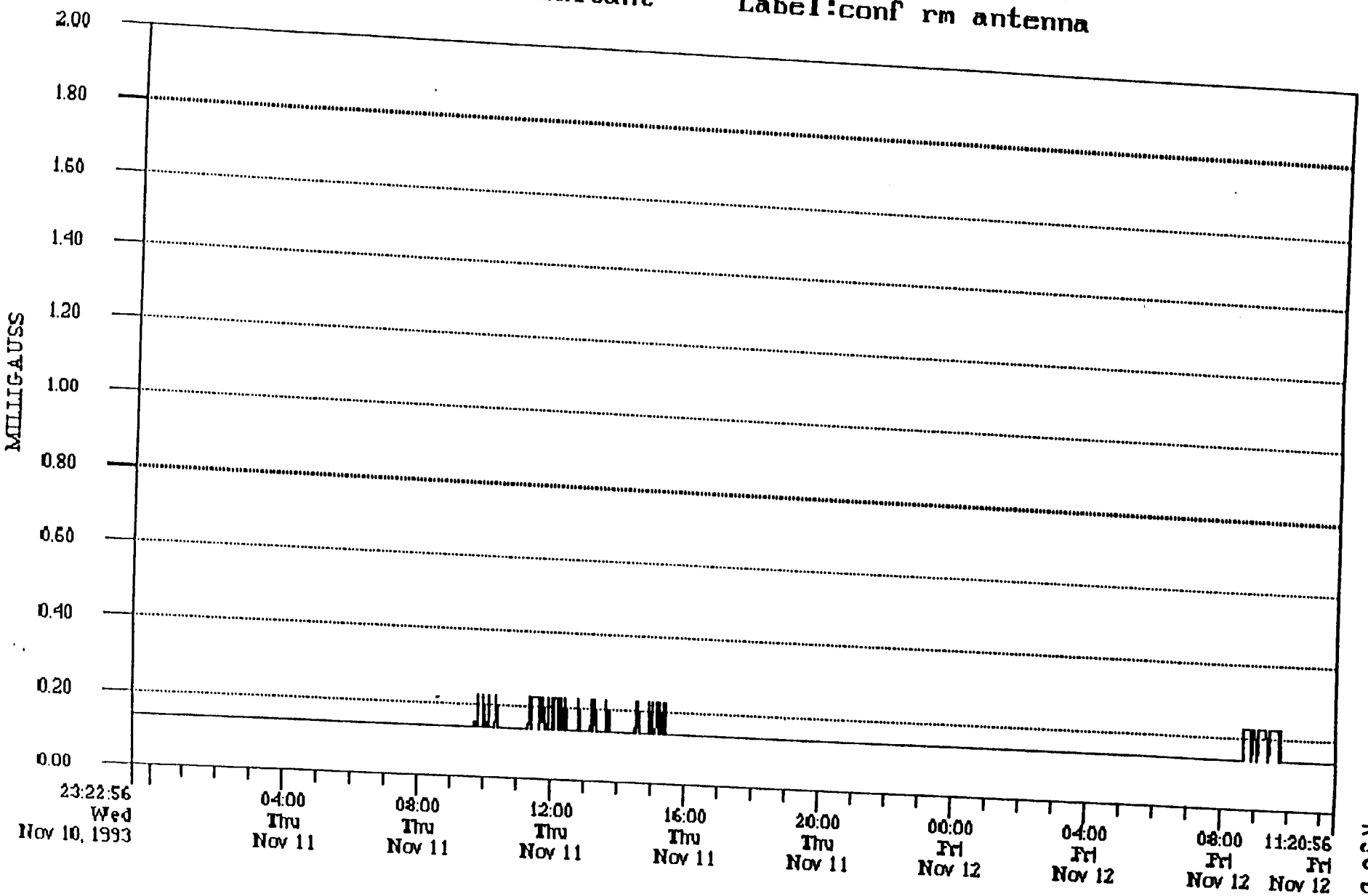

KSC-DF-3772

Fig. 30

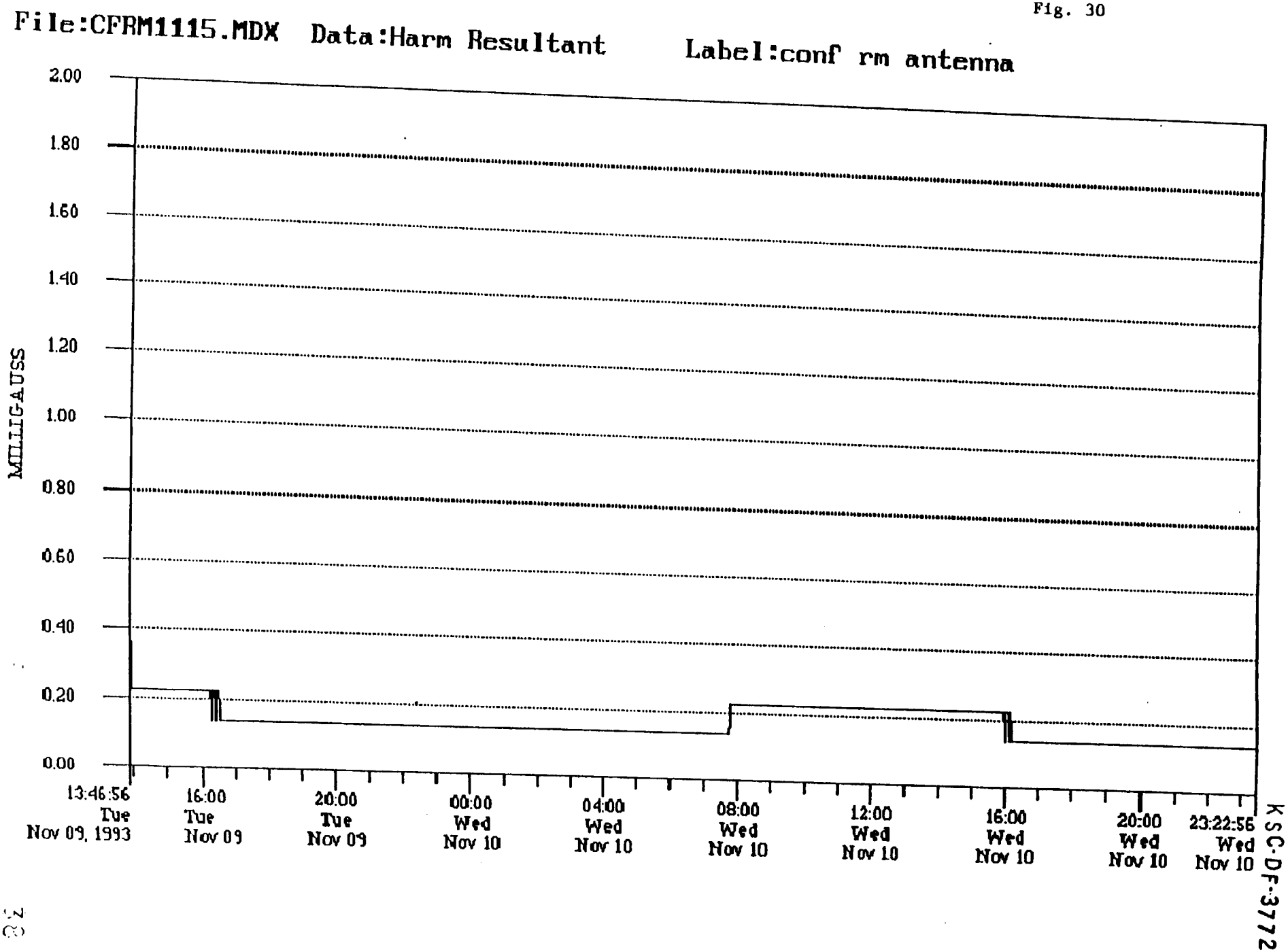
File:CFRM1115.MDX Data:Harm Resultant Label:conf rm antenna
MILLIGAUSS
2.00
1.80
1.60
1.40
1.20
1.00
0.80
0.60
0.40
0.20
0.00
13:46:56 Tue Nov 09, 1993
16:00 Tue Nov 09
20:00 Tue Nov 09
00:00 Wed Nov 10
04:00 Wed Nov 10
08:00 Wed Nov 10
12:00 Wed Nov 10
16:00 Wed Nov 10
20:00 Wed Nov 10
23:22:56 Wed Nov 10
KSC-DF-3772

Fig. 31

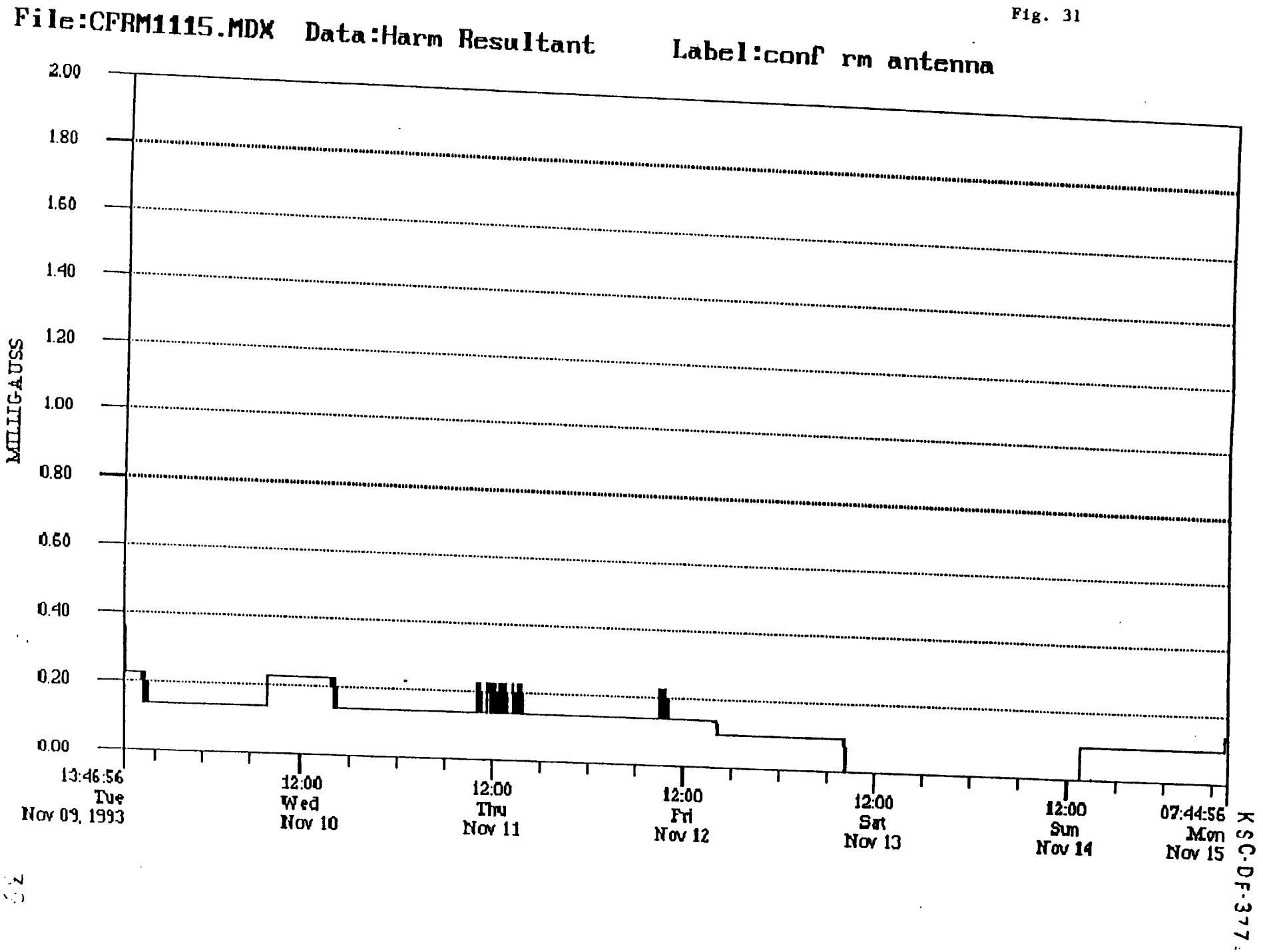
File:CFRM1115.MDX Data:Harm Resultant Label:conf rm antenna
2.00
1.80
1.60
1.40
1.20
1.00
0.80
0.60
0.40
0.20
0.00
MILLIGAUSS
13:46:56 Tue Nov 09, 1993
12:00 Wed Nov 10
12:00 Thu Nov 11
12:00 Fri Nov 12
12:00 Sat Nov 13
12:00 Sun Nov 14
07:44:56 Mon Nov 15
KSC-DF-377

3.4 Prototype Building

3.4.1 Measurements versus distance

A prototype building has been identified and a large number of measurements were taken in various locations of the building. Figures 32 through 37 depict the largest magnetic field levels observed in that building

From this group of measurements, the following locations in the prototype room recorded the highest magnetic field intensity levels:

1) Sub-station : about 27 mGauss

2) Lathe # 2 (running): about 19 mGauss

3) Office: (copier and fax place) - 8 mGauss

4) Conference room: about 7.2 mGauss

5) Drill # 1: about 6.0 mGauss

6) Office: (around a computer and a printer)- 3.3 mGauss

7) Walkway : about 0.8 mGauss

8) Supplies office: about 0.4 mGauss

9) Secretary area: 0.3 mGauss.

10) Lathe #1: west end: about 0.1 mGauss

11-13) Different paths for the same walkway : heighest about 1 mGauss

As expected the magnetic field level are high only in the vicinity of electrical equipment. Walkways, supply offices, and other spaces with no equipment at all exhibited very low levels of magnetic field.

Fig. 32

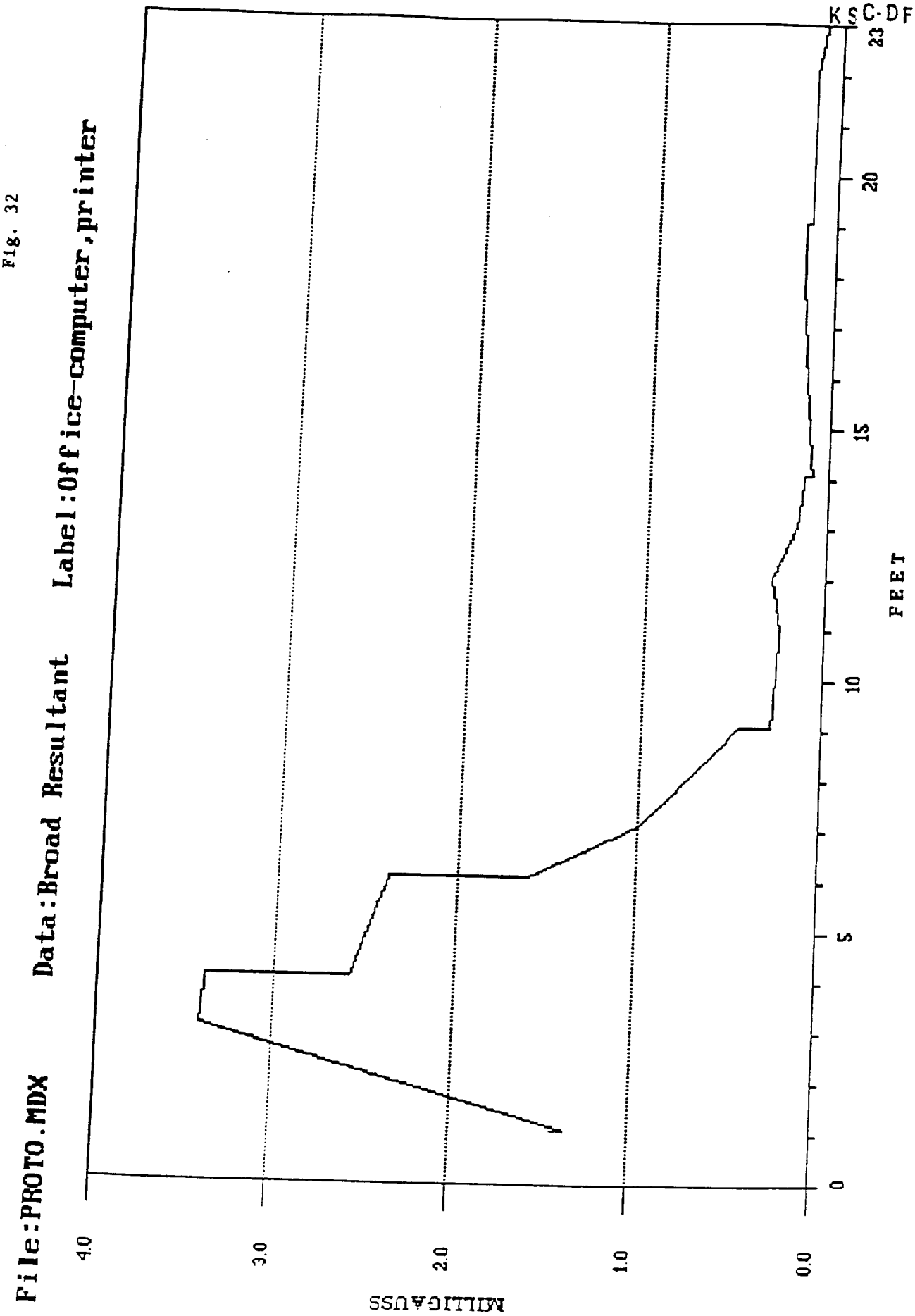
File:PROTO.MDX
Data:Broad Resultant
Label:Office-computer,printer
MILLIGAUSS
4.0
3.0
2.0
1.0
0.0
0
5
10
15
20
23
FEET

Fig. 33

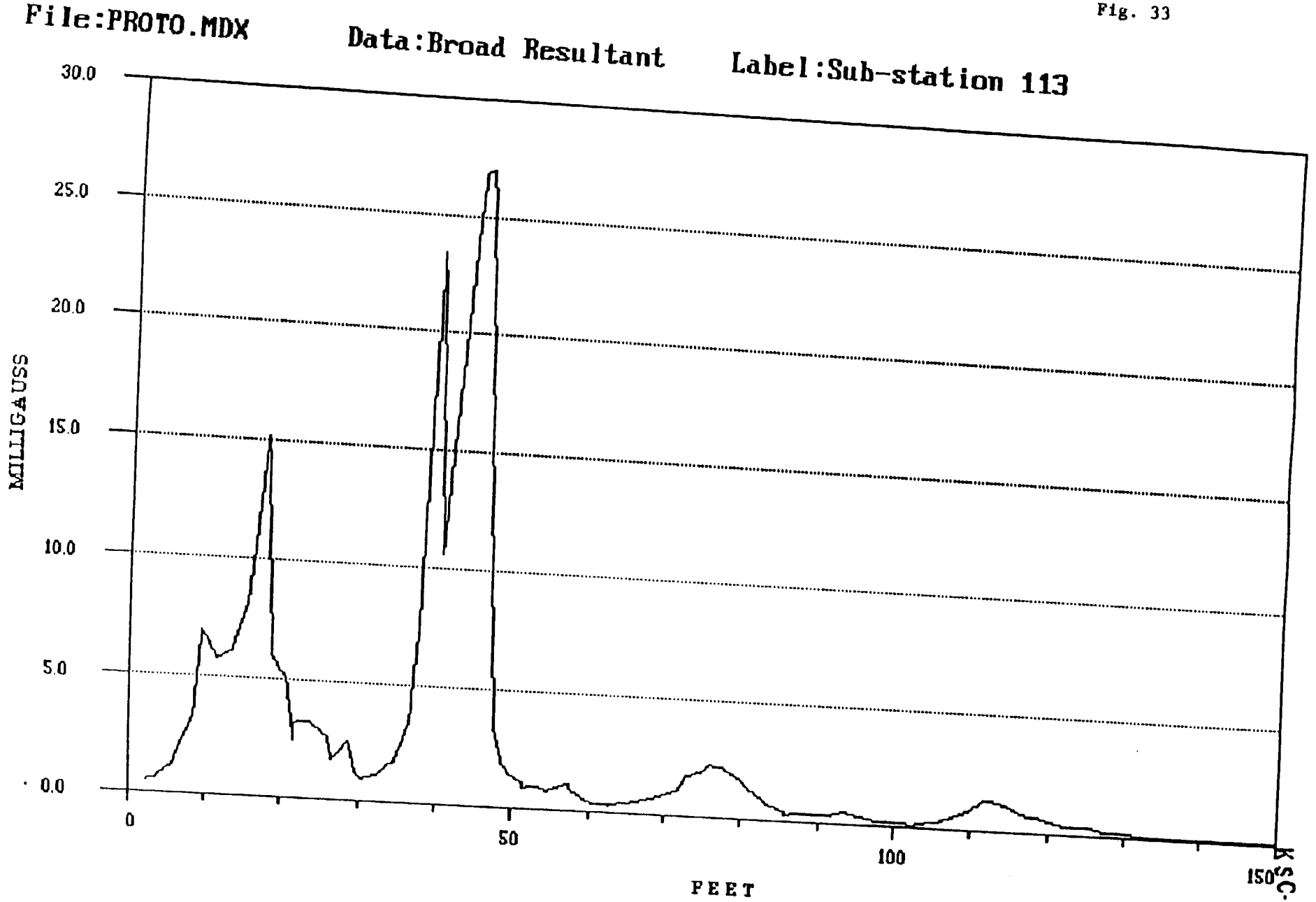

KSC-DF-377

Fig. 34

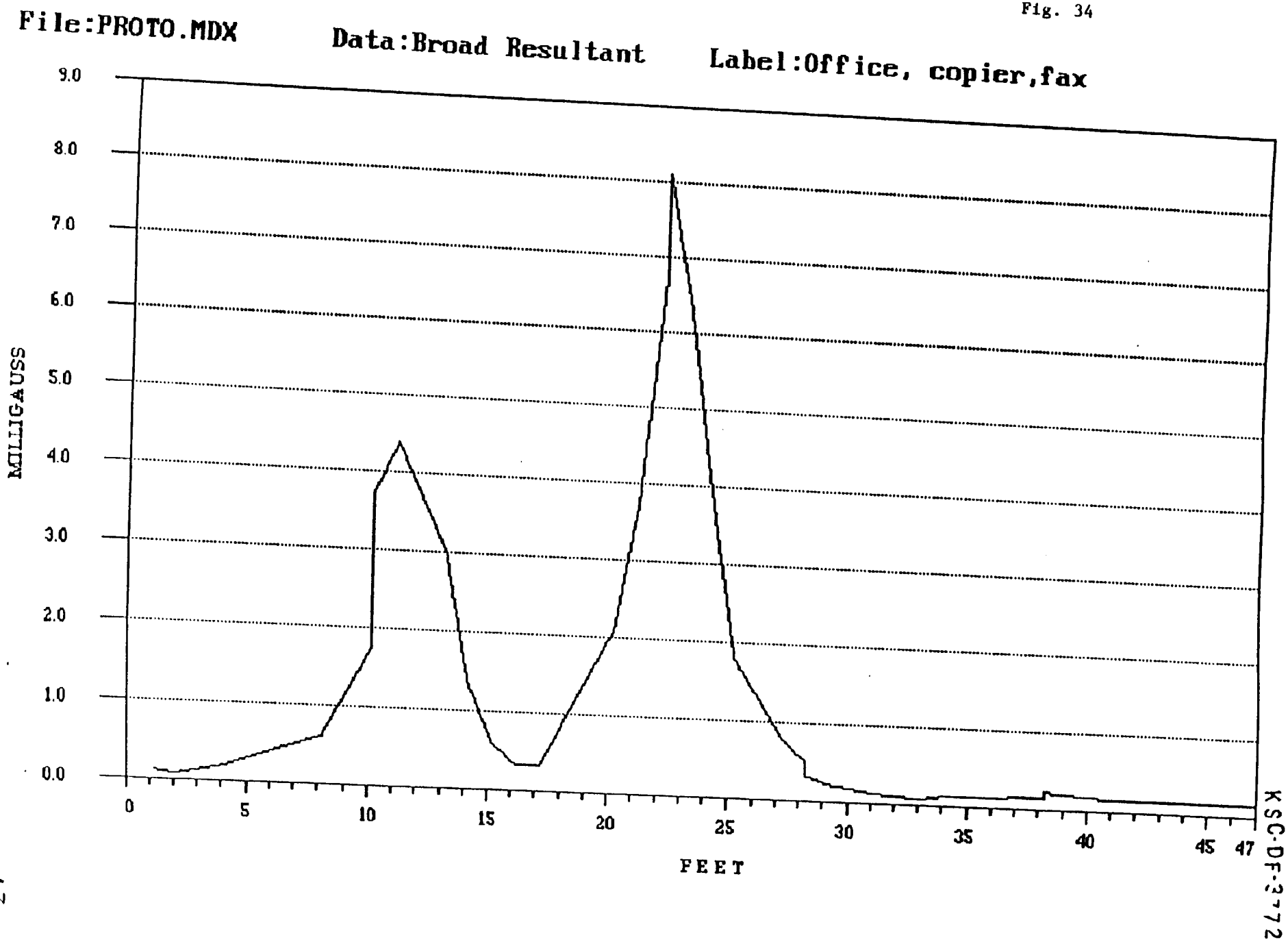
File:PROTO.MDX
Data:Broad Resultant
Label:Office, copier,fax
MILLIGAUSS
9.0
8.0
7.0
6.0
5.0
4.0
3.0
2.0
1.0
0.0
0
5
10
15
20
25
30
35
40
45
47
FEET
KSC-DF-3772

Fig. 35

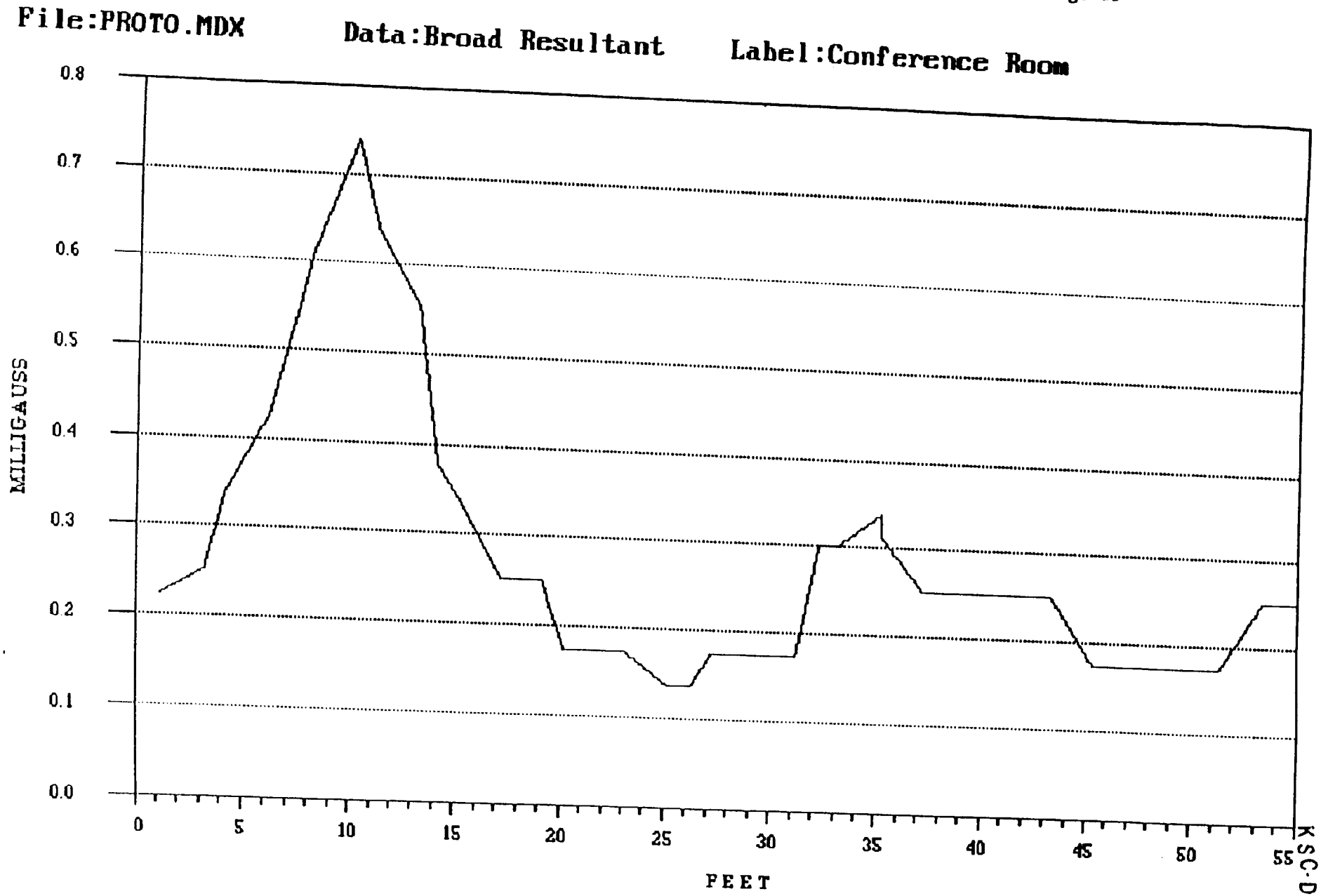
File:PROTO.MDX
Data:Broad Resultant
Label:Conference Room
0.8
0.7
0.6
0.5
0.4
0.3
0.2
0.1
0.0
MILLIGAUSS
0
5
10
15
20
25
30
35
40
45
50
55
FEET
KSC-DF-377

Fig. 36

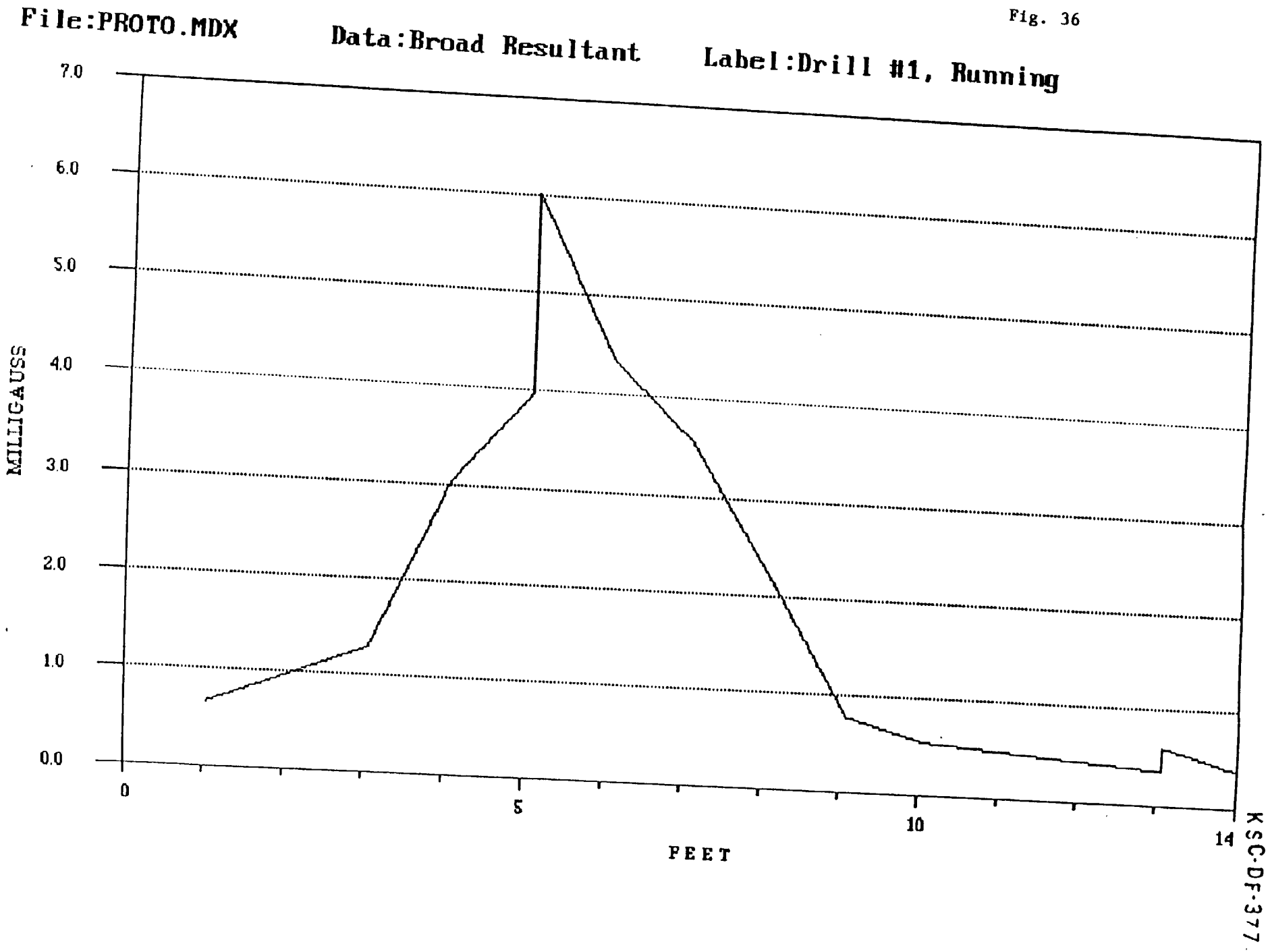
File:PROTO.MDX
Data:Broad Resultant
Label:Drill #1, Running
7.0
6.0
5.0
4.0
3.0
2.0
1.0
0.0
MILLIGAUSS
0
5
10
14
FEET
KSC-DF-377

Fig. 37

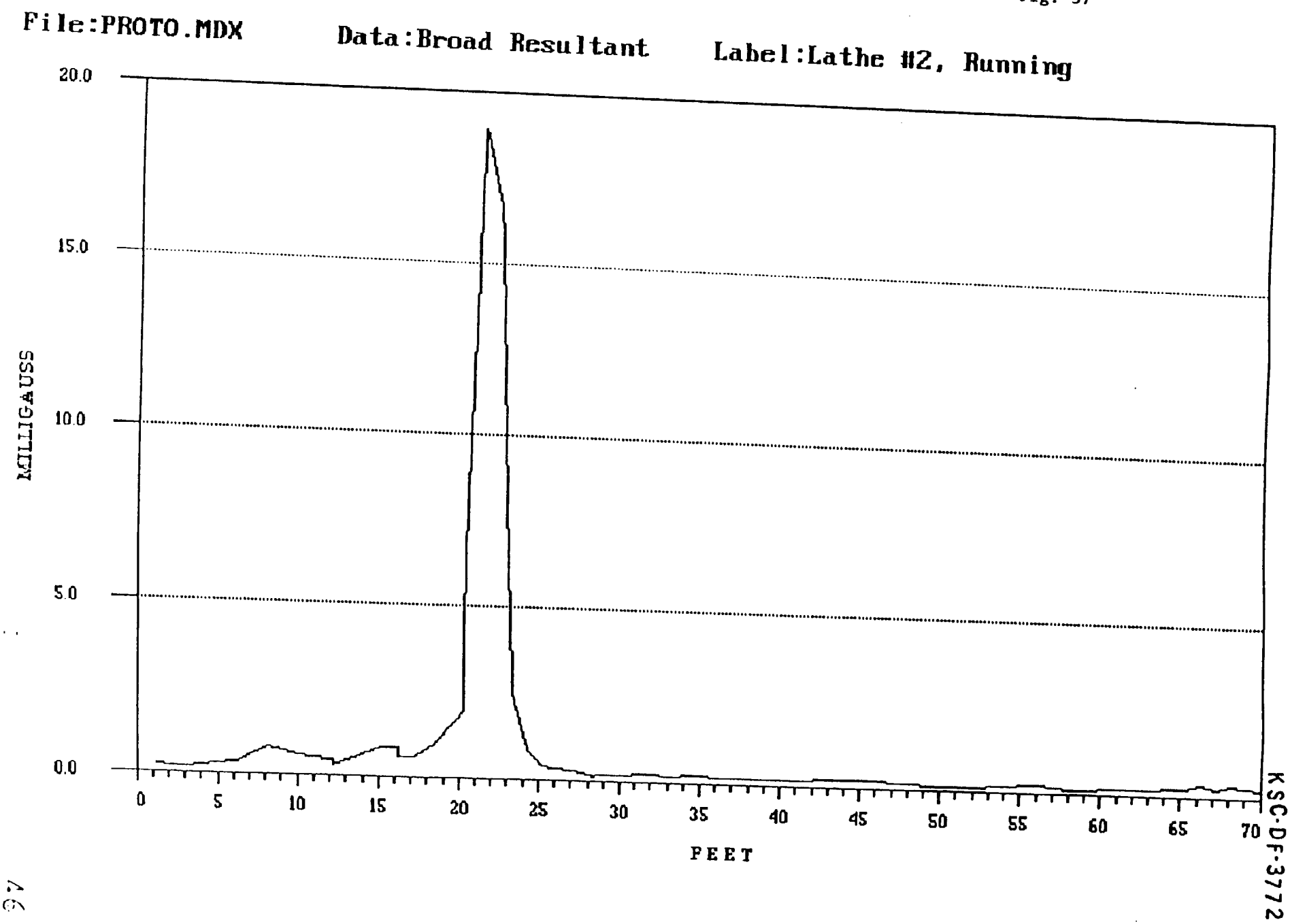
File:PROTO.MDX
Data:Broad Resultant
Label:Lathe #2, Running
20.0
15.0
10.0
5.0
0.0
MILLIGAUSS
0
5
10
15
20
25
30
35
40
45
50
55
60
65
70
FEET
KSC-DF-3772

3.4.2 Dependence of Results on the sensor location with respect to the source

Figures 38 through 58 depict measurements in different locations in the prototype building but as a function of time. Figures 38 through 52 show the magnetic field levels from lathes 1 and 2 in the building. The broadband, fundamental, and harmonic values are all shown. It can be seen that the magnetic fields due to the harmonic content was very small in all measurements.

Also, the location of the sensor with respect to the source was changed to see how different the levels would be for various locations. The results indicate that different values are observed for all different sensor locations in all lathe cases. In this group of measurements, tables with individual descriptive statistics were also included to indicate the minimum, maximum, mean values, and standard deviation values for the magnetic field intensities observed for each case. It is clear from the tables that the fields measured are totally due to the fundamental frequency and not any harmonics.

Next, 4 other items were tested for the generation of high magnetic field levels in the prototype building. These are :

1) The incoming power wiring unit - over 400 mGauss.

2) A disconnect panel and busway - over 100 mGauss.

3) A transformer vent - 2,000 mGauss.

4) A transformer - over 1,500 mGauss.

3.5 Ground Currents

We also looked into the problems that arise from various grounding practices. Since there are multiple connections for grounding purposes, currents can flow on different paths that include water pipes, TV cables, telephone lines etc. Magnetic fields generated by a pair of closely spaced wires tend to cancel each other but those produced

by currents on water pipes and other conductors do not. It is now known that high magnetic fields can be generated even from relatively small currents flowing on a pipe. That point can be simulated in the laboratory and analyzed to see if indeed one can avoid the generation of high magnetic fields by changing the grounding points. The understanding of that problem will enable researchers to make recommendation for various mitigation approaches. Measurements done in this area are included in the disks provided.

Fig. 38

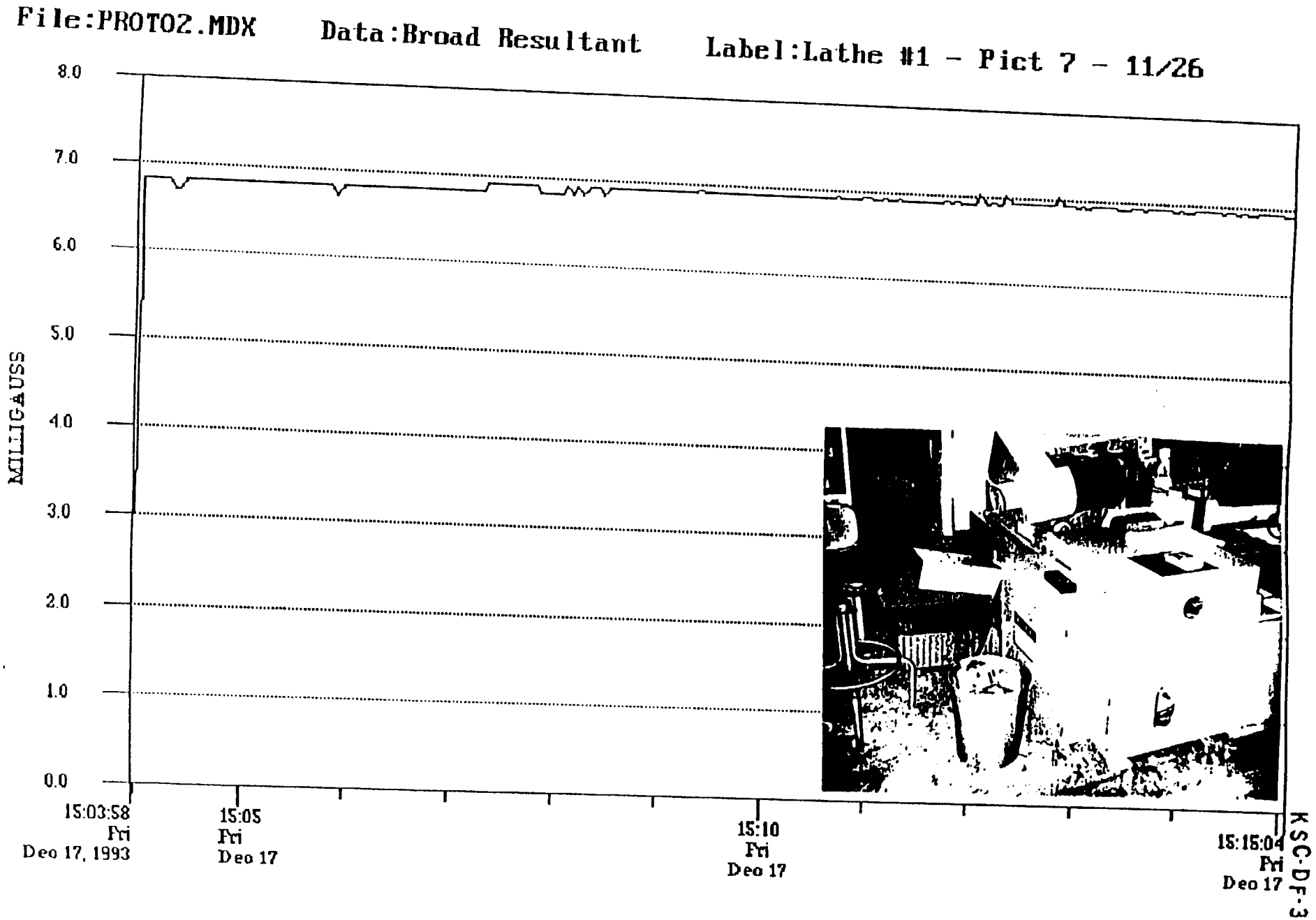

KSC-DF-3772

Fig. 39

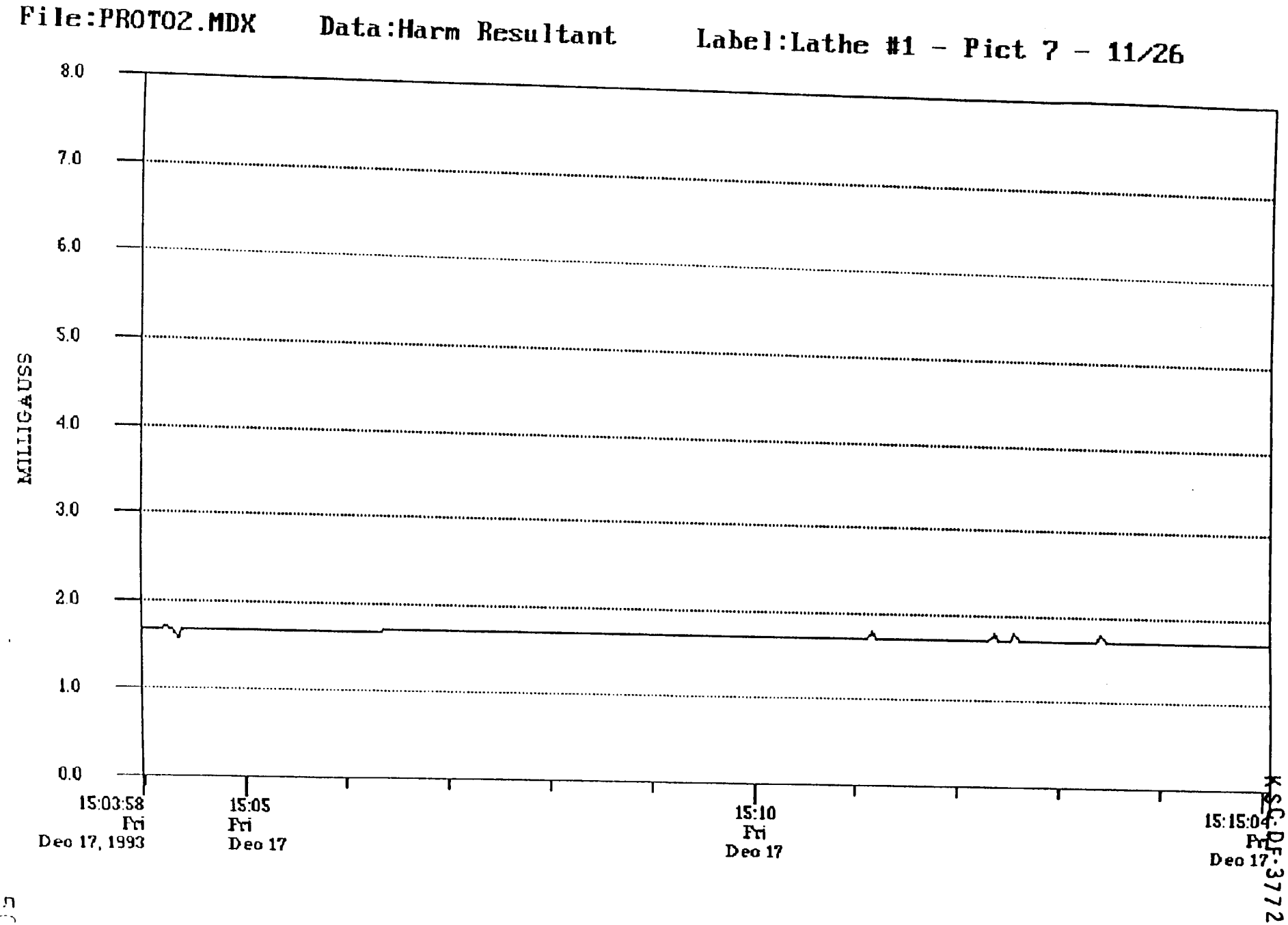
File:PROTO2.MDX
Data:Harm Resultant
Label:Lathe #1 - Pict 7 - 11/26
8.0
7.0
6.0
5.0
4.0
3.0
2.0
1.0
0.0
MILLIGAUSS
15:03:58
Fri
Deo 17, 1993
15:05
Fri
Deo 17
15:10
Fri
Deo 17
15:15:04
Fri
Deo 17
KSC-DF-3772

Fig. 40

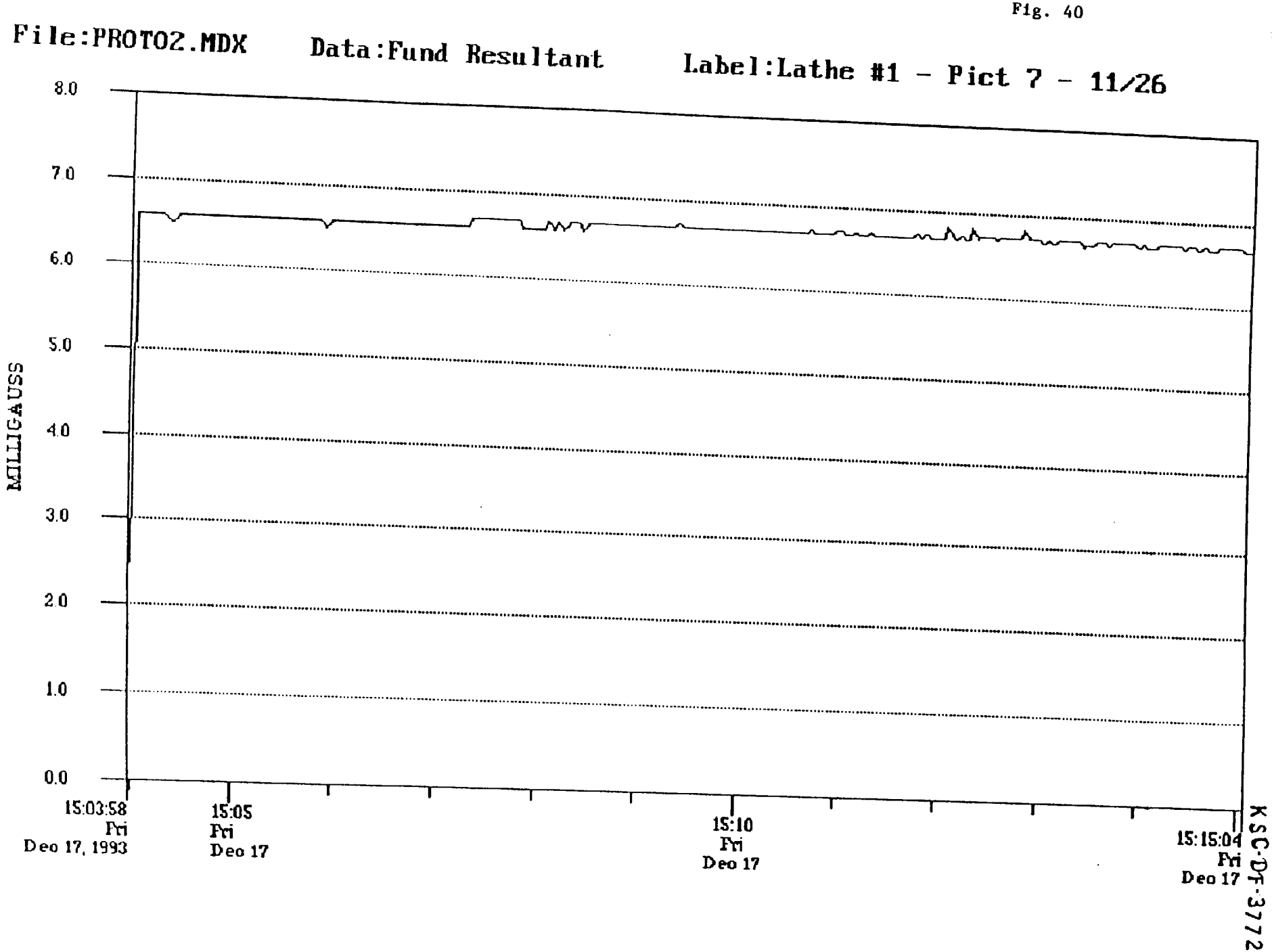
File:PROTO2.MDX
Data:Fund Resultant
Label:Lathe #1 - Pict 7 - 11/26
8.0
7.0
6.0
5.0
4.0
3.0
2.0
1.0
0.0
MILLIGAUSS
15:03:58
Fri
Dec 17, 1993
15:05
Fri
Dec 17
15:10
Fri
Dec 17
15:15:04
Fri
Dec 17
KSC-DF-3772

********** INDIVIDUAL ANALYSIS - NORMAL DESCRIPTIVE STATISTICS **********

Data File : C:\EMCALC21\PROTO2.MDX
Data Set Label : Lathe #1 - Pict 7 - 11/26
Data Set Number: 6
Data Set Start : Dec/17/93 15:03:58
Data Set Stop : Dec/17/93 15:15:04
Observations : 223

	Min	Max	Mean	Std Dev	Median
Broadband					
Result (mG)	3.02	7.02	6.86	0.26	6.89
X (mG)	0.21	6.61	6.44	0.42	6.51
Y (mG)	0.91	1.81	0.91	0.06	0.91
Z (mG)	2.11	2.41	2.13	0.05	2.11
Fundamental					
Result (mG)	2.51	6.81	6.63	0.28	6.67
X (mG)	0.01	6.41	6.24	0.42	6.31
Y (mG)	0.88	1.79	0.89	0.06	0.88
Z (mG)	2.02	2.36	2.05	0.05	2.02
Harmonic					
Result (mG)	1.59	1.82	1.72	0.02	1.73
X (mG)	1.51	1.71	1.61	0.01	1.61
Y (mG)	0.21	0.21	0.21	0.00	0.21
Z (mG)	0.51	0.61	0.59	0.04	0.61

Fig. 41

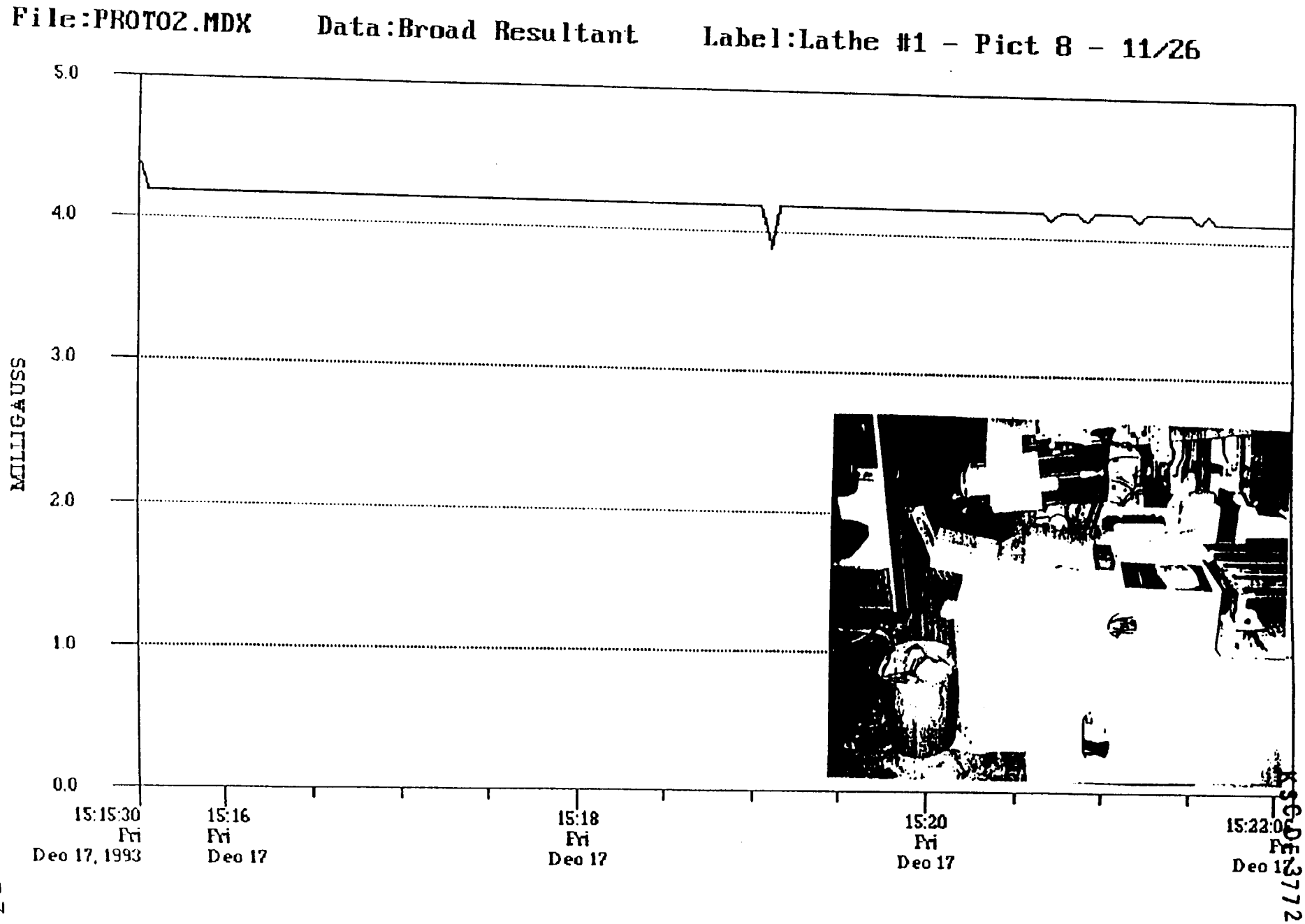

KSC-DE-3772

Fig. 42

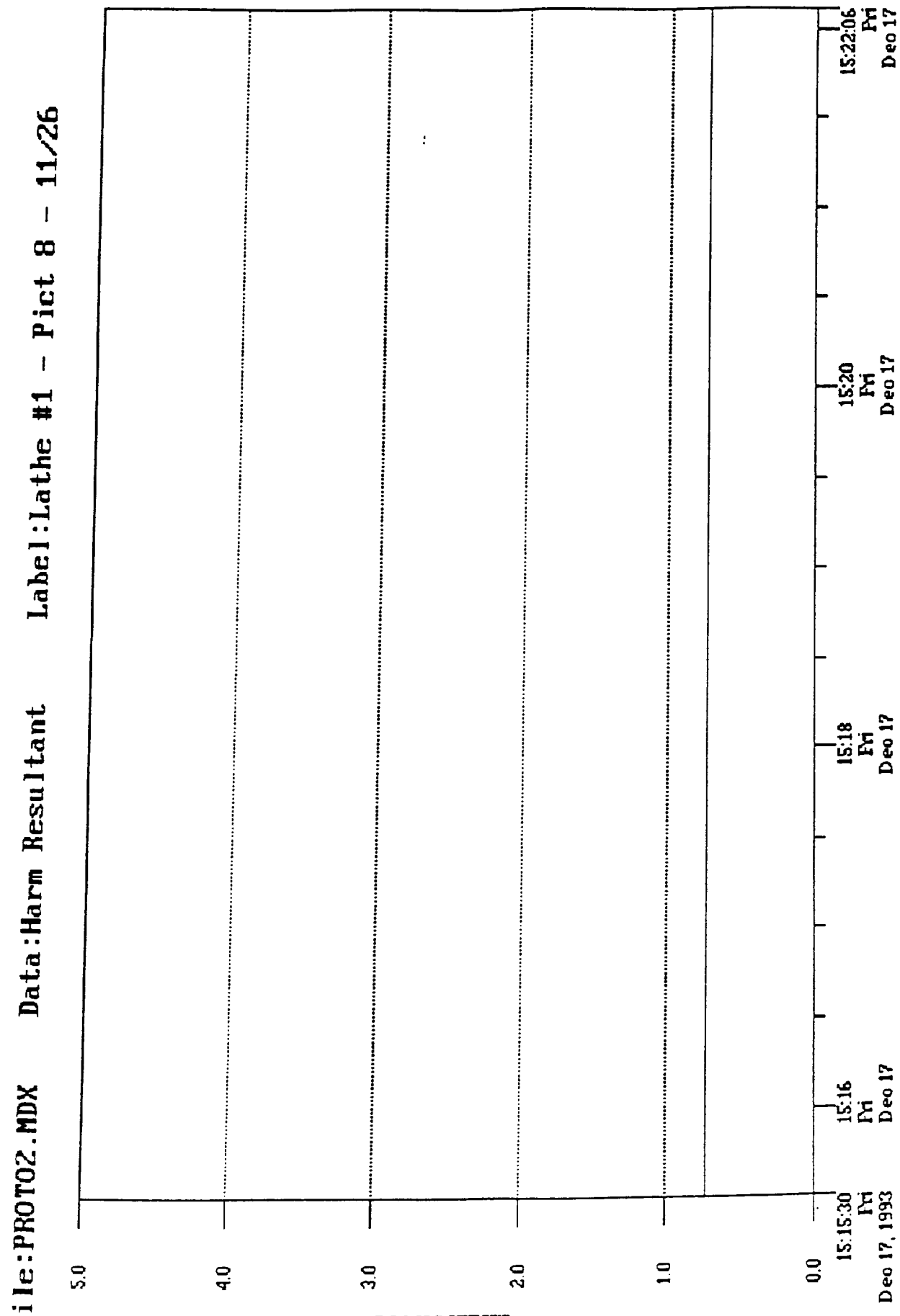
File:PROTO2.MDX
Data:Harm Resultant
Label:Lathe #1 - Pict 8 - 11/26
MILLIGAUSS
5.0
4.0
3.0
2.0
1.0
0.0
15:15:30 Fri Dec 17, 1993
15:16 Fri Dec 17
15:18 Fri Dec 17
15:20 Fri Dec 17
15:22:06 Fri Dec 17

Fig. 43

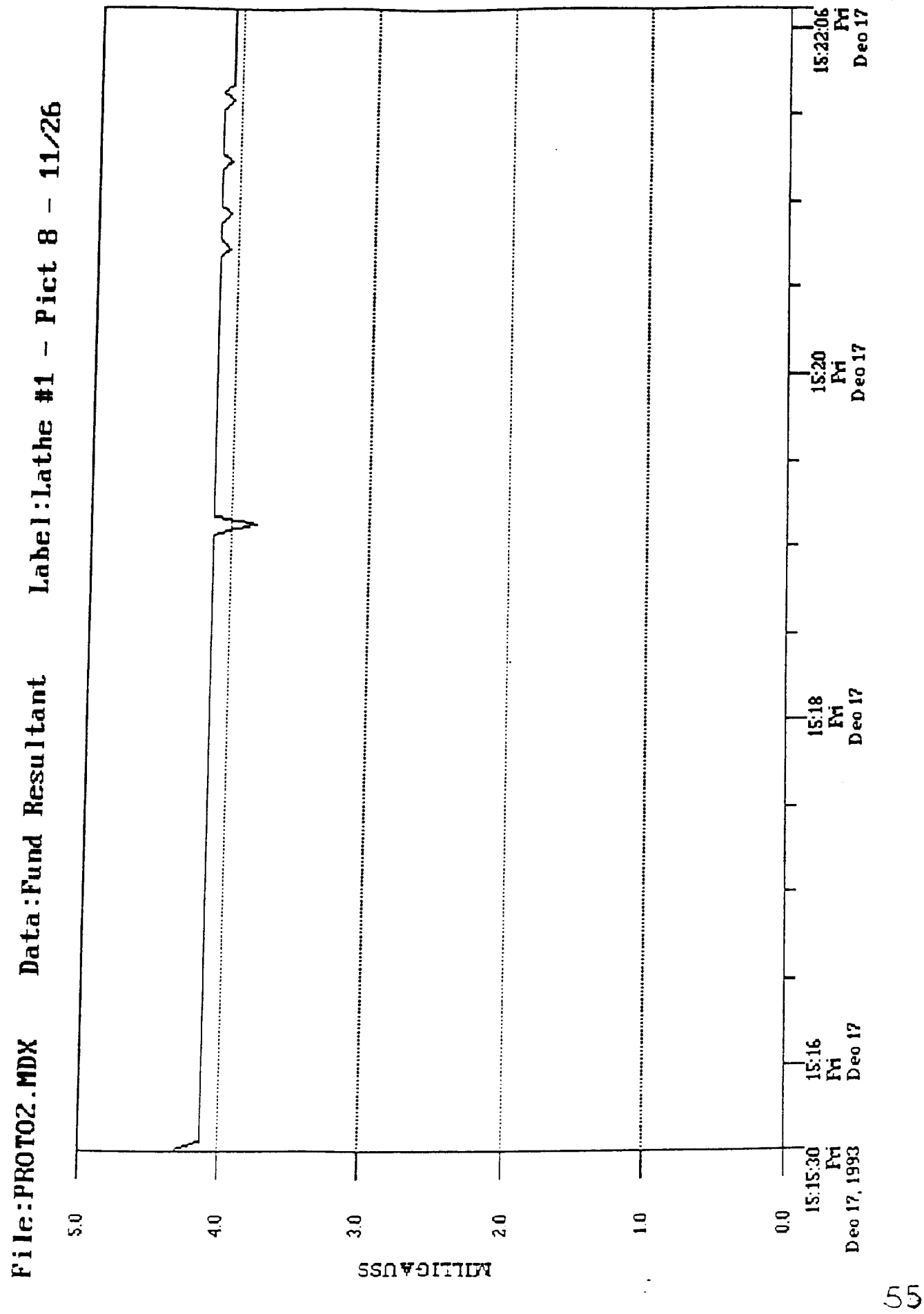
File:PROTO2.MDX Data:Fund Resultant Label:Lathe #1 - Pict 8 - 11/26
MILLIGAUSS
5.0
4.0
3.0
2.0
1.0
0.0
15:15:30 Fri Dec 17, 1993
15:16 Fri Dec 17
15:18 Fri Dec 17
15:20 Fri Dec 17
15:22:06 Fri Dec 17

********** INDIVIDUAL ANALYSIS - NORMAL DESCRIPTIVE STATISTICS **********

Data File : C:\EMCALC21\PROTO2.MDX
Data Set Label : Lathe #1 - Pict 8 - 11/26
Data Set Number: 7
Data Set Start : Dec/17/93 15:15:30
Data Set Stop : Dec/17/93 15:22:06
Observations : 133

	Min	Max	Mean	Std Dev	Median
Broadband					
Result (mG)	3.89	4.37	4.19	0.04	4.19
X (mG)	2.31	2.81	2.50	0.04	2.51
Y (mG)	0.51	0.61	0.60	0.01	0.61
Z (mG)	3.11	3.31	3.30	0.02	3.31
Fundamental					
Result (mG)	3.82	4.31	4.12	0.04	4.13
X (mG)	2.26	2.76	2.45	0.04	2.46
Y (mG)	0.47	0.57	0.57	0.01	0.57
Z (mG)	3.07	3.27	3.27	0.02	3.27
Harmonic					
Result (mG)	0.74	0.74	0.74	0.00	0.74
X (mG)	0.51	0.51	0.51	0.00	0.51
Y (mG)	0.21	0.21	0.21	0.00	0.21
Z (mG)	0.51	0.51	0.51	0.00	0.51

Fig. 44

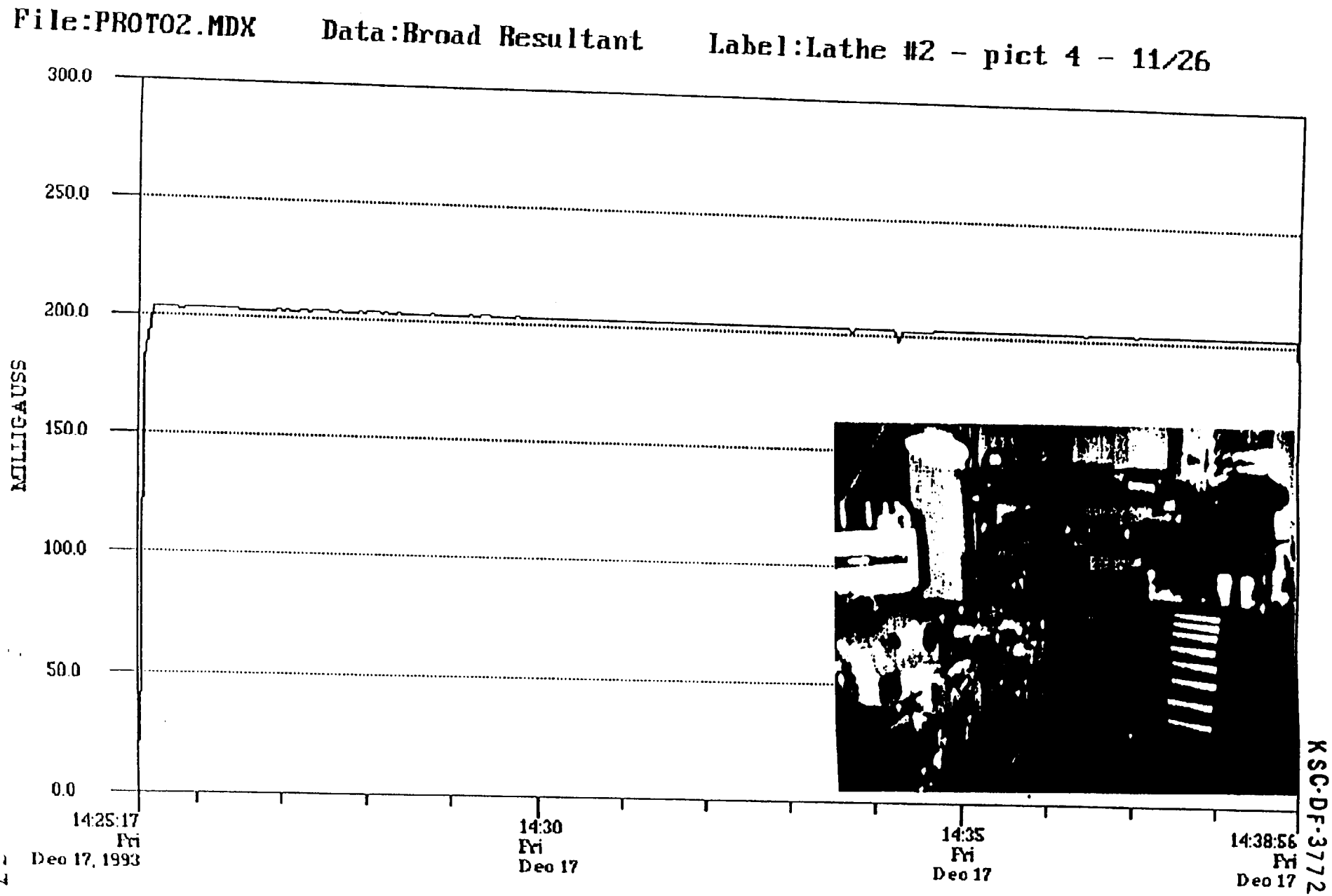
File:PROTO2.MDX
Data:Broad Resultant
Label:Lathe #2 - pict 4 - 11/26
300.0
250.0
200.0
150.0
100.0
50.0
0.0
MILLIGAUSS
14:25:17
Fri
Dec 17, 1993
14:30
Fri
Dec 17
14:35
Fri
Dec 17
14:38:56
Fri
Dec 17
KSC-DF-3772

Fig. 45

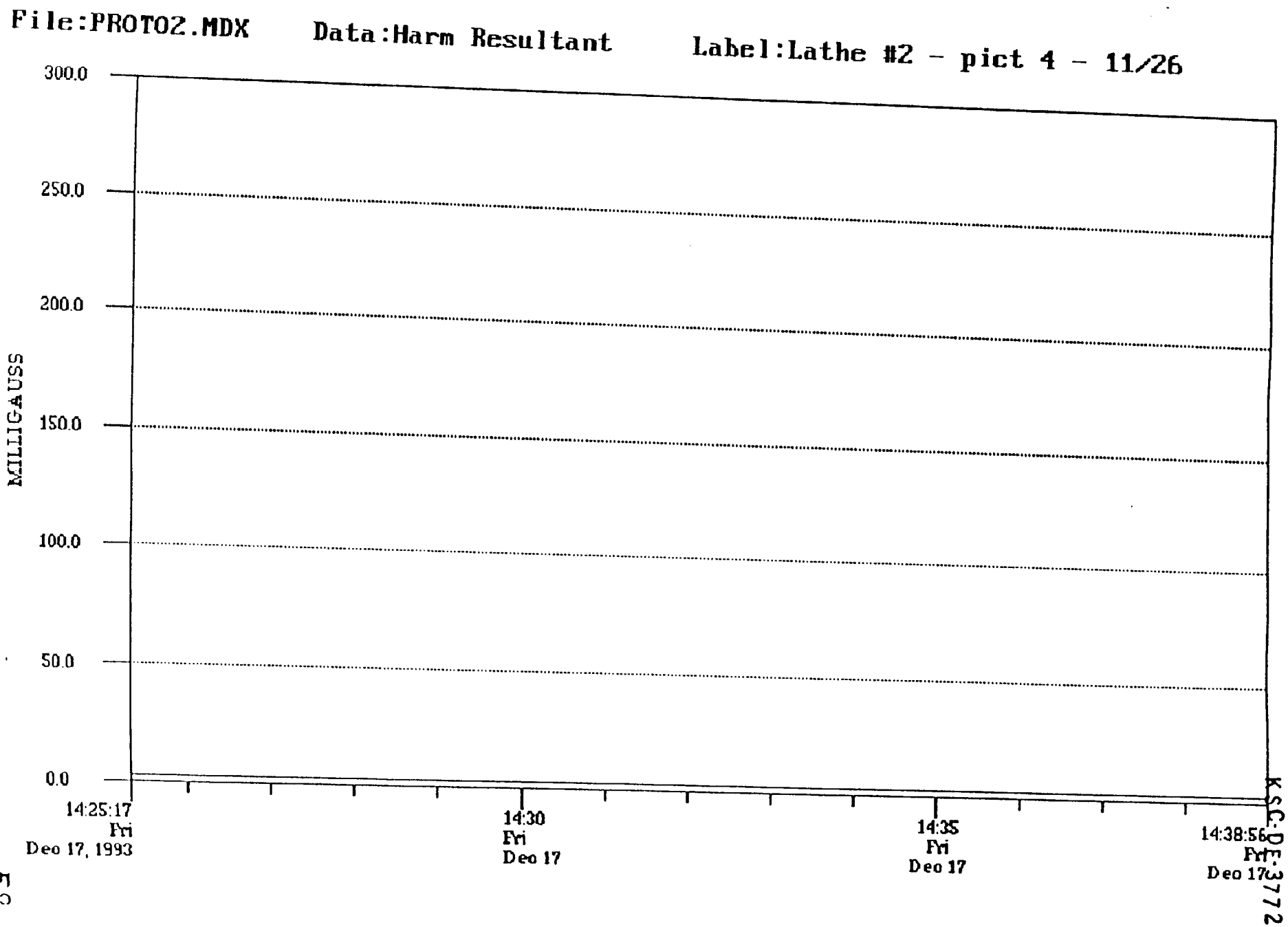
File:PROTO2.MDX
Data:Harm Resultant
Label:Lathe #2 - pict 4 - 11/26
300.0
250.0
200.0
150.0
100.0
50.0
0.0
MILLIGAUSS
14:25:17
Fri
Dec 17, 1993
14:30
Fri
Dec 17
14:35
Fri
Dec 17
14:38:56
Fri
Dec 17
KSC-DE-3772

Fig. 46

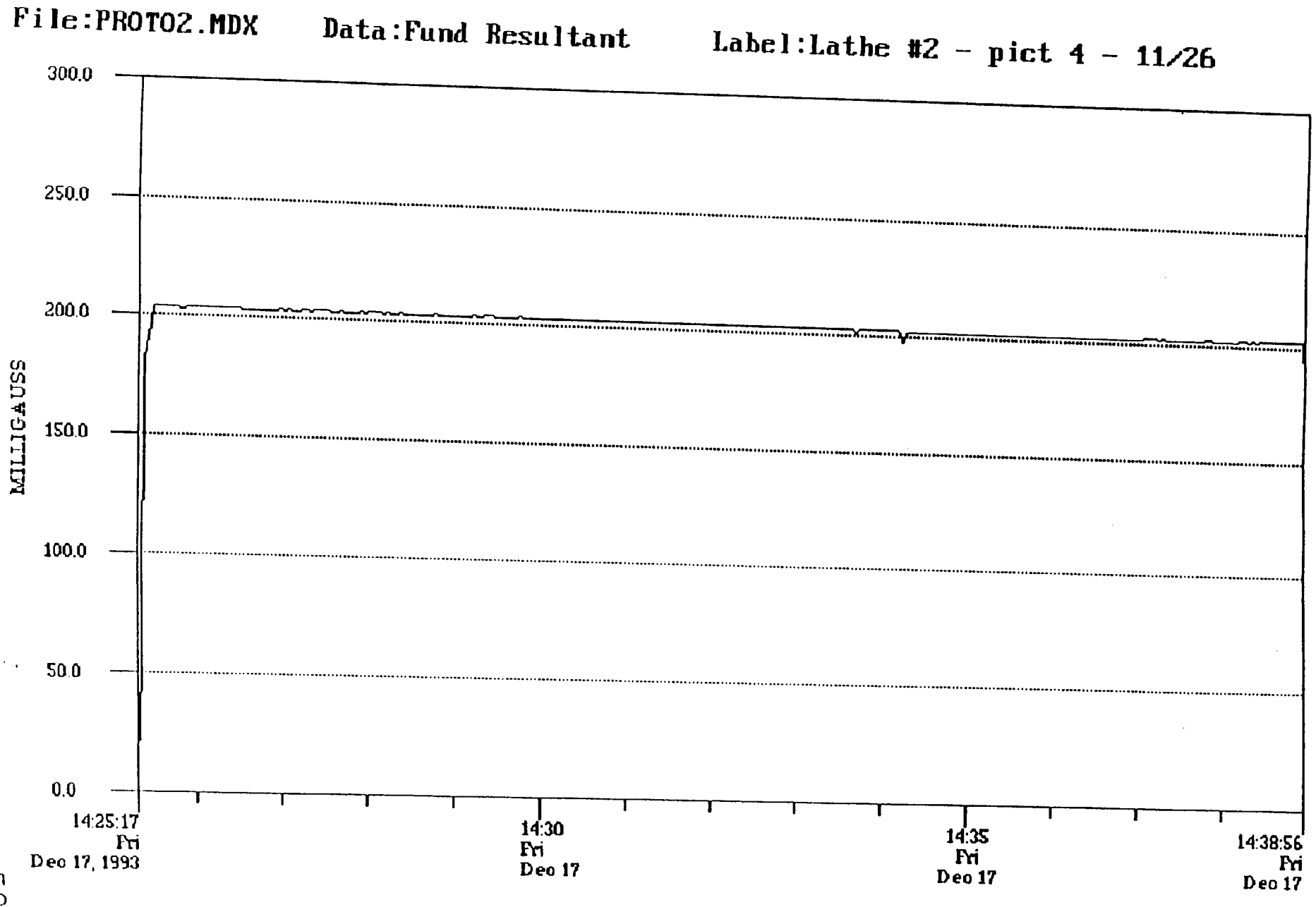

KSC-DF-3772

********** INDIVIDUAL ANALYSIS - NORMAL DESCRIPTIVE STATISTICS **********

Data File : C:\EMCALC21\PROTO2.MDX
Data Set Label : Lathe #2 - Pict 4 - 11/26
Data Set Number: 3
Data Set Start : Dec/17/93 14:25:17
Data Set Stop : Dec/17/93 14:38:56
Observations : 274

	Min	Max	Mean	Std Dev	Median
Broadband					
Result (mG)	22.01	203.30	201.52	11.65	202.50
X (mG)	4.50	12.71	7.14	0.39	7.11
Y (mG)	12.71	160.90	159.51	11.53	160.50
Z (mG)	12.71	132.10	122.88	6.92	123.30
Fundamental					
Result (mG)	21.82	203.30	201.52	11.66	202.50
X (mG)	4.50	12.69	7.14	0.39	7.11
Y (mG)	12.49	160.90	159.51	11.54	160.50
Z (mG)	12.61	132.10	122.88	6.92	123.30
Harmonic					
Result (mG)	1.10	3.10	3.04	0.15	3.09
X (mG)	0.50	0.70	0.64	0.09	0.71
Y (mG)	1.10	2.50	2.32	0.10	2.31
Z (mG)	0.30	1.90	1.89	0.10	1.91

Fig. 47

File:PROTO2.MDX Data:Broad Resultant Label:Lathe #2 - Pict 5 - 11/26

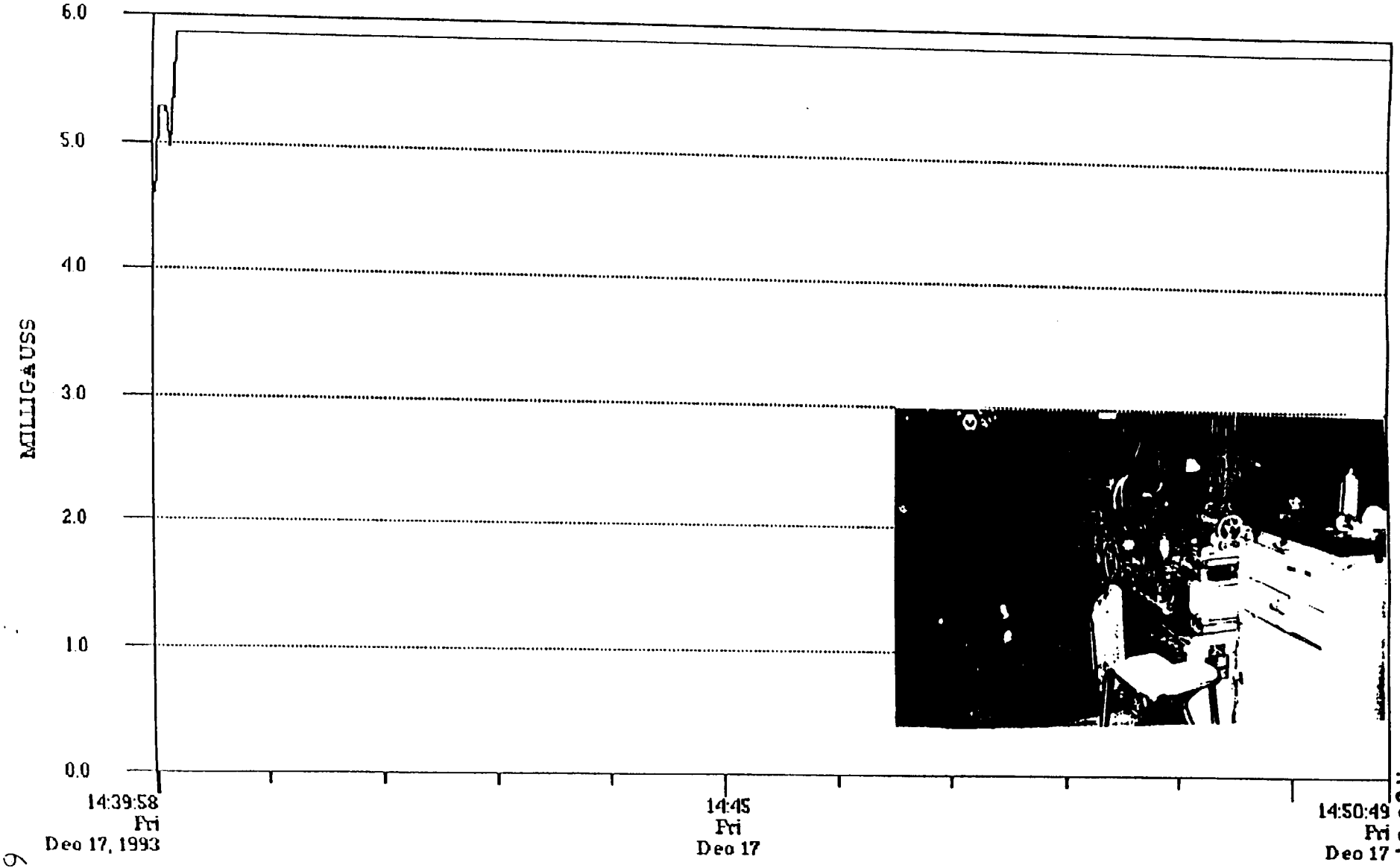

KSC-DF-3772

Fig. 48

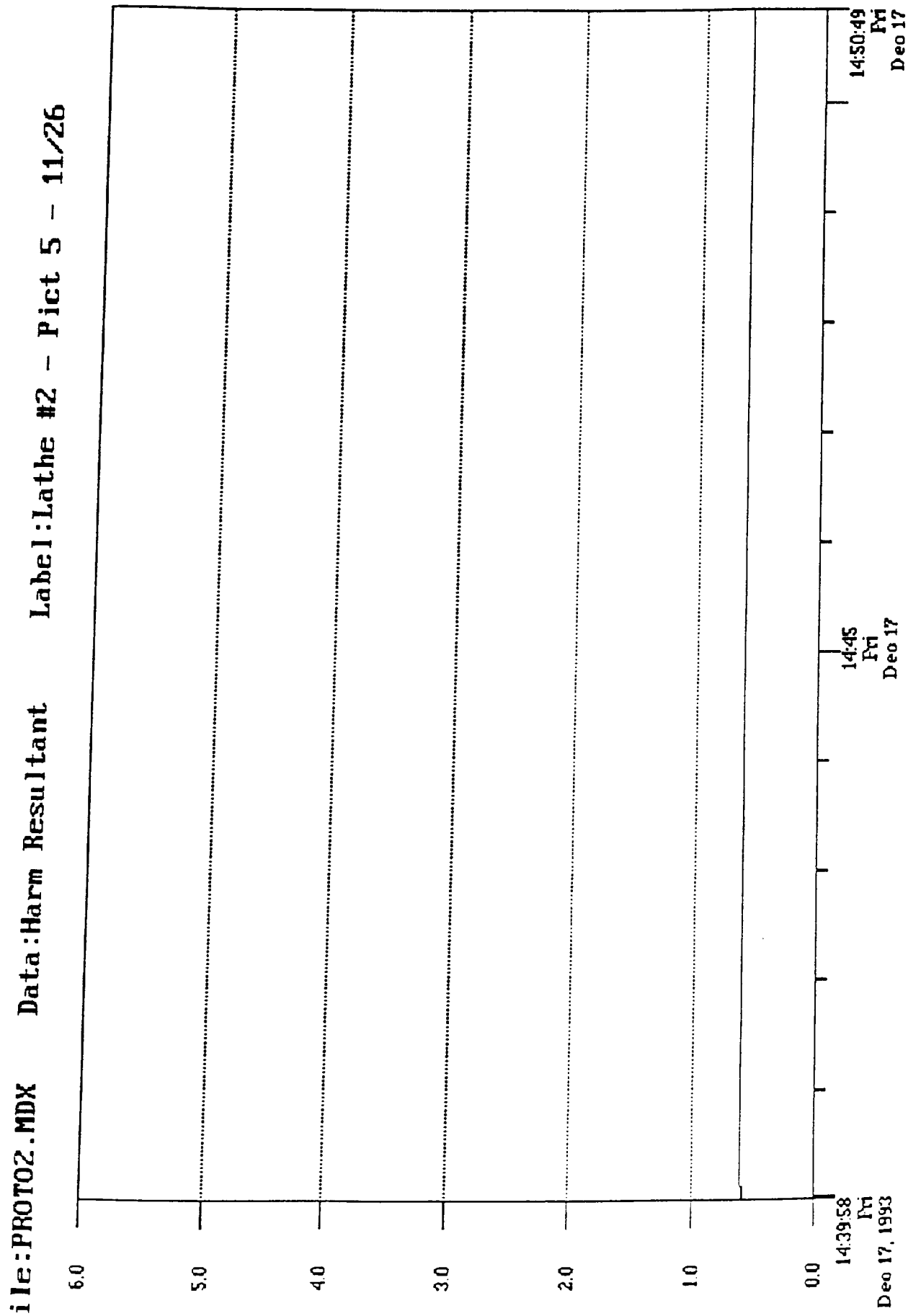
File:PROTO2.MDX
Data:Harm Resultant
Label:Lathe #2 - Pict 5 - 11/26
MILLIGAUSS
6.0
5.0
4.0
3.0
2.0
1.0
0.0
14:39:58 Fri Dec 17, 1993
14:45 Fri Dec 17
14:50:49 Fri Dec 17

Fig. 49

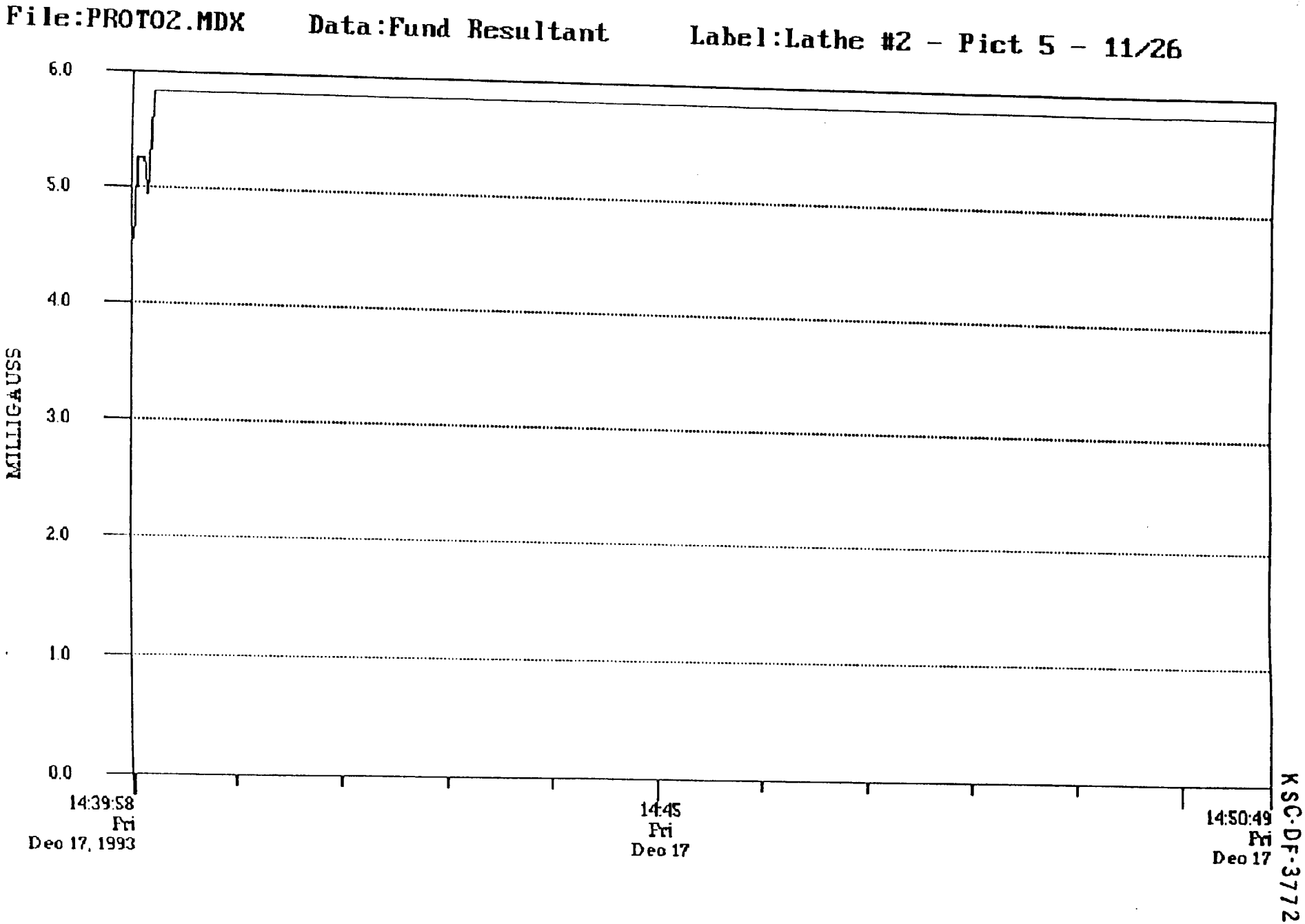
File:PROTO2.MDX
Data:Fund Resultant
Label:Lathe #2 - Pict 5 - 11/26
6.0
5.0
4.0
3.0
2.0
1.0
0.0
MILLIGAUSS
14:39:58
Fri
Dec 17, 1993
14:45
Fri
Dec 17
14:50:49
Fri
Dec 17
KSC-DF-3772

********** INDIVIDUAL ANALYSIS - NORMAL DESCRIPTIVE STATISTICS **********

Data File : C:\EMCALC21\PROTO2.MDX
Data Set Label : Lathe #2 - Pict 5 - 11/26
Data Set Number: 4
Data Set Start : Dec/17/93 14:39:58
Data Set Stop : Dec/17/93 14:50:49
Observations : 218

	Min	Max	Mean	Std Dev	Median
Broadband					
Result (mG)	4.59	5.86	5.84	0.12	5.86
X (mG)	2.11	4.41	4.38	0.22	4.41
Y (mG)	2.41	3.11	3.10	0.07	3.11
Z (mG)	2.31	3.31	2.32	0.12	2.31
Fundamental					
Result (mG)	4.56	5.82	5.80	0.12	5.82
X (mG)	2.07	4.38	4.35	0.22	4.38
Y (mG)	2.38	3.09	3.08	0.07	3.09
Z (mG)	2.29	3.29	2.31	0.12	2.29
Harmonic					
Result (mG)	0.59	0.62	0.62	0.00	0.62
X (mG)	0.41	0.51	0.50	0.01	0.51
Y (mG)	0.31	0.31	0.31	0.00	0.31
Z (mG)	0.21	0.31	0.21	0.01	0.21

Fig. 50

File:PROTO2.MDX Data:Broad Resultant Label:Lathe #2 - Pict 6 - 11/26

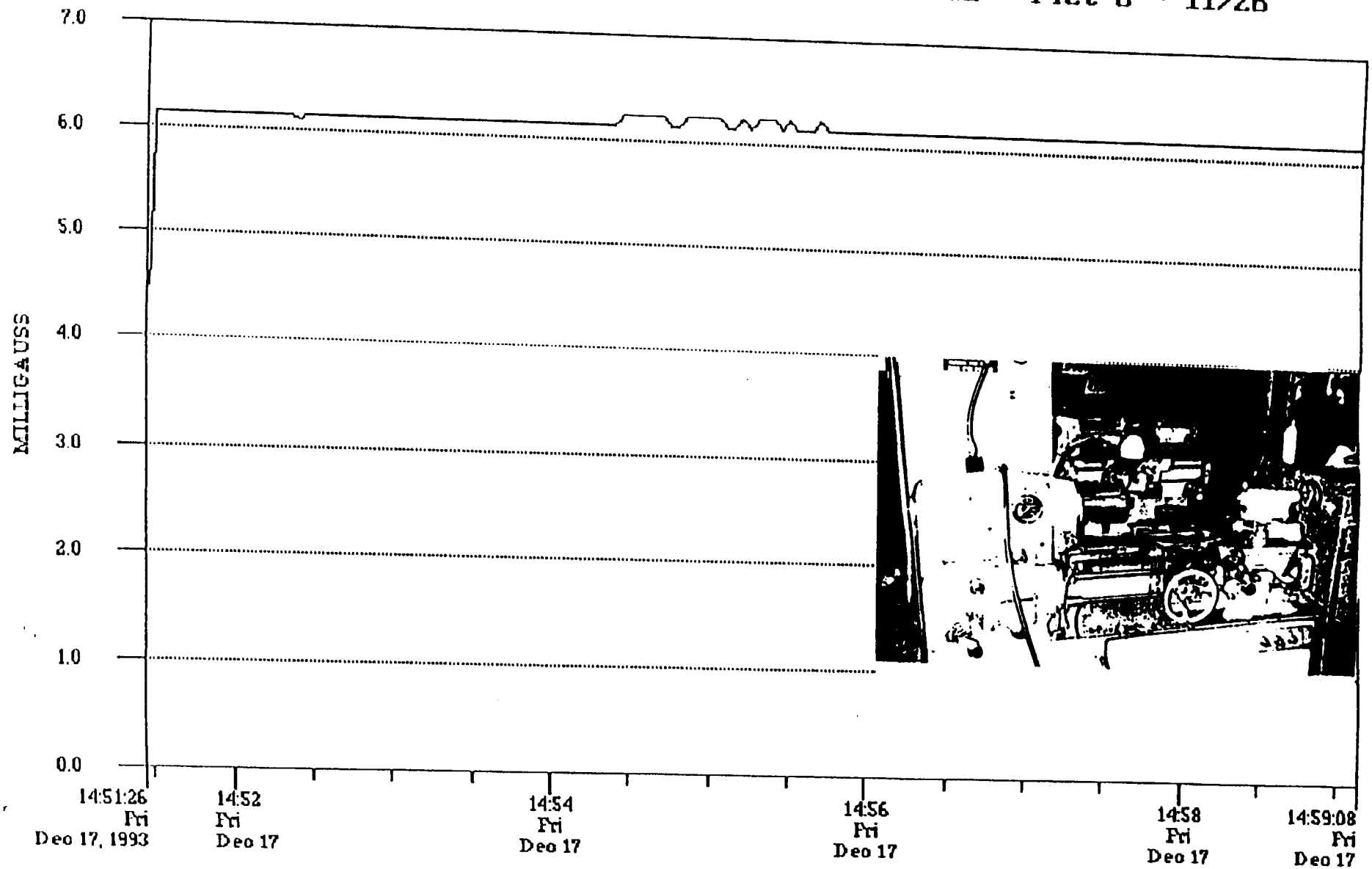

KSC-DF-3772

Fig. 51

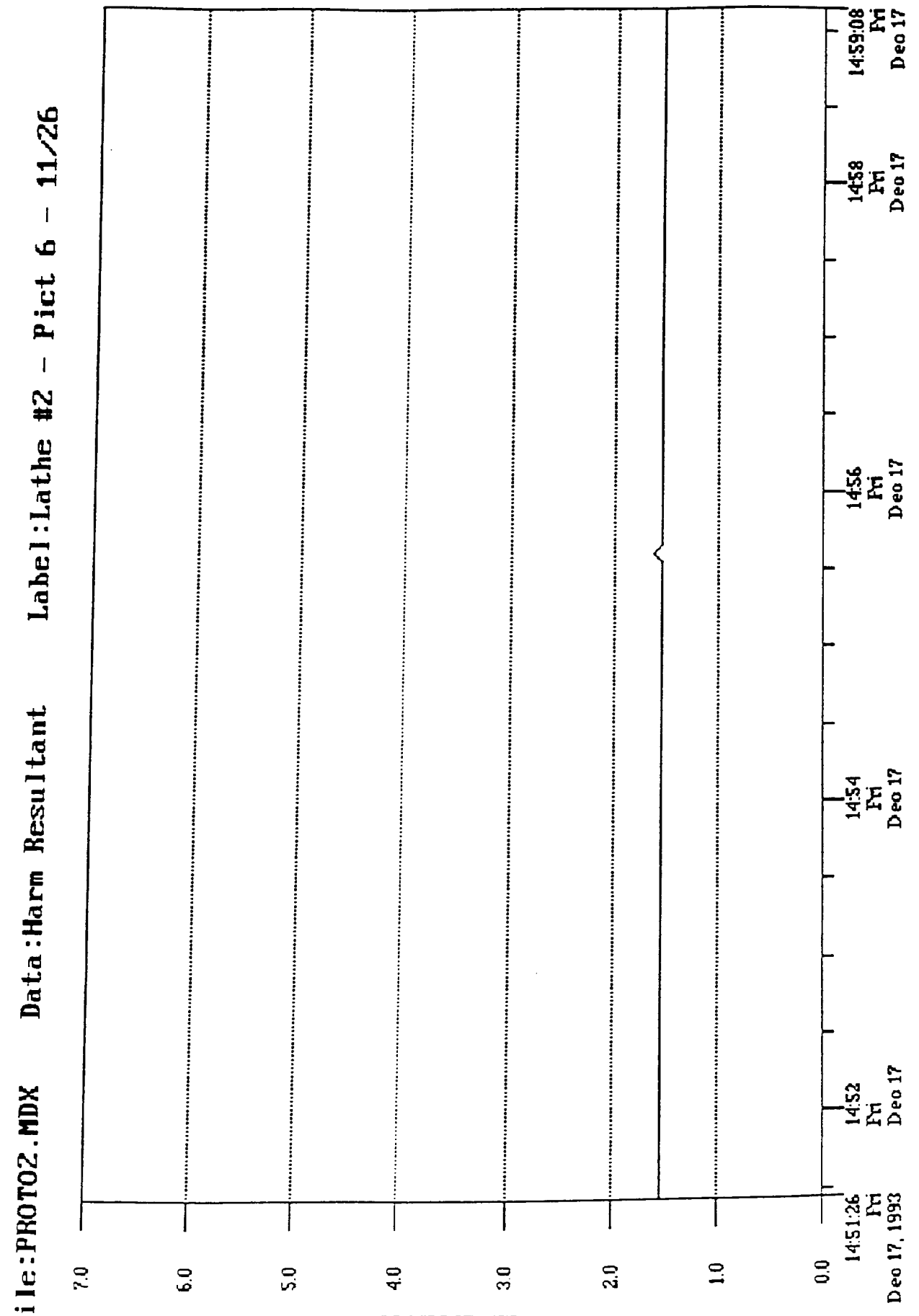
File:PROTO2.MDX
Data:Harm Resultant
Label:Lathe #2 - Pict 6 - 11/26
MILLIGAUSS
7.0
6.0
5.0
4.0
3.0
2.0
1.0
0.0
14:51:26 Fri Dec 17, 1993
14:52 Fri Dec 17
14:54 Fri Dec 17
14:56 Fri Dec 17
14:58 Fri Dec 17
14:59:08 Fri Dec 17

Fig. 52

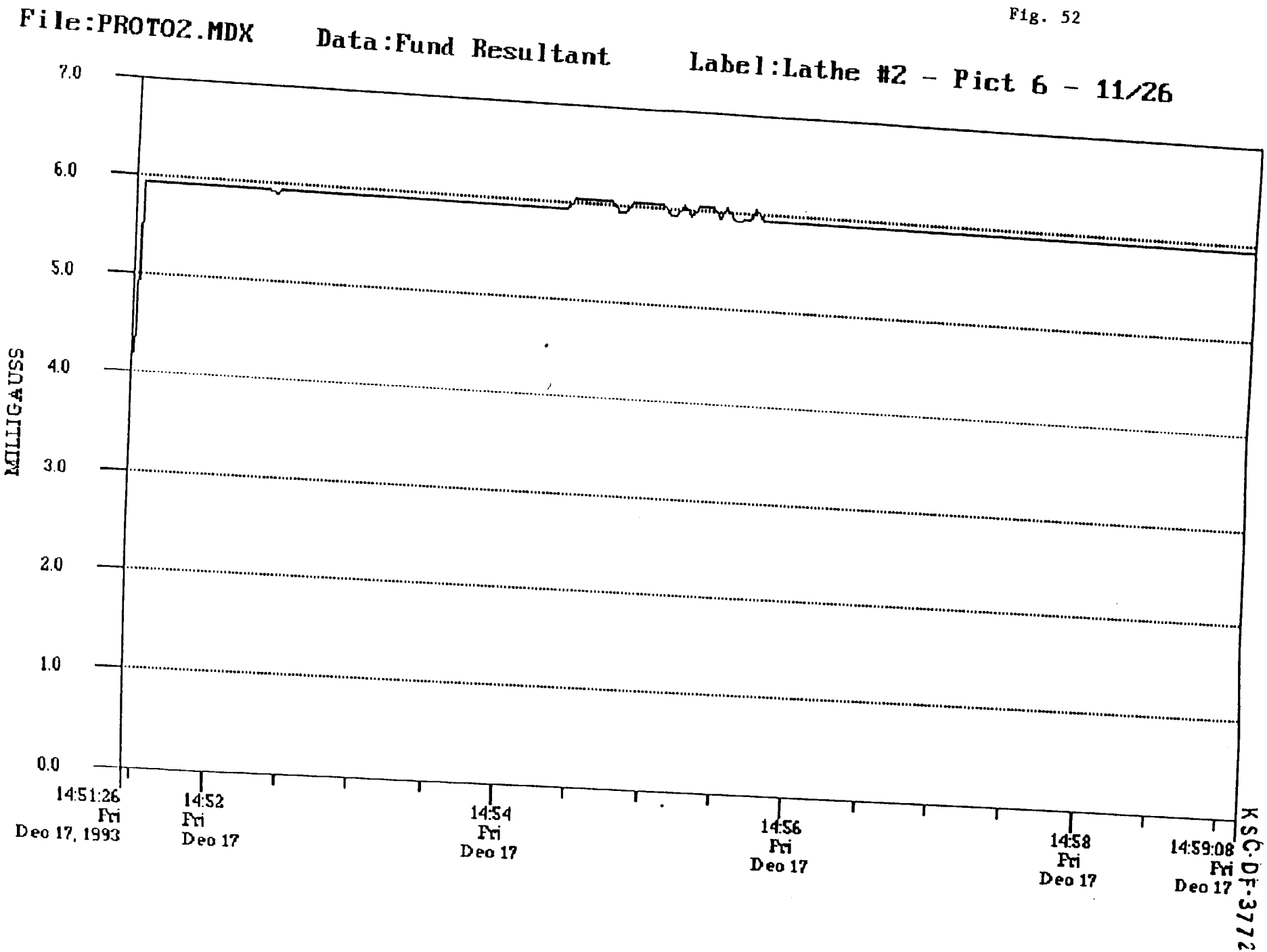
File:PROTO2.MDX
Data:Fund Resultant
Label:Lathe #2 - Pict 6 - 11/26
7.0
6.0
5.0
4.0
3.0
2.0
1.0
0.0
MILLIGAUSS
14:51:26
Fri
Dec 17, 1993
14:52
Fri
Dec 17
14:54
Fri
Dec 17
14:56
Fri
Dec 17
14:58
Fri
Dec 17
14:59:08
Fri
Dec 17
KSC DF-3772

********** INDIVIDUAL ANALYSIS - NORMAL DESCRIPTIVE STATISTICS **********

Data File : C:\EMCALC21\PROTO2.MDX
Data Set Label : Lathe #2 - Pict 6 - 11/26
Data Set Number: 5
Data Set Start : Dec/17/93 14:51:26
Data Set Stop : Dec/17/93 14:59:08
Observations : 155

	Min	Max	Mean	Std Dev	Median
Broadband					
Result (mG)	4.48	6.23	6.14	0.14	6.14
X (mG)	3.51	5.51	5.40	0.16	5.41
Y (mG)	1.51	1.71	1.51	0.02	1.51
Z (mG)	2.21	2.51	2.50	0.03	2.51
Fundamental					
Result (mG)	4.21	6.04	5.94	0.14	5.94
X (mG)	3.22	5.33	5.22	0.17	5.22
Y (mG)	1.42	1.63	1.42	0.02	1.42
Z (mG)	2.17	2.47	2.47	0.03	2.47
Harmonic					
Result (mG)	1.54	1.63	1.54	0.01	1.54
X (mG)	1.41	1.51	1.41	0.01	1.41
Y (mG)	0.51	0.51	0.51	0.00	0.51
Z (mG)	0.41	0.41	0.41	0.00	0.41

Fig. 53

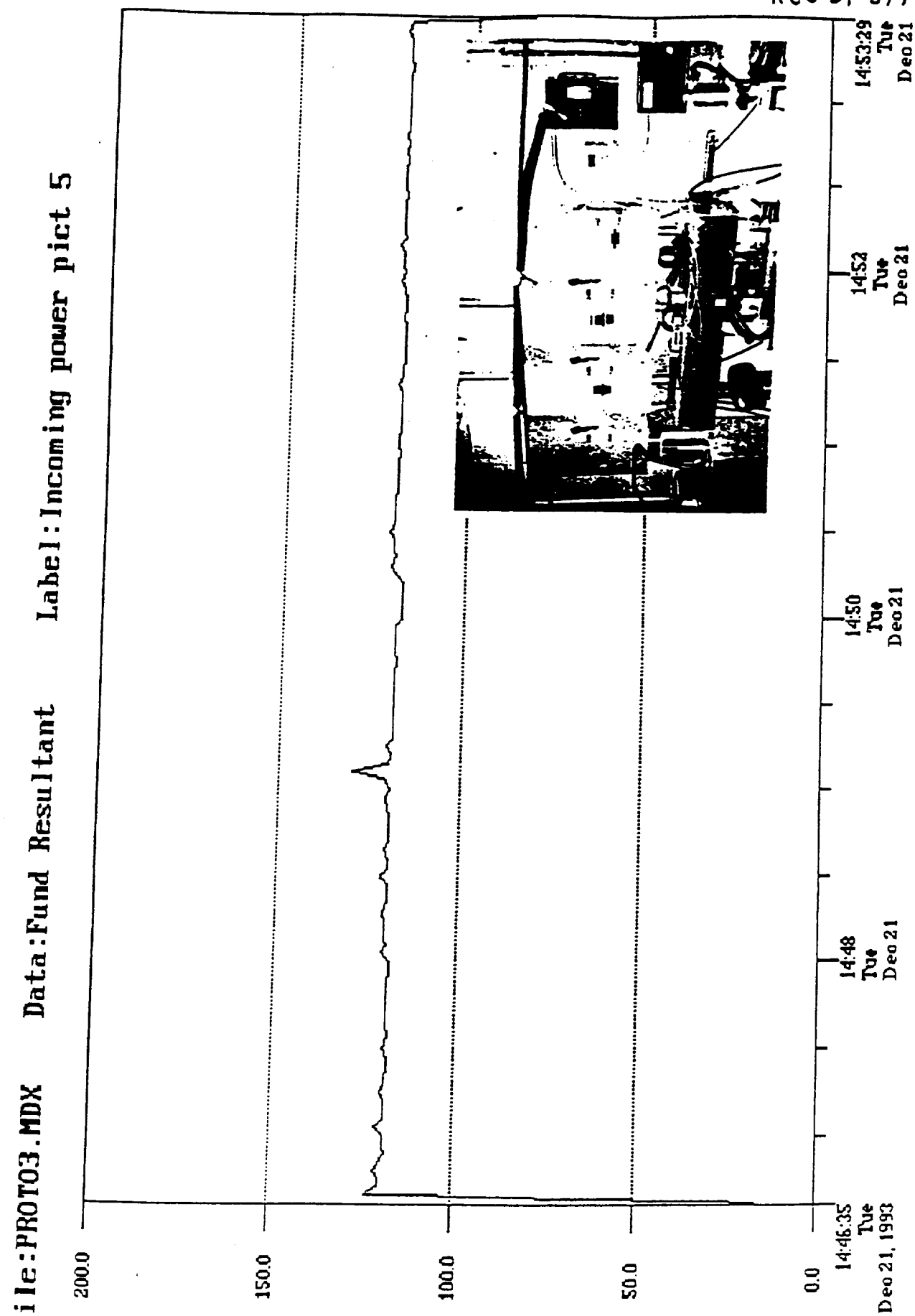
File:PROTO3.MDX
Data:Fund Resultant
Label:Incoming power pict 5
MILLIGAUSS
200.0
150.0
100.0
50.0
0.0
14:46:35 Tue Dec 21, 1993
14:48 Tue Dec 21
14:50 Tue Dec 21
14:52 Tue Dec 21
14:53:29 Tue Dec 21

Fig. 54

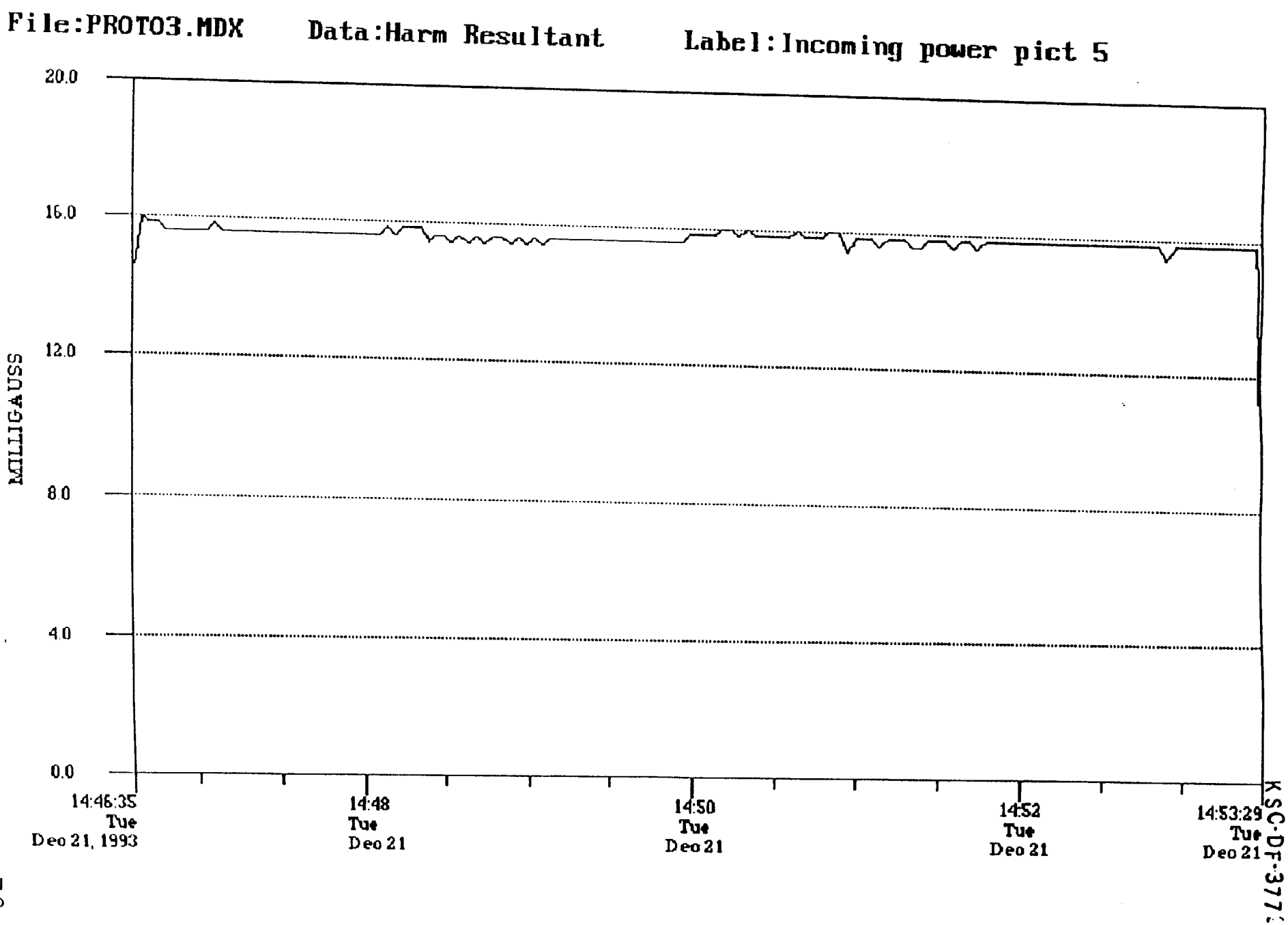
File:PROTO3.MDX
Data:Harm Resultant
Label:Incoming power pict 5
20.0
16.0
12.0
8.0
4.0
0.0
MILLIGAUSS
14:46:35
Tue
Dec 21, 1993
14:48
Tue
Dec 21
14:50
Tue
Dec 21
14:52
Tue
Dec 21
14:53:29
Tue
Dec 21

Fig. 55

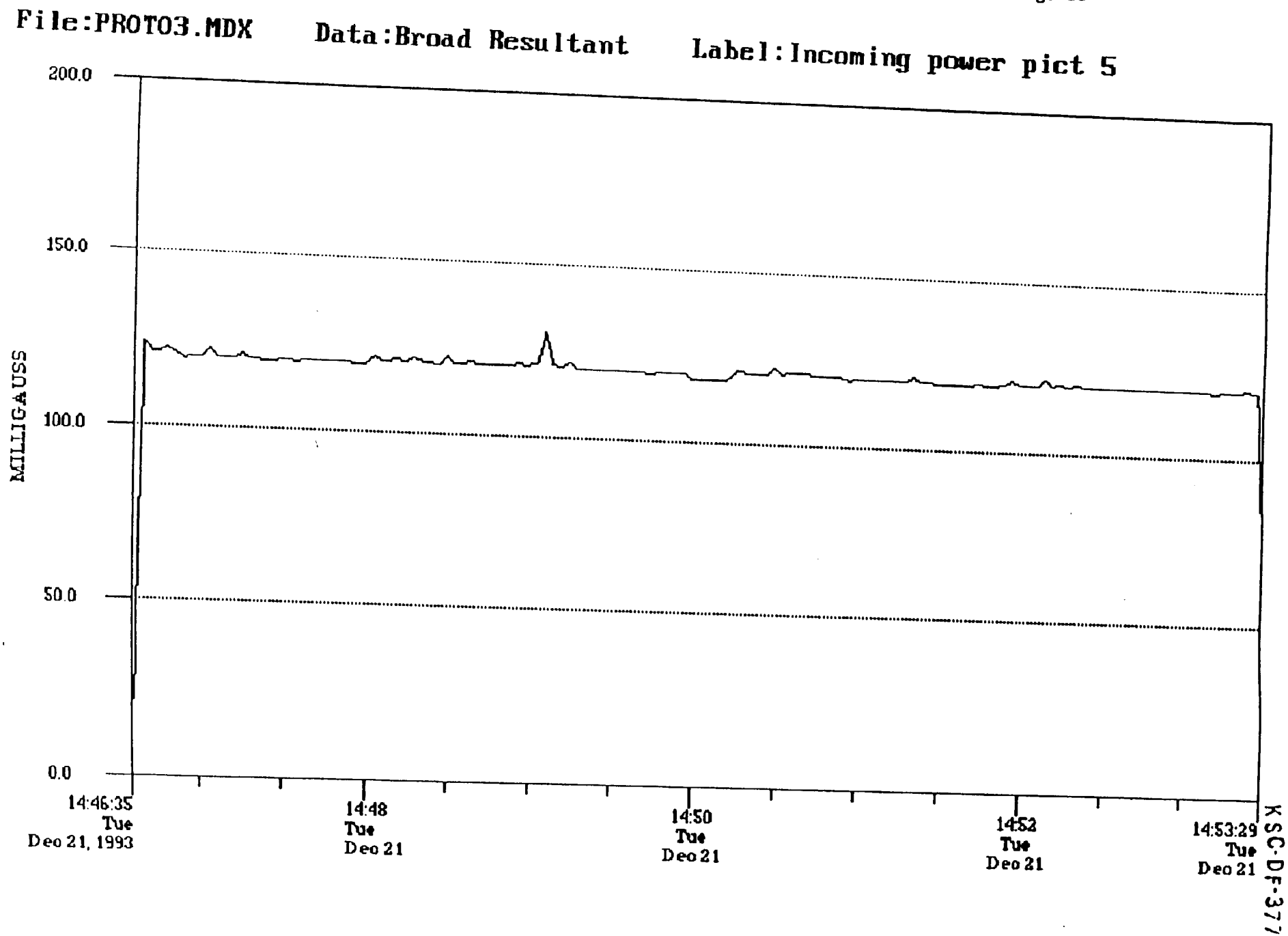

Fig. 56

File:PROTO3.MDX Data:Broad Resultant Label:Incoming power wireway pict 6

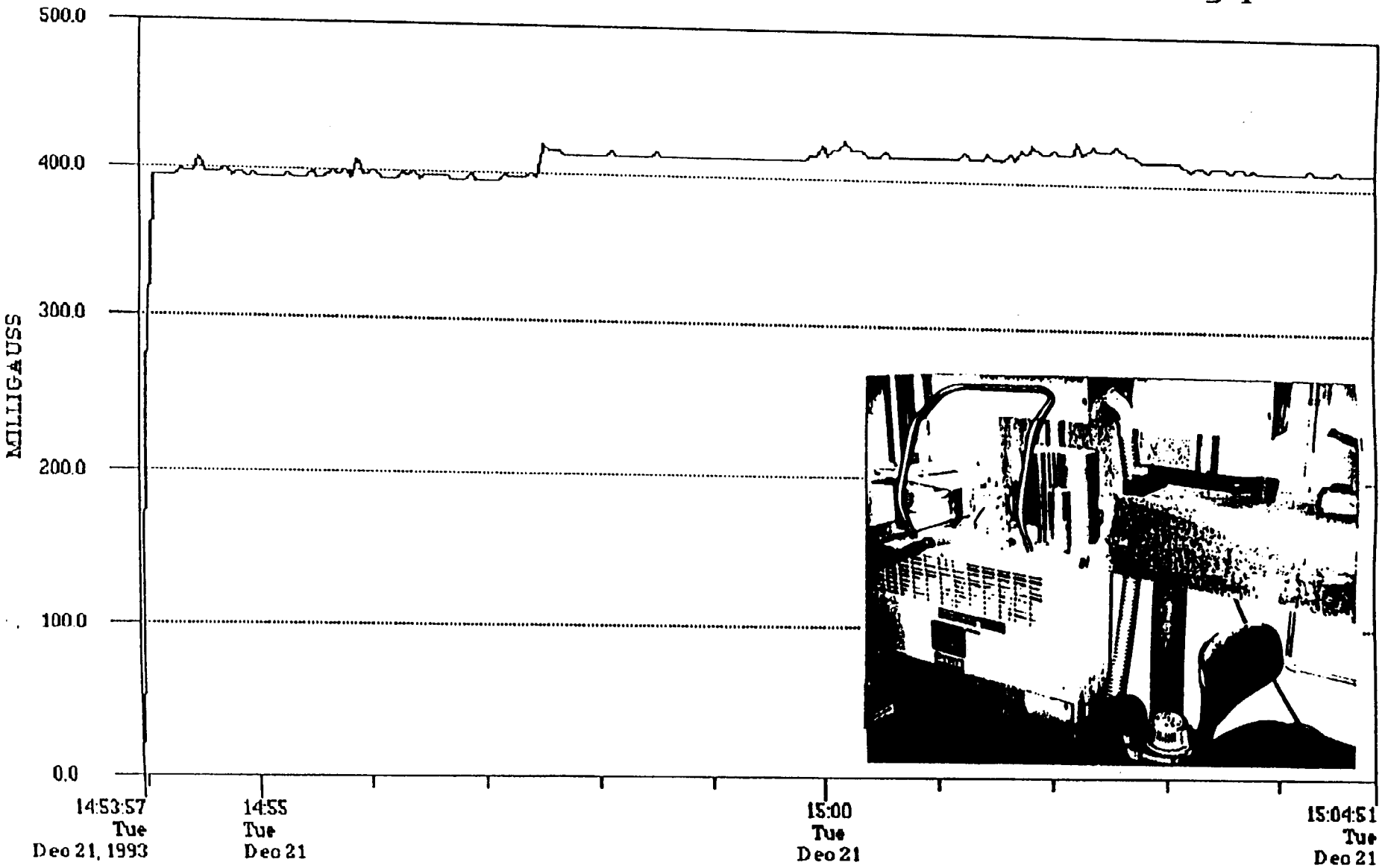

KSC-DF-3772

Fig. 57

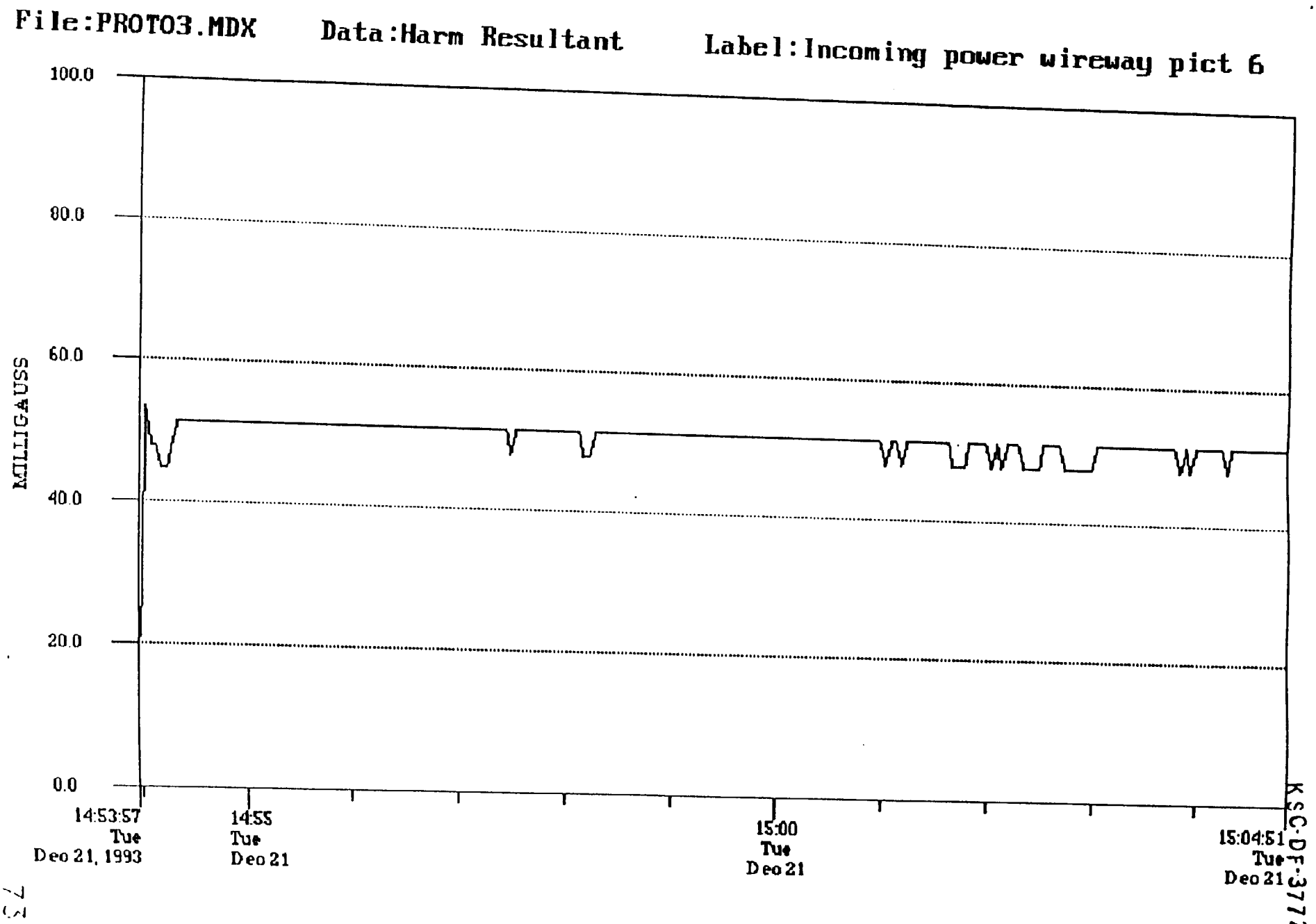
File:PROTO3.MDX
Data:Harm Resultant
Label:Incoming power wireway pict 6
100.0
80.0
60.0
40.0
20.0
0.0
MILLIGAUSS
14:53:57
Tue
Dec 21, 1993
14:55
Tue
Dec 21
15:00
Tue
Dec 21
15:04:51
Tue
Dec 21
KSC-DF-3772

Fig. 58

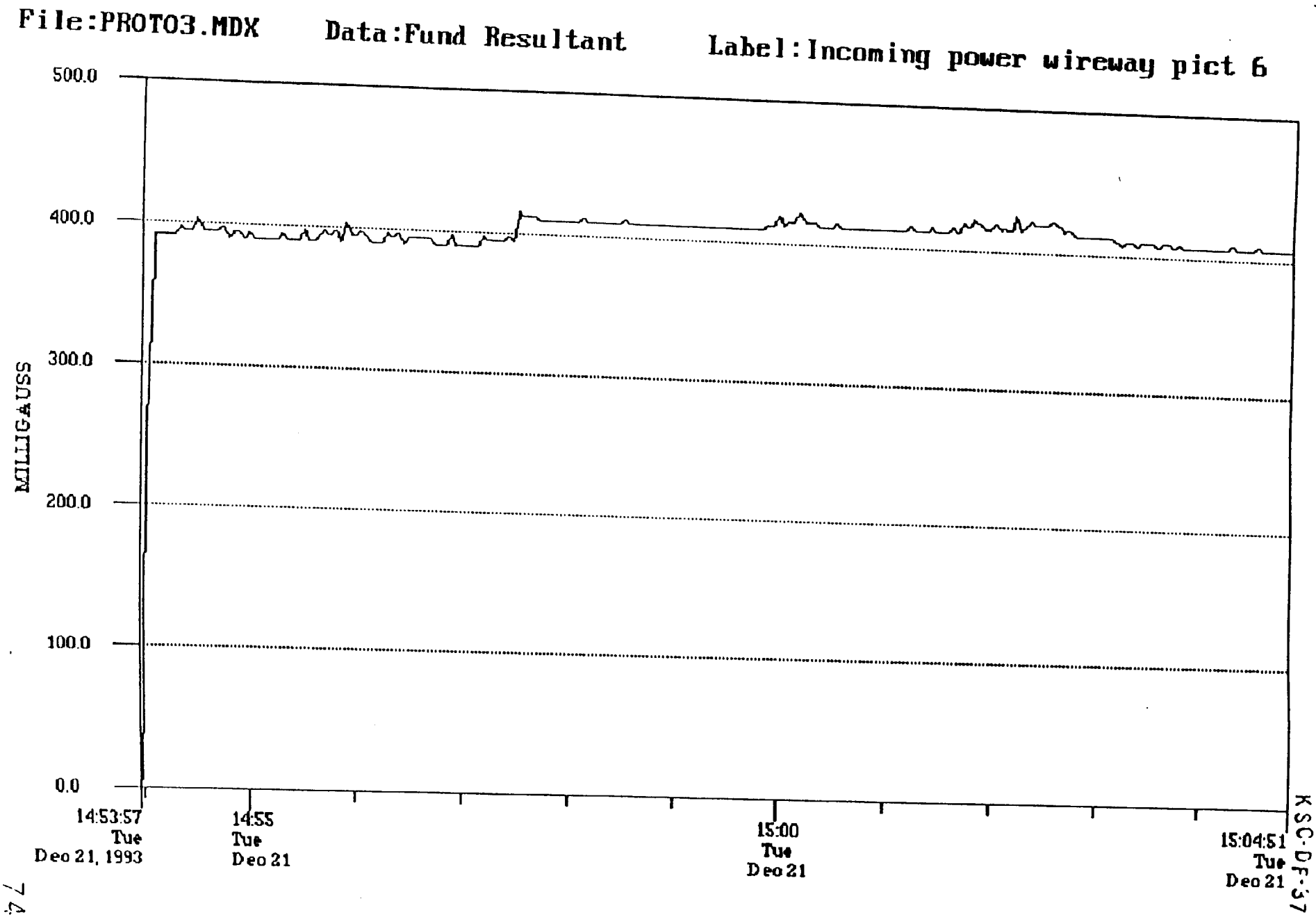

KSC-DF-3772

74

3.6 Electric Panels

During our measurements we noticed that electric panels, consistently, generated some of the highest magnetic field levels. Basically, some of the measurements were done with the panels covered and some with the panels uncovered to see if any difference occurs in the recording of the magnetic field levels. The results were very interesting. It was found that all original covers shielded magnetic fields to some extent but not enough, so additional shielding may be required to reduce the levels furthermore. Figures 59 to 73 depict some results from an uncovered panel containing 12 circuit breakers. The sensor was placed at five different locations on the panel. The maximum value recorded was 1,400 mGauss. That is a rather large value. The various locations yielded different magnitudes for the magnetic field. In Figures 74 to 76 the results at the center of the panel with the cover on are shown. Comparing these results with those in Figures 71 to 73 one can see that the cover itself attenuates both the broadband resultant and the harmonic resultant. The broadband resultant gets attenuated from about 450 mGauss to about 65 mGauss, whereas the harmonic resultant is cut from 120 mGauss to under 20 mGauss.

Another observation made in here was that the harmonic contribution to the magnetic field level was of the same magnitude as that of the fundamental one. This was the case for almost all panels in that place.

Next another set of panels located in the PDMS room (O & C building), shown in Figure 77, were evaluated. In Figures 78 to 83, with all panels covered, the highest value recorded was over 200 mGauss. Figures 84 to 92 represent measured data from a battery bank and a converter. Although, the UPS unit was covered still a level of 2,500 mGauss was measured. That suggests that shielding will be very appropriate in this case. An enclosure can be constructed of magnetically shielding material that

can further attenuate this high level of magnetic field. Again, the harmonic content contributed to the measured broad-band magnetic field level.

The next set of measurements demonstrate the effects of further shielding on these panels.

Fig. 59

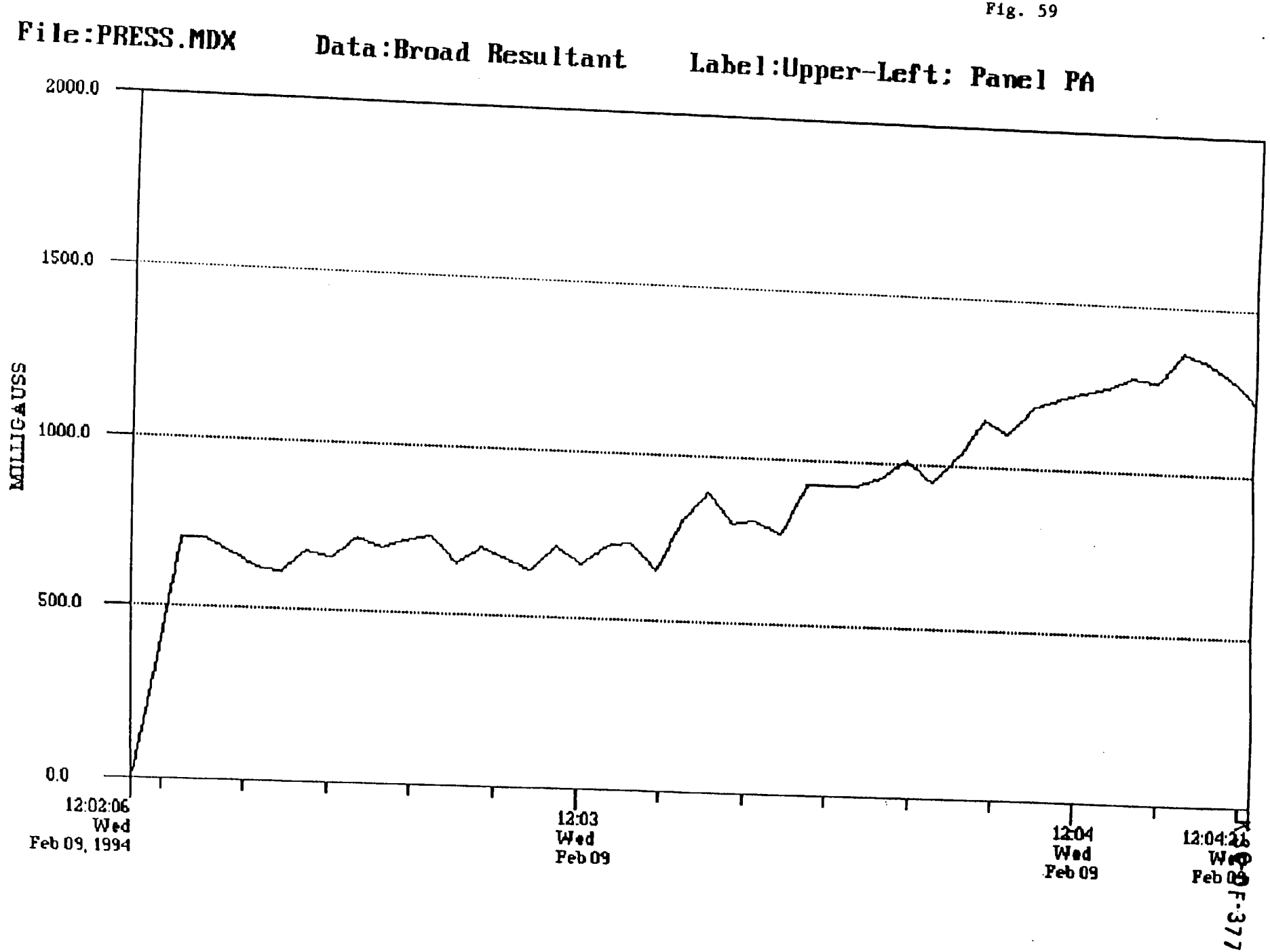
File:PRESS.MDX
Data:Broad Resultant
Label:Upper-Left: Panel PA
2000.0
1500.0
1000.0
500.0
0.0
MILLIGAUSS
12:02:06
Wed
Feb 09, 1994
12:03
Wed
Feb 09
12:04
Wed
Feb 09

Fig. 60

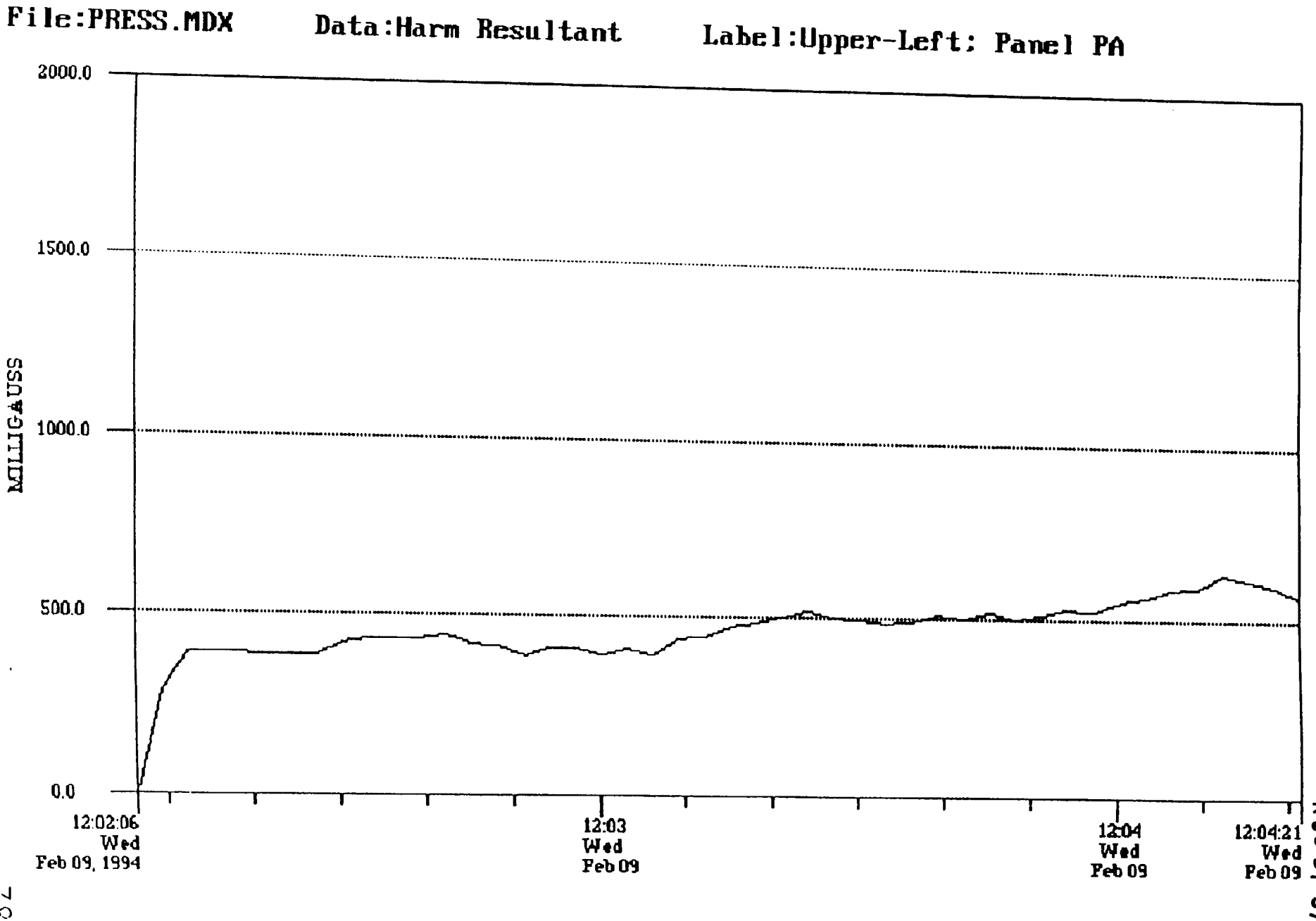
File:PRESS.MDX
Data:Harm Resultant
Label:Upper-Left: Panel PA
2000.0
1500.0
1000.0
500.0
0.0
MILLIGAUSS
12:02:06
Wed
Feb 09, 1994
12:03
Wed
Feb 09
12:04
Wed
Feb 09
12:04:21
Wed
Feb 09
KSC-DF-377

Fig. 61

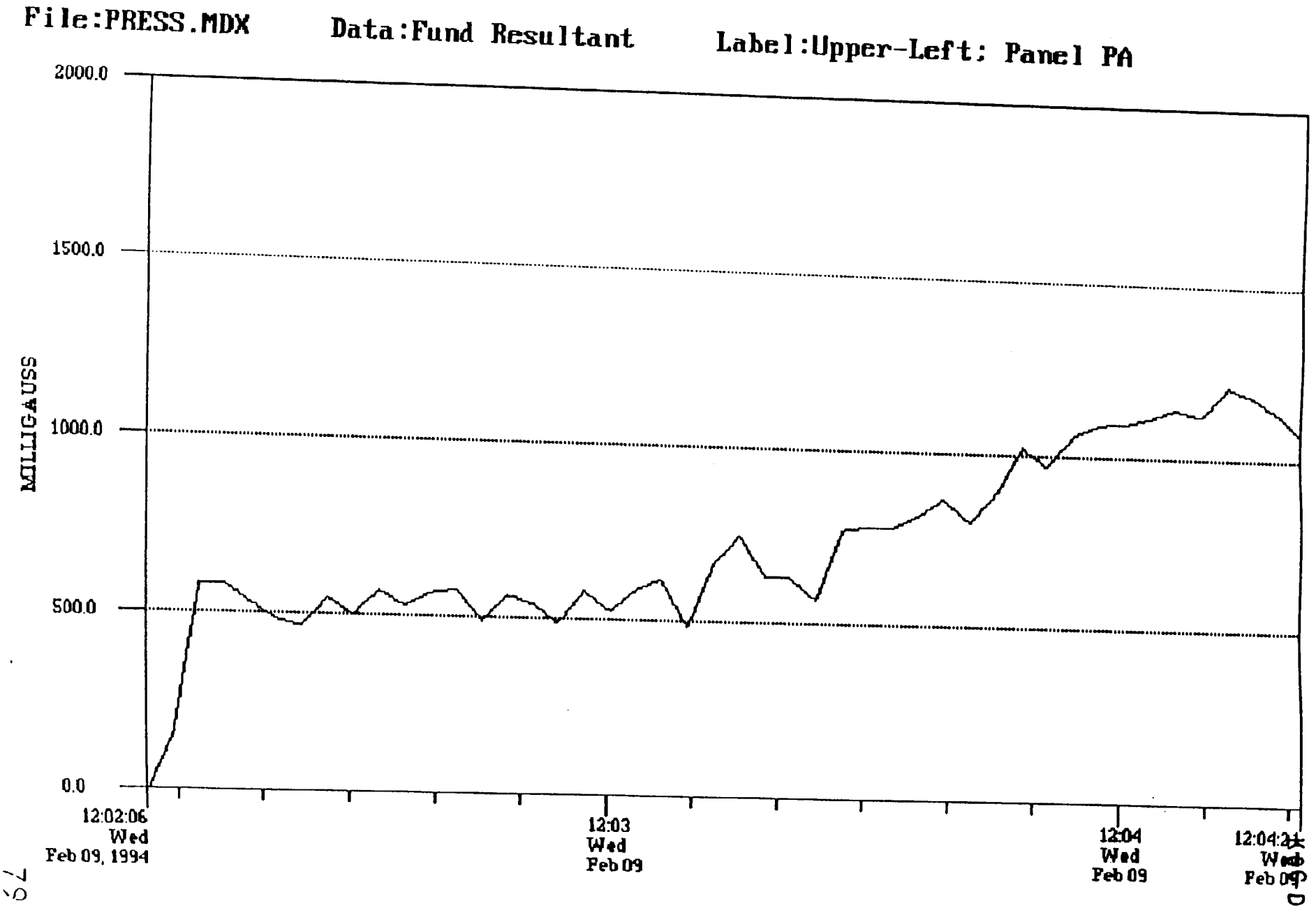
File:PRESS.MDX
Data:Fund Resultant
Label:Upper-Left; Panel PA
2000.0
1500.0
1000.0
500.0
0.0
MILLIGAUSS
12:02:06
Wed
Feb 09, 1994
12:03
Wed
Feb 09
12:04
Wed
Feb 09
DF-37

Fig. 62

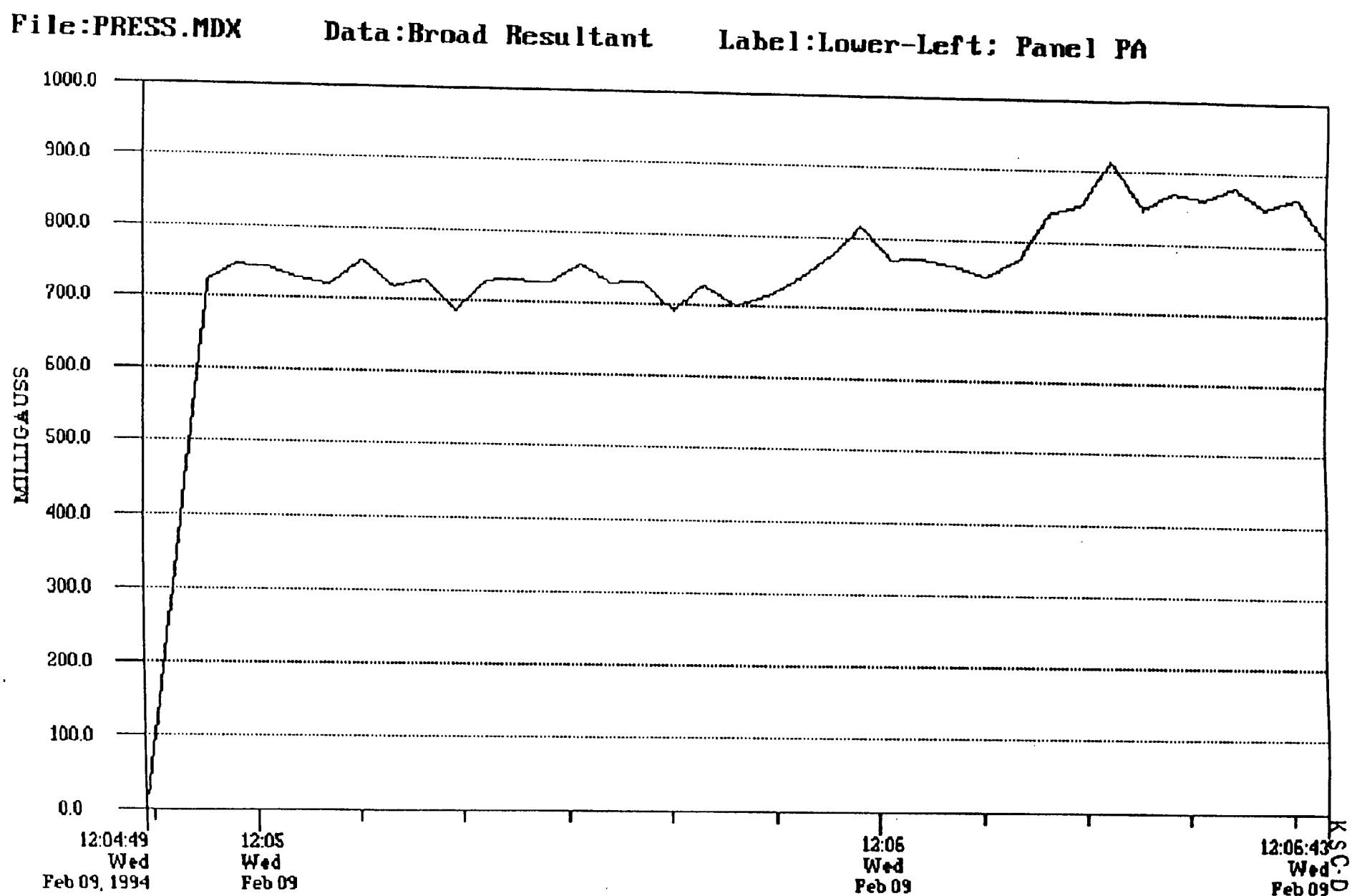
File:PRESS.MDX
Data:Broad Resultant
Label:Lower-Left: Panel PA
1000.0
900.0
800.0
700.0
600.0
500.0
400.0
300.0
200.0
100.0
0.0
MILLIGAUSS
12:04:49
Wed
Feb 09, 1994
12:05
Wed
Feb 09
12:06
Wed
Feb 09
12:06:43
Wed
Feb 09
KSC-DF-377

Fig. 63

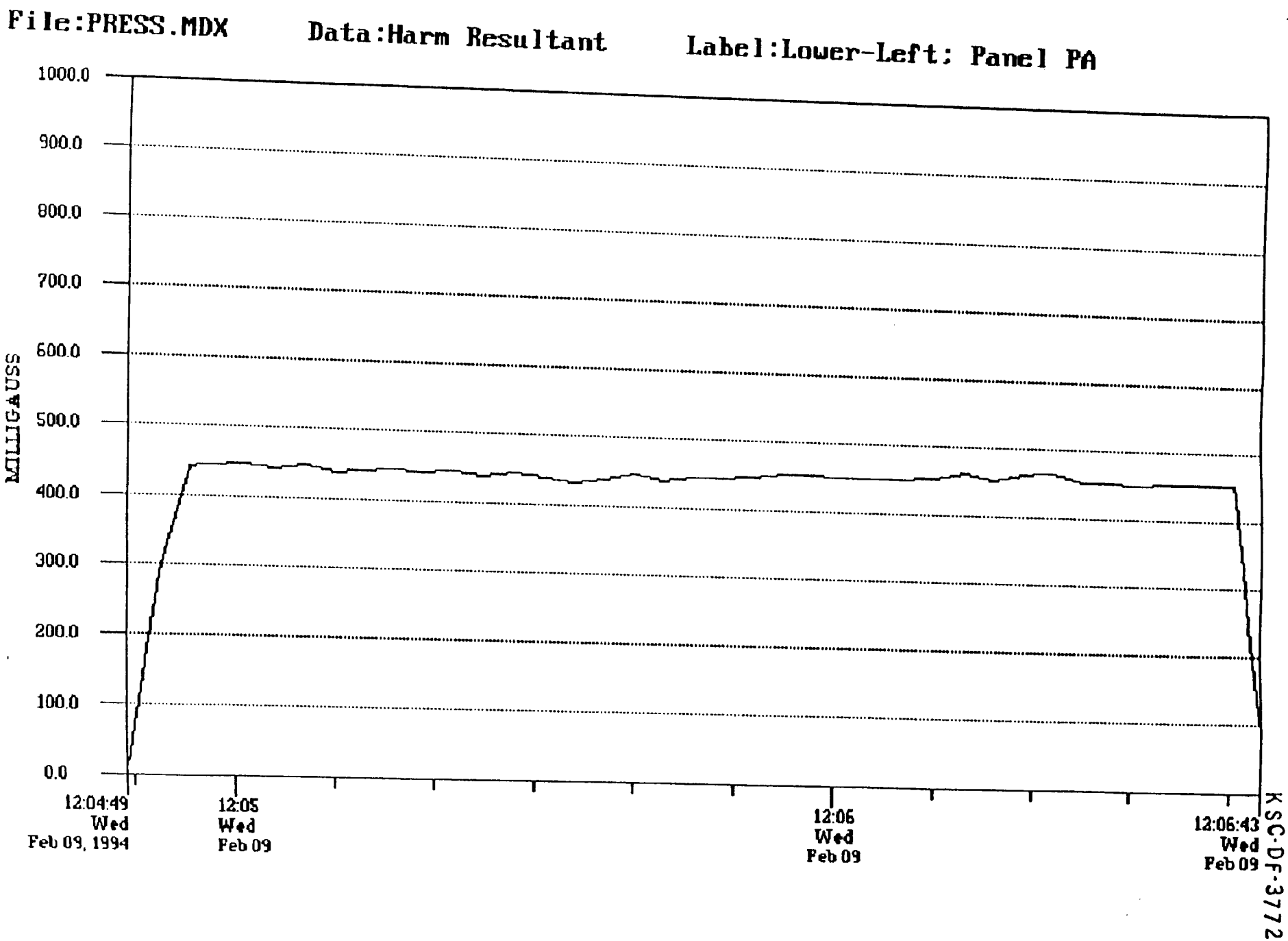
File:PRESS.MDX
Data:Harm Resultant
Label:Lower-Left: Panel PA
1000.0
900.0
800.0
700.0
600.0
500.0
400.0
300.0
200.0
100.0
0.0
MILLIGAUSS
12:04:49
Wed
Feb 09, 1994
12:05
Wed
Feb 09
12:06
Wed
Feb 09
12:06:43
Wed
Feb 09
KSC-DF-3772

Fig. 64

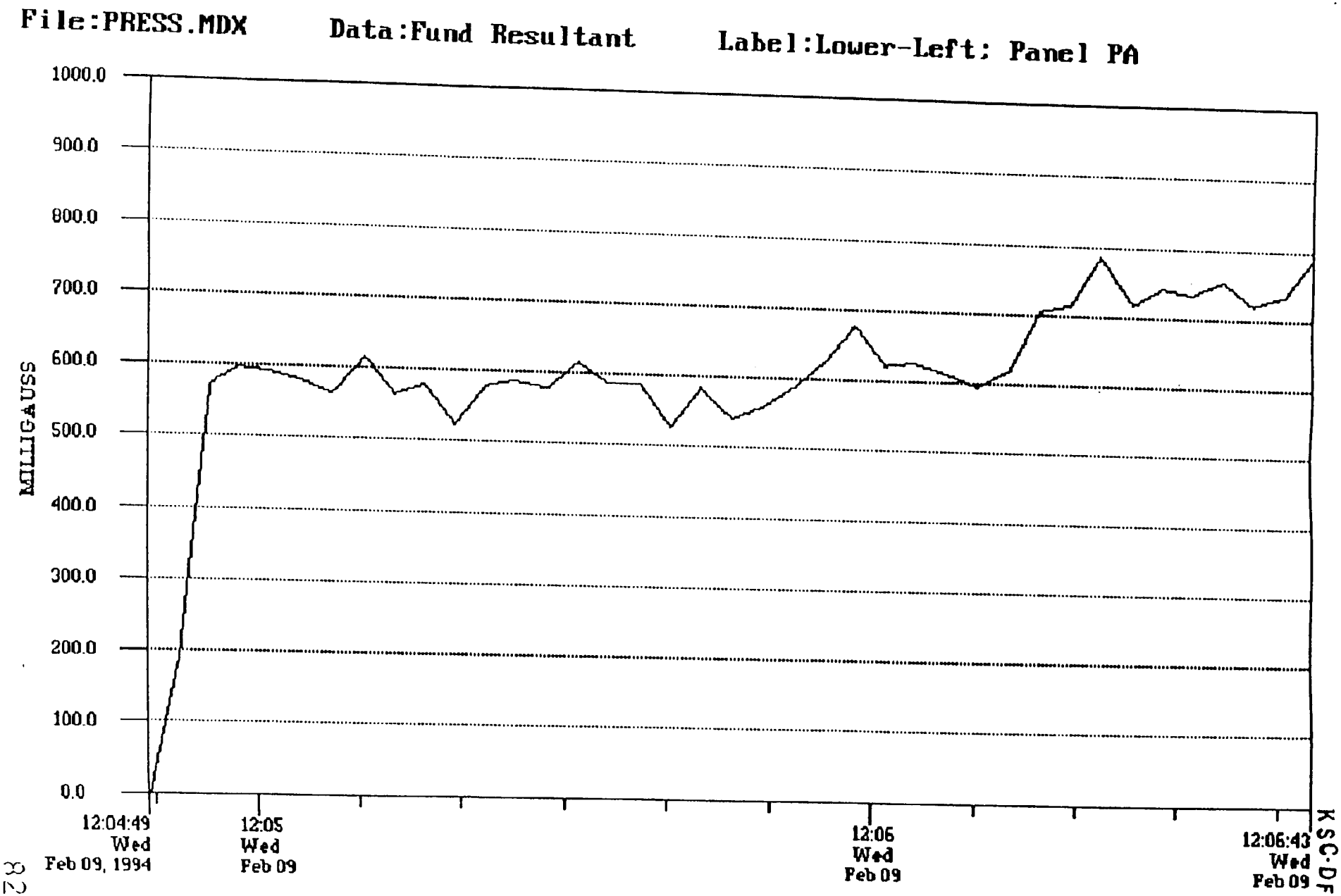

KSC-DF-3772

Fig. 65

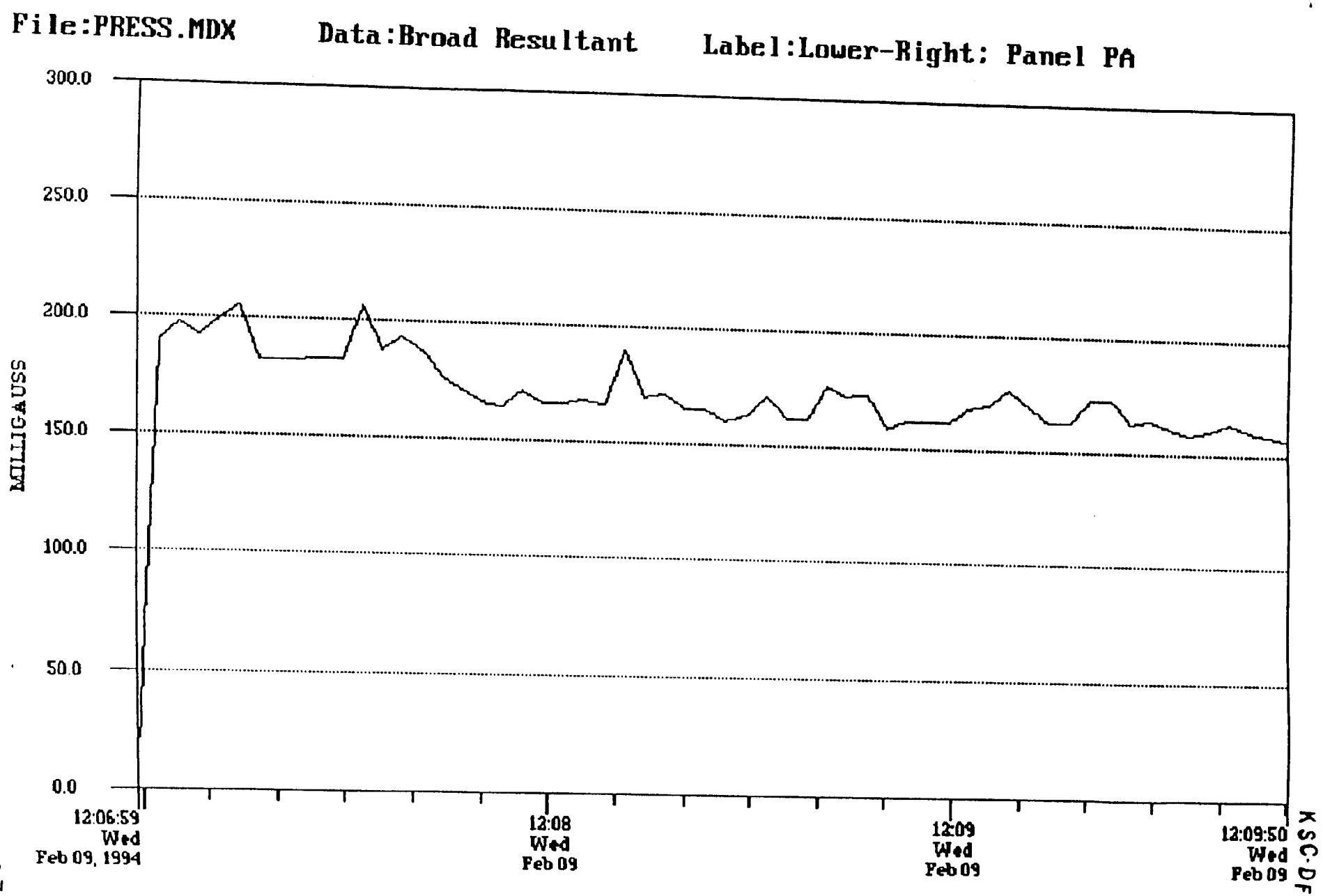

KSC-DF-377

Fig. 66

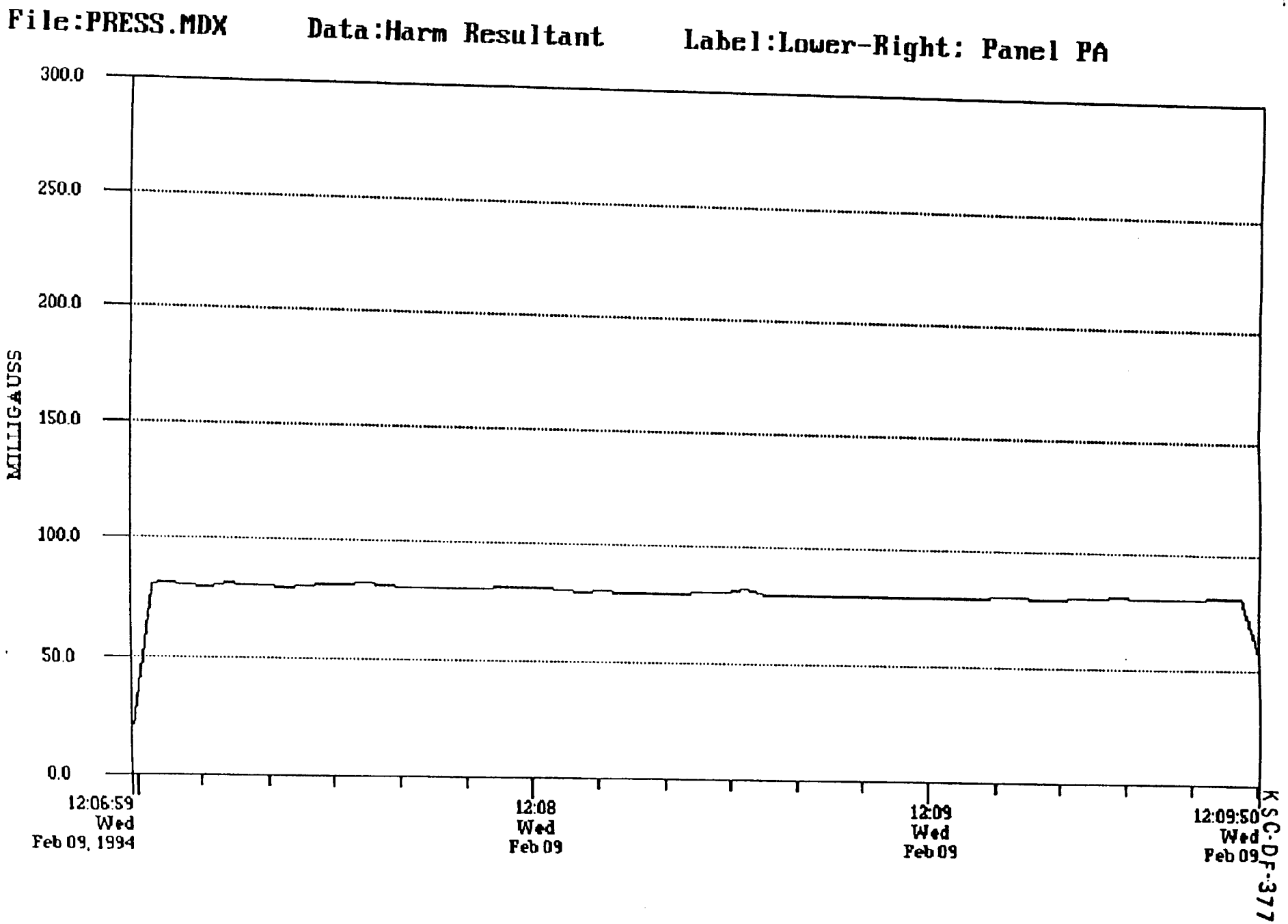
File:PRESS.MDX
Data:Harm Resultant
Label:Lower-Right: Panel PA
300.0
250.0
200.0
150.0
100.0
50.0
0.0
MILLIGAUSS
12:06:59
Wed
Feb 09, 1994
12:08
Wed
Feb 09
12:09
Wed
Feb 09
12:09:50
Wed
Feb 09
KSC-DF-377

Fig. 67

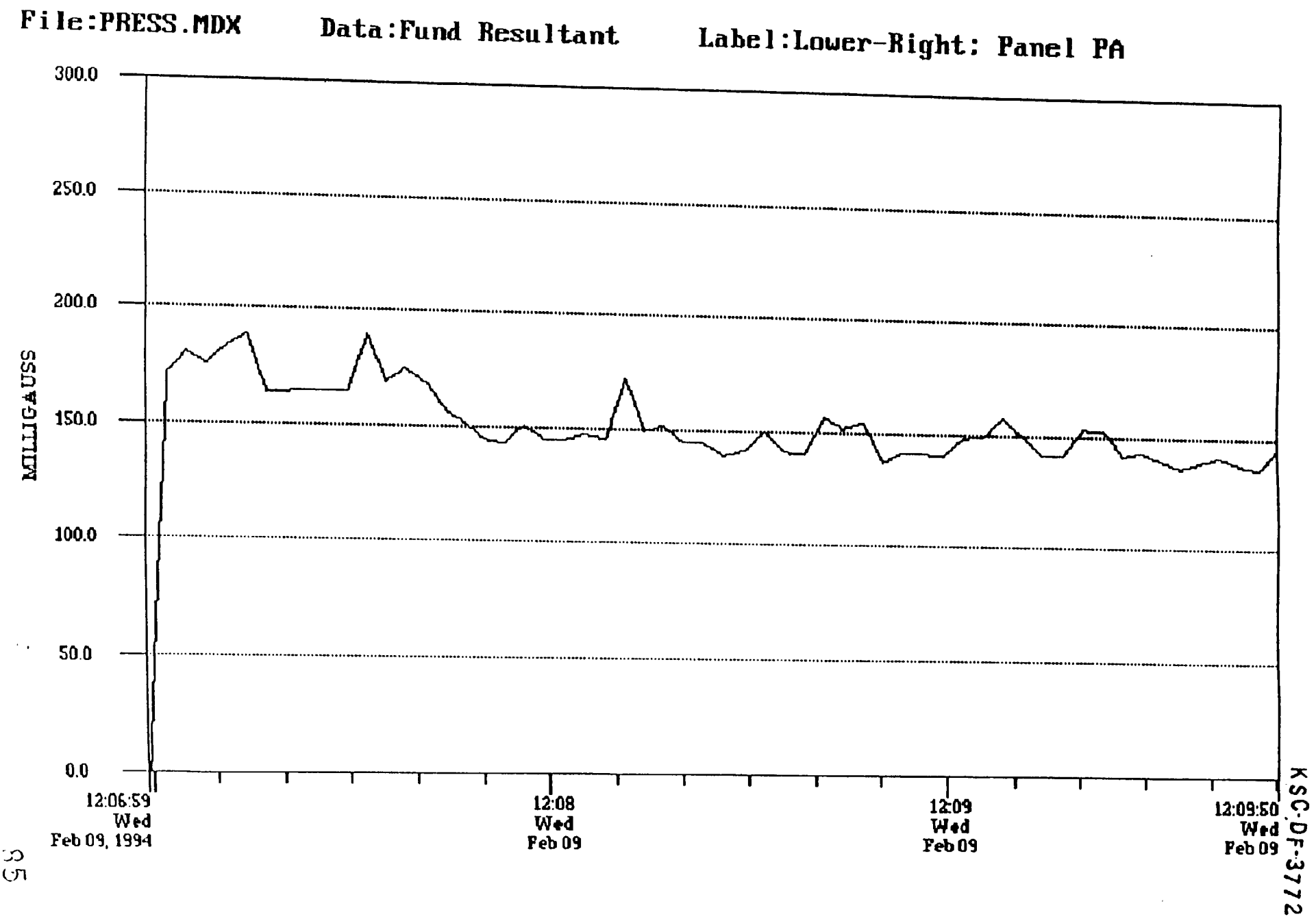
File:PRESS.MDX
Data:Fund Resultant
Label:Lower-Right: Panel PA
300.0
250.0
200.0
150.0
100.0
50.0
0.0
MILLIGAUSS
12:06:59
Wed
Feb 09, 1994
12:08
Wed
Feb 09
12:09
Wed
Feb 09
12:09:50
Wed
Feb 09
KSC-DF-3772

Fig. 68

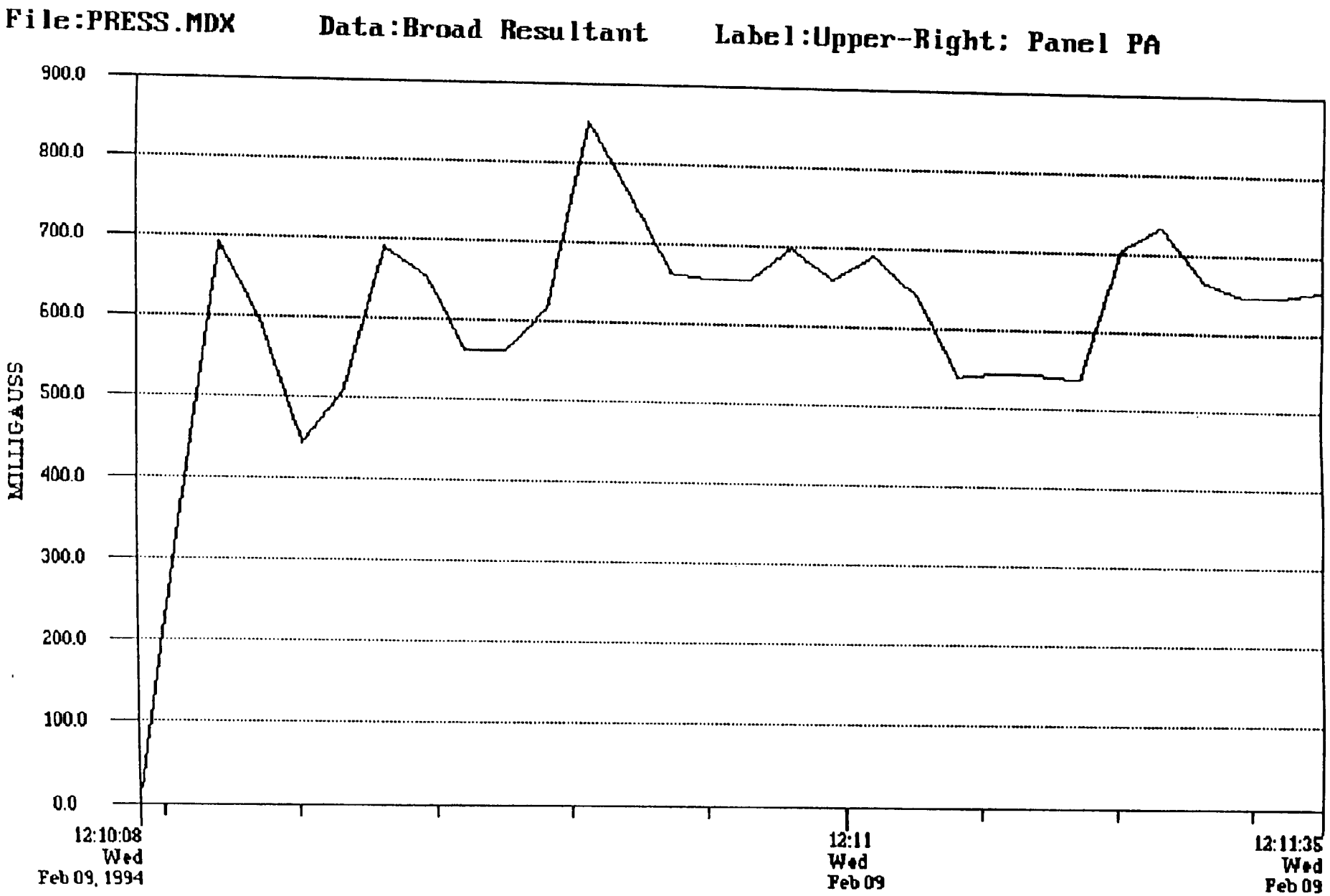

Fig. 69

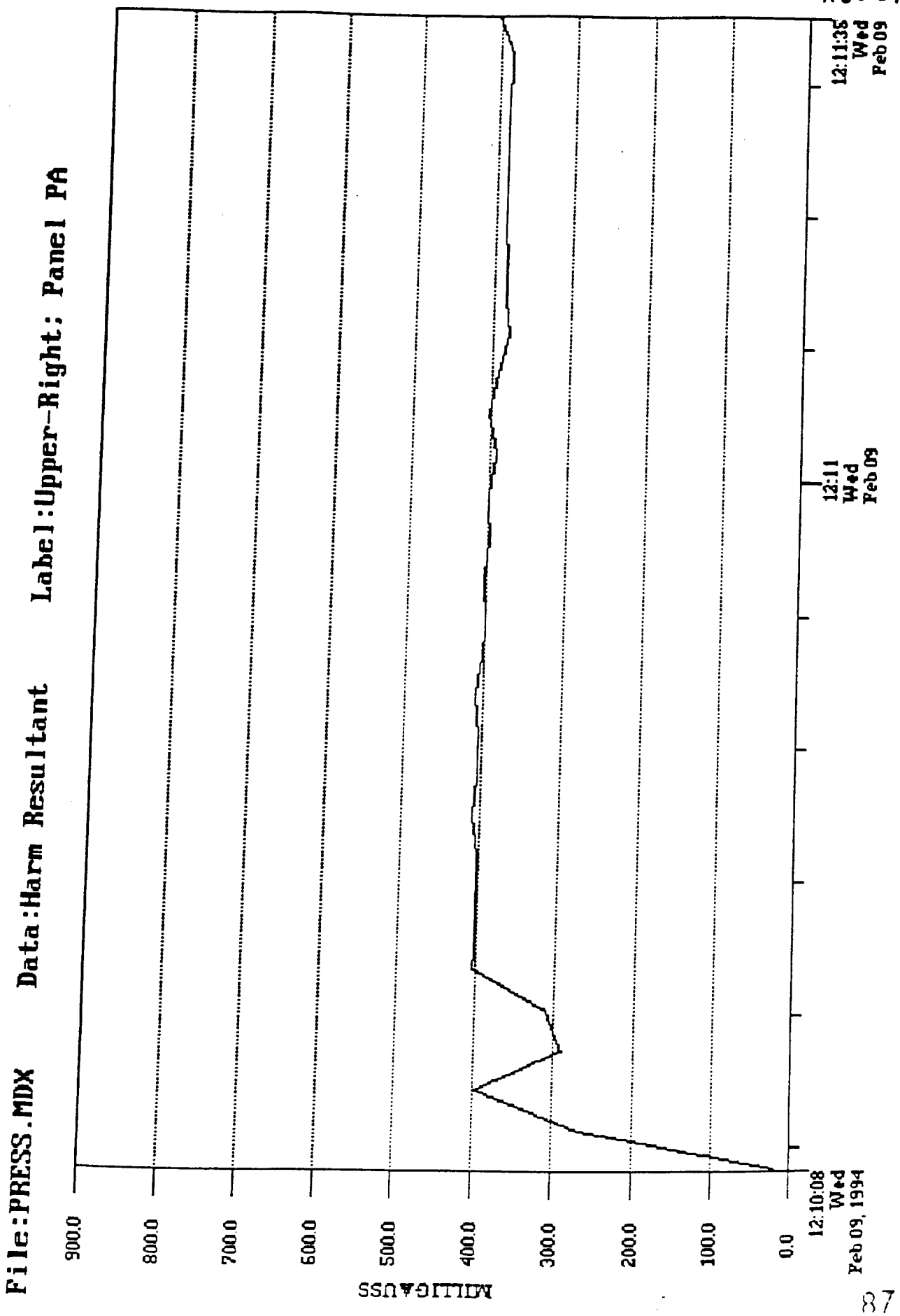
File:PRESS.MDX
Data:Harm Resultant
Label:Upper-Right: Panel PA
MILLIGAUSS
900.0
800.0
700.0
600.0
500.0
400.0
300.0
200.0
100.0
0.0
12:10:08
Wed
Feb 09, 1994
12:11
Wed
Feb 09
12:11:35
Wed
Feb 09

Fig. 70

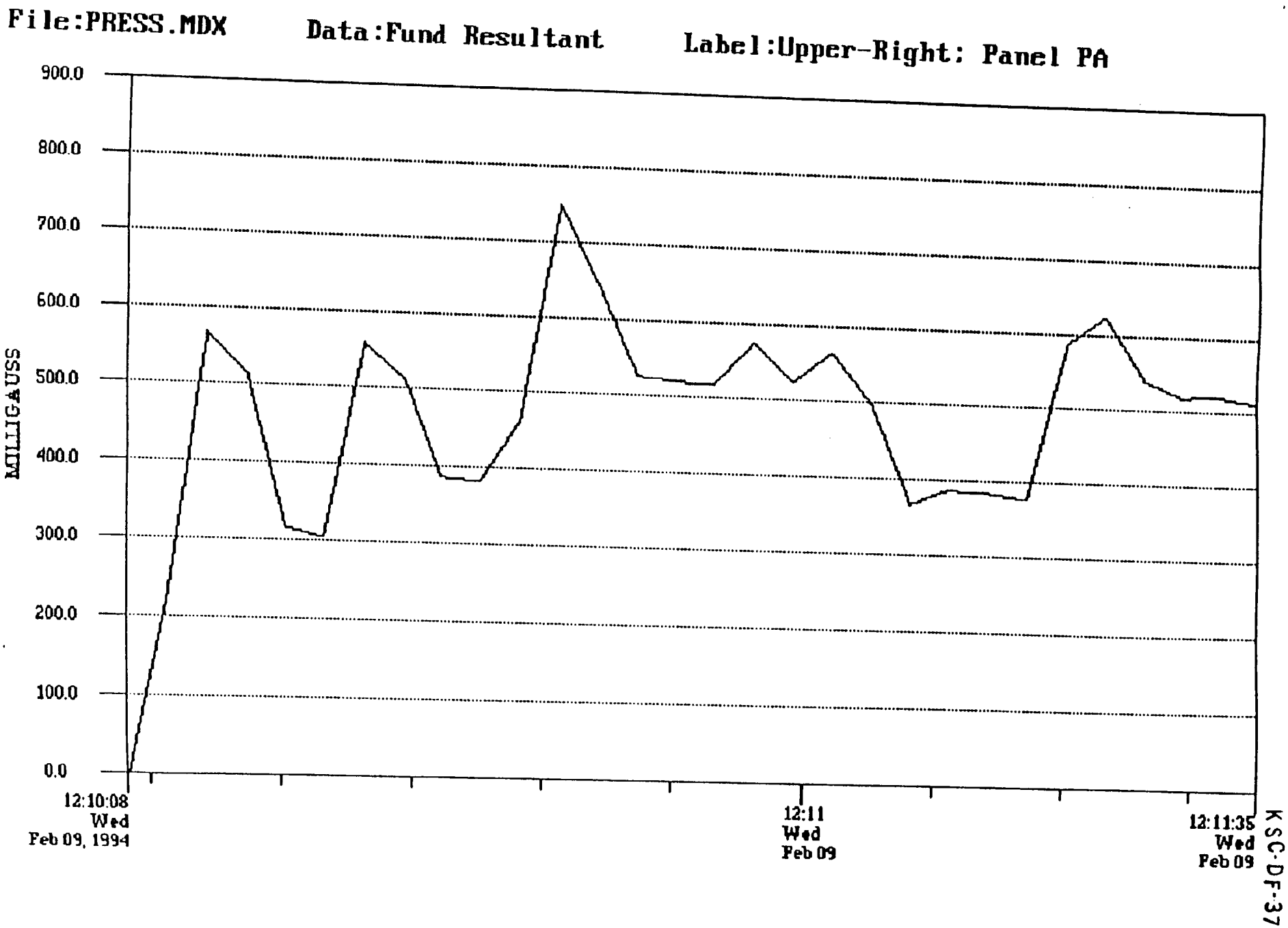
File:PRESS.MDX
Data:Fund Resultant
Label:Upper-Right: Panel PA
900.0
800.0
700.0
600.0
500.0
400.0
300.0
200.0
100.0
0.0
MILLIGAUSS
12:10:08
Wed
Feb 09, 1994
12:11
Wed
Feb 09
12:11:35
Wed
Feb 09
KSC-DF-37

Fig. 72

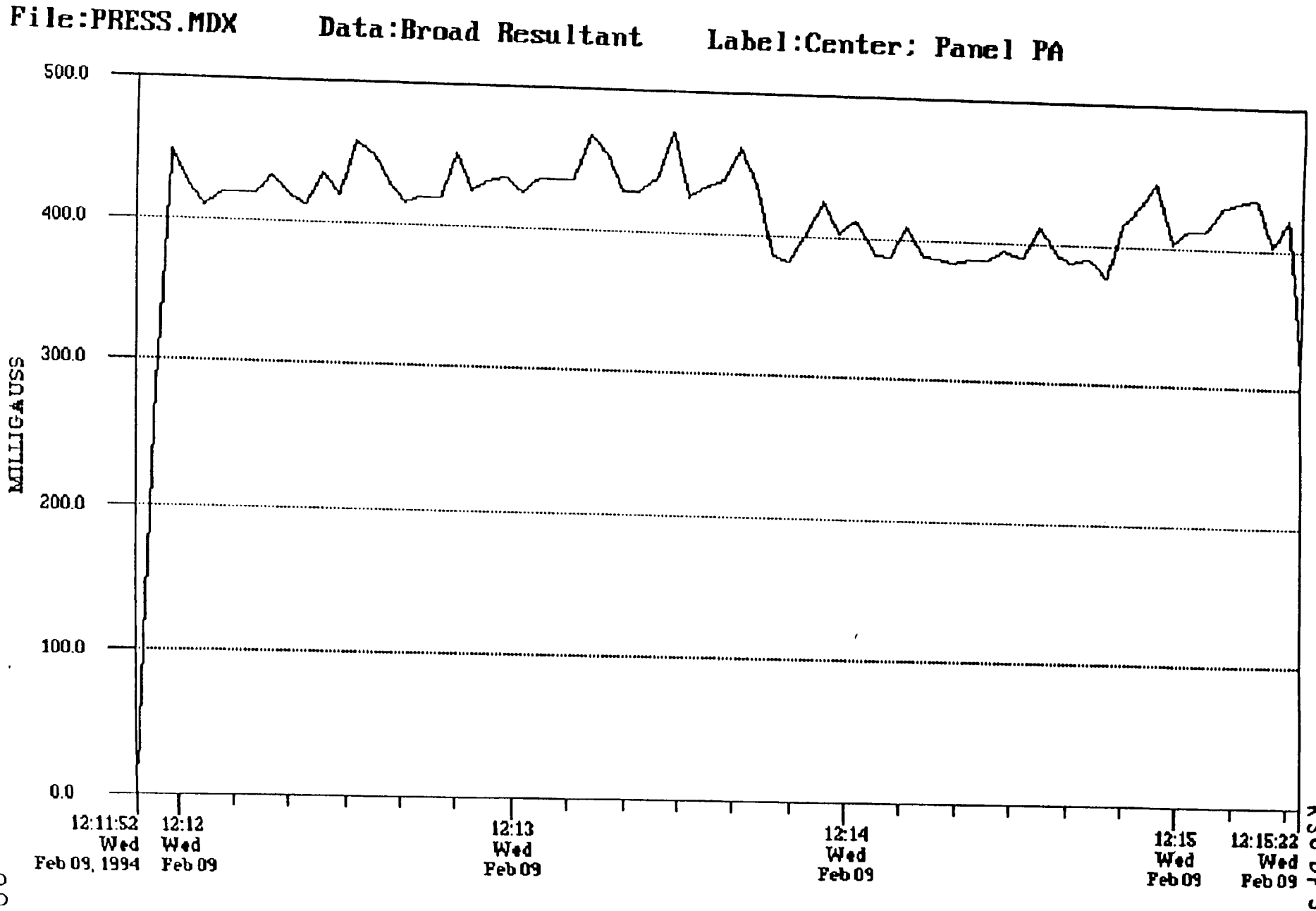
File:PRESS.MDX
Data:Broad Resultant
Label:Center: Panel PA
500.0
400.0
300.0
200.0
100.0
0.0
MILLIGAUSS
12:11:52 Wed Feb 09, 1994
12:12 Wed Feb 09
12:13 Wed Feb 09
12:14 Wed Feb 09
12:15 Wed Feb 09
12:15:22 Wed Feb 09
KSC-DF-3772

Fig. 72

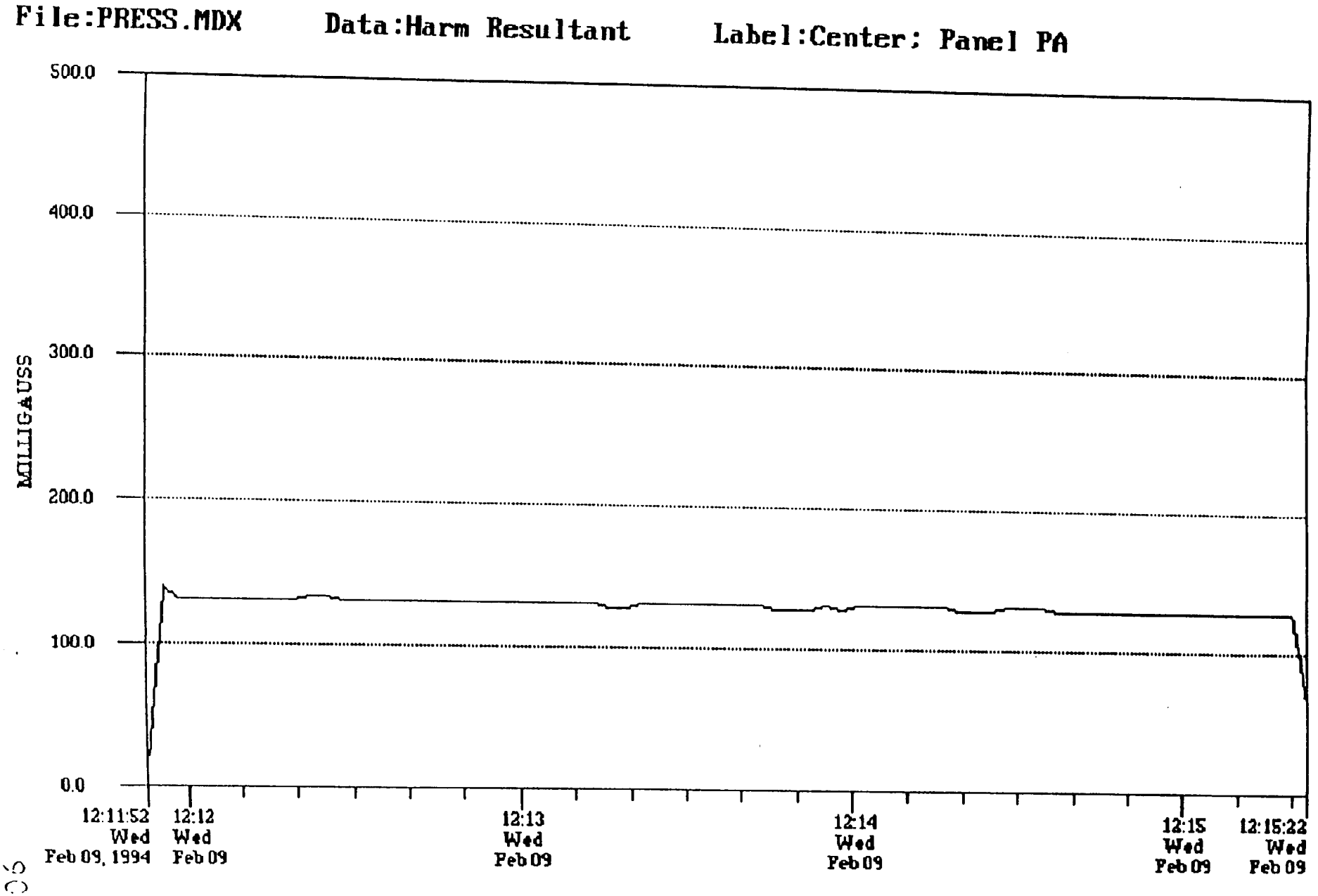

KSC-DF-571

Fig. 73

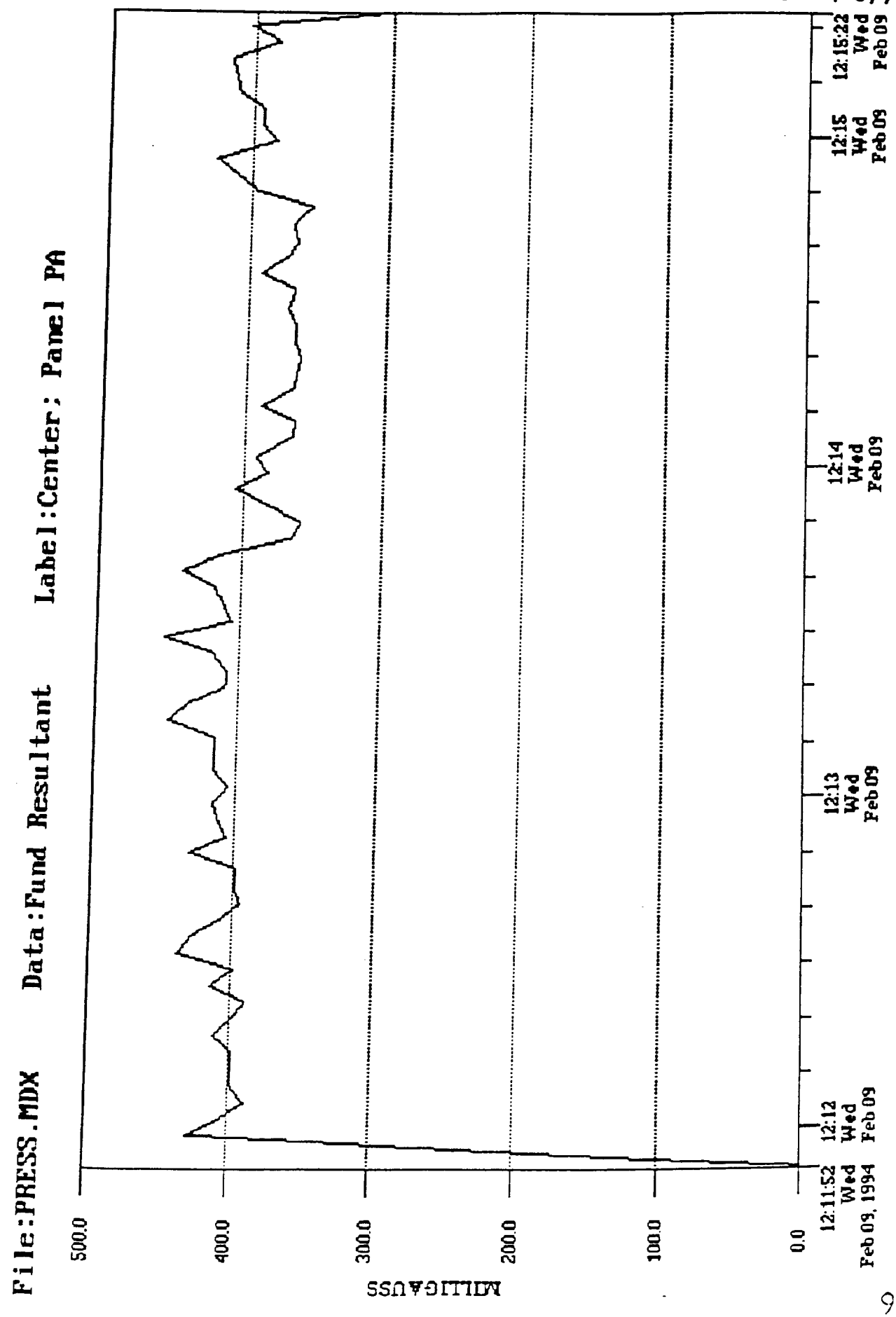
File:PRESS.MDX
Data:Fund Resultant
Label:Center; Panel PA
MILLIGAUSS
500.0
400.0
300.0
200.0
100.0
0.0
12:11:52 Wed Feb 09, 1994
12:12 Wed Feb 09
12:13 Wed Feb 09
12:14 Wed Feb 09
12:15 Wed Feb 09
12:15:22 Wed Feb 09

Fig. 74

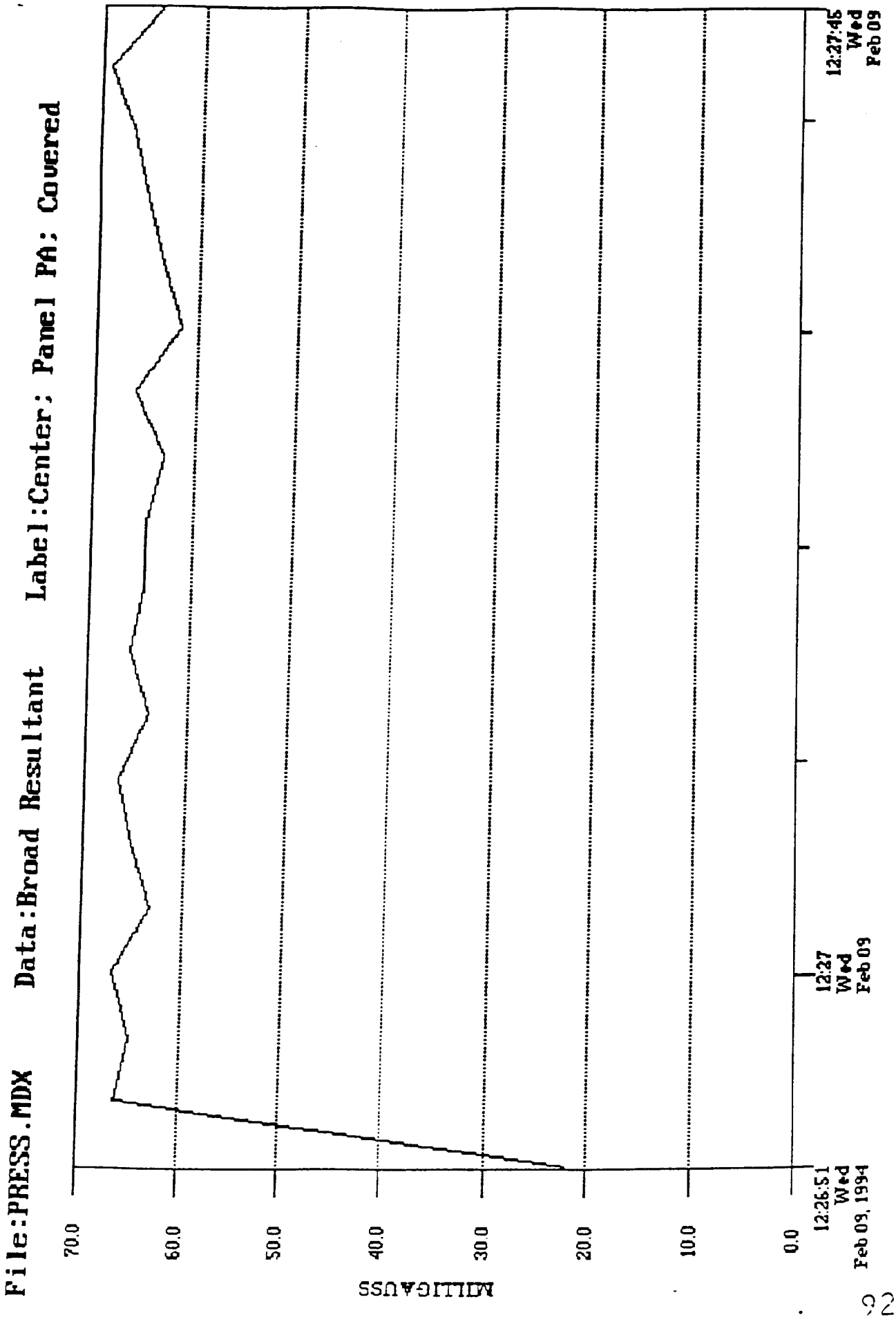
File:PRESS.MDX
Data:Broad Resultant
Label:Center: Panel PA: Covered
MILLIGAUSS
70.0
60.0
50.0
40.0
30.0
20.0
10.0
0.0
12:26:51
Wed
Feb 09, 1994
12:27
Wed
Feb 09
12:27:45
Wed
Feb 09

Fig. 75

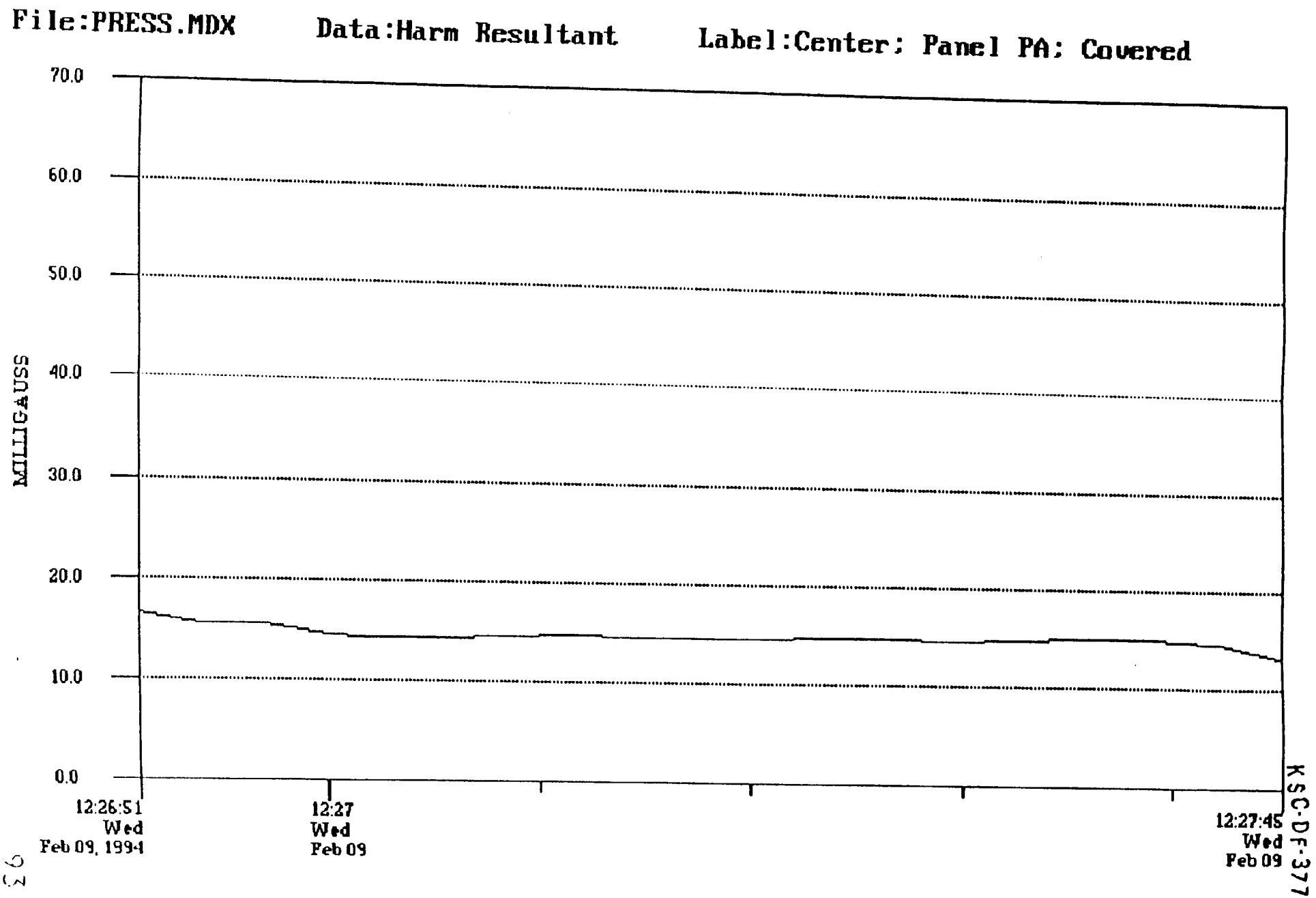
File:PRESS.MDX
Data:Harm Resultant
Label:Center; Panel PA; Covered
70.0
60.0
50.0
40.0
30.0
20.0
10.0
0.0
MILLIGAUSS
12:26:51
Wed
Feb 09, 1994
12:27
Wed
Feb 09
12:27:45
Wed
Feb 09
KSC-DF-3772

Fig. 76

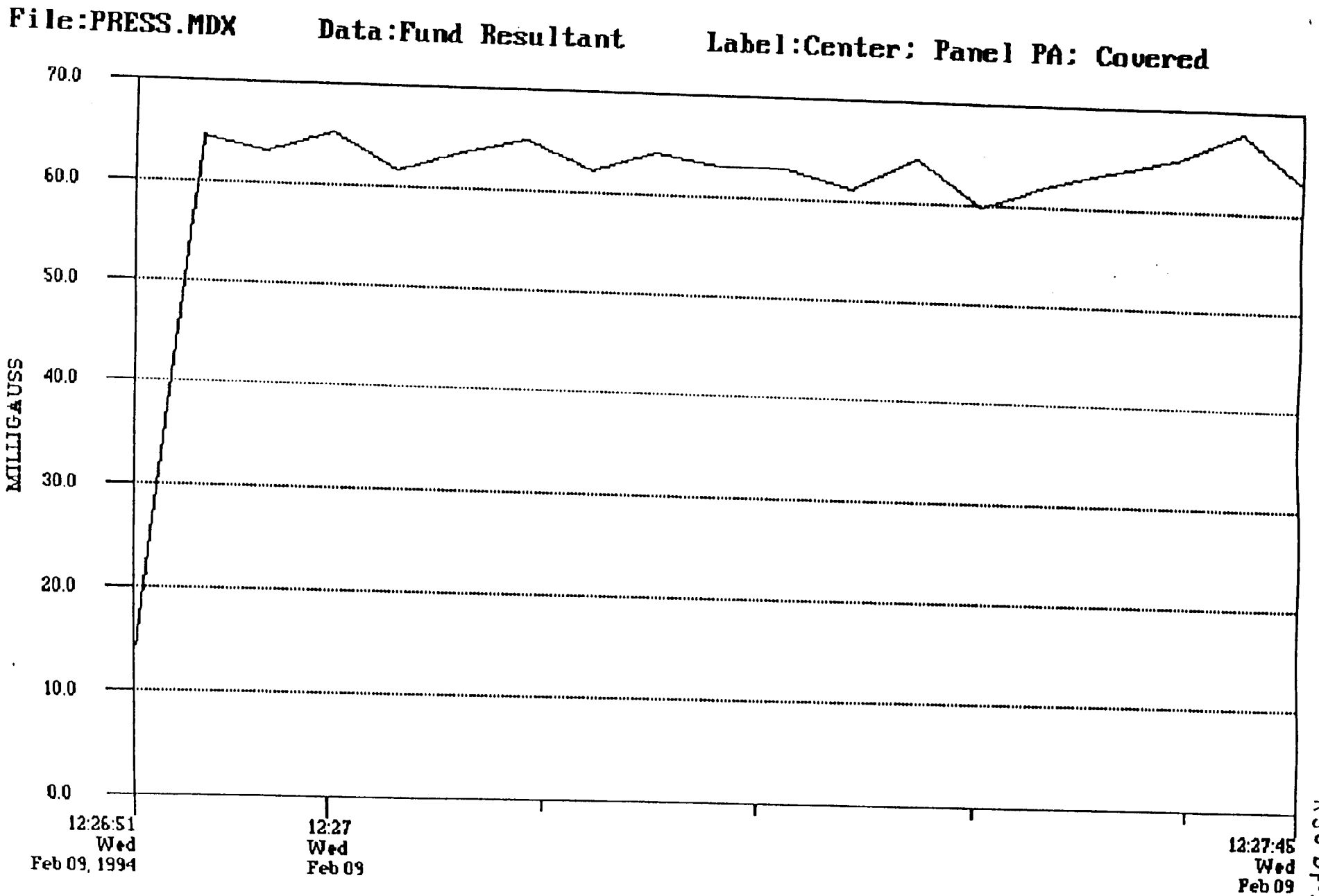

KSC-DF-3772

Fig. 77

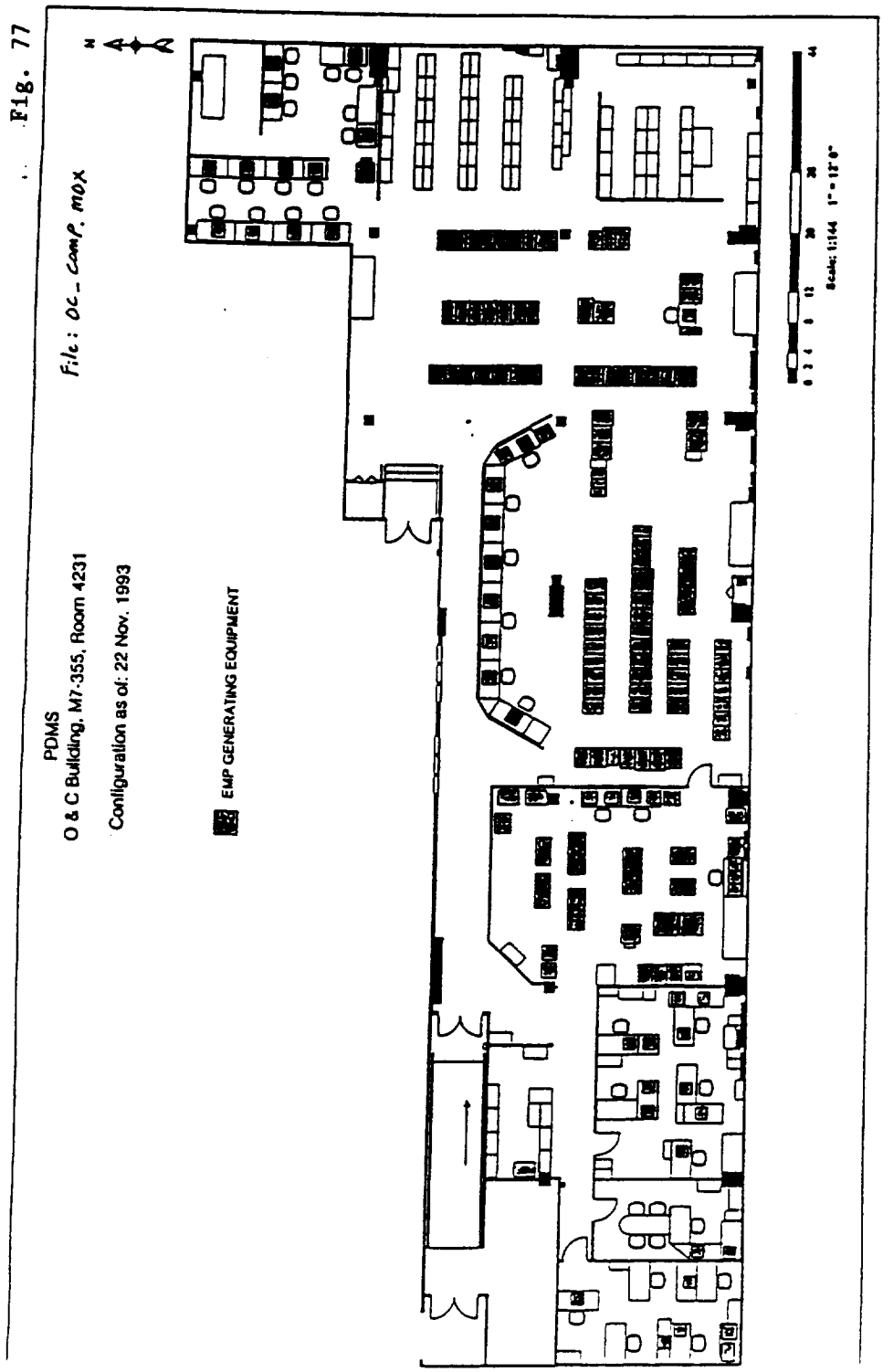
PDMS
O & C Building, M7-355, Room 4231
Configuration as of: 22 Nov. 1993
File: OC_comp. mox
EMP GENERATING EQUIPMENT

File:OC_COMP.MDX Data:Broad Resultant Label:Panel CRD-12P (#1) Fig. 78

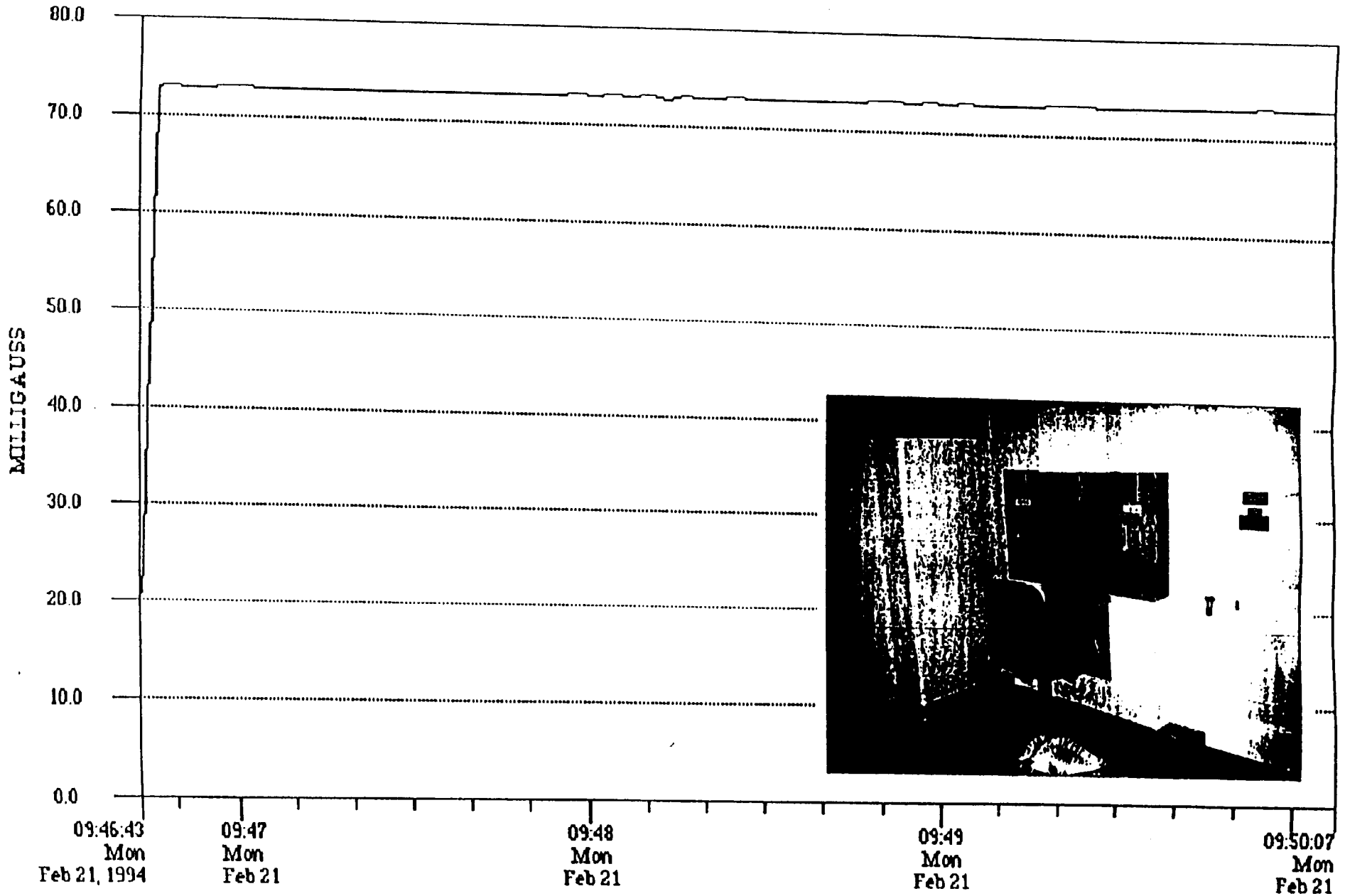

C-2

KSC-DF-3772

96

File:OC_COMP.MDX Data:Broad Resultant Label:Panel N6P (#2)

Fig.79

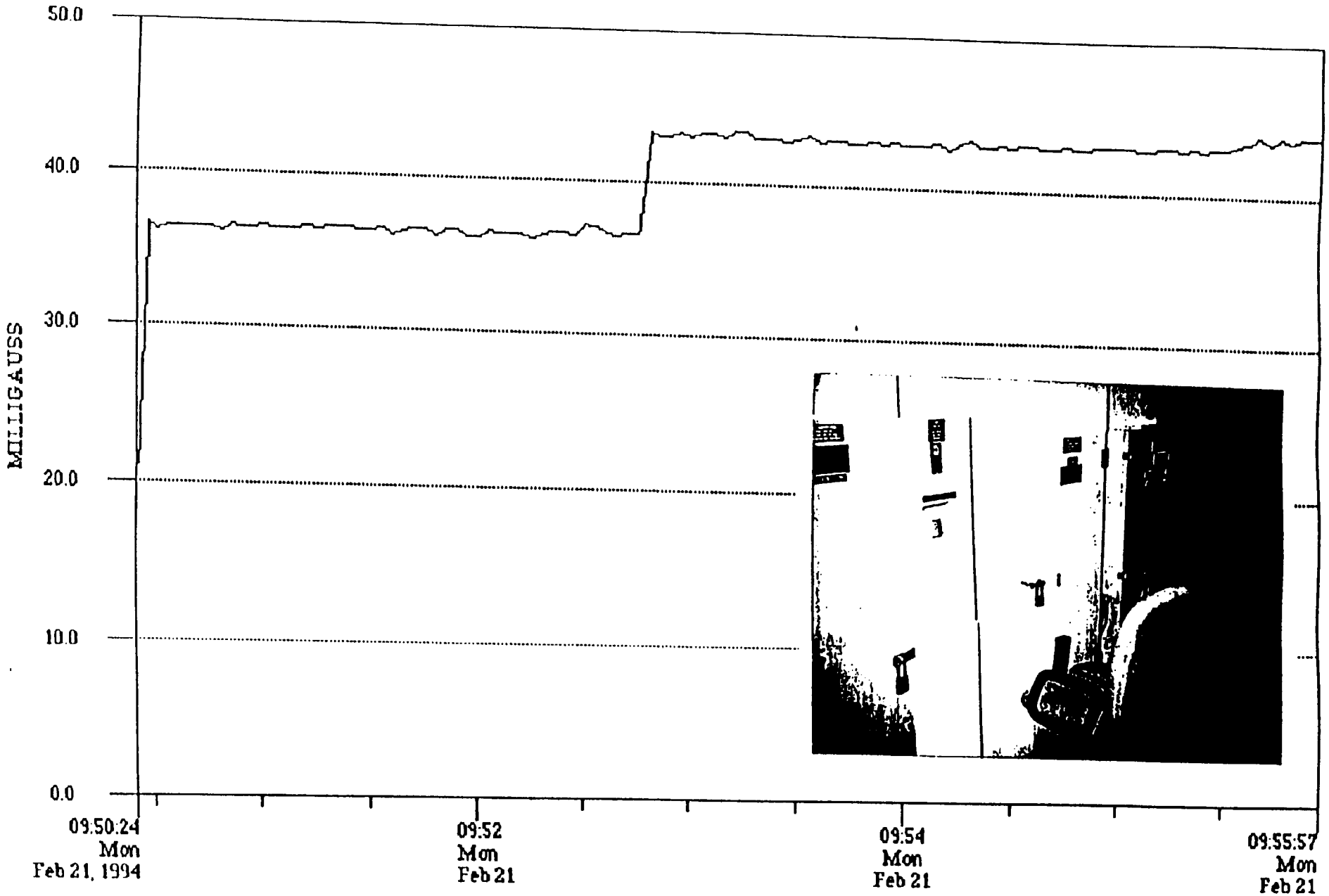

KSC-DF-377

File:OC_COMP.MDX Data:Broad Resultant Label:Panel CRD-4P (#3)

Fig. 80

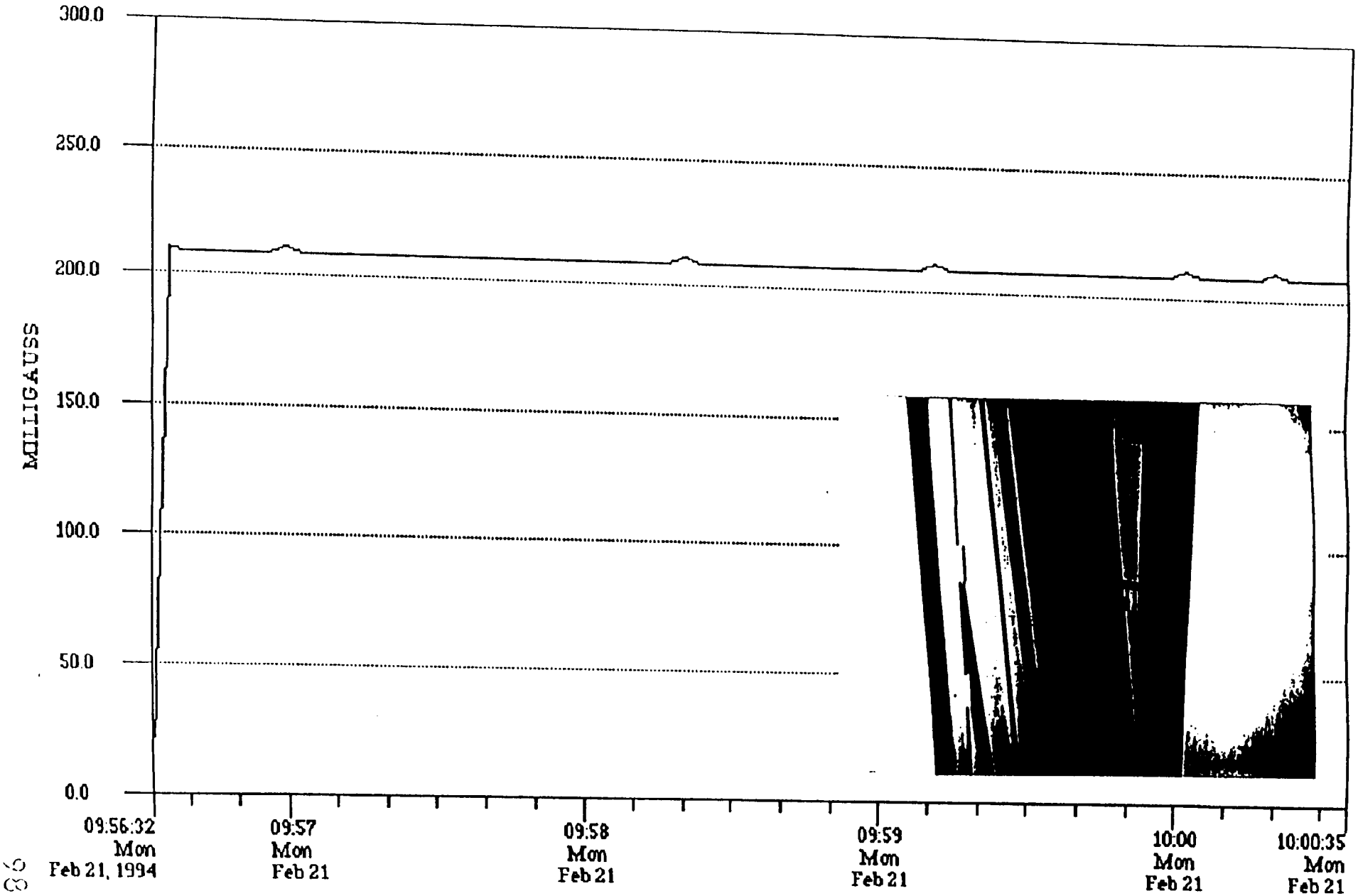

File:OC_COMP.MDX Data:Harm Resultant Label:Panel CRD-4P (#3)

Fig. 81

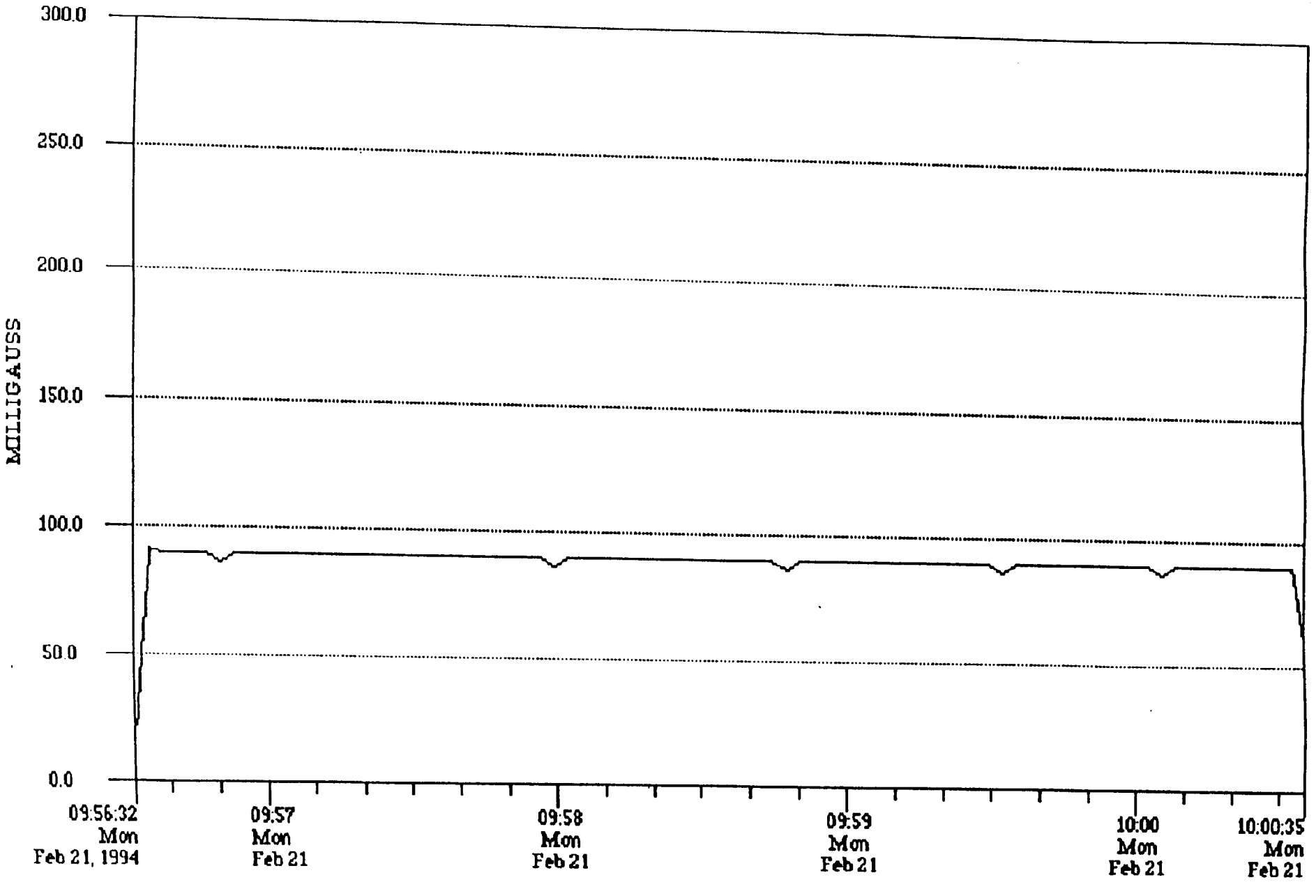

KSC-DF-3772

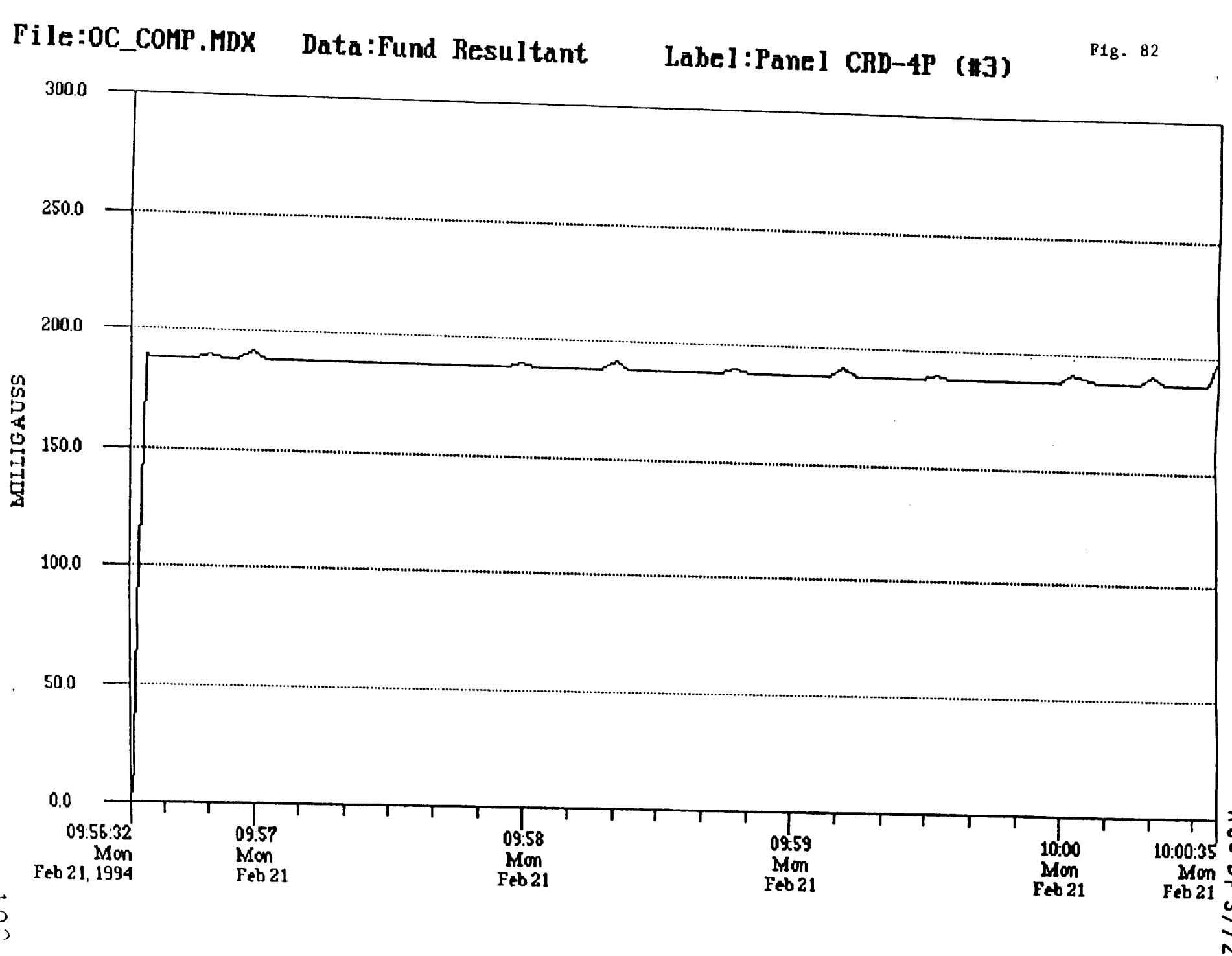
File:OC_COMP.MDX
Data:Fund Resultant
Label:Panel CRD-4P (#3)
Fig. 82
300.0
250.0
200.0
150.0
100.0
50.0
0.0
MILLIGAUSS
09:56:32
Mon
Feb 21, 1994
09:57
Mon
Feb 21
09:58
Mon
Feb 21
09:59
Mon
Feb 21
10:00
Mon
Feb 21
10:00:35
Mon
Feb 21
KSC-DF-3772

File:OC_COMP.MDX Data:Broad Resultant Label:Panel M1P (#4)

Fig. 83

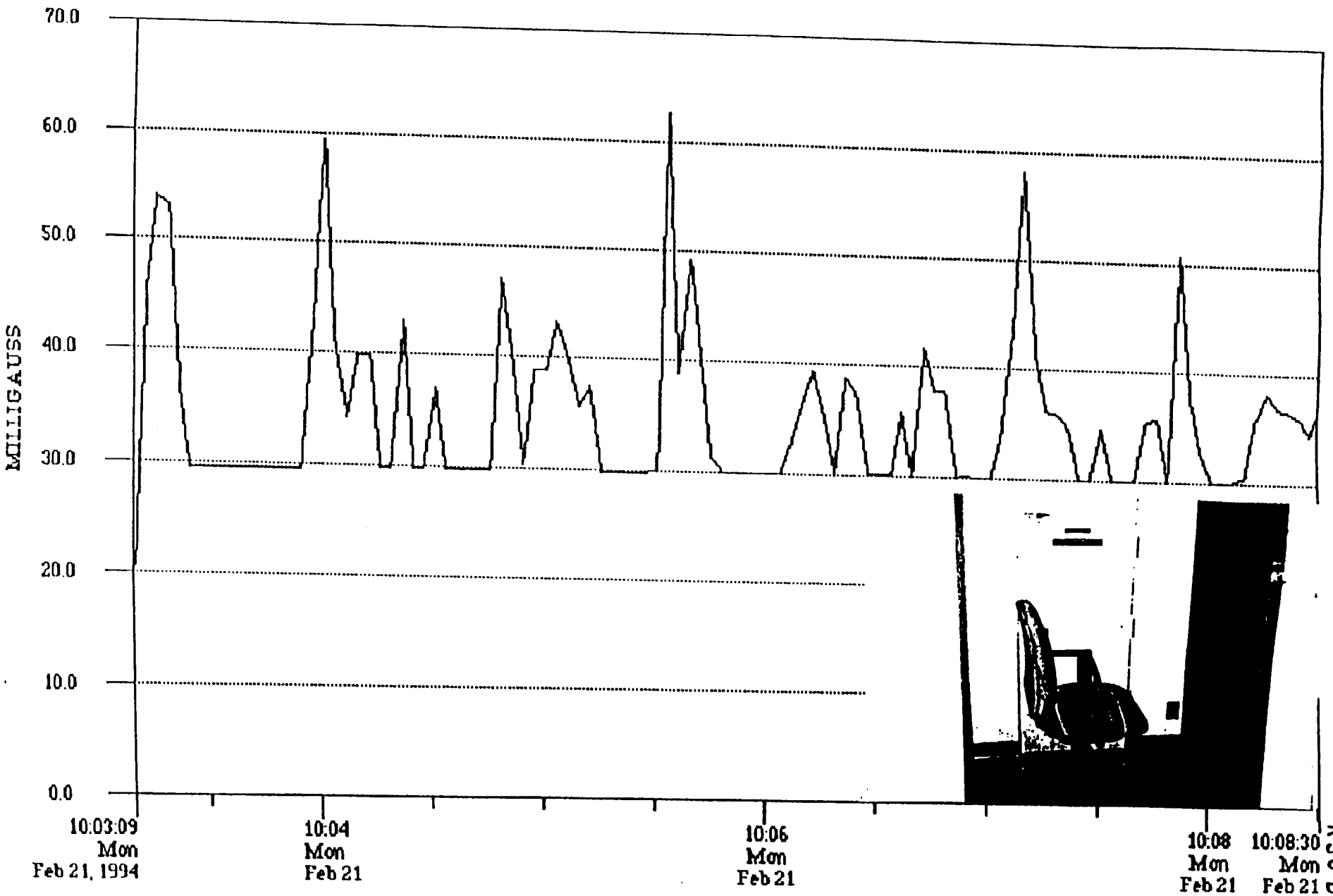

KSC-DF-377

File:OC_COMP.MDX Data:Broad Resultant Label:UPS No. 2 converter (#5)

Fig. 84

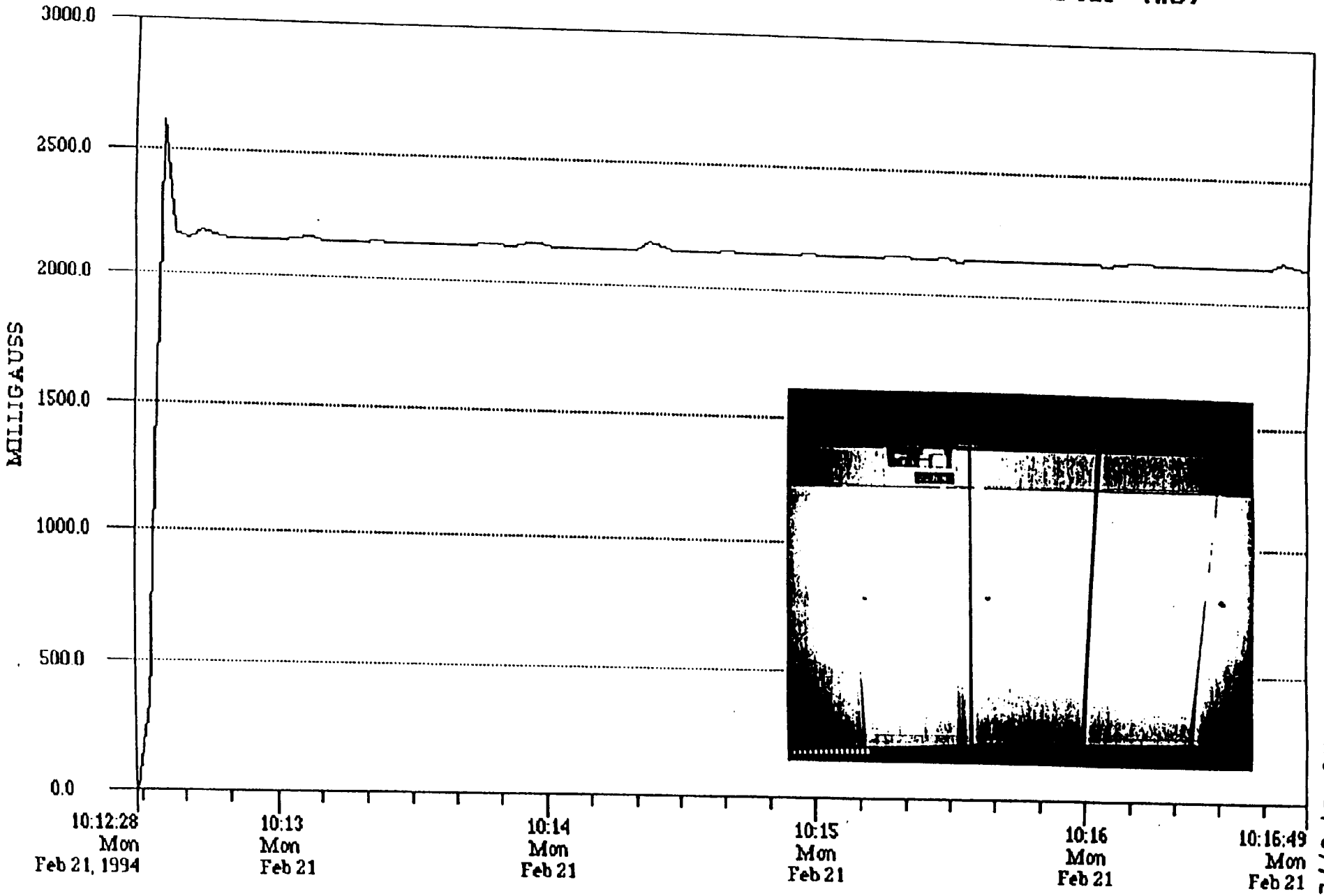

KSC-DF-3772

File:OC_COMP.MDX Data:Harm Resultant Label:UPS No. 2 converter (#5)

Fig. 85

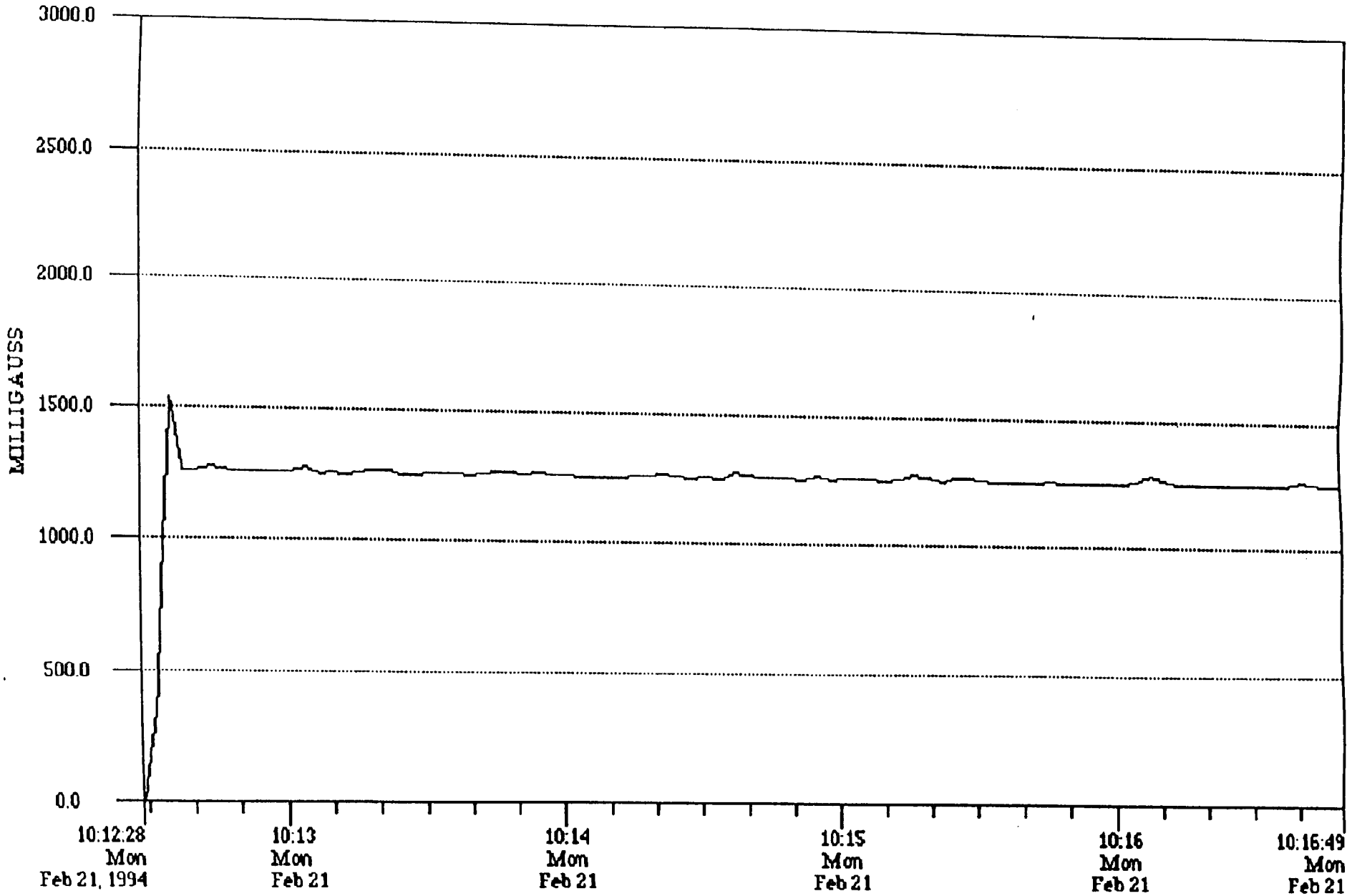

KSC-DF-3772

File:OC_COMP.MDX Data:Fund Resultant Label:UPS No. 2 converter (#5)

Fig. 86

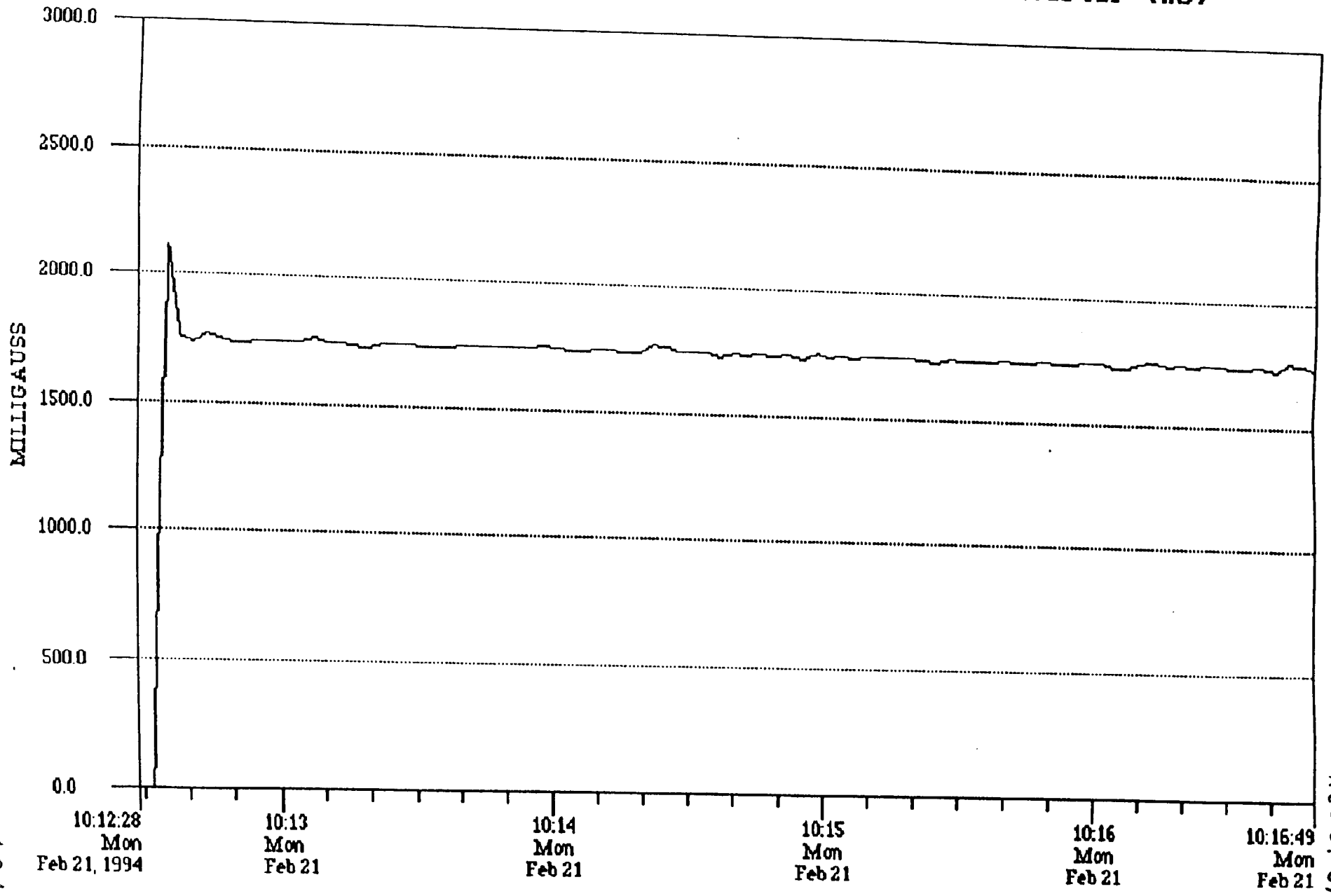

KSC-DF-3772

File:OC_COMP.MDX Data:Broad Resultant Label:UPS No. 2 2nd battery bank (6)

Fig. 87

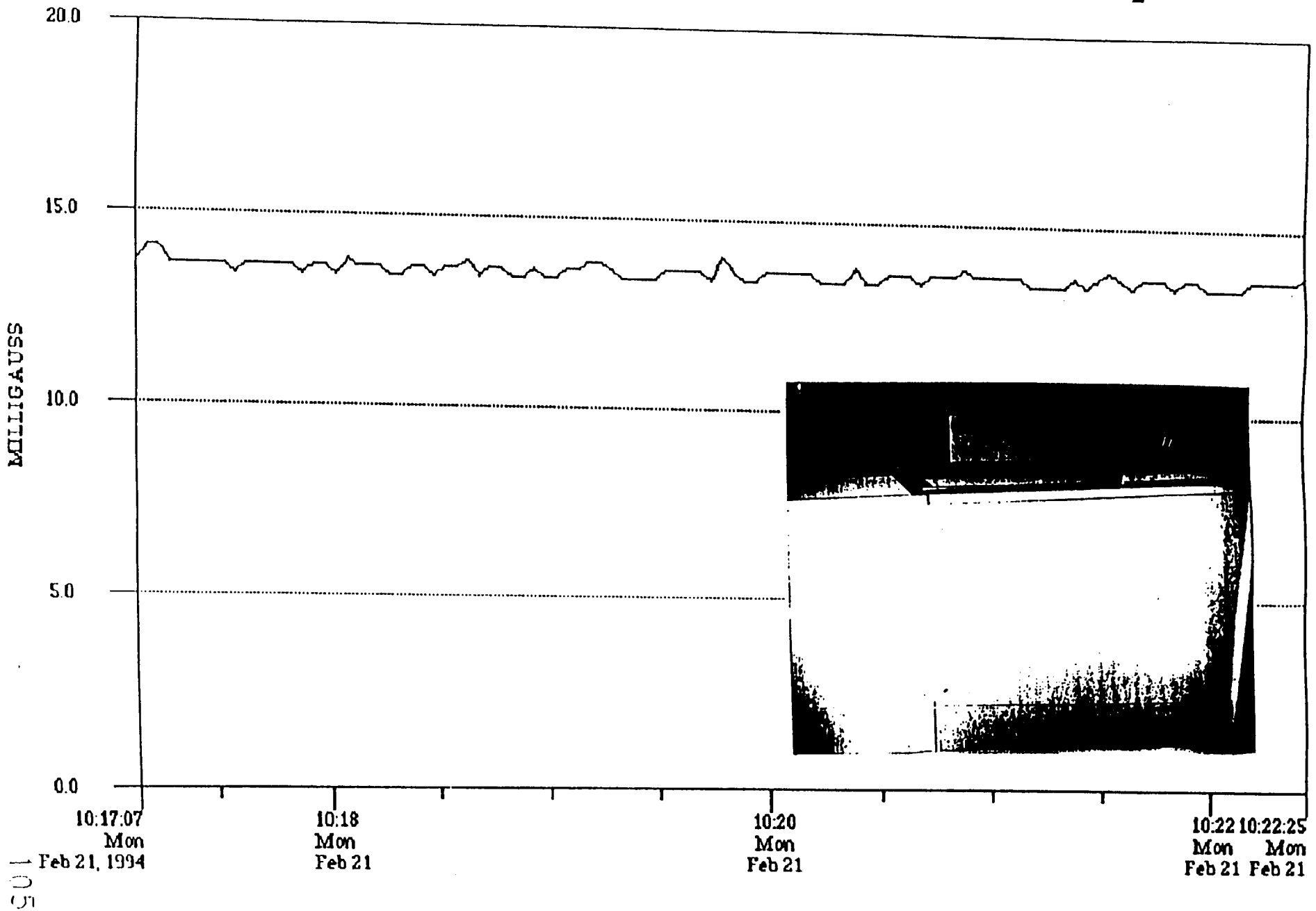

KSC-DF-3772

File:OC_COMP.MDX Data:Harm Resultant Label:UPS No. 2 2nd battery bank (6)

Fig. 88

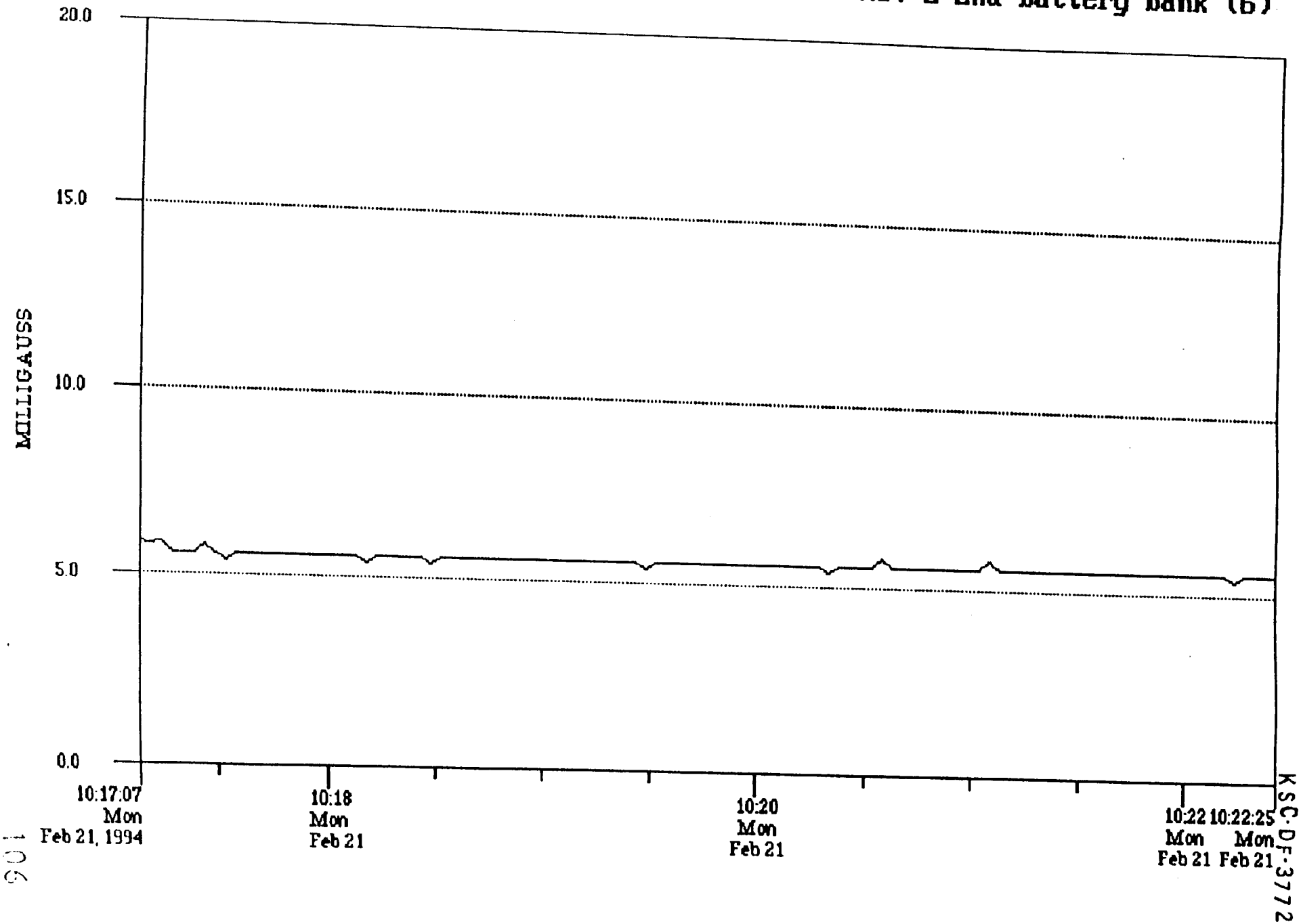

File:OC_COMP.MDX Data:Fund Resultant Label:UPS No. 2 2nd battery bank (6)

Fig. 89

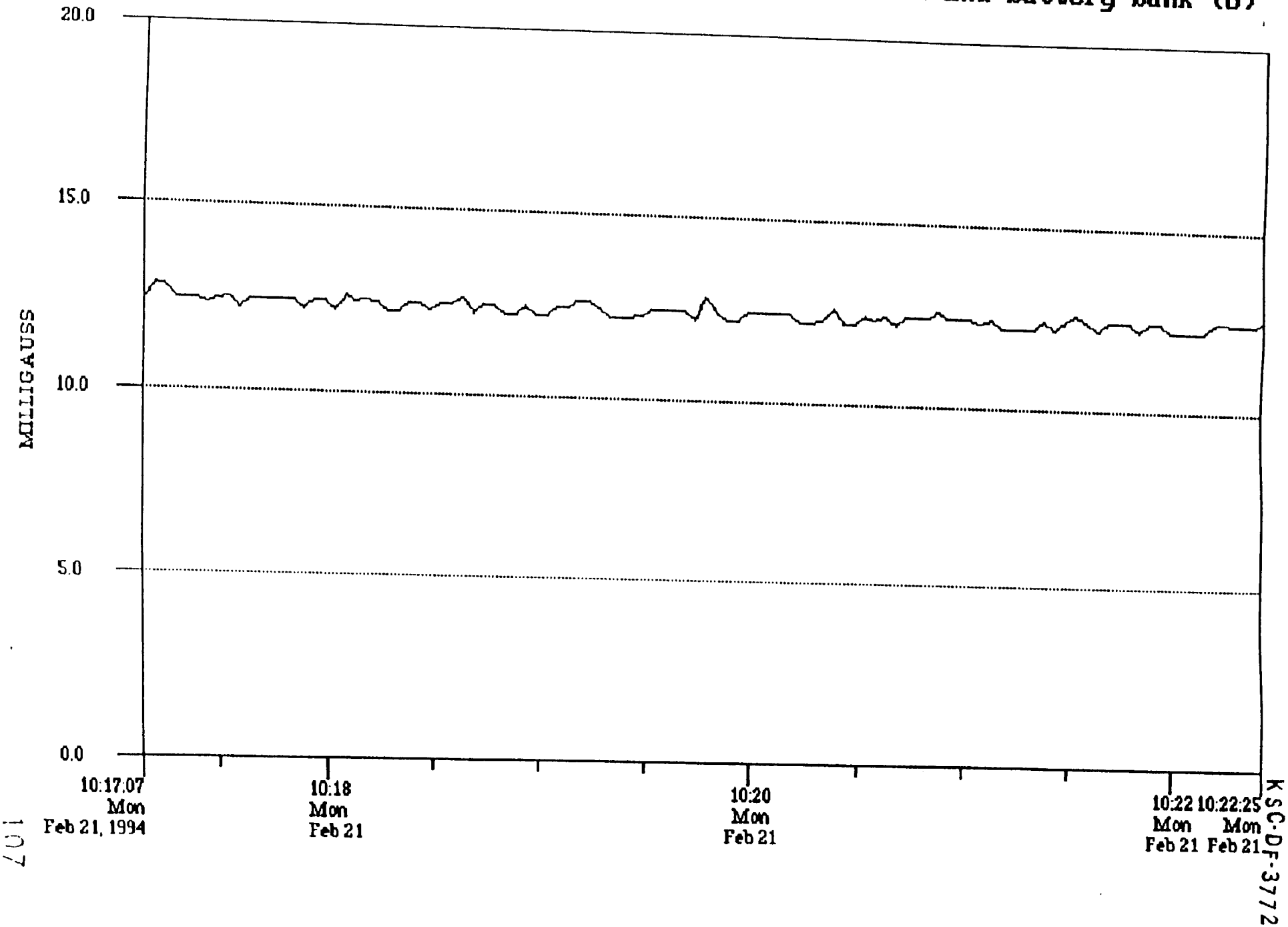

File:OC_COMP.MDX Data:Broad Resultant Label:UPS No. 2 back of conv/batt

Fig. 90

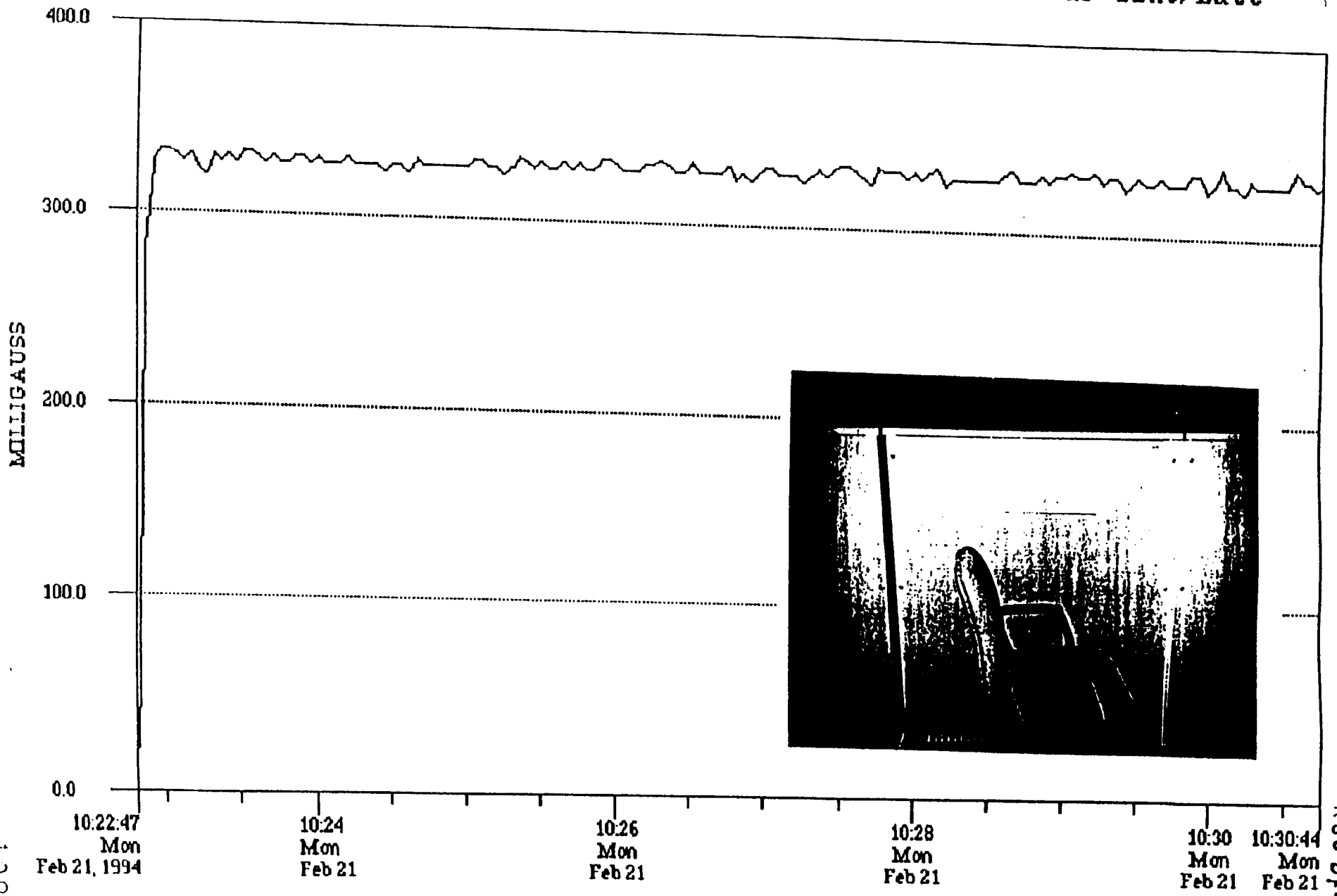

KSC-DF-3772

File:OC_COMP.MDX Data:Harm Resultant Label:UPS No. 2 back of conv/batt

Fig. 91

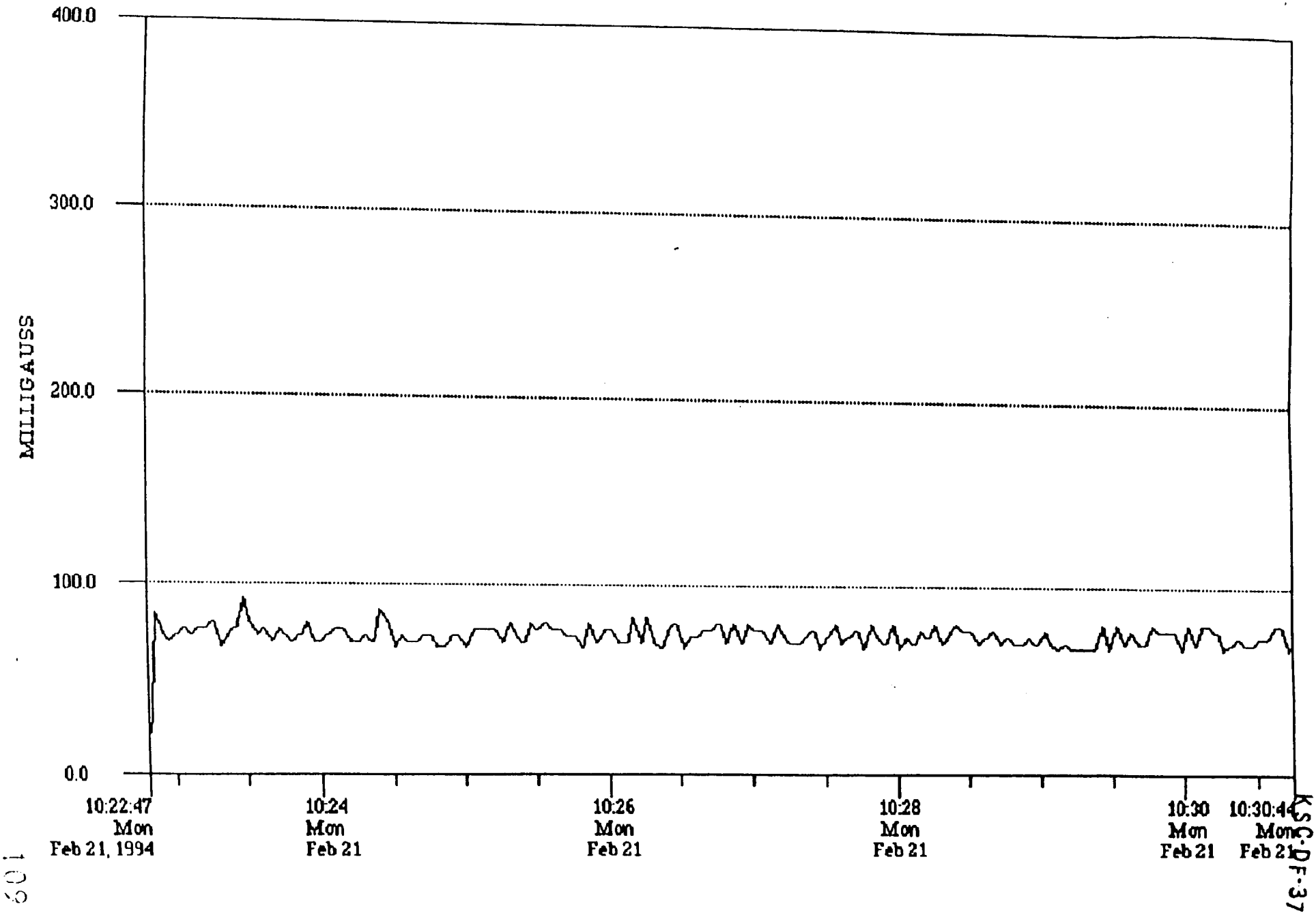

KSC-DF-377

File:OC_COMP.MDX Data:Fund Resultant Label:UPS No. 2 back of conv/batt

Fig. 92

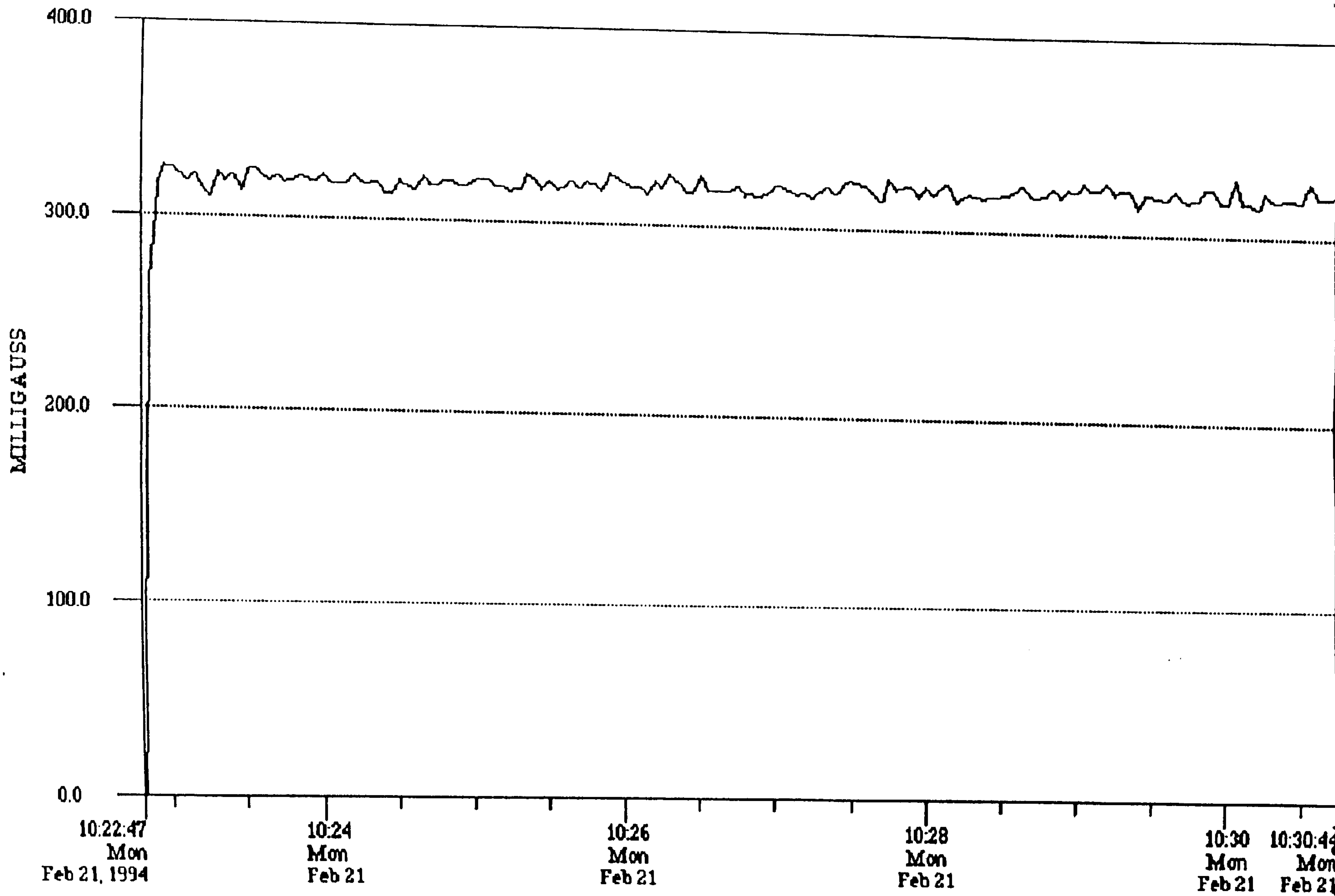

KSC-DF-377.

3.7 Shielding Measurements

In this section several panels were chosen to be shielded with different shielding materials. Figures 93 to 98 depict the results of this shielding. In Figure 93 the level of the magnetic field is about 35 mGauss (uncovered). For the covered case the magnetic field drops to 26 mGauss. In Figure 95 a sheet of Netic s3-6 (t=0.003) was used. The values get attenuated by about 10 mGauss. Next, in Figure 96, the Netic S3-6 (t=0.004) was tried and the level of the measured field dropped by about 12-13 mGauss with respect to the field of the covered panel. In Figure 97, the Conetic AA (t=0.004) attenuates the field by 17 mGauss, and finally in Figure 98, th Conetic AA (t=0.010) attenuates the field by 18 mGauss.

These results show that simple flat magnetic shielding sheets such as the Conetic type material can significantly shield electric panels. It is a very simple and rather inexpensive process.

To further demonstrate this point more testing was done on another panel with a different shielding arrangement. In here, the shield was placed with and without the original cover on. Again, different thicknesses and types of shielding materials were used. It can be seen from Figures 99 through 105 that the level of the magnetic field drops dramatically from 300 mG to 60 mG with proper shielding. The next table shows a direct comparison of these levels.

So one can see that shielding can drastically decrease the magnetic field level. What is also clear is that not every material can do the job. The AA type material did a much better job shielding fields than the S3-6 type even though a thicker S3-6 sheet was use.

Magnetic field levels from shielded and unshielded panels

case or panel	Max. value in mG
with out original cover	320
with original cover	110
without cover, shielded by s3-6 (t=0.004)	200
without cover, shielded by AA (t=0.004)	80
without cover, shielded by s3-6 (t=0.030)	250
without cover, shielded by AA (t=0.01)	60
without cover, shielded by AA (t=0.025)	60

Fig. 93

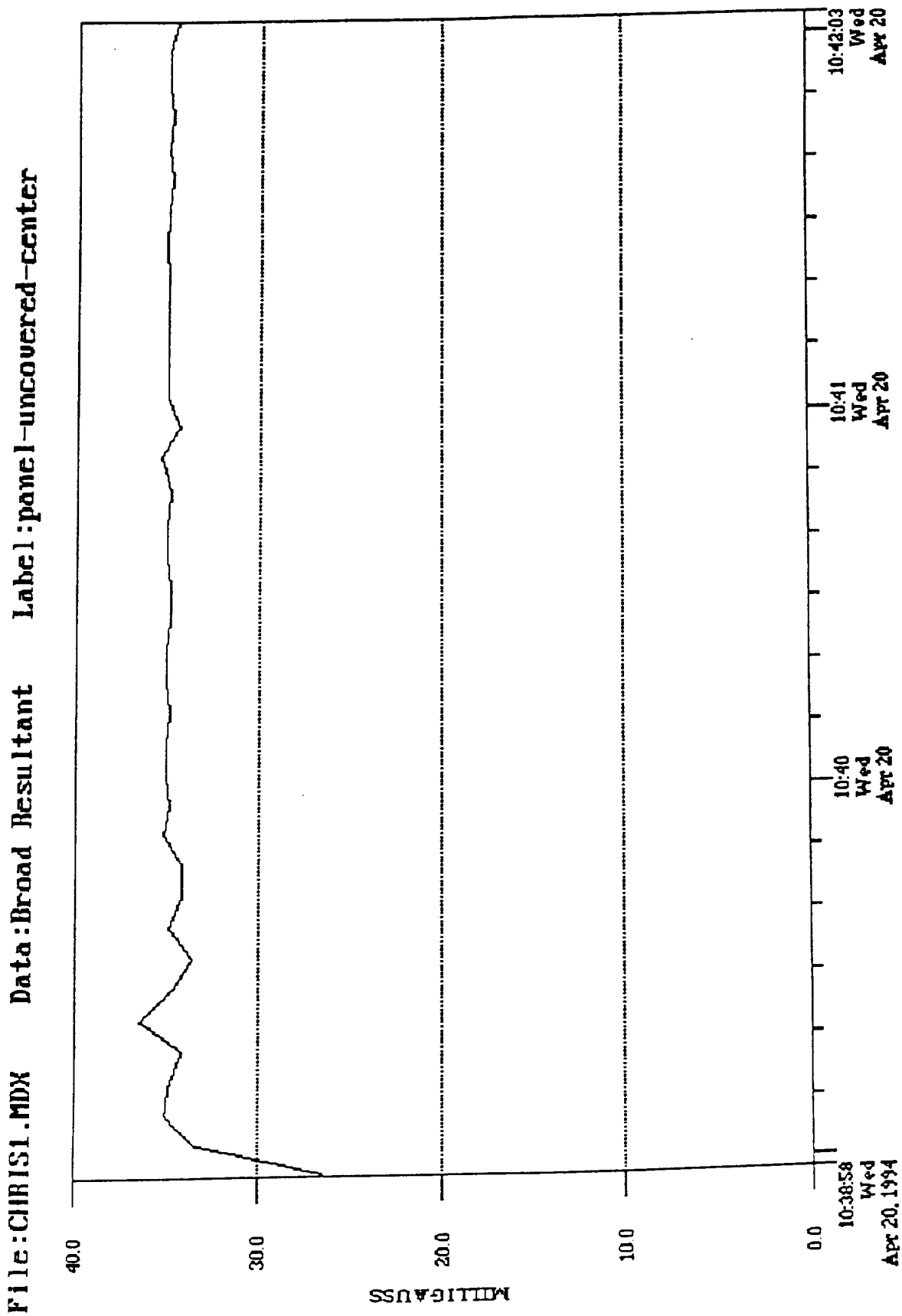
File:CIRIS1.MDX
Data:Broad Resultant
Label:panel-uncovered-center
MILLIGAUSS
40.0
30.0
20.0
10.0
0.0
10:38:58 Wed Apr 20,1994
10:40 Wed Apr 20
10:41 Wed Apr 20
10:42:03 Wed Apr 20

Fig. 94

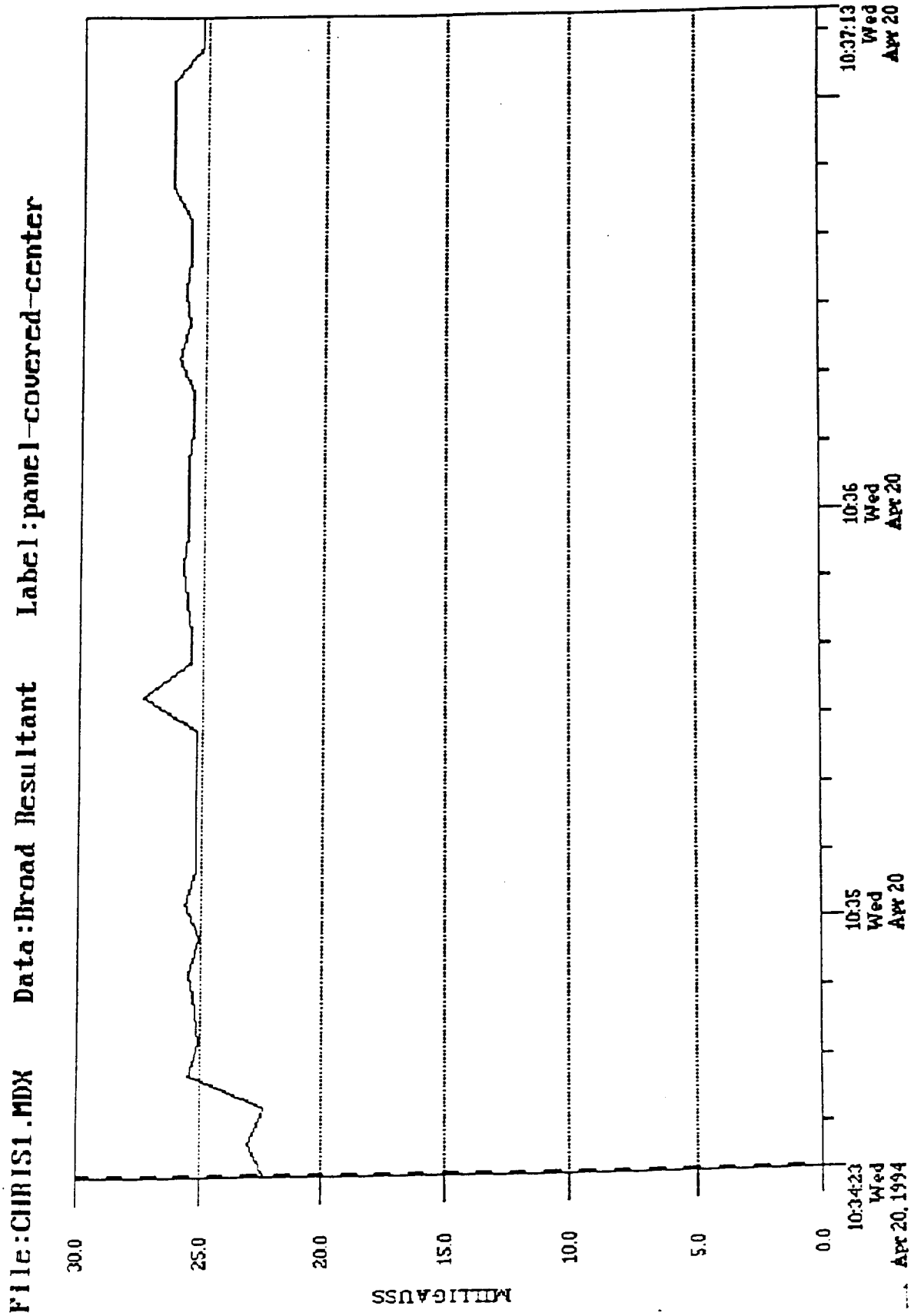
File:CHRIS1.MDX
Data:Broad Resultant
Label:panel-covered-center
MILLIGAUSS
30.0
25.0
20.0
15.0
10.0
5.0
0.0
10:34:23 Wed Apr 20, 1994
10:35 Wed Apr 20
10:36 Wed Apr 20
10:37:13 Wed Apr 20

Fig. 95

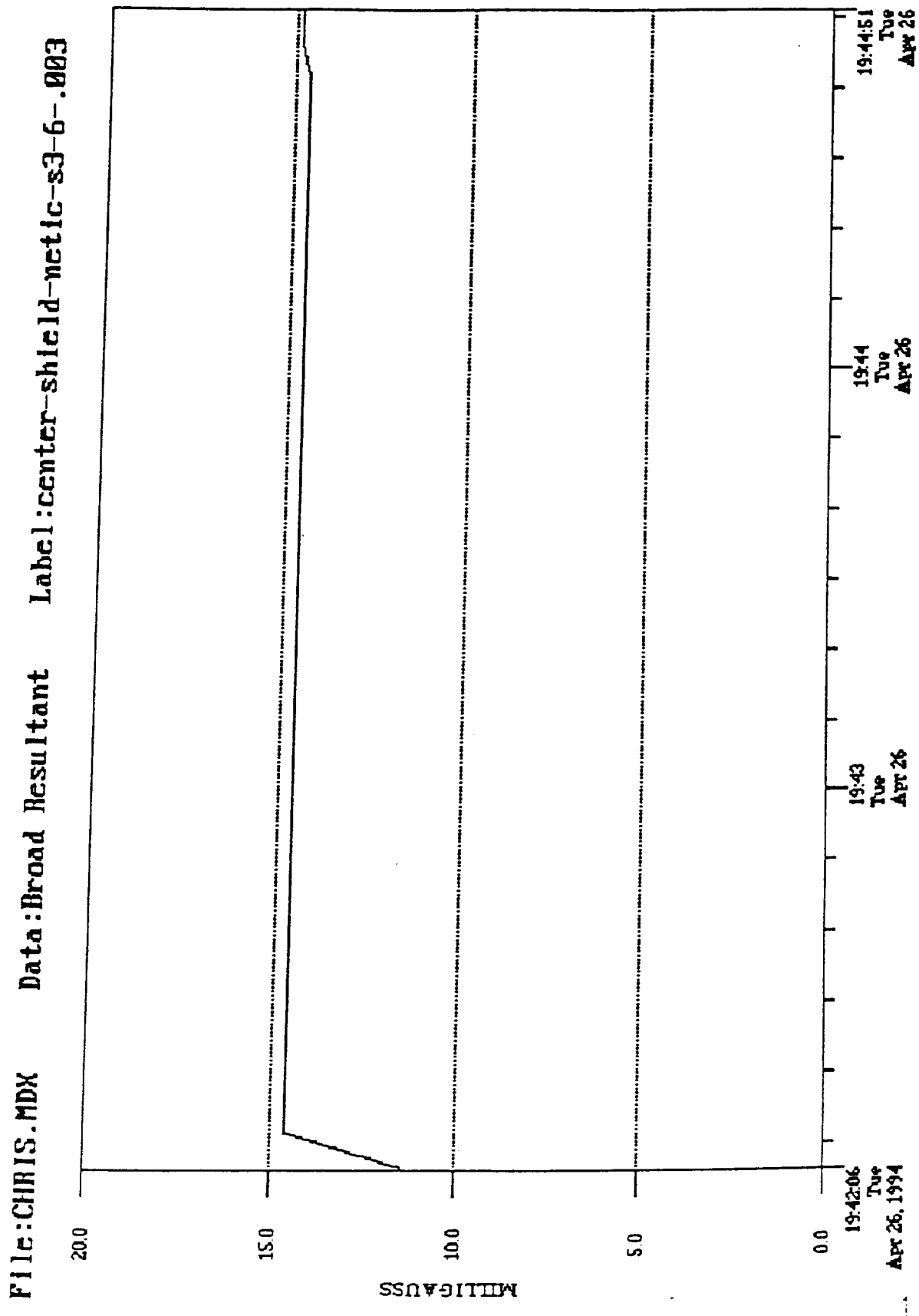
File:CHRIS.MDX
Data:Broad Resultant
Label:center-shield-metic-s3-6-.003
MILLIGAUSS
20.0
15.0
10.0
5.0
0.0
19:42:06 Tue Apr 26, 1994
19:43 Tue Apr 26
19:44 Tue Apr 26
19:44:51 Tue Apr 26

Fig. 96

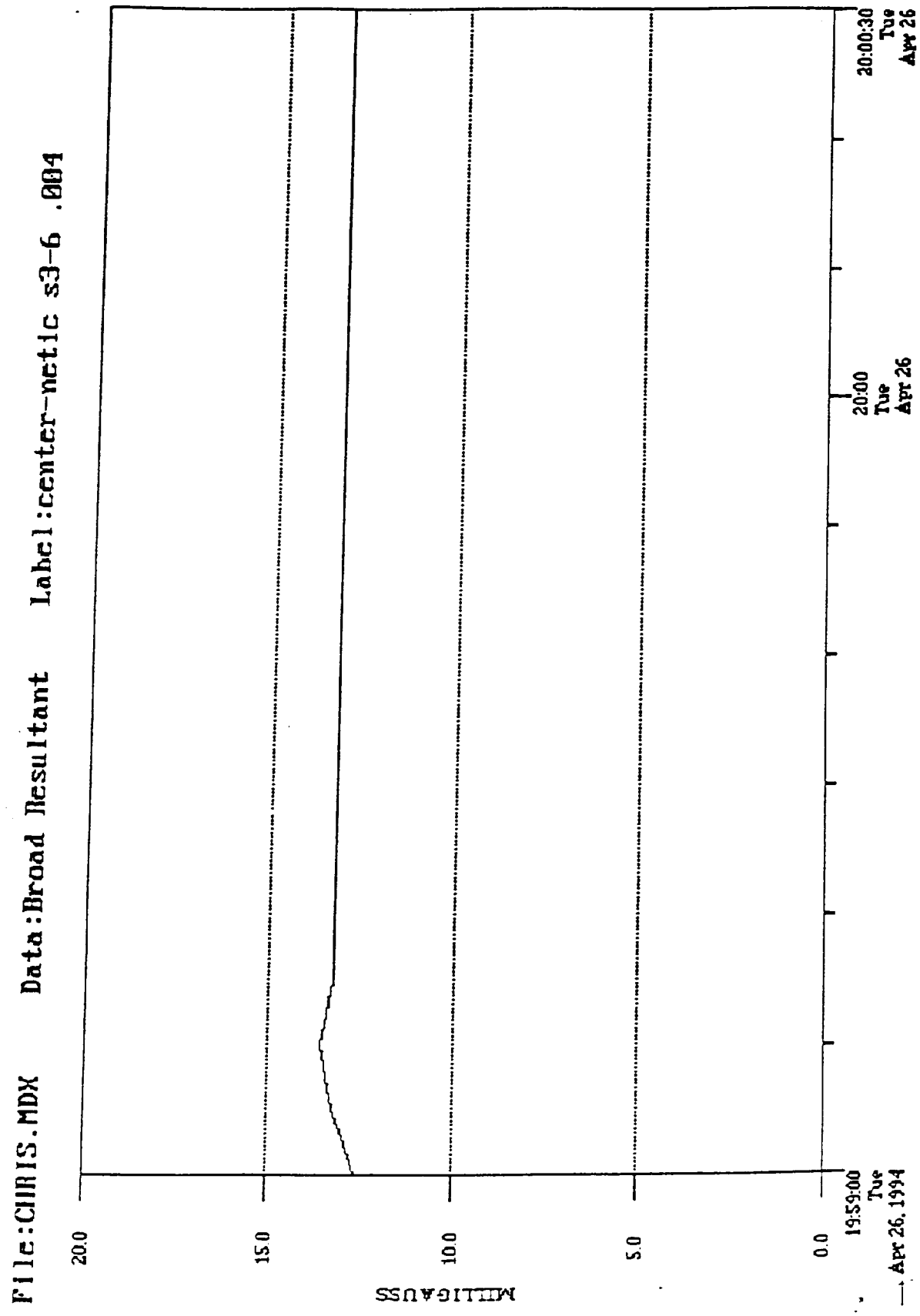
File:CHRIS.MDX
Data:Broad Resultant
Label:center-netic s3-6 .004
MILLIGAUSS
20.0
15.0
10.0
5.0
0.0
19:59:00
Tue
Apr 26, 1994
20:00
Tue
Apr 26
20:00:30
Tue
Apr 26

Fig. 97

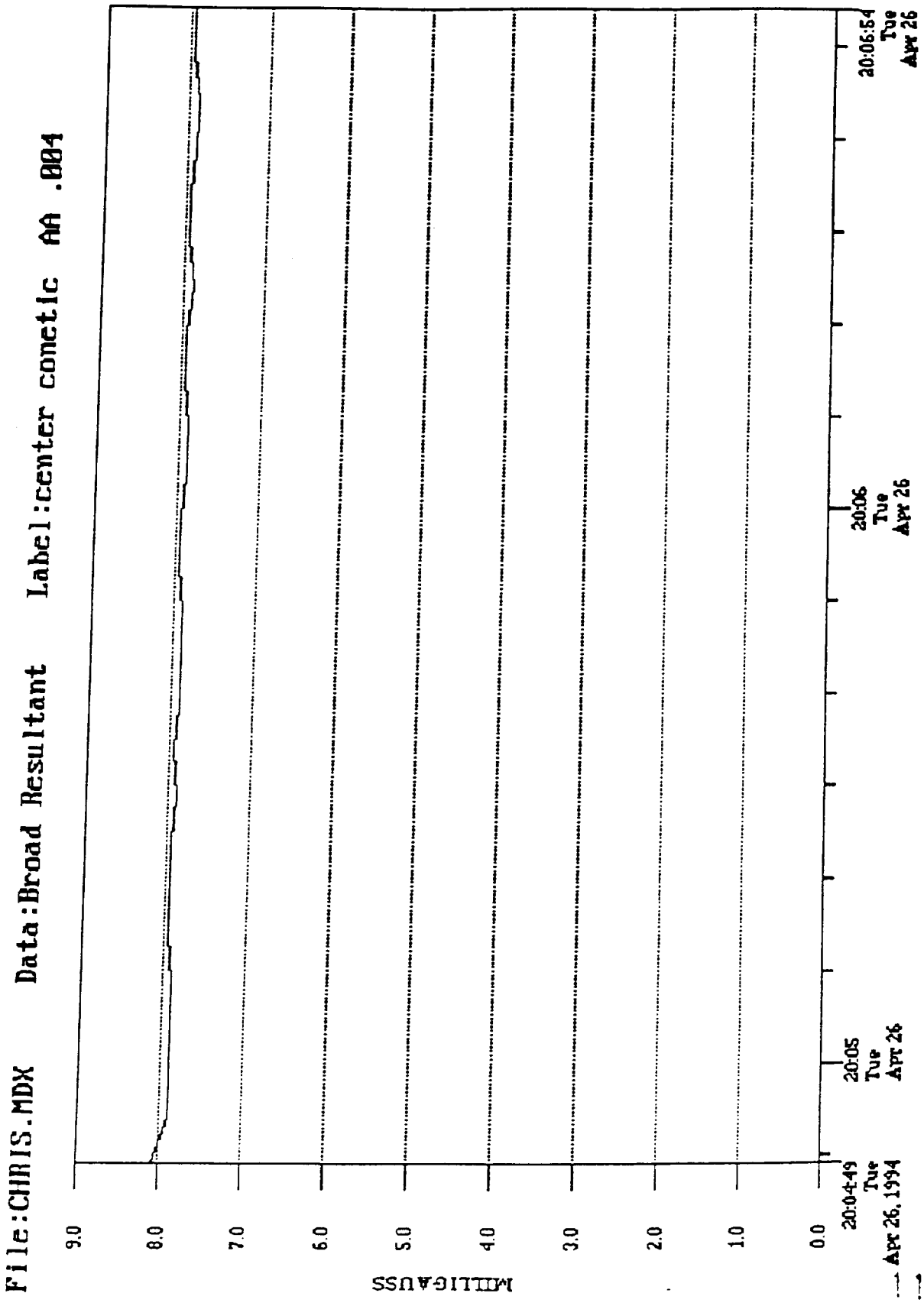
File:CHRIS.MDX
Data:Broad Resultant
Label:center cometic AA .004
MILLIGAUSS
9.0
8.0
7.0
6.0
5.0
4.0
3.0
2.0
1.0
0.0
20:04:49 Tue Apr 26, 1994
20:05 Tue Apr 26
20:06 Tue Apr 26
20:06:54 Tue Apr 26

Fig. 98

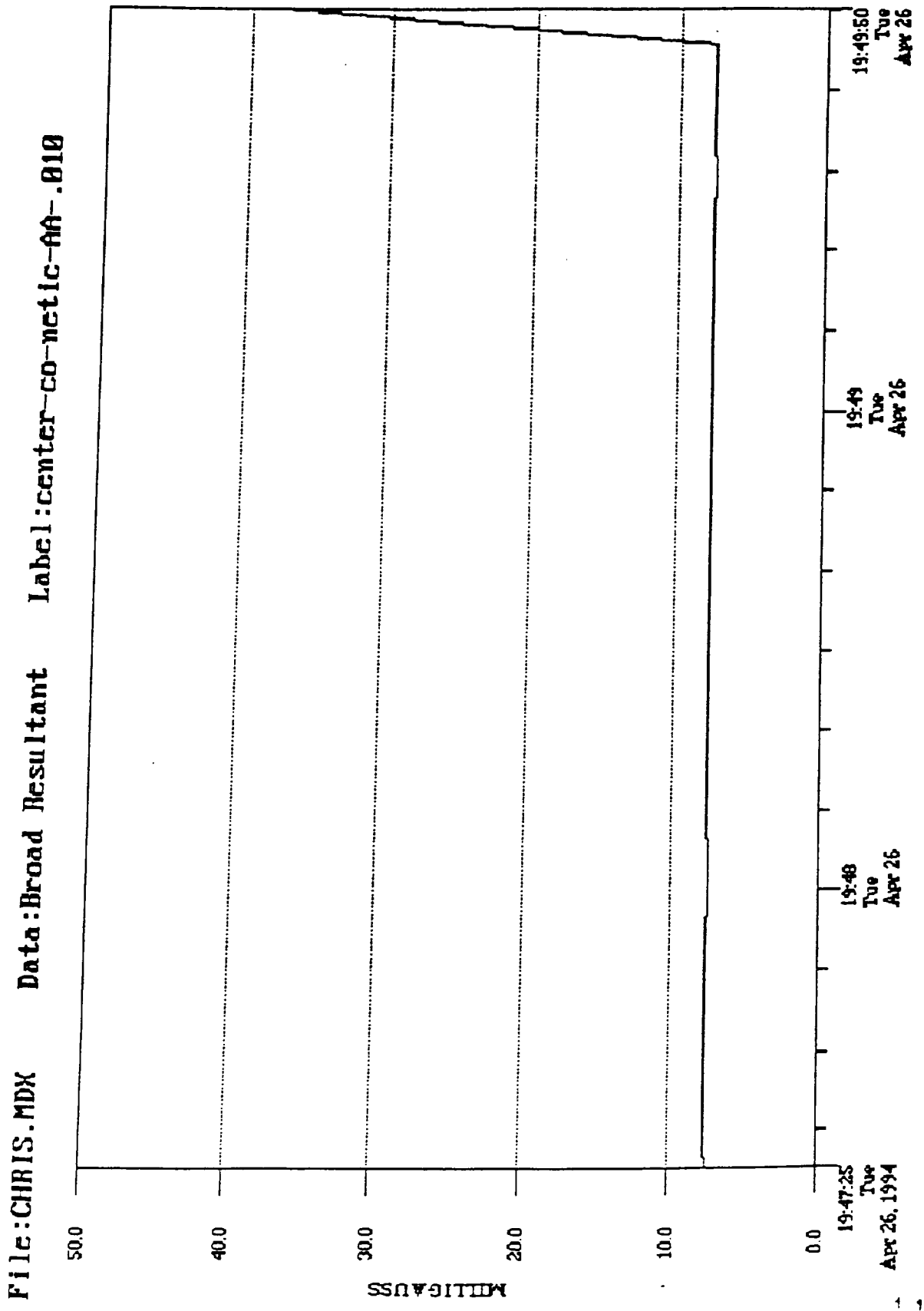
File:CHRIS.MDX
Data:Broad Resultant
Label:center-co-netic-AA-.810
MILLIGAUSS
50.0
40.0
30.0
20.0
10.0
0.0
19:47:25 Tue Apr 26, 1994
19:48 Tue Apr 26
19:49 Tue Apr 26
19:49:50 Tue Apr 26

Fig. 99

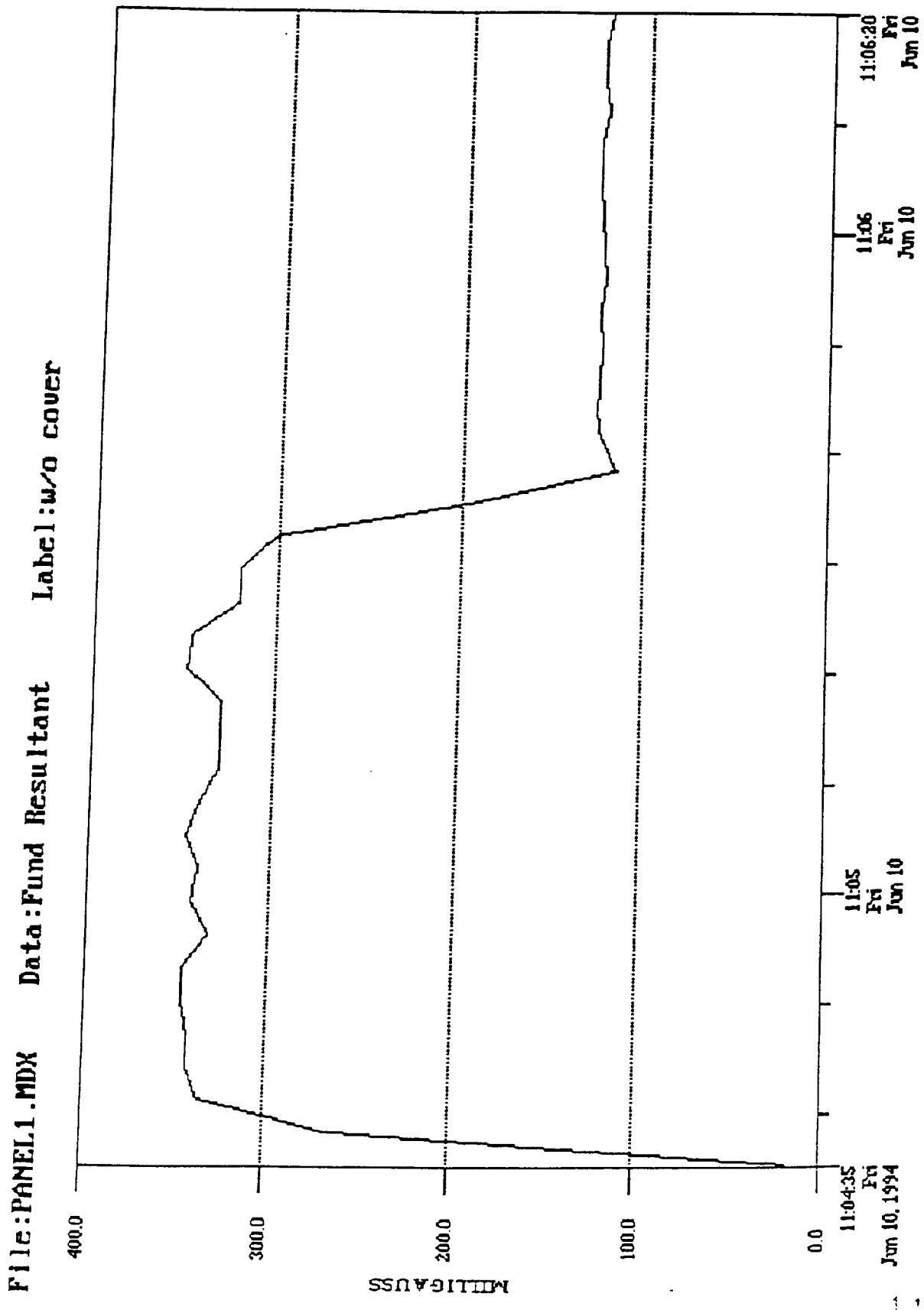
File:PANEL1.MDX
Data:Fund Resultant
Label:w/o cover
MILLIGAUSS
400.0
300.0
200.0
100.0
0.0
11:04:35 Fri Jun 10,1994
11:05 Fri Jun 10
11:06 Fri Jun 10
11:06:20 Fri Jun 10

Fig. 100

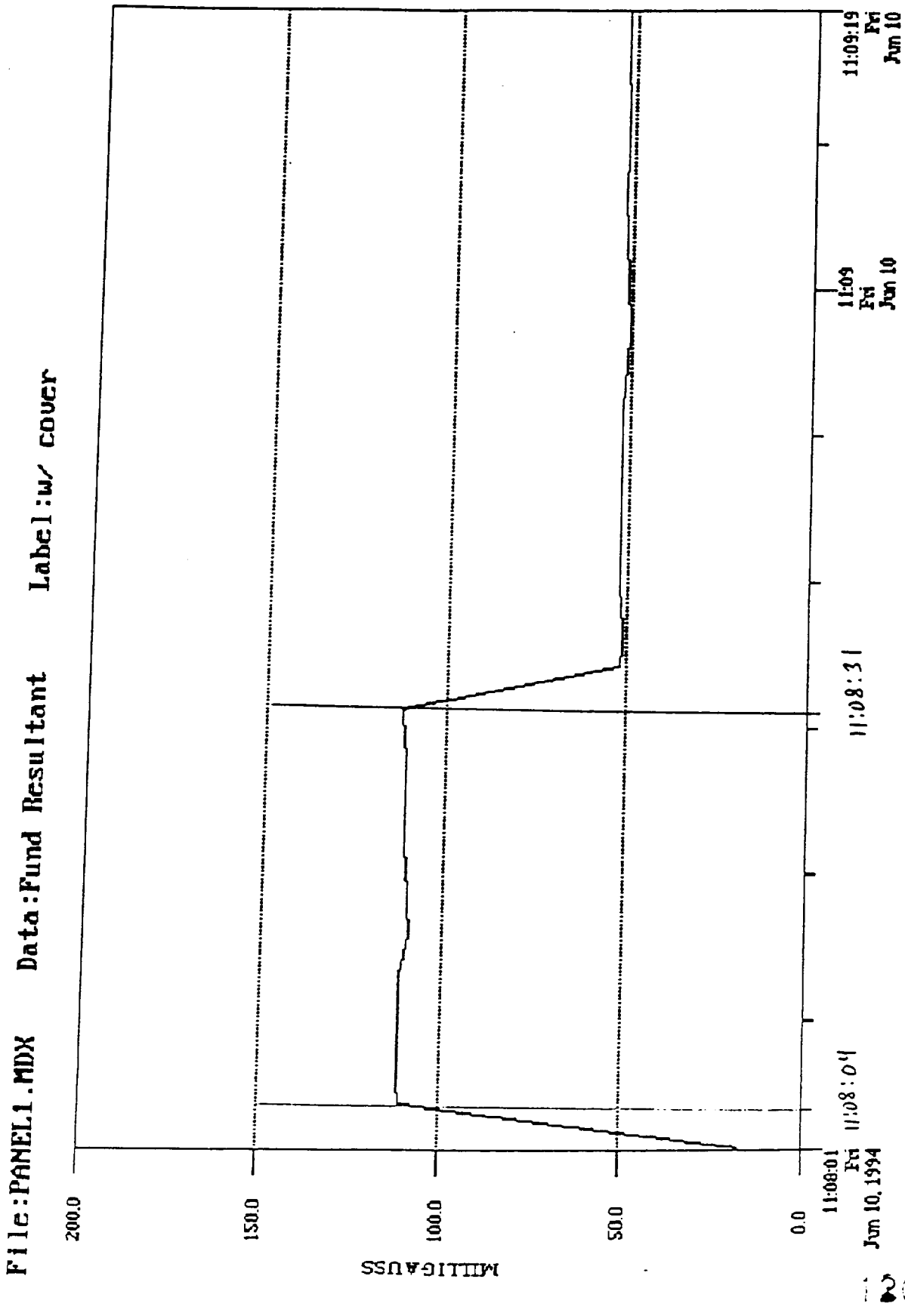
File:PANEL1.MDX
Data:Fund Resultant
Label:w/ cover
MILLIGAUSS
200.0
150.0
100.0
50.0
0.0
11:08:01
Fri
Jun 10, 1994
11:08:41
11:08:31
11:09
Fri
Jun 10
11:09:19
Fri
Jun 10

Fig. 101

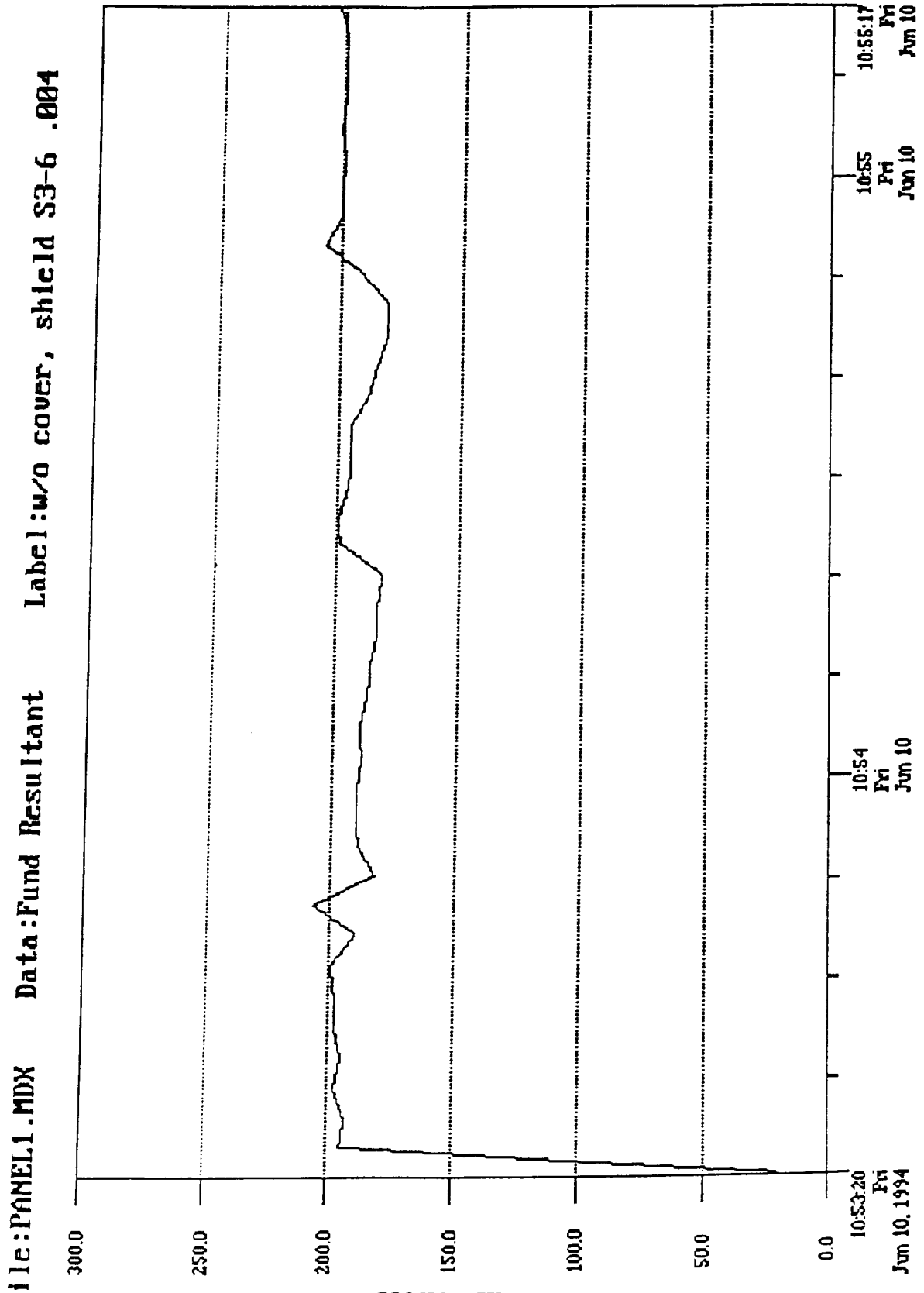
File:PANEL1.MDX
Data:Fund Resultant
Label:w/o cover, shield S3-6 .004
MILLIGAUSS
300.0
250.0
200.0
150.0
100.0
50.0
0.0
10:53:20 Fri Jun 10, 1994
10:54 Fri Jun 10
10:55 Fri Jun 10
10:56:17 Fri Jun 10

Fig. 102

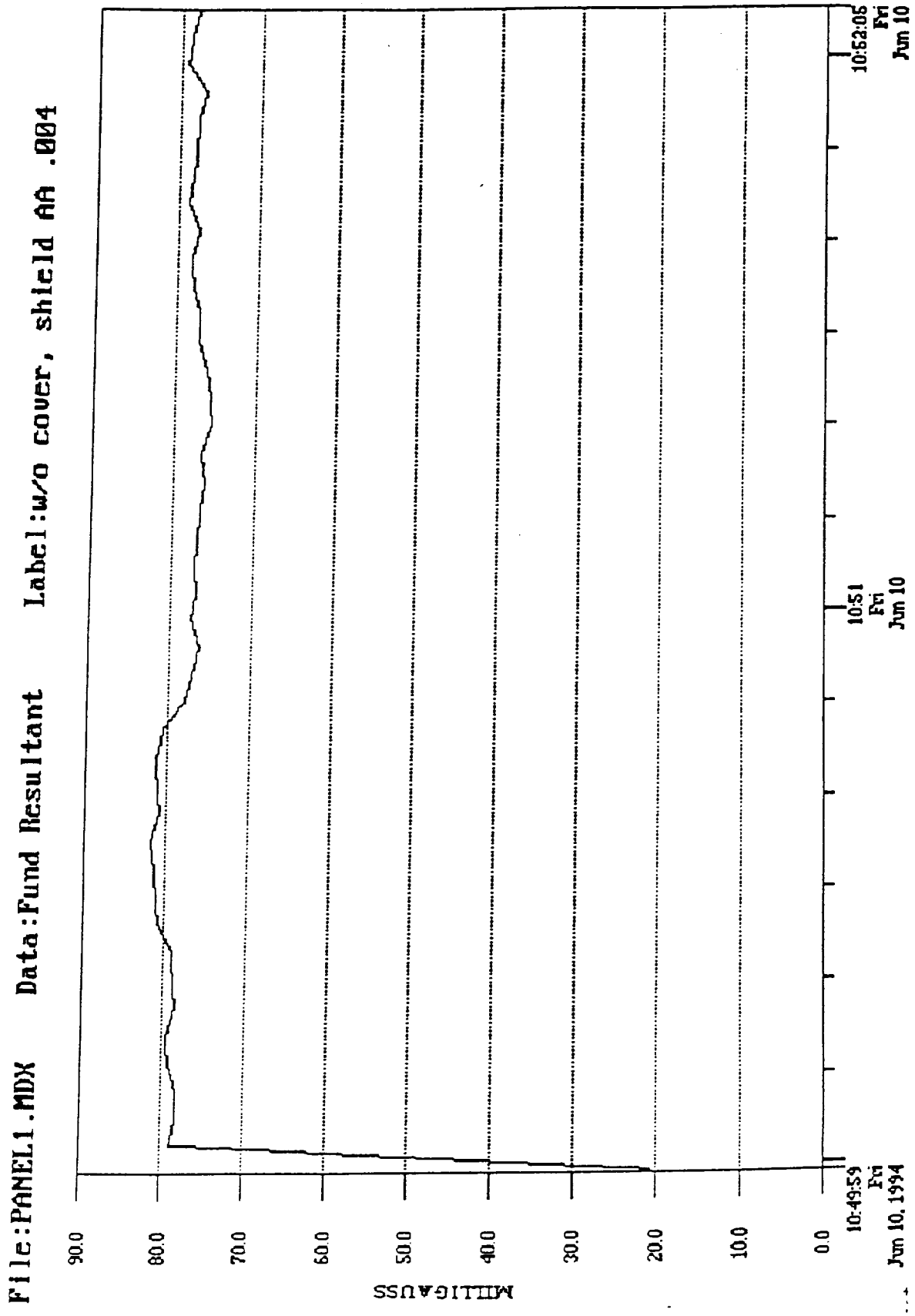
File:PANEL1.MDX Data:Fund Resultant Label:w/o cover, shield AA .004
MILLIGAUSS
90.0
80.0
70.0
60.0
50.0
40.0
30.0
20.0
10.0
0.0
10:49:59 Fri Jun 10, 1994
10:51 Fri Jun 10
10:52:05 Fri Jun 10

Fig. 103

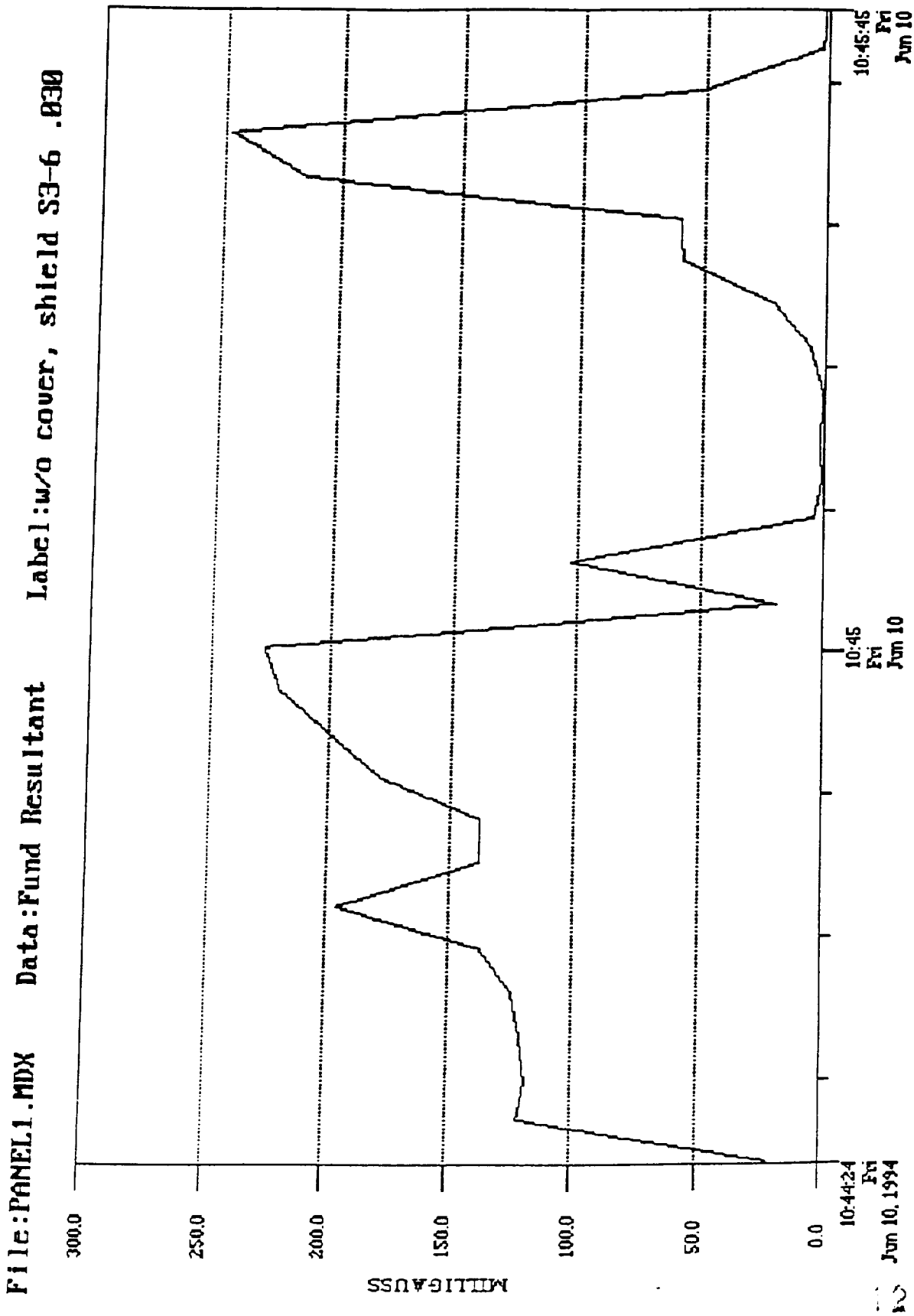
File:PANEL1.MDX
Data:Fund Resultant
Label:w/o cover, shield S3-6 .030
MILLIGAUSS
300.0
250.0
200.0
150.0
100.0
50.0
0.0
10:44:24 Fri Jun 10,1994
10:45 Fri Jun 10
10:45:45 Fri Jun 10

Fig. 104

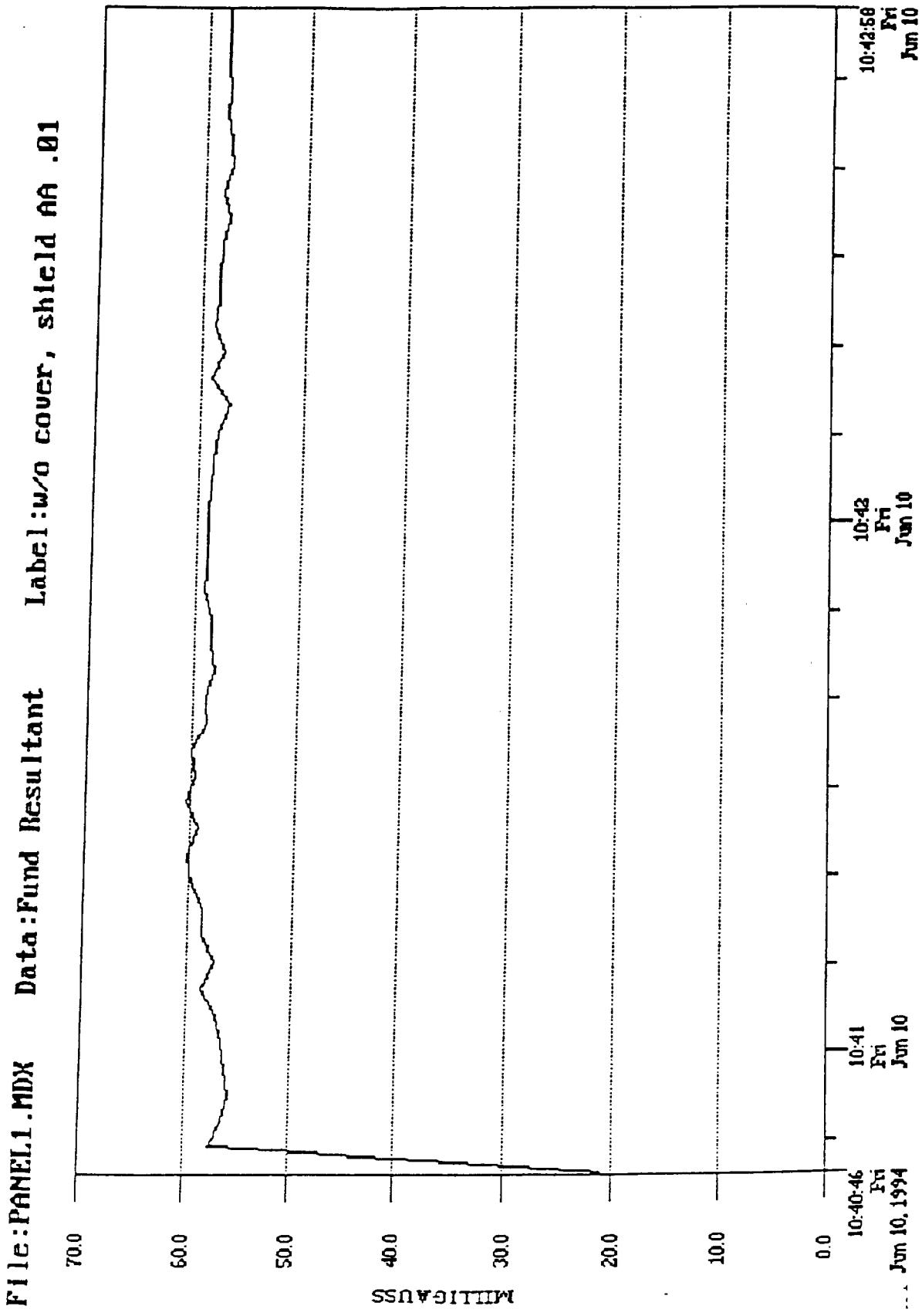
File:PANEL1.MDX
Data:Fund Resultant
Label:w/o cover, shield AA .01
MILLIGAUSS
70.0
60.0
50.0
40.0
30.0
20.0
10.0
0.0
10:40:46 Fri Jun 10,1994
10:41 Fri Jun 10
10:42 Fri Jun 10
10:42:58 Fri Jun 10

Fig. 105

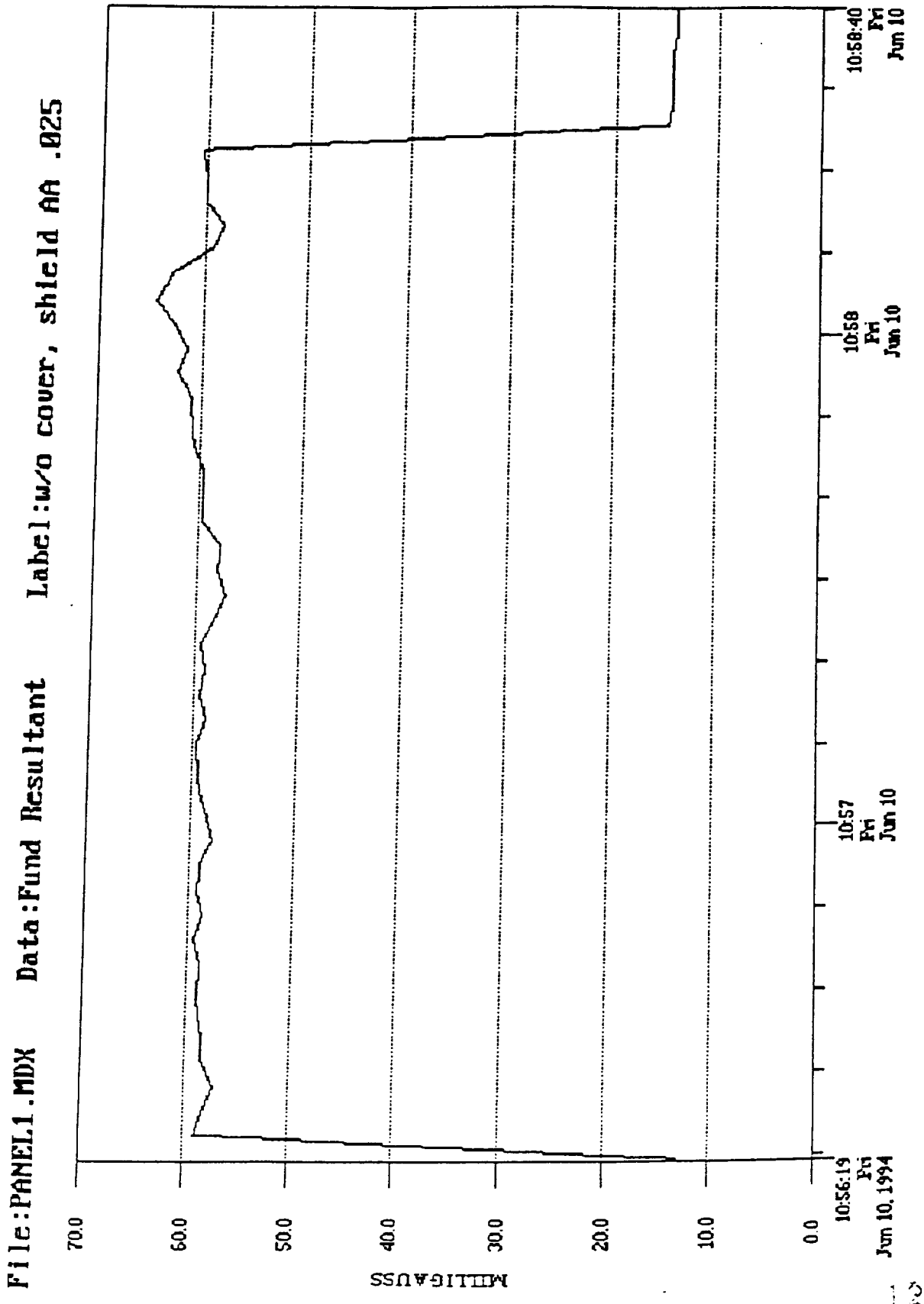
File:PANEL1.MDX
Data:Fund Resultant
Label:w/o cover, shield AA .025
MILLIGAUSS
70.0
60.0
50.0
40.0
30.0
20.0
10.0
0.0
10:56:19 Fri Jun 10,1994
10:57 Fri Jun 10
10:58 Fri Jun 10
10:58:40 Fri Jun 10

4 Measurements in the OPF location

Several measurements were also taken in the OPF room where several flight hardware equipment are located. Figures 106 through 111 show the levels of the magnetic field as a function of distance for two different locations in the OPF facility. In both cases the levels did not exceed the 6 mGauss mark. These two general measurements were taken for evaluating the general ambient magnetic field environment in the OPF location. Next, a number of measurements were taken around some panels and junction boxes. As it can be seen from Figures 112 through 117, a level of 70 mGauss was recorded in Figure 112 (east wall panel). This level of magnitude can potentially affect any sensitive flight hardware that are located in close proximity to the panel. Figure 115 shows that these levels, although they decrease as a function of distance away from the panel, there are still up to 20 mGauss in close proximity. Finally, Figure 118 shows the levels recorded from a junction box in the same room. In this case as the sensor moves away from the junction box the level of the magnetic field falls quickly.

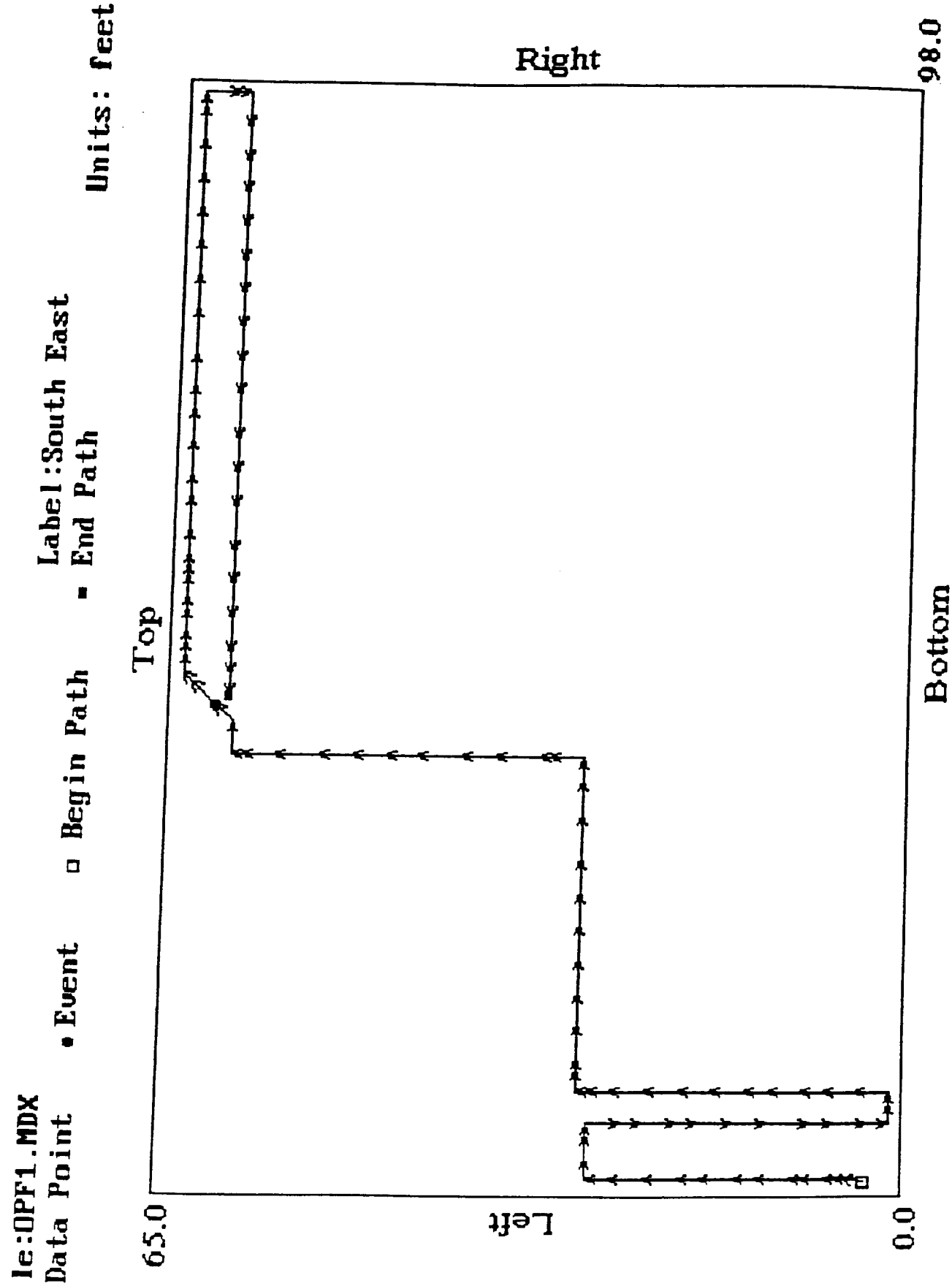
File:DPF1.MDX
< Data Point
• Event
□ Begin Path
▪ End Path
Label:South East
Units: feet
Right
98.0
Top
Bottom
65.0
Left
0.0

Fig. 106

Fig. 107

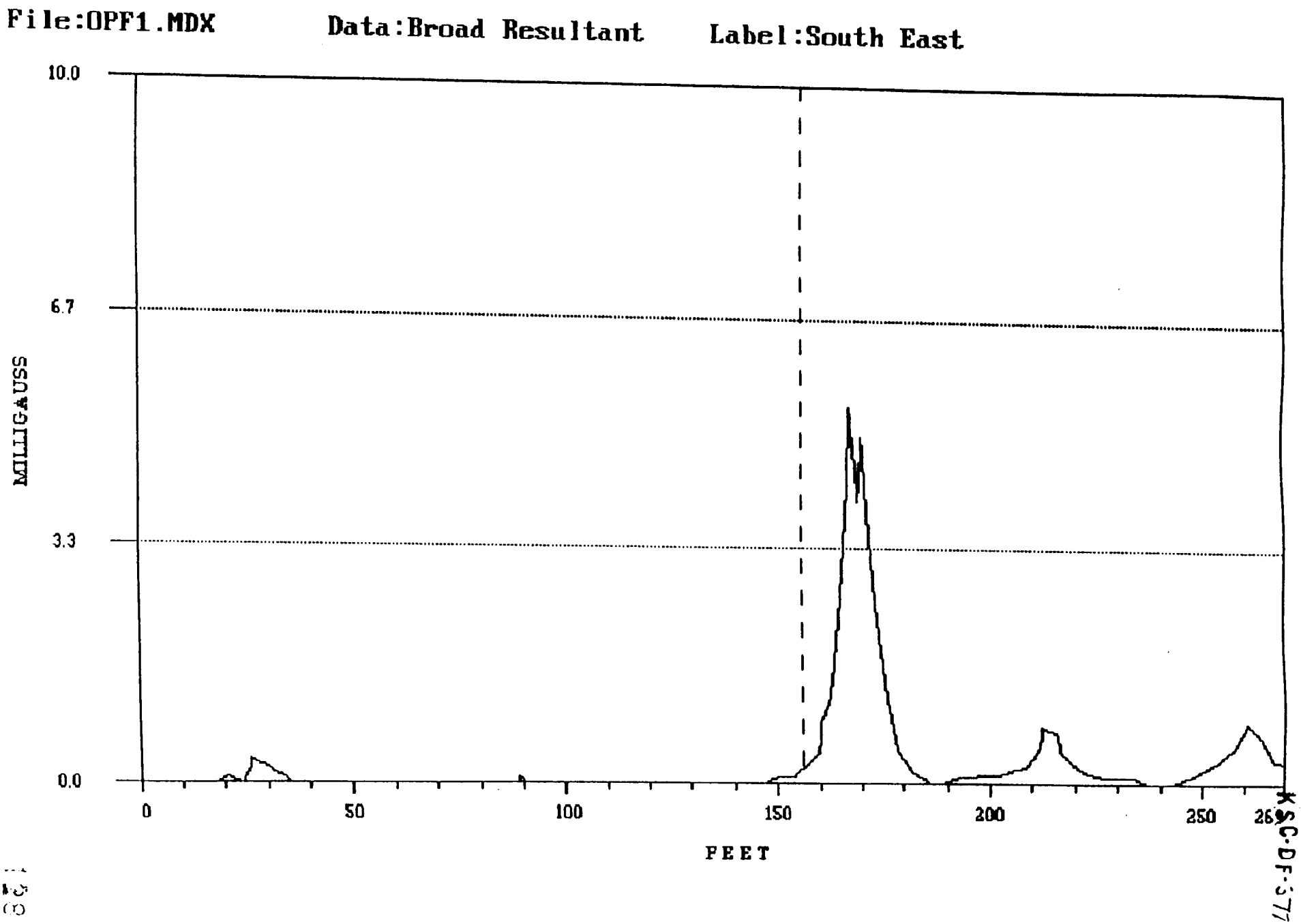

KSC-DF-37

Fig. 108

File:OPF1.MDX Data:Broad Resultant Label:South East

Units: feet

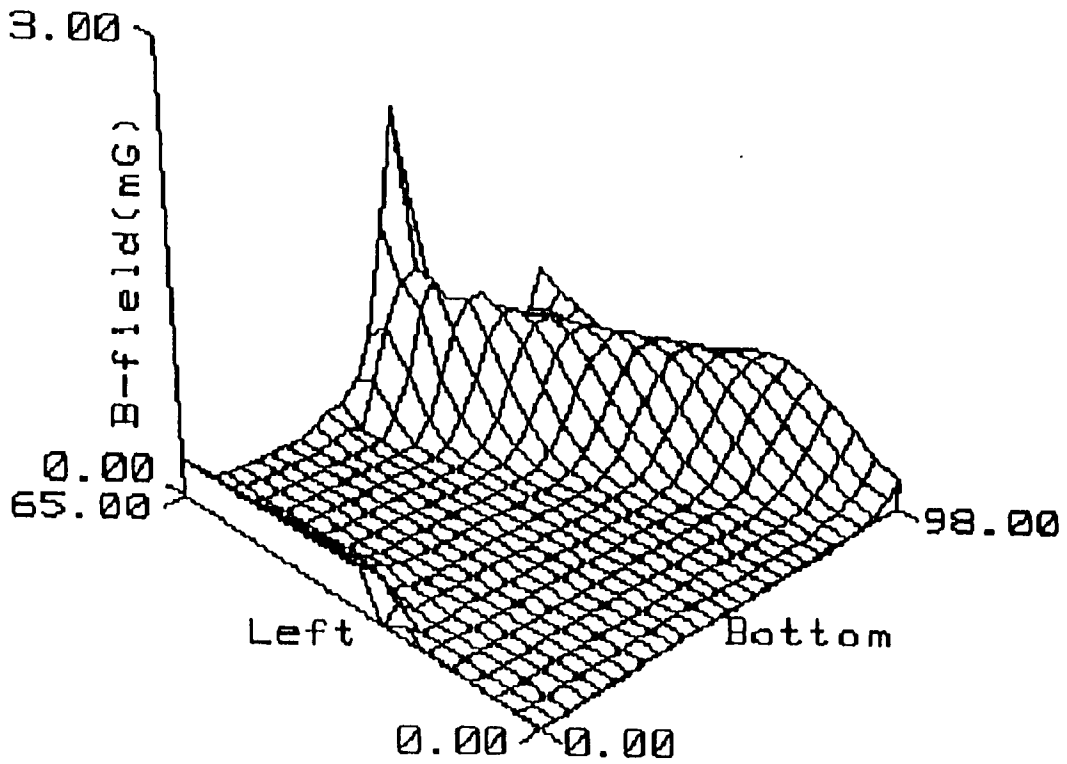

Fig. 109

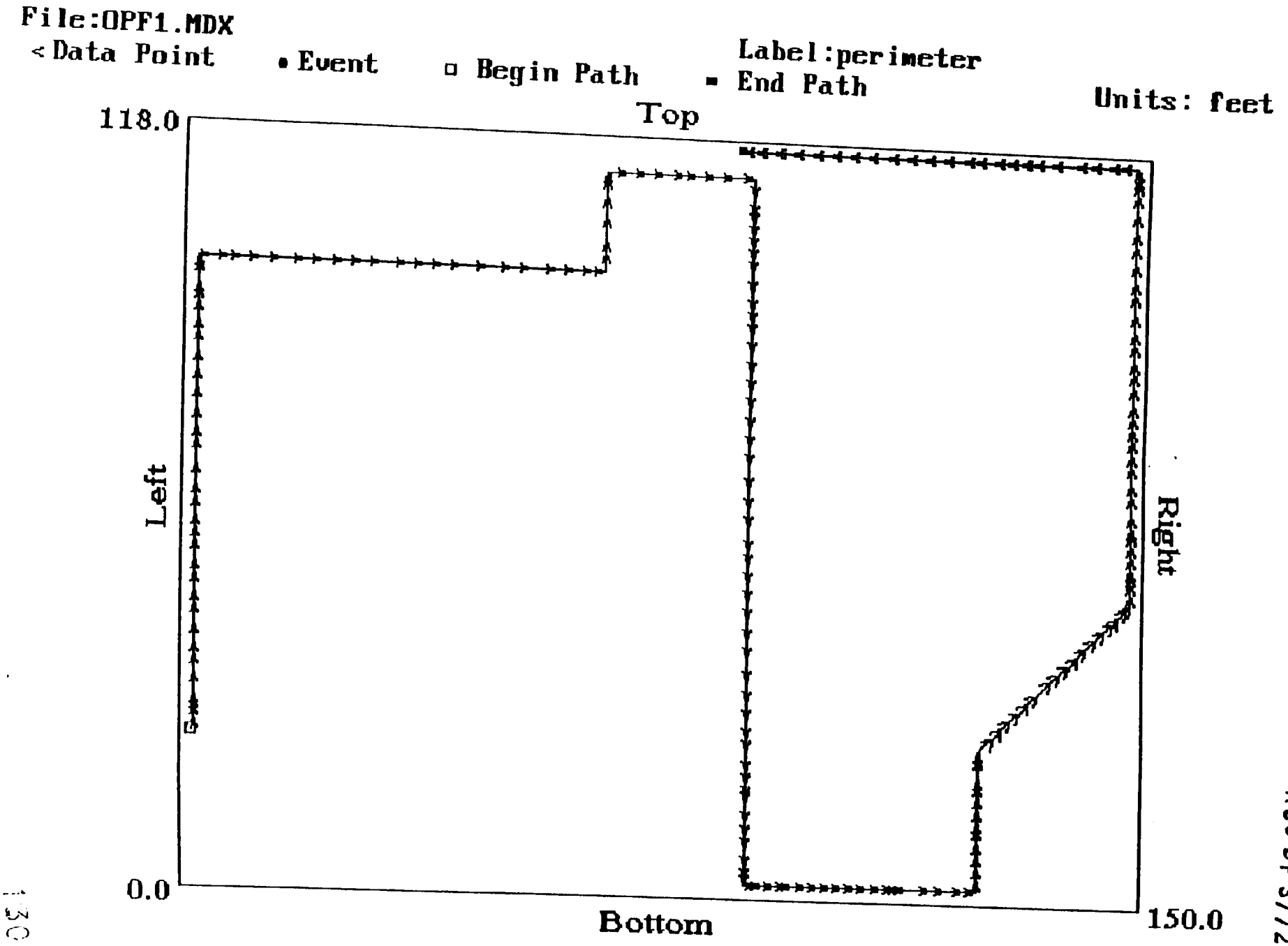

KSC-DF-3772

Fig. 110

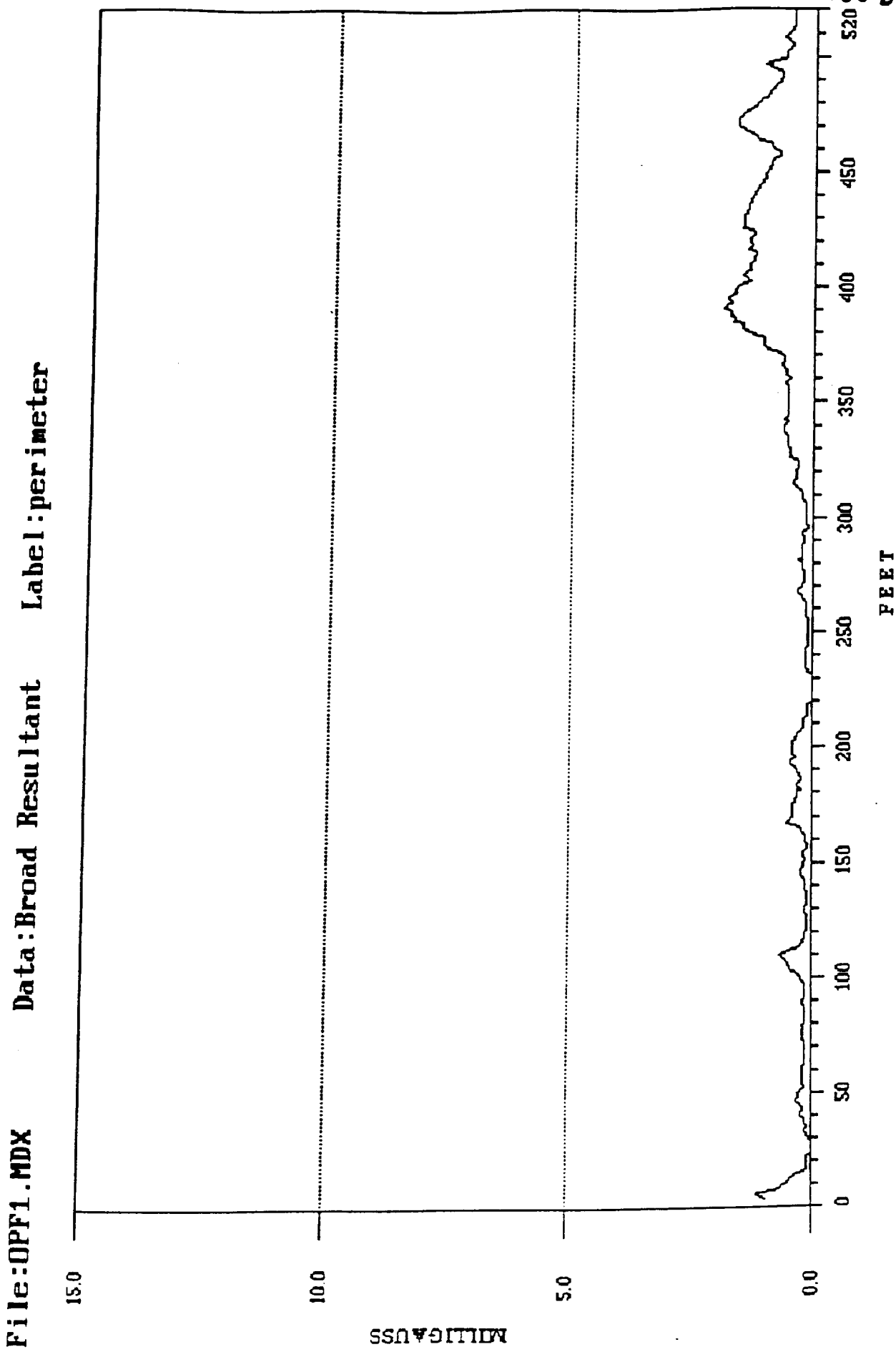
File:OPF1.MDX
Data:Broad Resultant
Label:perimeter
MILLIGAUSS
15.0
10.0
5.0
0.0
0
50
100
150
200
250
300
350
400
450
520
FEET

Fig. 111

File:OPF1.MDX Data:Broad Resultant Label:perimeter

Units: feet

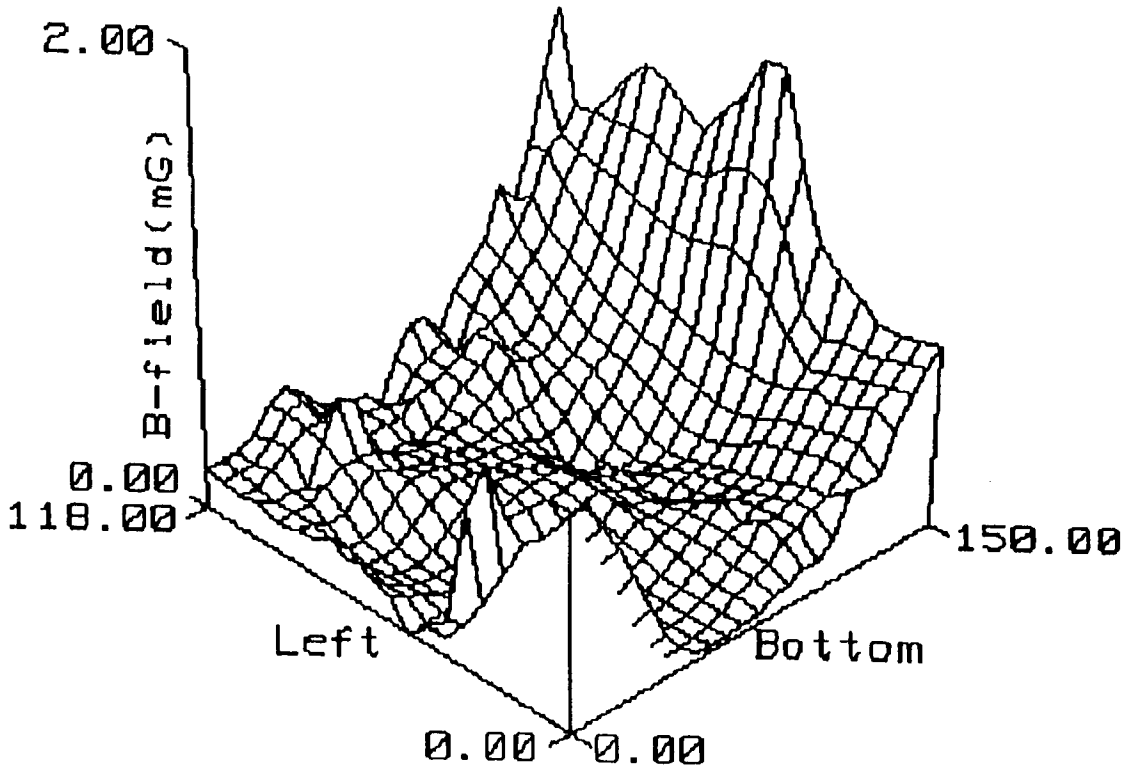

Fig. 112

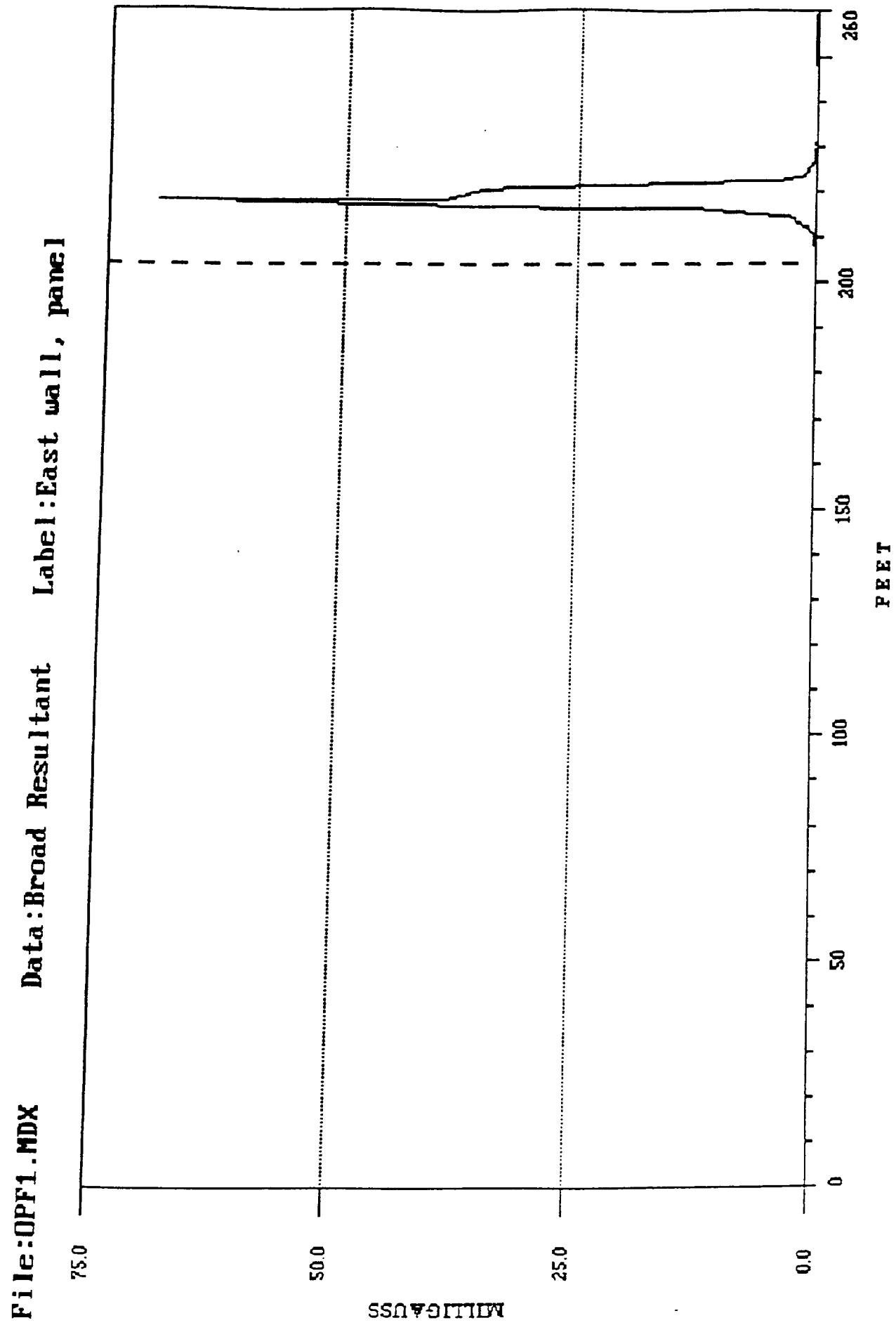
File:OPF1.MDX
Data:Broad Resultant
Label:East wall, panel
MILLIGAUSS
75.0
50.0
25.0
0.0
FEET
0
50
100
150
200
250

File:OPF1.MDX

< Data Point • Event □ Begin Path ▪ End Path

Label:East wall, panel

Units: feet

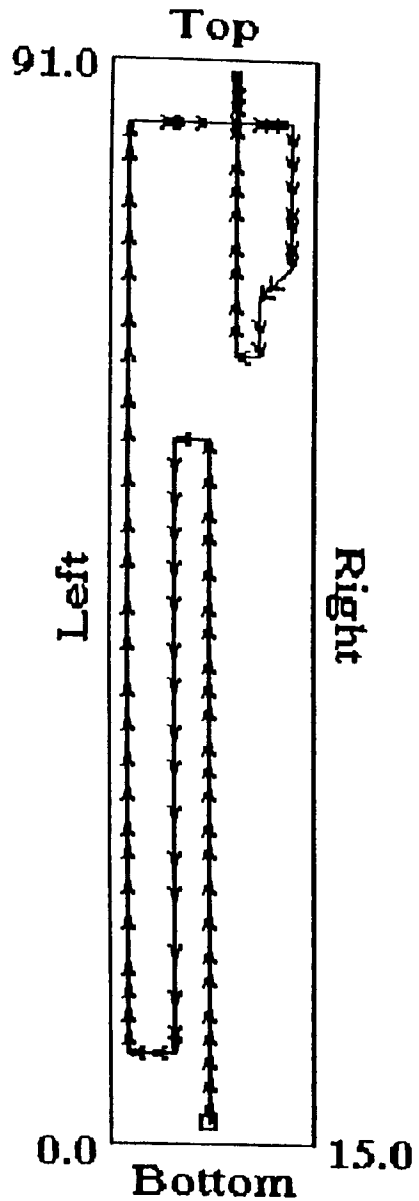

File:OPF1.MDX Data:Broad Resultant Label:East wall, panel

Units: feet

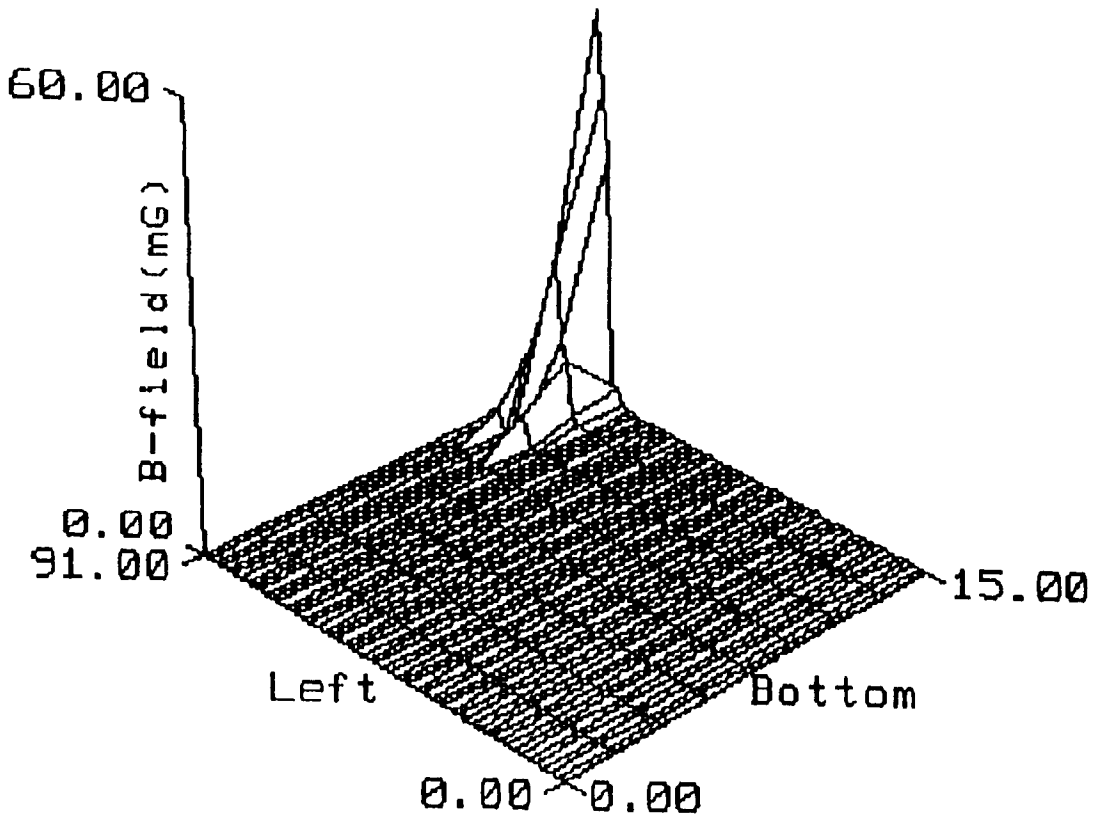

Fig. 115

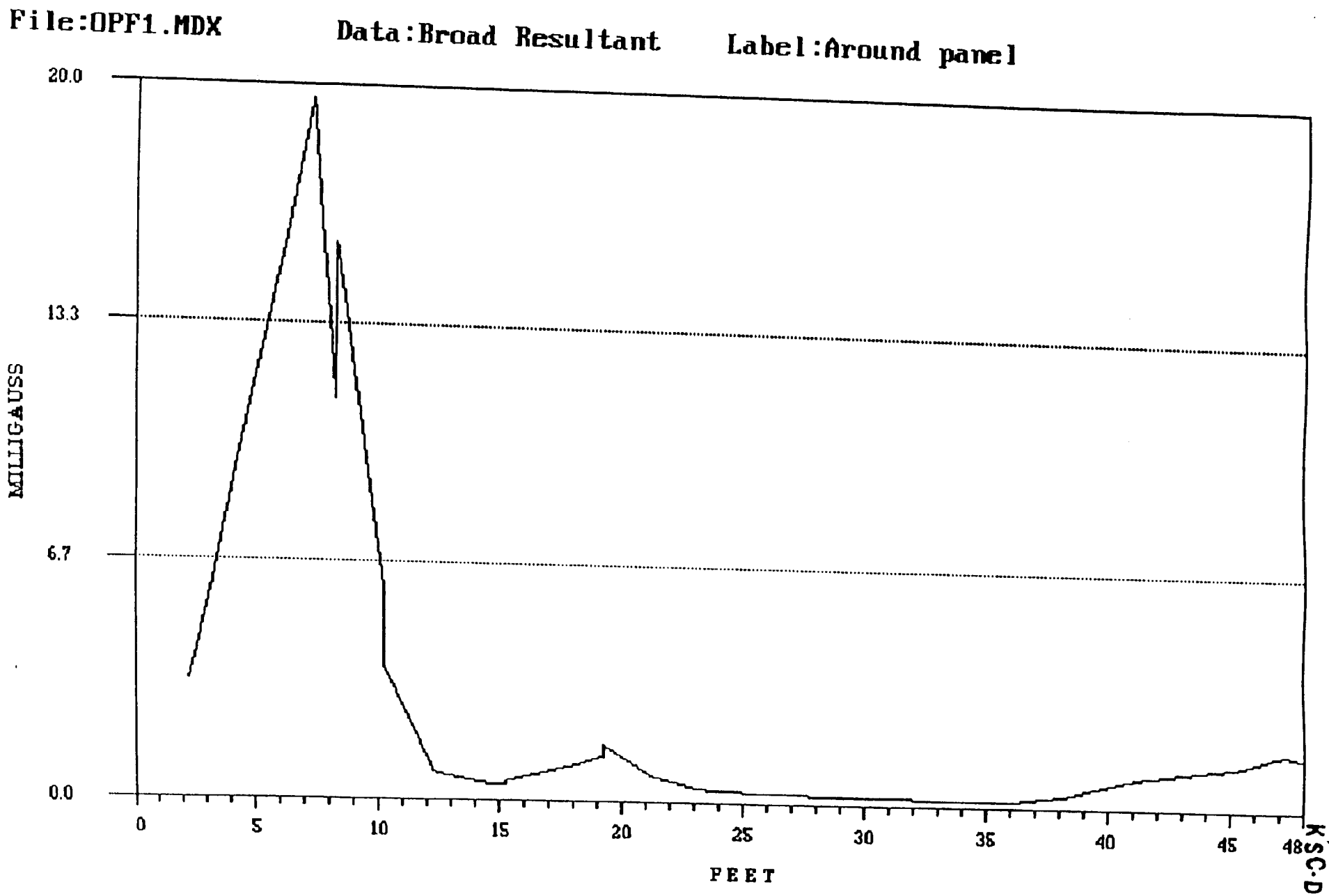
File:OPF1.MDX
Data:Broad Resultant
Label:Around panel
20.0
13.3
6.7
0.0
MILLIGAUSS
0
5
10
15
20
25
30
35
40
45
48
FEET
KSC-DF-377

File:OPF1.MDX
< Data Point • Event □ Begin Path ▪ End Path
Label:Around panel
Units: feet

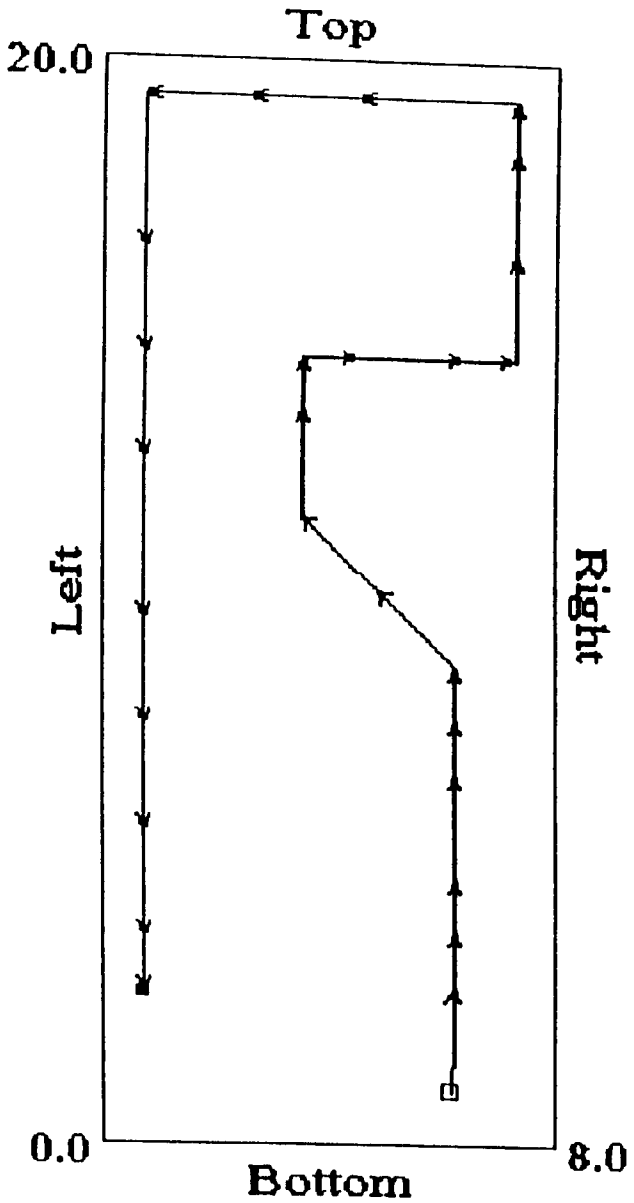

Fig. 117

File:OPF1.MDX Data:Broad Resultant Label:Around panel

Units: feet

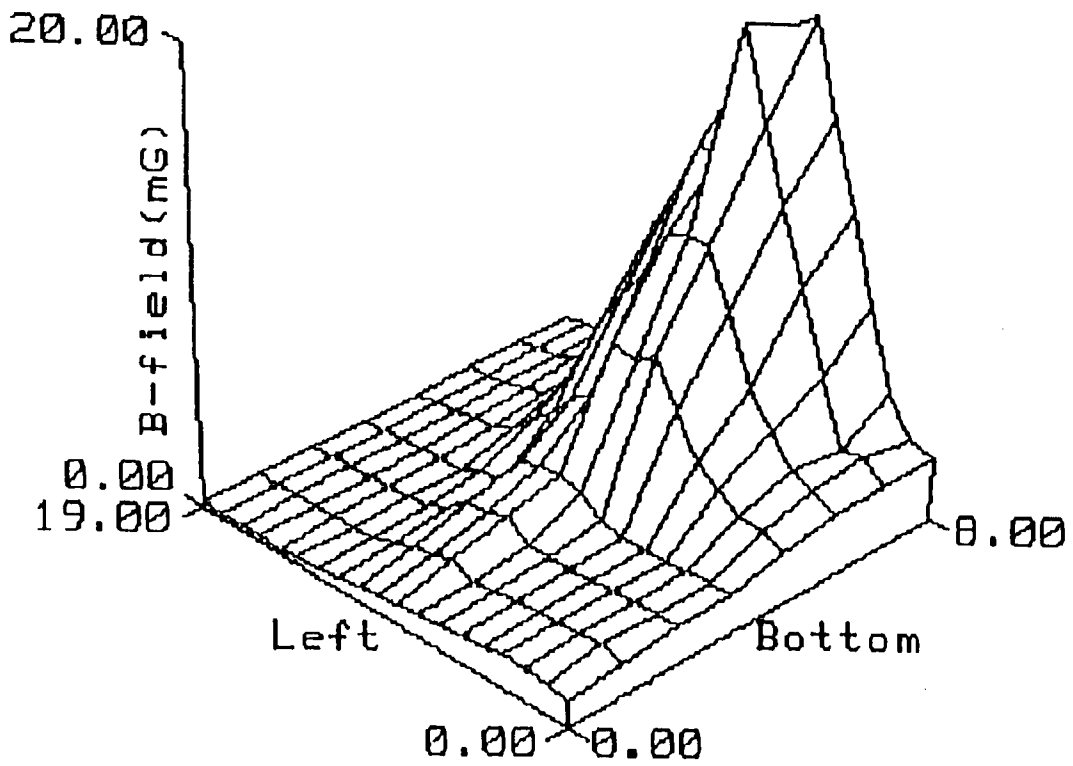

Fig. 118

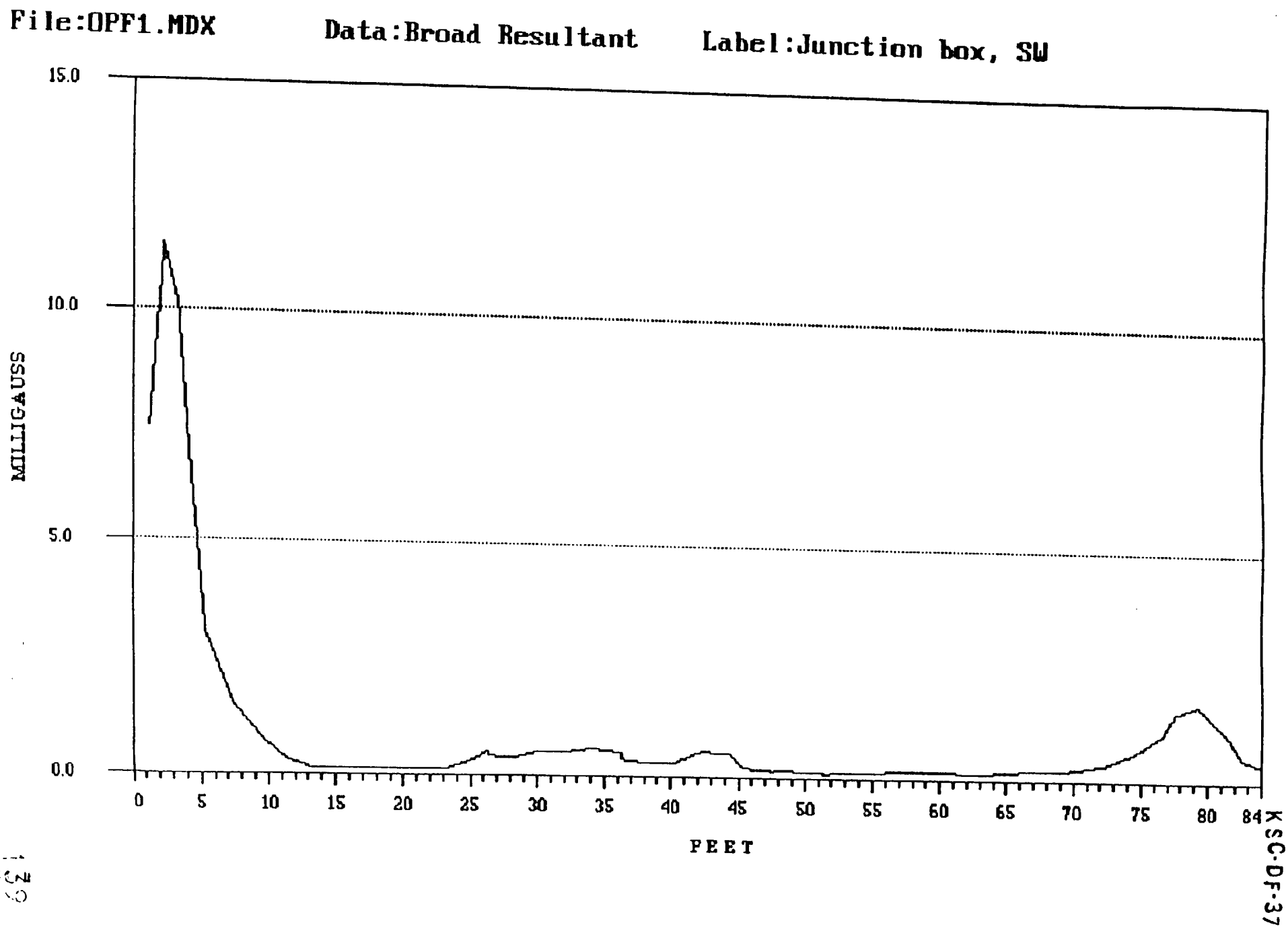
File:OPF1.MDX
Data:Broad Resultant
Label:Junction box, SW
15.0
10.0
5.0
0.0
MILLIGAUSS
0
5
10
15
20
25
30
35
40
45
50
55
60
65
70
75
80
84
FEET
KSC-DF-37

(This page left intentionally blank)

5 CONFORMITY WITH MIL-STD-461D and MIL-STD-462D

The military standards MIL-STD-461D and MIL-STD-462D which state the requirements for the control of electromagnetic interference emissions and susceptibility have been reviewed especially the following sections:

- Section 5.3.15 RS101(Radiated susceptibility, magnetic fields 30 Hz to 100 kHz) from MIL-STD-461D.
- Section 5.3.12 RE101(Radiated Emission, magnetic fields, 30 Hz to 50 kHz) from MIL-STD-461D
- Section 40.4 Ambient electromagnetic fields from MIL-STD-462D

It was determined that although we have tested for magnetic field levels within the region of 7cm and 50 cm from Equipment Under Test (EUT) these standards do not apply to our study case for the following reasons:

- The MIL standards require that tests on EUT are done in a reasonably shielded environment, whereas in this study our primary goal was to determine the ambient electromagnetic environment in the presense of one or more sources.
- Our test procedure required the movement of the sensor (actually mounted on a wheel), whereas in MIL-STD-462D the aim is to pick the maximum reading in whatever location it appears. As the sensor moves, the geomagnetic field of the earth creates a flux change in the sensor coil and a level of 0.3 mG is recorded. This is not the case in MIL-STD-462D set up.

6 CONCLUSIONS AND RECOMMENDATIONS

A study was done to identify sources generating magnetic fields at various locations at Kennedy Space Center. This study covered the following items:

- Power Lines
- Transformers
- Ground Currents
- Electric panels
- Several industrial equipment
- Several offices (in a prototype building)

This work included measurements of the magnetic fields at both the fundamental (60 Hz) frequency and its harmonics. Measurements were done as a function of distance around the source and as a function of time. The last part of the study was focused on the levels of fields from electric panels and the effectiveness of some shielding materials. A large data set was generated that can be used by other researchers.

As part of our work we would like to recommend the following:

- We recommend that some electric panels and power supply sources that yield a level of over 500 mG to be shielded if any computer or sensitive equipment are in close proximity. 500 is chosen here as an example since most of the equipment that could easily be shielded do not produce much more than 500 mG. A good shield can reduce this level to about 50 mG or less and then any magnetic field leaking from the shield will decay as a function of distance very quickly. In a distance of 4 to 5 feet from the shielded source the level of the magnetic field

will be insiginificant. The reduction of the magnetic field level due shielding depends on the available shielding materials.

Shielding can be achieved by using flat metalic panels with high permeability.

In working towards shielding sources in a room one has to keep in mind that the functional workspace is usually defined as 6" away from all walls and the floor and 90" above the floor. In this area the magnetic field should be less than 10 mG if possible. That can be achieved by shielding various sources around the building. Greater than 10 mG [12] could cause interference with video display terminals, computers, and other equipment.

It should also be noted that since gaps and welds in a shield alter the flux within the shield. Care should be exercised in shielding specific equipment.

- We also reccomend that the data set generated should be used for verifying any analytical models that simulate magnetic fields from various sources, such as panels, computers, lathes, transformers, etc.
- Furthermore, it is recommended that the data set should be used for further parametric studies and ways to shield electric panels.
- Finally, we recommend that more measurements are taken to understand the effects of transients on the generation of magnetic field levels.

7 References

- 1) Deno, D. W., "Transmission Line Fields", *IEEE Trans. on Power Apparatus and Systems*, vol. 95, Sept/Oct. 1976, pp. 1600-1611.
- 2) Magnetic Shielding Corporation manual, pp. 4-7.
- 3) Wait, J. R. and K.P. Spies, "On the Image Representation of the Quasi-static Fields of a Line Current Source Above the Ground" *Canadian Journal of Physics*,vol. 47, 1969, pp. 2731-2733.
- 4) Olsen R. G., "Electromagnetic Fields from Power Lines" *IEEE Intern. Symp. on EMC*, at Dallas Texas, pp.138-143, 1993
- 5) "EMDEX System Manuals", Vols. 1-2, *EPRI*, Oct. 1989, EPRI EN-6518. Prepared by Enertech Consultants, Campell, CA.
- 6) Afifi, A., R.S. Banks, L.I. Kheifets, and B. Newman, "Proceedings: Discussion of an EMF Protocol", *EPRI*, July 1990, EPRI EN-6829. Prepared by Robert S. Banks Associates, Inc., Minneapolis, MN.
- 7) Gauger, J. R., "Household Applicance Magnetic Field Survey", *IEEE Transactions on Power Apparatus and Systems*, 1986, PAS-104, pp. 2436-2444.
- 8) Zaffanella, L. E., "Pilot Study of Residential Power Frequency Magnetic Field", *EPRI*, Sept. 1989, EPRI EL-6509. Prepared by General Electric Company, Lenox, MA.
- 9) Bracken, T. D., " Analysis of BPA Occupational Electric Field Exposure Data", Jan. 1986, DOE/BP-36303-1. Prepared for Bonneville Power Administration.
- 10) " The EMDEX Project: Technology Transfer and Occupational Measurements", vols. 1-3, *EPRI*, Nov. 1990, EPRI EN-7048.
- 11) "Silva, M., H. Hummon, D. Rutter, and C. Cooper, "Power Frequency Magnetic Fields in the Home", *IEEE Transactions on Power Delivery*, 1989, pp. 465-478.
- 12) "Proceedings:Substation Magnetic Field Management Workshop", *EPRI*, April 1993, EPRI TR-101852. Prepared by Electric Research & Management, Inc., Felton, CA, page. A-7.

8 APPENDICES

8.1 Appendix I - EMDEX II

The EMDEX II System for measuring magnetic field (developed by EPRI) was acquired and tested for proper operation.

The pieces of equipment ordered are :

EMDEX II Magnetic Field Meter
(Includes meter, 256K memory,
software, read-out cable, user manual
storage case)
Amplogger Model 100A
(Current probe for measuring Amps)
Technical Reference Manual
Nylon Carrying Pouch
Technical Support Package
Shipping, Insurance and Handling

LINDA Measurement Wheel
(Includes wheel, field vs distance
software, and user manual)
Enhanced Contour and 3-D Mapping
LINDA Shipping Case

8.2 Appendix II - Error Analysis for the Calculated Fundamental Value

(from EMDEX Operational Manual)

Potential Errors in the Fundamental Frequency Calculation

The EMDEX II meter was originally envisioned as a meter to measure magnetic fields generated by load currents in transmission and distribution systems. Measurements can be made over two frequency ranges: the *broadband* frequency range from 40 to 800 Hz, and the *harmonic* frequency range from 100 to 800 Hz. The broadband measurement includes the *fundamental* power frequency of 50/60 Hz out to the 13th harmonic, whereas the harmonic measurement includes only the harmonics and excludes the fundamental. Values for the fundamental are calculated from the measured broadband and harmonic values in the EMCALC software. Errors in the calculated fundamental can result from small errors in the measured broadband and harmonic values.

In most typical power frequency EMF environments, the dominant component of the magnetic field is the 50/60 Hz fundamental. In these cases, the calculated values of the fundamental are accurate. However, one may encounter an environment where harmonic components dominate (such as commercial airliners operating at 400 Hz). In this special case, EMCALC may report a calculated fundamental value that is substantially in error. The EMDEX II is reporting the values of the broadband and harmonic within its specifications, but in special cases where the harmonic frequencies are dominant, small filter and tolerance errors can affect the calculated fundamental values.

Although the circumstances in which this problem occurs are unusual, it is important to fully understand the potential calculation error so that data can be interpreted in a meaningful way. ***This discussion applies only to the calculated fundamental, and that the results reported for the broadband and harmonic resultant are not affected.***

The calculated fundamental, F_c is given by the expression:

$$F_c = \sqrt{B_m^2 - H_m^2} \qquad H_m \le B_m$$
$$F_c = 0 \qquad H_m \ge B_m \tag{1}$$

where B_m and H_m are the measured RMS values of the broadband and harmonic components, respectively. Consider a particular case where an EMDEX II is in a pure 300 Hz magnetic field of 100 mG. Suppose the measured broadband value is 100 mG (i.e., no error) and the measured harmonic value is 99 mG (i.e., 1% error). The fundamental (50/60 Hz) value that would be calculated by EMCALC in this case would be:

$$\sqrt{(100mG)^2 - (99mG)^2} = 14.1\ mG.$$

That is, a 1 mG (1%) error in the harmonic measurement could result in a 14 mG error in the calculated 50/60 Hz fundamental value reported by EMCALC.

Now consider the other extreme, where the field has a pure fundamental frequency of 50/60 Hz (no harmonic frequencies present). Again assume that the measured broadband value is 100 mG (no error) but assume that the measured harmonic value is 1 mG rather than the true value of 0 mG. In this case, the calculated value for the fundamental is 100.005 mG, which is in error by only 0.005 mG. These examples illustrate the fact that the ***fundamental calculation error under consideration here is only of concern when the broadband and harmonic signals have similar magnitudes (i.e. a high harmonic content with little or no fundamental)***.

Error Analysis of the Fundamental Calculation

The error in the calculated fundamental value can be determined as follows: Let the true fundamental, harmonic, and broadband RMS amplitudes be designated F, H, and B respectively. F, H, and B are related by the equation:

$$B = \sqrt{F^2 + H^2} \tag{2}$$

Assume the broadband signal is measured without error (i.e., $B_m = B$), but that the harmonic value is in error by the amount δ, so that:

$$H_m = (1-\delta)H \tag{3}$$

Combining equations 1, 2, and 3, and simplifying yields:

$$F_c = \sqrt{F^2+(2\delta-\delta^2)H^2} \tag{4}$$

Solving this equation for the true fundamental gives:

$$F = F_c\sqrt{1-(2\delta-\delta^2)\frac{H^2}{F_C^2}} \tag{5}$$

Then the ratio of the true value of the fundamental to the calculated value is:

$$\frac{F}{F_c} = \sqrt{1-(2\delta-\delta^2)\frac{H^2}{F_c^2}} \tag{6}$$

In terms of measured quantities, this ratio is:

$$\frac{F}{F_c} = \sqrt{1-\frac{(2\delta-\delta^2)}{(1-\delta)^2}\frac{H_m^2}{(B_m^2-H_m^2)}} \tag{7}$$

The value under the radical is always less than or equal to 1, so the expression shows that the calculated value is always equal to or larger than the true value.

This expression is used to establish a criteria for limiting the error to a specified fractional value, ϵ, or equivalently to a percentage error of ϵ x 100.

The fractional error is given by:

$$\frac{F_c-F}{F} \le \epsilon \tag{8}$$

or, equivalently,

$$\frac{F}{F_c} \ge \frac{1}{1+\epsilon}$$

Substituting the value for F/F_e given above yields:

$$\sqrt{1-\frac{(2\delta-\delta^2)\ H_m^2}{(1-\delta)^2\ B_m^2-H_m^2}} \geq \frac{1}{1+\epsilon} \qquad (9)$$

Solving this equation for the ratio of H_m to B_m gives:

$$\frac{H_m}{B_m} \leq \sqrt{\frac{(1-\delta)^2}{1+\frac{2\delta-\delta^2}{2\epsilon+\epsilon^2}}} \qquad (10)$$

For given values of δ and ϵ, this expression determines the maximum ratio between the measured harmonic and broadband values for which the error in the calculated fundamental is less than ϵ x 100%.

Examples

Example 1. Consider a case where the true broadband field is 100 mG and the true harmonic field is 10 mG. The true fundamental field would therefore be 99.5 mG. If the error in filtering and component tolerance of the EMDEX II is assumed to be 5%, then the measured broadband value would be 100 mG and the measured harmonic value could be 9.5 mG (5% low). The calculated fundamental value would be 99.55 mG.

Equation 10 provides the formula for establishing an acceptance criteria for the ratio H_m/B_m. In Example #1, we assumed a tolerance of 5% (δ = 0.05) and an acceptable error limit of 20% (ϵ = 0.20). Therefore, the acceptance ratio for H_m/B_m is 0.86 or less. The actual ratio H/B is 9.5/100 or 0.095, which is much less than 0.86 and is acceptable.

Example 2. Next suppose that the true broadband field is again 100 mG and the true harmonic field is 70 mG. The true fundamental field would be 71.4 mG. Assuming a 5% error in the harmonic measurement, the broadband value would be 100 mG and the harmonic

8.3 Appendix III - Shielding Materials

I Introduction

Magnetic shielding assures optimum performance for many types of equipment.

- MRI magnet systems are protected from outside magnetic field interference by layers of CO-NETIC AA Perfection Annealed alloy used outside of soft iron shielding.
- Electron microscopes, operating in a sensitive mode while examining state-of-the-art IC chips, are protected from magnetic field changes by CO-NETIC modular enclosures.
- High-temperature superconducting material experiments are enclosed in magnetic shields to allow precise measurements of material properties.
- Biomagnetic diagnosis equipment using SQUID (Superconducting Quantum Interference Device) technology operates inside a magnetically shielded room to measure the extremely small magnetic fields from brainwaves.

II Magnetic vs. RF Shielding

Magnetic shielding provides interference control of H-fields from DC to 100 kHz and differs fundamentally from RF shielding. RF shielding constructions, or "screen rooms," typically use copper foil, copper mesh or galvanized steel to block E-fields at radio frequencies. The main shielding effect is from eddy current reflection and is primarily dependent on skin effect. Material bulk is usually not important, but tight, secure joints are critical.

Magnetic shielding, in contrast, relies on the induction of the impinging magnetic flux into the shielding alloy, bypassing the enclosed magnetically sensitive apparatus. Shielding of stronger H-fields therefore requires proportionately thicker walls of high permeability material. Unlike RF enclosure design practice, small openings and gaps may have little effect on the attenuation at the center of a magnetic shield.

Magnetic shielding alloys are conductive. Therefore, a magnetic shield enclosure, if grounded and designed with proper RF practice, can provide some degree of RF shielding.

Magnetic shield rooms enclosing very strong magnets, particularly unshielded types used in some MRI systems, typically require tons of iron plate. This is due to the need for thick layers of high saturation point material to prevent saturation by the magnetic field. This shield's primary purpose is to limit the magnetic field level outside the room to a level acceptable for incidental personnel exposure. High permeability CO-NETIC AA alloy can be useful as an outer layer to prevent external magnetic field sources from affecting the magnet. CO-NETIC AA alloy can also be used to protect self-shielded MRI magnets from outside disturbances.

III Application

Specification of magnetic shield enclosures requires consideration of several factors:

- SIZE: Required magnetic shield thickness is proportional to enclosure size, so the minimum practicable volume of enclosure should be chosen. As size increases, the cost per dB of attenuation increases. For example, 60 dB attenuation in a 12" x 12" x 12" chamber is reasonable. However, if all space dimensions are multiplied by 12, volume increases 1728 times, making the 60 dB figure difficult to attain. The internal height, width and length should be specified, and any limitations on outer dimensions noted.
- FIELD STRENGTH: Incoming field strengths must be known for proper design. Measurements of DC and AC field strengths allow calculation of the required wall thickness to avoid saturation. Magnetic Shield Corporation offers Magnetic Field Evaluator Probes to aid in measurements.
- INSIDE FIELD REQUIRED: A practical estimate of the maximum allowable inside field is necessary to avoid unrealistic blanket requirements such as "zero leakage" or "no magnetic field inside." Minimize sources of interference inside the enclosure by evaluating lighting, instruments and equipment for magnetic field emissions.
- ENTRY: Any number of doors may be incorporated in a room, but for both maximum field reduction and lowest cost, it is desirable to limit a room to one door. The door latch mechanism is usually operable by one man from the inside or outside, though other lock and alarm arrangements may be used. Conventional hinge doors may be used, but they should be a pressure fit to provide a better magnetic joint.

- MOUNTING: The base to which the room will be mounted should be specified. In particular, vibration or seismic isolation requirements must be noted.

- VENTILATION: The minimum air flow in cfm should be specified, along with any special temperature or filtering requirements. This air may also be used to pressure seal the door.

- LIGHTING: The minimum illumination level at a given height above the floor should be specified. This frequently runs about 75 to 100 lumens at 30 in. above the floor. From a performance viewpoint, the type of light can be most important. Incandescent lamps are acceptable, although they do introduce some field. Fluorescent lighting usually has intolerable magnetic noise. For thoroughly nonmagnetic lighting, consider propane lamps.

- POWER: The required electrical power into the room should be stated. Normally this means AC power for lights and equipment, plus DC outlets. Cables inside of the enclosure can be shielded with CO-NETIC Braided Sleeving or Spira-Shield Flexible Conduit. Filters may be required. Circuit breakers and DC power supplies are best located outside the room to minimize interference.

  CABLE PENETRATIONS: The number, size and location of access openings to allow the introduction of connecting cables from outside should be specified. The shield designer has several ways of gaining cable access without significant effects on the shielding. Power and signal leads do not require extension tubes if the diameter at the opening is smaller than five percent of the largest overall dimension of the enclosure.

IV Configuration

The ideal theoretical shape for a shield is a closed sphere. In practice, cans with lids or box shapes are normally used. Complete enclosures that fully surround a device provide best results.

Shielding attenuation decreases as shapes progress from cans with lids to open cans or open cylinders, particularly as the length to diameter ratio decreases. For rectangular shapes, 6-sided boxes are best, followed by 5-sided boxes, 4-sided sleeves, 3-sided channels, and L-Shapes. Flat plate shields can be effective if both dimensions of the shield wall substantially exceed the distance between the source and receiver of magnetic interference.

Due to the highly unsymmetrical nature of flat shields, the formulas on page 6, which give results for closed shapes, cannot be used for flat plate calculations. Field trials are often necessary to determine actual performance.

V Construction

FREE STANDING ENCLOSURE

The material must support its own weight plus that of any attachments. Because fully annealed CO-NETIC AA alloy has a low yield strength, thicker layers than those found from attenuation equations may be required. A non-magnetic core material should be used to separate alloy layers, adding strength and improving attenuation performance. Core thicknesses of 1/4" to 1/2" provide optimum attenuation.

Secure joints between panels are important for maximum flux conductance and best shielding results. Preferred construction uses flux transfer strips, of the same alloy and thickness as the main panels, to cover all seams between panels. The width of the strips is usually determined by bolt spacing requirements (non-magnetic fasteners must be used) and is not critical for shield performance. Flux transfer strips may require reinforcing battens to assure that pressure is evenly applied.

Magnetic shielding alloy floor panels should be covered with rigid plywood or hardboard to prevent applied loads from causing local flexing, which leads to work hardening and loss of permeability. Raised floors may be necessary in order to provide access to flux transfer strip hardware.

Required access points may be constructed with bolted panels where infrequent access is necessary, or with slip-fit covers that mate with short tubular extensions permanently attached to the enclosure. Doors must be designed to provide close-fitting joints when latched.

Components made of CO-NETIC AA Stress Annealed alloy must be fully annealed to achieve high attenuations. To avoid the complications of annealing after fabrication, flat panels may be made from the factory annealed, CO-NETIC AA Perfection Annealed sheet stock. Angles and other pieces can also be constructed from Perfection Annealed stock if bending dies having radius at least two times material thickness are used. Components that are severely deformed from the flat condition, such as small cylinders, should be annealed according to the specifications in our MG-5 Material and Fabrication guide after fabrication has been completed.

APPLICATION TO EXISTING STRUCTURE

Magnetic Shield Corporation shielding alloys can be applied directly to the walls, floors and ceilings of a room.

Two forms of CO-NETIC AA shielding alloy are available for applications of this type. CO-NETIC AA foils are available in 15" widths in 004", .006" and .010" thicknesses, in large coils. When applying to room surfaces, care should be taken to avoid severe, repetitive flexure, which will lead to loss of permeability. Adjacent strips should be overlapped about 1" and the securing method should aid in keeping the strips in contact at the overlaps. Reversing the overlap lay at alternate joints will help avoid re-radiation of flux.

Non-preferred Overlaps:

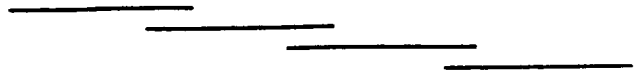

Preferred Overlaps:

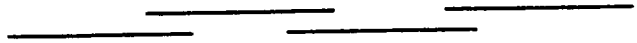

Views of overlap methods

CO-NETIC AA Perfection Annealed sheets are available in standard gauges .014" through .062" thick, in flat sheet sizes up to 30" x 59". As with foil constructions, flexure should be avoided. Protective flooring is required over the CO-NETIC and can be accomplished with a raised false floor or with rigid subflooring material overlaying the CO-NETIC alloy.

Fastening of sheets to the walls must be done with non-magnetic fasteners, spaced so as to keep the sheets in contact at the overlaps. Wall coverings can be applied as desired, but if smooth finishes are required, additional wallboard or paneling may be needed over the CO-NETIC alloy. Any required attachments for this finishing layer must also avoid penetration of CO-NETIC by magnetic fasteners.

Joints at corners can be made by forming the CO-NETIC alloy, using as large a bending radius as possible (which minimizes loss of attenuation). Corner bends should be protected from repeated flexing.

VI Additional Design Information

A design guide cannot anticipate all questions that may arise in the application of magnetic shielding to large enclosures. The engineers at Magnetic Shield Corporation are available for consultation regarding the specifications of magnetic shielding.

VII Calculation

The following is a basic method for determining an approximate shield design. Engineers at Magnetic Shield Corporation are available for consultation on calculations.

SATURATION LIMIT

(A) Minimum Wall Thickness (t) $= \dfrac{D \cdot H_o \cdot 1.25}{B_{Max}}$

t = Minimum wall thickness of shielding alloy (inches)

D = Diameter of cylindrical shield or Diagonal of largest face of rectangular box (inches)

H_o = Outside Field Strength (Oersteds)**

**Note: A minimum of 0.5 Oersteds must be used to assure that Earth's field does not saturate the enclosure preventing shielding of AC fields.

B_{Max} = Maximum Induction (Gauss)
7,500 for CO-NETIC AA;
21,000 for NETIC S3-6

CO-NETIC AA alloy, Perfection Annealed for maximum permeability, is normally preferred for construction of high attenuation shields. CO-NETIC Magnetic Shielding alloy is available in thicknesses up to .100". If Equation (A) indicates that thicker gages are required, multiple layers of shielding alloy will be necessary. In that case, choose two layers either of equal thickness or with heavier gage on the outside, totaling at least the required thickness.

If more than two layers would be required to meet the saturation limit, either the enclosure size should be reduced, or a NETIC S3-6 alloy layer should be added to reduce the field before CO-NETIC can be used.

ATTENUATION

The attenuation factor must be calculated for each layer individually:

(B) $B_m = \dfrac{1.25 \cdot D \cdot H_o}{t}$

B_m = Flux Density in the Alloy (Gauss)

t = thickness of layer (inches)

Refer to graph and find μ, which is the permeability corresponding to B_m on the vertical scale. If B_m exceeds the saturation limit (7,500 Gauss for CO-NETIC, 21,000 Gauss for NETIC), see Section C, otherwise proceed to D.

(C) If Outer Layer(s) Saturate

If B_m exceeds the saturation limit, the calculation must be modified. For CO-NETIC, assume $B_S = 7{,}000$ Gauss (20,000 for NETIC) as the limit for the first layer, and that any additional field passes directly through that layer unattenuated.

1. $H_i\,(U) = \dfrac{B_m - B_S}{B_m} \cdot H_o$

H_i (U) = Field penetrating unattenuated (Oersteds)

B_S = Saturation induction limit (Gauss)

Now calculate attenuation for the portion of the field that does not exceed the limit.

2. $A = \dfrac{\mu \cdot t}{D} + 1$

μ = Permeability at the assumed B_S Gauss Level (100,000 for CO-NETIC, 500 for NETIC)

3. $H_i\,(A) = \dfrac{B_S \cdot H_o}{B_m \cdot A}$

H_i (A) = Attenuated portion of field

The total field inside this layer is then

4. $H_i = H_i\,(U) + H_i\,(A)$

This H_i then becomes the input (H_o) into the next layer.

Calculations proceed using the standard formulas to calculate attenuations for the remaining layers.

(D) $A = \dfrac{\mu \cdot t}{D}$

A = Attenuation Factor

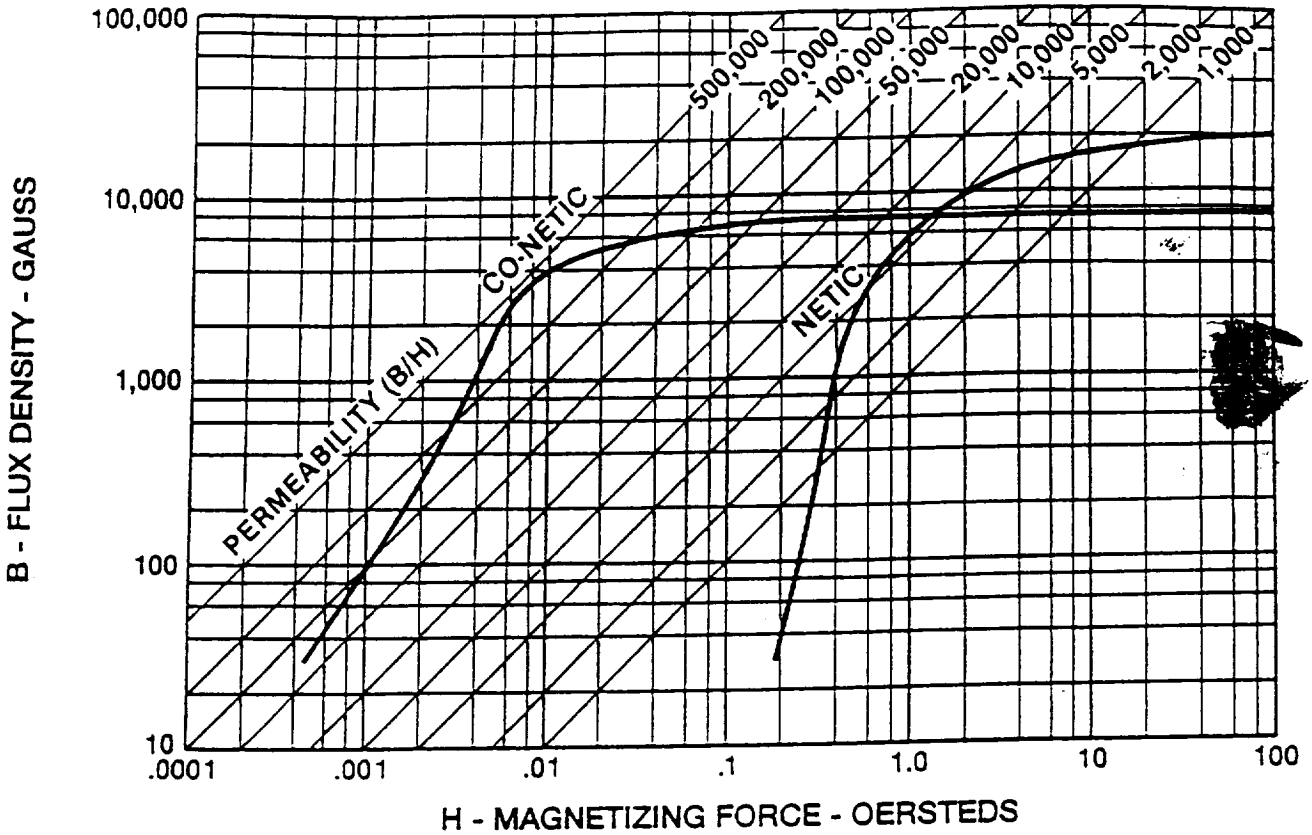

(E) $H_i = \frac{H_o}{A}$

H_i = Field inside the enclosure (Oersteds)

For multilayer shields, the H_i from the outermost layer becomes H_o for the next layer. Attenuation is calculated in a similar manner for each layer.

If B_m is very small, use μ = 30,000 (initial permeability) in calculations for CO-NETIC inner layers.

Attenuation factors calculated in the above manner give theoretical attenuations only attainable in ideal conditions. Designating individual layer attenuations as A_1, A_2, A_3 ... A_n (A_1 as the outer layer) allows calculation of the minimum theoretical inside field as:

(F) $H_i = \frac{H_o}{A_1 \cdot A_2 \cdot A_3 \ldots \cdot A_n}$

Some theories maintain that attenuations of this magnitude are only possible with ideal combinations of spacing, annealing and shape. A more conservative view holds that attenuations may, in the worst case, only add; giving the inside field as:

(G) $H_i = \frac{H_o}{A_1 + A_2 + A_3 + \ldots + A_n}$

Experiments with actual enclosures typically provide results between the upper and lower limits. If attenuations higher than those given by equation (G) are required, additional layers of shielding material should be added.

VIII Specification of Shielding

The following is a list of essential items that should be shown on your drawings.

- Alloy: CO-NETIC AA or NETIC S3-6
- Anneal: Perfection (for CO-NETIC AA Alloy).
- Thickness: See MG-5 catalog for standard thicknesses and sizes.
- Source: **Magnetic Shield Corporation**
  740 N. Thomas Drive
  Bensenville, IL 60106, USA
  Phone: 708-766-7800
  Fax: 708-766-2813